“Studies on Solid-Phase Organic Reactions & Catalysis: Greener Approaches”

A Thesis submitted to the University of North Bengal

For the Award of

Doctor of Philosophy

in

Chemistry

BY

Babli Roy

GUIDE

Prof. Basudeb Basu

Department of Chemistry
University of North Bengal
July-2016

Dedicated
TO
My Parents
&
My Beloved Subir

DECLARATION

I declare that the thesis entitled **"Studies on Solid-Phase Organic Reactions & Catalysis: Greener Approaches"** has been prepared by me under the guidance of Dr. Basudeb Basu, Professor of Chemistry, University of North Bengal. No part of this thesis has formed the basis for the award of any degree or fellowship previously.

Babli Roy 30.06.16

Babli Roy
Department of Chemistry
University of North Bengal
Darjeeling–734013
West Bengal
India

Date: 30.06.16

UNIVERSITY OF NORTH BENGAL

Dr. B. BASU
Professor of Chemistry
DEPARTMENT OF CHEMISTRY
North Bengal University,
Darjeeling – 734 013
India

Phone: +91 353 2776 381
Fax: +91 353 2699 001
Cell: +91 9434428477
Email: basu_nbu@hotmail.com

CERTIFICATE

I certify that Smt. Babli Roy has prepared the thesis entitled "**Studies on Solid-Phase Organic Reactions & Catalysis: Greener Approaches**", for the award of Ph.D. degree of the University of North Bengal, under my guidance. She has carried out the work at the Department of Chemistry, University of North Bengal.

30.06.2016

Dr. Basudeb Basu
Professor of Chemistry
Department of Chemistry
University of North Bengal
Darjeeling-734013
West Bengal
India

DATE: 30.06.2016

Acknowledgment

*This thesis entitled "**Studies on Solid-Phase Organic Reactions & Catalysis: Greener Approaches**" is by far most significant scientific endeavor in my life and it is my great honor to acknowledge the persons who supported me all through with their help and co-operation for the successful conception of the thesis work.*

It is my humble duty and great pleasure to express my indebtedness and respect to my prudent mentor Prof. Basudeb Basu, Department of Chemistry, NBU for his active guidance, painstaking supervision, valuable advice and constant encouragement that he rendered for the present work. His constant vigilance and care has been lavishly bestowed upon me in every stage of this work. He is the key person to steer my academic career in right direction. Any words of gratitude would not be enough to express my thanks for his tremendous support and advice. I would also like to take this opportunity to sincerely thank the better half of my guide, Mrs. Monidipa Basu for her kind words of inspiration.

I take immense pleasure to show great appreciation to all respected teachers of my department, especially Prof. Swapan Kumar Saha, Prof. Pranab Ghosh, Prof. Ashish Kumar Nanda and Dr. Sajal Das. Every meeting with them motivated me more to thrive for success. I do not have enough words to express my gratefulness to my teachers.

I feel pride to have acquainted with all non-teaching staffs like Guru da, Amar Da, Samit Da, Subrata Da, Jogen Da, Amit Da, Sankar Da, Narayan da and also Heera Da; who always stood beside me for constant support and spent a lot of their valuable time to motivate me in my darker hours. I suppose, any word would not fit the gravity to express how indispensable, their presence was for my research. My special thanks to my labmates, Sekhar da, Susmita di, Bablee di, Kinkar, Sujit, Debashish, Samir, Sankar, Prasun and Suchandra for their immense co-operation and co-ordination for the research work which made me capable to adhere to the schedule of the study.

I am also thankful to all other labmates/scholars especially Gourab, Gulmi, Madhurima, Biplab, Ambika, Dipu, Gyan Da, Mainul Da for their continuous co-operation throughout my time at NBU. My heartiest thanks to Abhiseck Saha, Biswasjit Saha, Indradweep Chakrabarty, Neha Choudhury and Nandita Biswas, M.Sc. 4th Semester, 2014 for their assistance during my project work.

I offer cordial thanks to Dr. Goutam De, Chief Scientist & Head, Nano-Structured Materials Division, CSIR-CGCRI, Kolkata, who is an important advisor during my project work and provide me with his valuable support through his scholar Mr. Koushik Bhowmik to facilitate characterization of my samples.

I also express my deep respect to Dr. Debashish Chatterjee, Principal, Tufanganj Mahavidyalaya and all colleague faculties and non-teaching staffs over there for their able advice and supportive ideas. I am also thankful to 'Barobabu' (Ex) Sri Brajodulal Paul of my institute for his never tiring help.

My sincere thanks to Mr. Nitish Biswas, Prof. Raghunath Ghosh and Dr. Minakshi Chakraborty, for their continuous co-operation during the research work.

Words of thanks would be too meager for profound support and blessings rendered to me by my parents Mrs. Arati Roy and Mr. Ramesh Chandra Roy, who remain deprived of my time and attention during the preparation of this thesis. My family, my brothers, my sweet sister-in-law and also my little nephew have always been a constant source of inspiration and energy during my work. I feel pride to take my grandparents name late Narendranath Roy and Bhubaneswari Roy who always remain as my inspirations. I also like to take this opportunity to thank my friends Banani, Anusree, Suranjan, Hossain Aziz, Antara, Sushma, Narottam, Indrajit da and others for their beautiful friendship and support they rendered me always.

I am indebted to my friend Subhanil and also his parents to motivate me throughout my research work.

I would like to convey my thanks to CSIR, New Delhi, for awarding me Junior Research Fellowship and University of North Bengal for providing the infrastructural facilities.

I am really grateful to UGC, Kolkata for giving me the Teacher Fellowship under UGC–FDP programme.

Finally, yet importantly, I would like to express my heartfelt thanks to my beloved husband Mr. Subir Roy for his unending enthusiasm to inspire me at every stage of the research and helping me silently and invisibly to navigate through every obstacle I faced.

Before I finish, I want to express my gratitude to all the chemists, the scientists and research scholars in this field of work whose studies have guided me to complete this work. However, the words might not reach, but I feel it is important to thank my almighty. I have possibly left out the names of many other people who helped me in a way or other during this research work and I express my sincere thanks to all of them.

–Babli Roy

.

ABSTRACT

The research work embodied in this thesis entitled **"Studies on Solid-Phase Organic Reactions & Catalysis: Greener Approaches"** was initiated in February 2009 as a CSIR–NET–JRF and became successful with the kind support of UGC for Teacher Fellowship under the scheme of 'Faculty Development Program'. The research work is primarily motivated to develop new approaches for conducting organic reactions under greener conditions by following solid-phase techniques as well as catalysis. The entire work was emphasized on different types of solid supports mainly silica, graphene-based carbon materials and poly-ionic resins to promote various organic reactions. The thesis has been divided into five chapters.

At the beginning, the **CHAPTER I** is started with a brief review mainly focusing on solid-phase organic reactions and catalysis promoted by different types of inorganic and organic solid-supports. 'Silica gel' which is generally used as an adsorbent in chromatography is also known as an efficient inorganic solid support to promote diverse organic reactions. Recently, graphene and graphene-based materials have attracted synthetic organic chemists due to their unusual behavior towards sustainable organic synthesis. Among various organic polymer supports, poly-ionic resins have a major role for developing diverse polymer-supported reagents and catalysts as well as metal nanoparticles which are efficient to promote solid-phase organic reactions.

CHAPTER II demonstrates the tuning surface behavior of silica gel under pre-calcined and moistened states to promote regioselective addition of excess thiol with allyl bromide to produce 1,2- or 1,3-dithioethers respectively. The presence of physically adsorbed water on the silica surface influenced for the anti-Markonikov addition of thiols to inactivated allylic double bond to produce 1,3-dithioether. On the hand, HBr which is produced in the first step of the reaction activate the allylic double bond and assist the sulfur atom of excess thiol to couple with the more stable secondary carbocation resulting in the Markonikov addition to form exclusively 1,2-dithioether.

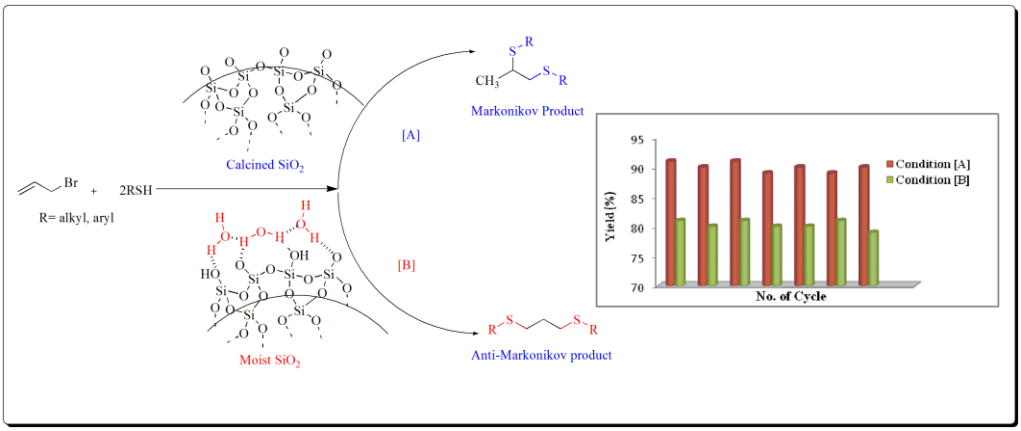

[This work entitled **"**Silica: An efficient catalyst for one-pot regioselective synthesis of dithioethers" has been published on ***Beilstein J. Org. Chem.*****, 2014, *10*, 26-33**]

CHAPTER III is divided into two sections: **Section A** & **Section B. Section A** represents an efficient and greener method for the synthesis of open chain, cyclic and unsymmetrical dithioacetals from aryl/hetero-aryl/aliphatic aldehydes catalyzed by graphene oxide (GO). The reaction conditions are mild, solvent-free and aerobic. Notable features of this methodology are operational simplicity, nil or negligible formation of disulfide, chemoselectivity, recyclability and environmental compatibility.

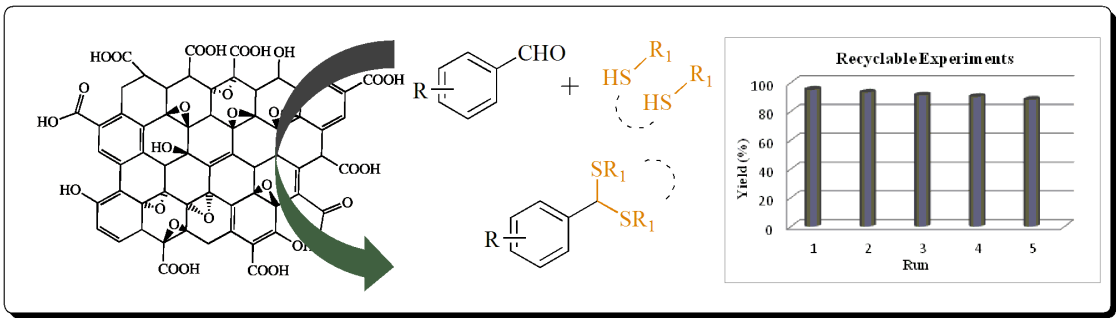

[The work entitled "Graphene Oxide (GO)–catalyzed chemoselective thioacetalization of aldehydes under solvent-free conditions" has been published on ***Tetrahedron Lett.*, 2014, *55*, 6596–6600]**

Section B demonstrates a straightforward and green synthesis of bio-active scaffold quinoxalines directly from 2-nitronilines *via* one-pot reduction-condensation reactions using hydrazine hydrate as the reductant and GO/rGO as the catalysts under complete metal free conditions. The catalyst has been recovered, characterized and recycled for four consecutive runs.

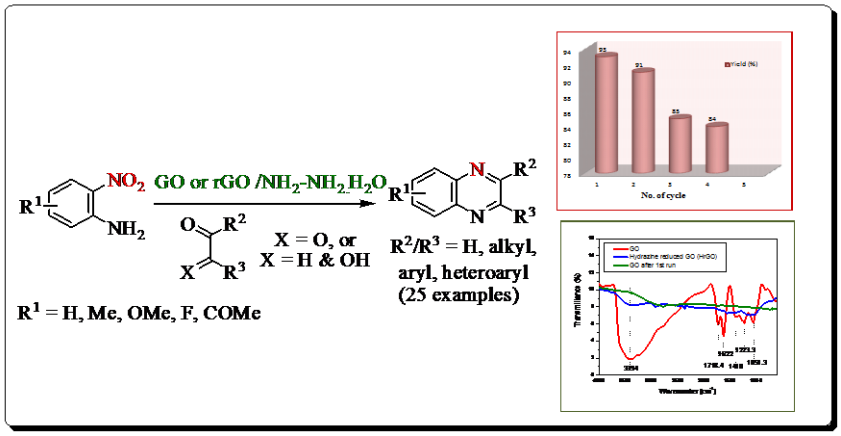

[This work entitled "Graphene oxide (GO) or reduced graphene oxide (rGO): efficient catalysts for one-pot metal-free synthesis of quinoxalines from 2-nitroaniline" has been published on ***Tetrahedron Lett.*, 2015, *56*, 6762–6767**]

CHAPTER IV portrays about the comparative evaluation of diverse properties of chemically and biologically reduced graphene oxides (rGOs). Reduced graphene oxides (rGOs) can be prepared from graphene oxide (GO) by several methods and reducing sources including some phyto– and fungi–extracts. However, rGOs obtained by different methods might exhibit different properties depending on the extent of residual oxygen–containing functional groups, though textural aspects of rGOs seem to be rather similar. The present study has been aimed at making a comparative evaluation of various properties of reduced graphene oxides (rGOs), prepared by using chemical and biological reducing sources, and to establish specific reducing agent, in particular from greener sources, which might be more effective in exhibiting catalytic activity. Four different plants extracts viz. *Adathoda Vasika* (Malabar nut), *Azadirachta Indica* (Neem), *Camellia Sinensis* (Tea), *Moringa Oleifera* (Drumstick), and a fungi *Volvereilla Volvacea* (Mushroom), all are edible to human beings, and one chemical reductant (hydrazine hydrate) were used to obtain rGOs from GO. Each rGO was characterized by UV–Vis, FT–IR, Raman spectroscopic techniques, and surface morphological aspects were obtained by powder XRD, Scanning and Transmission electron microscopic images. The acidic nature (pH) of rGOs in aqueous suspension was measured with a pH meter and their

cation–exchange capacity was calculated by potentiometric titration in the presence of an electrolyte. Further, the catalytic activity of rGOs was measured in a model reduction of nitrobenzene to aniline at room temperature and monitoring the progress by UV–Vis spectroscopy. While textural aspects of various rGOs are fairly similar, various physicochemical properties like pH, cation–exchange ability etc. are found to be different for rGOs obtained by using different reductants. Moreover, there is significant variation observed in their catalytic activity in the reduction of nitrobenzene. By comparison, it was found that rGOs obtained by using plant leaf extract of *Adathoda Vasika*, (brGO–AV) and *Volvereilla Volvacea*, (brGO–VV) exhibit significantly better catalytic efficiency than others.

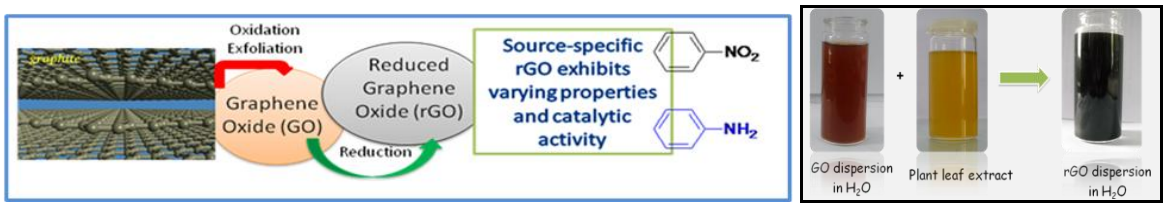

[This work titled **"**Reduced Graphene Oxides (rGOs): Source–dependent Properties and Catalytic Activity" has been communicated.]

CHAPTER V depicts about the catalytic applications of poly-ionic resins embedded with Pd/Cu bimetallic NPs in two most important C–C bond forming reactions, Suzuki-Miyaura and Mizoroki-Heck coupling reactions. A comparative study between monometallic Pd–ARF and bimetallic Pd/Cu-ARF towards Suzuki and Heck coupling reactions demonstrates the more catalytic efficiency of bimetallic NPs compared to monometallic Pd NPs as catalysts. The Pd/Cu–ARF bimetallic NPs have been found to be recyclable for seven consecutive runs without loss of any catalytic activity as well as without any leaching of metals.

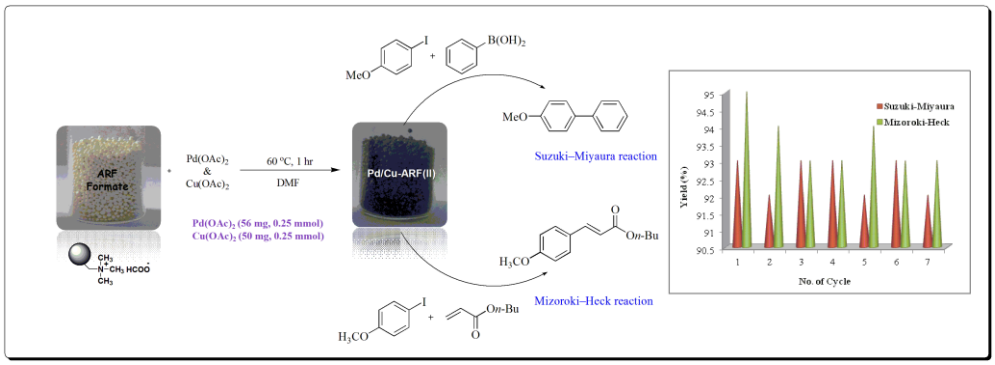

[This work titled "Bimetallic Pd/Cu NPs embedded on macroporous ion-exchange resins: Application to Suzuki–Miyaura and Mizoroki–Heck reactions" manuscript under preparation]

PREFACE

The ever increasing demand for efficient syntheses of novel organic compounds remains the major driving force for the development of new and efficient solid-supported technologies. Solid-phase organic synthesis has emerged as a powerful tool for the generation of compound library. Polymer-supported reagents/substrates and polymer-supported catalysts have been widely employed in various fields of chemistry such as drug discovery, material sciences and asymmetric catalyses. Such process offers several advantages, which include possibility to use excess reagents to drive the reactions to completion, simplification of product work-up, separation and isolation as well as reuse of the catalysts, thereby providing an environmentally benign technique for green and cleaner reactions. The current emphasis for organic transformations requires high selectivity, easy separation and production of minimum waste. Immobilized reagents/substrates and immobilized catalysts can afford to greener organic transformations for laboratory to large-scale operations. As pointed out by Steven V. Ley, "the face of organic synthesis is changing rapidly as it should if it is to stay a healthy, vibrant subject. I feel, therefore, I should end with a vision of where we see the potential use of these immobilised systems in the future."

The development of new approaches for conducting organic reactions under greener reaction conditions constitutes an attractive area of synthetic organic chemistry. Solid-phase organic reactions and solid-phase immobilized catalysts have played a significant role in combinatorial synthesis small molecules of pharmaceutical interest. Over the last two decades, there has been insurgency in developing green chemistry and catalysis for sustainable organic synthesis.

In the recent years, graphene and graphene-based materials; such as graphene oxide (GO) and reduced graphene oxide (rGO) have been found to be extremely useful as alternative metal-free heterogeneous reusable catalysts for diverse organic transformations.

The present research work represents the development of some new approaches towards selective organic reactions promoted by inexpensive solid-surface like silica gel as well as catalyzed by GO and rGO. The present dissertation also includes the development of new polymer-immobilized metal catalysts for their applications in C–C bond-forming reactions.

The present works begin with **CHAPTER I** describing a brief introduction on solid-phase organic reactions mediated by heterogeneous solid supports such as silica, graphene-based materials and poly-ionic resins. **CHAPTER II** demonstrated about the silica gel promoted one-pot regioselective synthesis of dithioethers. **CHAPTER III** divided into two sections; **Section A and Section B**. **Section A** deals with "carbocatalysis" where graphene oxide (GO) has been exploited as a solid "carbocatalyst" for the chemoselective dithioacetalization of aldehydes. **Section B** demonstrates further utilization of GO or reduced graphene oxide (rGO) as efficient catalysts for one-pot metal-free synthesis of quinoxalines directly from 2-nitroaniline. In **CHAPTER IV** a comparative evaluation of diverse properties of chemically and biologically reduced graphene oxide along with their catalytic activity towards reduction of nitrobenzene has been described. Finally, **CHAPTER V** focused on the application of poly-ionic resins embedded with Pd/Cu bimetallic nanoparticles in Suzuki–Miyaura and Mizoroki–Heck reactions.

TABLE OF CONTENTS

Abstract			i-iii
Preface			iv
List of Tables			ix
List of Schemes			x-xiii
List of Figures			xiv-xv
List of Appendices			xvi
Appendix A: List of Publications			xvii
Appendix B: Oral Presentation & Poster Presentation			xviii
Abbreviation			xix
CHAPTER I			
A brief review on solid-phase organic reactions & catalysis by heterogeneous solid supports: Silica, Graphene-based materials and Poly-ionic resins			1–27
I.1.	General Introduction		2–3
I.2.	Catalysis		3
	I.2.1.	Homogenous Catalysis	3
	I.2.2.	Heterogeneous Catalysis	4
1.3	Heterogeneous solid supports and their catalytic applications		5
	I.3.1.	Amorphous silica	5–9
	I.3.2.	Ordered mesoporous silica	9–10
	I.3.3.	Carbon materials	10–11
		I.3.3.1. Graphene-based materials and their catalytic applications in diverse organic reactions	10–18
I.4.	Organic polymers		18–19
	I.4.1.	Microporous gel-type resins	19
		I.4.1.1. Polystyrene (PS) resins	19–20
		I.4.1.2. Poly (ethylene glycol)-polystyrene resins (PEG–PS)	20
		I.4.1.3. Hydrophilic PEG-based resin	20–21
		I.4.2.1. Ion-exchange resins	21–23
	I.4.2.	Macroporous resins	22–27
I.5	References		27
CHAPTER II			
Silica: An efficient inorganic solid support to promote one-pot regioselective synthesis of dithioethers			28–55
II.1.	Introduction		29–30
II.2.	Present Work: Background and Objective		31–36
II.3.	Present work: Results and Discussion		36–40
	II.3.1.	Optimization of reaction conditions	36–37

	II.3.2.	Applications of our optimized reaction conditions in one-pot tandem reactions of allyl bromide with a variety of thiols	38–40
	II.3.3.	Mechanism	41–42
	II.3.4.	Recyclability of the catalyst	43–44
II.4.	Conclusion		44
II.5.	Experimental Section		44–56
	II.5.1.	General Information	44–45
	II.5.2.	General procedure for the preparation of 1,2- and 1,3-dithioethers (Table II.2, Route A or B)	45
	II.5.3.	Procedure for the reaction using a mixture of silica and sodium silicate under condition [A] (Table II.2, Entry 20)	45–46
	II.5.4.	II.5.4. Physical properties and spectral data of compounds	46–54
II.6.	References		55

CHAPTER III

Section A

Graphene oxide (GO): A convenient metal-free "Carbocatalyst" for diverse organic reactions 56–87

III.A.I.	Introduction		57–58
IIIA.2.	Present Work: Background and Objectives		58–64
III.A.3.	Present work: Results and Discussion		64–72
	III.3.1.	Preparation and characterization of graphene oxide	64–65
III.A.4.	Conclusion		72
III.A.5.	Experimental Section		72–84
	III.A.5.1.	General Information	72–73
	III.A.5.2.	General procedure for the preparation of dithioacetals	73
	III.A.5.3.	HPLC analysis	73–74
	III.A.5.4.	Physical properties and spectral data of dithioacetals	75–86
III.A.6.	References		87

CHAPTER III

Section B

Graphene oxide (GO) or reduced graphene oxide (rGO): Efficient catalysts for one-pot metal-free synthesis of quinoxalines from 2-nitroaniline 88–115

III.B.1.	Introduction		89–90
III.B.2.	Present Work: Background and Objectives		90–94
III.B.3.	Present work: Results and Discussion		93–102
	III.B.3.1.	Preparation and characterization of graphene oxide	94–96
	III.B.3.2.	DLS study of GO	95
	III.B.3.3.	AAS study of GO	96
	III.B.3.4.	Optimization of reaction conditions	96–98
	III.B.3.5.	Applications of our optimized condition in a variety of 2-nitroanilines and benzil derivatives	98–101
	III.B.3.6.	Recyclability of the catalyst	101–102

	III.B.3.7.	Characterization of the recovered catalyst after 1st run of the reaction and also the hydrazine reduced GO	102
	III.B.3.8.	Mechanism	102-103
III.B.4.	Conclusion		104
III.B.5.	Experimental Section		104-114
	III.B.5.1.	General Information	104
	III.B.5.2.	Preparation of reduced graphene oxide (rGO)	104–105
	III.B.5.3.	General procedure for the preparation of quinoxaline derivatives	105
	III.B.5.4	HPLC Analysis	105–106
	III.B.5.5.	Spectral data and melting points of quinoxaline compounds	107–114
III.B.6.	References		115

CHAPTER IV

	Chemically and Biologically Reduced Graphene Oxides: Comparative Evaluation of Diverse Properties and Catalytic Activity		116–137
IV.1.	Introduction		116–117
IV.2.	Present Work: Background and Objectives		117–123
IV.3.	Present work: Results and Discussion		123–132
	IV.3.1	Experimental	123
		IV.3.1.1 Materials	123
		IV.3.1.2. Preparation of plants and fungi extracts	123
		IV.3.1.3. Preparation of graphene oxide (GO)	124
		IV.3.1.4. General procedure for the preparation of different biologically reduced graphene oxides (brGOs)	124
		IV.3.1.5. Preparation of chemically reduced GO (crGO)	124
	IV.3.2.	Characterizations	124–132
		IV.3.2.1. UV–Vis spectroscopy	125–126
		IV.3.2.2. FT–IR spectroscopy	126–127
		IV.3.2.3. Raman spectroscopy	127–128
		IV.3.2.4. Powder X–ray diffraction patterns	129
		IV.3.2.5. FESEM & HRTEM studies	130–131
		IV.3.2.6. The pH measurements	131–132
V.4.	Catalytic applications		132–135
V.5.	Conclusion		136
V.6.	References		136

CHAPTER V

	Poly-ionic resins embedded with Pd/Cu bimetallic NPs: Applications in Suzuki–Miyaura and Mizoroki–Heck Coupling reactions	137–162
V.1.	Introduction	138–142
V.2.	Background and Objectives	143–144

V.3. Present work: Results and Discussion 144–150
V.3.1. Preparation of heterogeneous Pd/Cu-ARF nanocomposite 144
V.3.2. Suzuki–Miyaura reaction catalyzed by Pd/Cu−ARF 144–146
V.3.3. Mizoroki–Heck reaction catalyzed by Pd/Cu−ARF 147–148
V.3.4. Application of Pd/Cu–ARF bimetallic NPs for the preparation of 3-Methyl-1*H*-indole 149
V.3.4. Comparative study 149–150
V.3.5. Hot filtration test 150–151
V.3.6. Recyclability of the catalyst 151
V.3.7. Characterization of the recovered catalyst 151–152
V.4. Conclusion 152
V.5. Experimental Section 152–153
V.5.1. General Information 153
V.5.2. Preparation of Pd/Cu−ARF bimetallic nanocomposite 153
V.5.3. Preparation of monometallic ARF–Pd 153
V.5.4. General procedure for Suzuki–Miyaura cross-coupling using Pd/Cu−ARF 153
V.5.5. General procedure for Mizoroki–Heck coupling using Pd/Cu−ARF 154
V.5.6. Preparation of 3-Methylindole 154
V.5.7. Physical properties and spectral data of compounds 155–162
V.6. References 162
Bibliography 162–190
Index 191–196

LIST OF TABLES

Table No.	Title	Page No.
Table I.1.	Comparison of various synthetic methods for the preparation of GO	16
Table II.1.	Optimization of one-pot sequential substitution-hydrothiolation of allylic substrate with excess benzenethiol over silica at room temperature	37
Table II.2.	Regioselective one-pot synthesis of 1,2- and 1,3-dithioethers using dry (pre-calcined) or moist silica gel at room temperature	39–40
Table III.A.1.	Optimization of dithioacetal formation from *p*-anisaldehyde and *n*-pentane thiol	66
Table III.A. 2.	GO–catalyzed thioacetalization of aldehydes with different thiols	67–68
Table III.A.3.	GO–catalyzed thioacetalization of heteroaryl aldehydes	69
Table III.A.4.	Unsymmetrical thioacetals from aryl aldehydes using two different thiols	70
Table III.B.1.	Optimization of reaction conditions for GO–catalyzed one-pot reduction and heterocyclization of 2-nitroaniline (1 mmol) and benzil (1 mmol)	97
Table III.B.2.	GO–catalyzed reduction of various 2-nitroanilines and subsequent heterocyclization with 1,2-dicarbonyl compounds or with α-hydroxy ketones	99–101
Table III.B.3.	Recycling of the catalyst tested with 2-nitroaniline and benzil in one-pot reactions	102
Table IV.1.	UV–Vis spectra of GO, crGO and different brGOs	126
Table IV.2.	Comparative chart for FT–IR data of GO and various rGOs	126
Table IV.3.	Raman peak position of D and G band and their intensity ratio	128
Table IV.4.	XRD value of GO and different rGO's	129
Table IV.5.	pH variation of GO and different brGO and their cation exchange capacity	132
Table IV.6.	Rate constants of different rGO samples for the reduction of nitrobenzene to aniline	136
Table V.1.	Optimization of Suzuki–Miyaura reaction using Pd/Cu–ARF	145
Table V.2.	Suzuki–Miyaura cross-coupling using Pd/Cu−ARF	146
Table V.3.	Optimization of Mizoroki–Heck reaction using Pd/Cu−ARF	147
Table V.4.	Mizoroki–Heck cross-coupling using Pd/Cu−ARF	148

LIST OF SCHEMES

Scheme No.	Title	Page No.
Scheme I.1.	Silica gel promoted various organic transformations	8
Scheme I.2.	Synthesis of 2-bromobenzoate in the one-pot method catalyzed by silica gel	9
Scheme I.3.	A schematic presentation for the preparation of suspended graphene sheets through consecutive graphite oxidation, exfoliation to GO and its eventual reduction to graphene	12
Scheme I.4.	Chemical reduction of GO to rGO by means H_2, $NaBH_4$ or N_2H_4	12
Scheme I.5.	Graphene–catalyzed oxidation of cyclohexane	13
Scheme I.6.	*N*-doped graphene–catalyzed oxidation of alcohols	13
Scheme I.7.	CCG–catalyzed oxidation of benzene to phenol	14
Scheme I.8.	KOH-G–catalyzed aerobic oxidation of 9*H*-fluorene to 9-fluorenone	14
Scheme I.9.	Reduced graphene oxide (rGO)–catalyzed dehydrogenation of various hydrazo compounds	14
Scheme I.10.	Conversion of hemicellulosic materials to xylose and then furfural	14
Scheme I.11.	Reduced graphene oxide (rGO)–catalyzed disulfiram formation from dibenzylamine and CS_2	15
Scheme I.12.	Preparation of isoamyl benzoate using rGO-PSSA	15
Scheme I.13.	Polymerization of 3-amino-phenylbpronic acid catalyzed by GO or rGO	15
Scheme I.14.	Reduction of nitrobenzene catalyzed by rGO	15
Scheme I.15.	GO as an efficient oxidant for various organic transformations.	18
Scheme I.16.	GO–catalyzed various organic transformations	18
Scheme I.17.	The formation of Merrifield's polystyrene resin	20
Scheme I.18.	Microencapsulated PS-$RuCl_2(PPh_3)$–catalyzed organic transformations	23
Scheme I.19.	Amberlyst A-26 catalyzed disulfide formation	24
Scheme I.20.	Amberlyst-15 catalyzed various organic transformations	24
Scheme I.21.	Synthesis of ARF and Pd–catalyzed catalytic transfer hydrogenation of alkenes, imines and nitroarenes	25
Scheme I.22.	ARF–Pd catalyzed various C-C cross coupling reactions	26
Scheme I.23.	Synthesis of phenothiazine using poly-ionic resin supported CuO NPs	26
Scheme I.24.	Amberlite supported tetraphenylborate as a phenylating agent for Suzuki reaction	27
Scheme II.1.	$[Ni(NH_3)_6]Cl_2$–catalyzed vicinal-dithioethers of norbornene derivatives *via* S_8 activation	31

Scheme II.2.	Bis(bipyridine)nickel(II) bromide complex catalyzed synthesis of alkenyl sulfides and ketene thioaetals	32
Scheme II.3.	Cp*RuCl(cod)–catalyzed stereoselective synthesis of *vicinal*-dithioethers	32
Scheme II.4.	$GaCl_3$–catalyzed disufidation of alkynes and alkenes	32
Scheme II.5.	$Pd(PPh_3)_4$–catalyzed stereoselective addition of aromatic disulfides to terminal alkynes	33
Scheme II.6.	$Pd(PPh_3)_4$ catalyzed one-pot carbonylative addition of disulfides to alkynes	33
Scheme II.7.	$Pd(PPh_3)_4$–catalyzed *syn*-addition of bis(triisopropylsilyl)disulfide to alkynes in benzene at 80 °C	33
Scheme II.8.	Synthesis of disubstituted dithioethers by $Pd(OAc)_2$/Xantphos promoted tandem elimination/ring opening/C−S cross coupling of 1,3-dithianes	34
Scheme II.9.	$FeCl_3/AlCl_3$–catalyzed disulfenylation of cylohexene with aromatic sulphide	34
Scheme II.10.	"On water" synthesis of vicinal dithioethers from alkynes and thiols and region- and stereoselective monohydrothiolation of propargyl alcohols	34
Scheme II.11.	Silica NPs–catalyzed anti-Markonikov addition of thiols to alkenes/allyl halides and also the synthesis of 1,3-dithioether	35
Scheme II.12.	Silica gel promoted various organic transformations	35
Scheme II.13.	S-allylation of thiohenols promted by silica gel surface at room temperature	36
Scheme II.14.	Sequential substitution-addition reactions of thiols with allyl halides leading to the formation of 1,2- or 1,3-dithioethers	36
Scheme II.15.	Plausible mechanisms for the regioselective formation of vicinal and 1,3- dithioethers in the presence of dry or moist silica gel	41
Scheme II.16.	Addition of thiophenol to allylphenylsulfane with thiophenol in the presence of an exogenous base	42
Scheme II.17.	Reaction of allylphenylsulfane with thiophenol in the presence of dry HCl gas	43
Scheme II.18.	Plausible mechanism for the formation of 2-D-1,3-dithioether following condition [B]	43
Scheme III.A.1.	GO–catalyzed various organic transformations	58
Scheme III.A.2.	Michael addition reaction of *trans*-β-nitrostyrene and 2,4-pentanedione	58
Scheme III.A.3.	GO–catalyzed Aza-Michael addition reaction	59
Scheme III.A.4.	GO–catalyzed synthesis of dipyrromethane and calix[4]pyrrole	59
Scheme III.A.5.	One-pot sequential dehydration-hydrothiolation catalyzed by graphene oxide	60

Scheme III.A.6.	GO–catalyzed one-pot multi-component synthesis of 3-sulfenylimidazo[1,2-*a*]pyridines	60
Scheme III.A.7.	GO/TEMPO–catalyzed aerobic oxidation of 5-hydroxymethylfulfural to 2,5-diformylfuran	60
Scheme III.A.8.	Organosulfates present in GO prepared *via* the Hummers method; susceptible to hydrolysis, leading to the formation of acidic sulfate species in the final product	61
Scheme III.A.9.	GO–catalyzed ring opening of styrene oxide in methanol	61
Scheme III.A.10.	Acetalization of aldehydes at room temperature using GO as a solid acid catalyst	61
Scheme III.A.11.	Hetero poly acid catalyzed dithioacetalization	62
Scheme III.A.12.	Dithioacetalization of carbonyl compounds using *p*-toluenesulfonic acid and silica gel	62
Scheme III.A.13.	Montmorillonite K–10 clay catalyzed oxathioacetalization of carbonyl compounds	63
Scheme III.A.14.	Silica sulphuric acid catalyzed dithioacetalization of aldehydes	63
Scheme III.A.15.	Dithioacetalization of aldehydes and ketones by resin-bound reagents	63
Scheme III.A.16.	GO–catalyzed diverse dithioacetals formation	64
Scheme III.B.1.	Solid-phase synthesis of quinoxaline on SynPhase™ Lanterns.	90
Scheme III.B.2.	Ru/C–catalyzed one-pot synthesis of quinoxalines	90
Scheme III.B.3.	Quinoxaline synthesis on heterogeneous KF/Alumina basic surface	91
Scheme III.B.4.	Graphite–catalyzed quinoxalie synthesis	91
Scheme III.B.5	Ruthenium catalyzed quinoxaline synthesis from various nitroanilines and symmetrical vicinal diols	92
Scheme III.B.6.	Synthesis of 2,3-dimethylquinoxalines and 2,3-diphenylquinoxaline in the presence of indium and $InCl_3$ in different condition	92
Scheme III.B.7	Fe/S–catalyzed redox condensation reaction of 2-arylethylamines with various *o*-nitroanilines	93
Scheme III.B.8.	Au/CeO_2–catalyzed one-pot three-step synthesis of quinoxaline derivatives	93
Scheme III.B.9.	The synthesis of quinoxalines by the reaction of 2-Nnitroanilines and 1,2-dicarbonyl compounds mediated by $SnCl_2 \cdot 2H_2O$	93
Scheme III.B.10.	One-pot reduction of nitro compounds and subsequent condensation resulting quinoxalines	94
Scheme III.B.11.	Plausible mechanism for the quinoxaline synthesis	103
Scheme IV.1.	Reduction of nitrobenzene using brGO as a catalyst	133
Scheme V.1.	Suzuki–Miyaura and Heck reactions catalyzed by Au-Pd	139

	bimetallic nanoparticles	
Scheme V.2.	Suzuki cross-coupling reaction using Au-Pd/SiO_2 as a catalyst	140
Scheme V.3.	Ag–Pd@rGO bimetallic nanoparticles catalyzed Suzuki reaction	140
Scheme V.4.	Graphene supported Pd–Co bimetallic nanoparticles catalyzed Suzuki-Miyaura coupling	140
Scheme V.5.	Suzuki and Heck coupling reactions catalyzed by bimetallic Pd-Ni nanoclusters	141
Scheme V.6.	Pd–Ni core-shell nanoparticles catalyzed Suzuki coupling reaction	141
Scheme V.7.	Pd/Cu (4:1) catalyzed Heck–Mizoroki coupling reaction	142
Scheme V.8.	Suzuki and Heck reactions catalyzed by Pd–M/C	142
Scheme V.9.	Preparation of monometallic Pd NPs and CuO NP embedded on Amberlite Resin Formate (ARF).	143
Scheme V.10.	Sonogashira cross-coupling catalyzed by Pd/Cu–ARF(II)	143
Scheme V.11.	Preparation of bimetallic Pd/Cu–ARF NPs.	144
Scheme V.12.	Synthesis of 3-methylindole *via* Mizoroki–Heack coupling with Pd/Cu−ARF(II) catalyst	149

LIST OF FIGURES

Figure No.	Title	Page No.
Figure I.1.	The formation of silanol groups on the silica surface: (a) Condensation polymerization; (b) Rehydroxylation	6
Figure I.2.	Various types of silanol groups and siloxane bridges present on the surface of amorphous silica along with internal silnanol groups	7
Figure I.3.	Graphene, 2D building material wrapped up into 0D buckyballs, rolled into 1D nanotubes or stacked into 3D graphite	11
Figure I.4.	Various structural models of graphene oxide	17
Figure I.5.	Structures of some common polymeric resins	21
Figure II.1.	Some flexible dithioether ligands involved in the formation of metal-organic coordination complexes	29
Figure II.2.	Structural variation of thioether-based copper complexes	
Figure II.3.	Recclyabilty of silica gel for the one-pot regioselective addition of thiophenols to allyl bromide under pre-calcined silica (Condition [A]) and moistened silica (condition [B])	30
Figure III.A.1.	Various active sites present in the graphene-based materials like GO and rGO	57
Figure III.A.2.	FT-IR spectra of GO	65
Figure III.A.3.	Recyclability of GO in the thioacetalization of *p*-anisaldehyde and *n*-pentanethiol	71
Figure III.A.4.	Comparative FT-IR spectra of GO before and after 1st use in the reaction between *p*-anisaldehyde and *n*-pentanethiol under neat condition.	72
Figure III.A.5.	HPLC analysis showing retention times of two different symmetrical dithioacetals (Table III.A.2, entry 1 and entry 10)	74
Figure III.A.6.	HPLC analysis showing area percentage of three possible dithioacetals obtained from *p*-anisaldehyde, *n*-pentanethiol and benzenethiol (Table III.A.4, entry 3).	74
Figure III.B.1.	Some important drugs containing quionxaline moieties	89
Figure III.B.2.	The FT–IR Spectra of GO	95
Figure III.B.3.	Particle size distribution plot of graphene oxide obtained from dynamic light scattering (DLS)	96
Figure III.B.4.	The comparison between the FT-IR spectra of GO before and after 1st use in the one-pot reduction and heterocyclization reaction between 2-nitroaniline and benzil with hydrazine reduced GO (HrGO)	103
Figure III.B.5.	HPLC of crude reaction mixture (Table III.B.1, Entry 13 reaction), the area percentage of quinoxaline product and starting benzil is in the ratio of 95:5	106

Figure III.B.6.	HPLC analysis of a pure mixture of two regioisomer (Table III.B.2, Entry 19)	106
Figure IV.1.	UV–Vis spectra of GO, brGO–CS, brGO–MO, brGO–AV, brGO–VV, brGO–AI, crGO (0.5 mg/ml in water)	125
Figure IV.2.	FTIR spectra of GO, brGOs and crGO	127
Figure IV.3.	Raman spectra of GO and different rGOs	128
Figure IV.4.	XRD pattern of GO and different rGOs	129
Figure IV.5.	FESEM images of GO and different brGOs	130
Figure IV.6.	HRTEM images of GO, brGO–CS, brGO–MO, brGO–AV, brGO–VV, brGO–AI respectively	130
Figure IV.7.	Titration curves for GO and different brGO in aqueous NaCl with 0.1 M NaOH solution	132
Figure IV.8.	UV–Vis absorption spectra of pure nitrobenzene and aniline (I) and of the reduction of nitrobenzene without catalyst (II)	133
Figure IV.9.	Spectral decay at different time intervals using brGO–AV (III) and plot of ln (C_t/C_0) *vs.* reduction time (IV)	134
Figure IV.10.	Spectral decay at different time intervals using brGO–VV (V) and plot of ln (C_t/C_0) *vs.* reduction time (VI)	134
Figure IV.11.	Spectral decay at different time intervals using brGO–CS (VII) and plot of ln (C_t/C_0) *vs.* reduction time (VIII)	134
Figure IV.12.	Spectral decay at different time intervals using brGO–AI (IX) and plot of ln (C_t/C_0) *vs.* reduction time (X)	135
Figure IV.13.	Spectral decay at different time intervals using brGO–MO (XI) and plot of ln (C_t/C_0) *vs.* reduction time (XII)	135
Figure IV.14.	Spectral decay at different time intervals using crGO (XIII) and plot of ln (C_t/C_0) *vs.* reduction time (XIV).	135
Figure V.1.	Time conversion plot for (a) Suzuki–Miyaura and (b) Mizoroki–Heck coupling reaction using Pd/Cu−ARF and ARF–Pd	150
Figure V.2.	Comparison of the reaction under normal condition and the reaction after hot filtration test for (a) Suzuki–Miyaura and (b) Mizoroki–Heck coupling reaction catalyzed by Pd/Cu−ARF	150
Figure V.3.	Recycling experiments using Pd/Cu−ARF for Suzuki–Miyaura cross–coupling between 4-iodoanisole and phenylboronic acid and Mizoroki–Heck cross–coupling between 4-iodoanisoleand *n*-butyl acrylate	151
Figure V.4.	XRD analysis of Pd/Cu−ARF catalyst recovered after 7^{th} consecutive runs in Mizoroki–Heck reaction	152

LIST OF APPENDICES

APPENDIX A:

List of Publications xvii

APPENDIX B:

Oral Presentation & Poster Presentation xviii

APPENDIX A

List of Publications

1. "Silica: An efficient catalyst for one-pot regioselective synthesis of dithioethers" Samir Kundu, **Babli Roy** and Basudeb Basu, *Beilstein J. Org. Chem.*, **2014**, *10*, 26–33.

2. "Graphene Oxide (GO)–catalyzed chemoselective thioacetalization of aldehydes under solvent-free conditions" **Babli Roy**, Debasish Sengupta and Basudeb Basu, *Tetrahedron Lett.*, **2014**, *55*, 6596–6600.

3. "Graphene oxide (GO) or reduced graphene oxide (rGO): efficient catalysts for one-pot metal-free synthesis of quinoxalines from 2-nitroaniline" **Babli Roy**, Sujit Ghosh, Pranab Ghosh, Basudeb Basu, *Tetrahedron Lett*., **2015,** *56*, 6762–6767.

4. **"**Chemically and Biologically Reduced Graphene Oxides (rGOs): Comparative Evaluation of Diverse Properties and Catalytic Activity**"** **Babli Roy** and Basudeb Basu (Communicated).

Review Article

1. "Microwave-assisted Formation of Organic Disulfides of Biochemical Significance" Debasish Sengupta, **Babli Roy** and Basudeb Basu, *Curr. Med. Chem.*, **2016**, *23*, 1–11.

APPENDIX B

Oral Presentation

- "In quest of greener approaches towards reduction of graphene oxide and subsequent catalytic applications" **Babli Roy**, *National Seminar On Frontiers In Chemistry*-**2015**, Department of Chemistry, University of North Bengal, Darjeeling-734013.

Poster Presention

- "Reduced Graphene Oxide (rGO) – an eco-friendly and reusable carbocatalyst for the synthesis of biologically potent N-based hetereocycles" Babli Roy and Basudeb Basu, *National Seminar On Frontiers In Chemistry*-**2015**, Department of Chemistry, University of North Bengal, Darjeeling-734013, February 17-18, 2015.

- ""Graphene oxide (GO) – an efficient carbocatalyst for the one–pot tandem reduction and cyclization for quinoxaline synthesis", **Babli Roy**, Kinkar Biswas, Sujit Ghosh and Basudeb Basu, *National Symposium on Recent Trends and Perspectives in Chemistry (RTPC*-**2015***)*, National Institute of Technology, Sikkim, India, January 23–24, **2015**.

- Pd/Cu bimetallic nanoparticles soaked on poly-ionic resins: an excellent heterogeneous catalyst for Suzuki-Miyaura and Heck coupling reactions, Debasish Sengupta, **Babli Roy**, Samir Kundu and Basudeb Basu, *National Seminar on Frontiers in Chemistry*-**2014**, held at University of North Bengal, Darjeeling, March 11, 2014.

- "Role of additives in triggering stereoselective switch in alkyne hydrothiolation", Sujit Ghosh, Kinkar Biswas, **Babli Roy**, Susmita Paul, Bablee Mandal, Basudeb Basu, *12th CRSI National Symposium in Chemistry & 4th CRSI–RSC Symposium in Chemistry*-**2010** ,Indian Institute of Chemical Technology (IICT), Hyderabad, India, February 4–7, 2010.

ABBREVIATION

AAS	Atomic absorption spectroscopy	mol%	Mol percent
ARF	Amberlite resin formate	MOF	Metal-organic framework
Bu	Butyl	NMP	*N*-Methylpyrrolidone
^{o}C	Degree Celsius	nm	Nanometer
CCG	Chemically converted graphene	NMR	Nuclear Magnetic Resonance
CLEAR	Poly(ethylene glycol) cross-linked ethoxylate acrylate resin	NPs	Nanoparticles
CMG	Chemically modified graphene	PEG	Polyethylene glycol
CNT	Carbon nanotube	PEGA	Poly acrylamides cross-linked with PEG
CTH	Catalytic transfer hydrogenation	PEG–PS	Poly(ethylene glycol)–Polystyrene Resin
CVD	Chemical vapor deposition	ppm	parts per million
dd	Doublet of doublet	PS	Polystyrene
DCM	Dichloromethane	PSSA	Polystyrene sulfonic acid
DMF	Dimethyl formamide	PVP	Poly vinyl pyrrolidone
DMSO	Dimethyl sulfoxide	QHE	Quantum Hall Effect
DLS	Dynamic light scattering	rt	Room temperature
DVB	Divinyl benzene	s	Singlet
EDA	Ethylenediamine	SBA-15	Santa Barbara Amorphous
HMF	5-hydroxymethylfulfural	SEM	Scanning electron microscopy
HPLC	High performance liquid chromatography	SPOS	Soild-phase organic synthesis
HRTEM	High-resolution transmission electron microscopy	SPPS	Solid-phase peptide synthesis
HRMS	High resolution mass spectra	SSA	Silica sulphuric acid
h/hr	Hours	t	Triplate
IUPAC	International Union of Pure and Applied Chemistry	TBAB	Tetrabutylammonium bromide
LDHs	Layered double hydroxides	TEOS	Tetraethyl orthosilicate
$LiAlH_4$	Lithium aluminium hydride	TPOS	Tetrapropyl orthosilicate
MCM	Mobil crystalline materials	TMOS	Tetramethyl orthosilicate
MCR	Multi-component reaction	TFA	Trifluoro acetic acid
meso-G	Mesoporous graphene	THF	Tetrahydrofuran
min	Minute	TOF	Turnover frequency
m	Multiplet	TON	Turnover number
mg	Milligram	UV-Vis	Ultraviolet-Visible Spectroscopy
MHz	Mega hertz	XRD	X-ray Diffraction

CHAPTER I

A brief review on solid-phase organic reactions & catalysis by heterogeneous solid supports: Silica, Graphene-based materials and Poly-ionic resins

I.1. General Introduction

The concept of green chemistry and sustainable development towards "meeting the needs of the present generation without compromising the ability of future generations" is now acknowledged universally. "Green Chemistry" is a philosophy towards invention, design, development and application of chemical products or processes to reduce or eliminate the use or generation of substances hazardous to human health as well as environment which was coined by the US Environmental Protection Agency (EPA) during the early 1990s. After that, green chemistry has become a common practice in industry, education and research to achieve sustainability.[1] Our modern society is unimaginable without the industrial products of chemicals and pharmaceuticals.[2] But the ever increasing demands of our overcrowded world for the production of various synthetic chemical products and pharmaceutical needs; waste prevention and environmental protection have become major requirements in the field of synthetic organic chemistry. Therefore, due to growing concern towards protection of environment by human society, the development of eco-friendly methodologies has become a foremost criterion in organic synthesis among which solid-phase synthesis draws upon emphasis.

Solid-phase synthesis is a methodology which relates to the chemical reactions carried out either on the surface of various solid supports (inorganic or organic polymers) or by attaching one of reactant molecules to solid support.[3] Solid-phase organic reactions involve adsorption of reactants molecules on the surface of solid supports which either may be physisorption or chemisorptions followed by desorption.

After the revolutionary work on solid-phase peptide synthesis by R. B. Merrifield,[4] in 1963, the concept of organic synthesis has been drastically changing from conventional liquid-phase to solid-phase synthesis due to diverse advantages like ease of work up, separation and isolation of the product as well as solid supported reagents and catalysts, accessibility to use excess reagents, recyclability of the recovered catalyst, ease of handling and non toxic nature of solid supports.[3]

For a long time, carbon materials such as charcoal, carbon nanotube (CNT), fullerene etc. have been widely used as solid supports for metal catalysts. After the breakthrough synthesis of monolayer graphene by A. Geim and K. Novoselov,[5] graphene and graphene-based materials have taken a major attraction in materials science as well as in catalysis due to their unique physical and chemical properties. Graphene oxide (GO) and its derivatives[5] have now become one of the most accepted graphene-based materials used in various organic

transformations either as a catalyst or a metal support due to their high surface area, abundant active sites such as acidic and basic sites, low-cost preparation and overall their sustainability.[6] As carbocatalysts, these are also well recognized as a convenient alternatives for reducing transition metal dependence on organic reactions.[6a,c] Owing to extensive applications of such carbon materials in multidisciplinary fields of science,it won't be much of a surprise if the future is termed Carbon age.

The present chapter represents a brief review on the catalytic applications of inorganic solid supports such as silica and graphene-based materials comprising graphene oxide (GO) and reduced graphene oxide (rGO) and organic solid supports like poly-ionic resins.

I.2. Catalysis

"Catalysis" is one of the most fundamental and important principle among twelve principles of green chemistry where an external entity called "catalyst" accelerates the rate of a chemical reaction without being consumed or produced in the process. When a major source of waste in the (fine) chemicals industry is derived from the stoichiometric use of various inorganic salts for organic synthesis, the catalysts play an important role by accelerating industrially important reactions under practically attainable conditions. In addition, catalytic process can be designed in such a way that raw materials can be used more efficiently to minimize the waste production. Consequently, the chemical industry is largely based upon catalysis and it is reported that approximately 85–90% of industrial process is driven by catalysis.

Catalysis is mainly divided into two types, homogeneous and heterogeneous. The main difference between two is the phase; when catalysts and reactants are in same phase (mainly liquid), it is called homogeneous catalysis. However, when reactants and catalysts remain in different phases (usually catalysts are in solid state); the catalysis is called heterogeneous.

I.2.1. Homogeneous Catalysis

Homogeneous catalysis occurs on the same phase, most likely in liquid phase where the catalysts are dissolved in the reaction media. A large number of homogeneous catalysts ranging from Bronsted and Lewis acids, metal complexes, metal ions, organometallic complexes, organic molecules up to biocatalysts (enzymes, artificial enzymes etc.) are known to be widely used in various organic syntheses.[7] Aromatic substitution reactions like, nitration, Friedel-Crafts alkylation and acylation using homogeneous Lewis acid catalysts have widely been used in chemical industry.

I.2.2. Heterogeneous Catalysis

Heterogeneous catalysis involves a solid catalyst that is brought into contact with a gas phase or liquid phase reactant medium in which it remains insoluble. In heterogeneous catalysis, the distinct phase of catalysts with respect to the reaction media leads to major advantages like easy separation, re-utilization compared to homogeneous catalysis.[8]

The major advantages of heterogeneous catalysis over homogeneous catalysis are-

- The catalyst recovery is very easy and economical while it is very difficult and expensive in case of homogeneous catalysis.
- Much better thermal stability of catalyst is obtained in heterogeneous catalysis.
- Surface modifications of the catalysts can be achieved easily by approaches like nanotechnology and nanoscience or controlling the pore structure.

The major disadvantage is the poor selectivity with respect to homogeneous catalysts, due to multiple active sites of heterogeneous catalysts such as oxides or supported metal particles. In homogeneous catalysts, every single entity can act as a single active site which makes them more active and selective.

The mechanism of such heterogeneous catalysis can be described by the sequence of elementary reaction steps of the catalytic cycle including adsorption, diffusion, chemical transformation of the adsorbed species and desorption. This is the basis for the kinetics of the catalytic chemical reaction. Necessary first step in a heterogeneous catalytic reaction involves activation of a reactant molecule by adsorption onto catalyst surface. Therefore, various essential physical properties of heterogeneous catalysts like surface area (often very large measured in hundreds of square metres per gram), pore volume, pore size distribution, the size and shape of the particles and their strength are vital requirements for heterogeneous catalysis. The solid catalyst provides a surface, usually internal, for the substrates to adsorb and facilitate the reaction. Thus the surface characteristics like roughness, functional groups, organophilicity, hydrophobicity etc. of the surface are also very vital for performance in the catalytic cycle.

The two most important characteristics of a catalyst are its activity, expressed in terms of turnover number (TON) or turnover frequency (TOF) and selectivity. The turnover number is the number of product molecules produced per molecule of the catalyst. The turnover frequency is the turnover number per unit time. In general, homogeneous and heterogeneous catalysts do not differ by an order of magnitude in their activities when either type of catalyst can catalyze a given reaction.

1.3. Heterogeneous solid supports and their catalytic applications

In heterogeneous catalysis, both inorganic and organic solid supports are used as solid catalysts as well as catalyst supports. Inorganic supports are mainly inorganic metals, metal oxides, sulphides metal complexes and metal salts.[3,8] A plenty of inorganic oxides such as alumina, silica, modified silica, zeolites, sand clays or layered silicates (*e.g.* montmorillonite, saponite) have been employed to promote various organic reactions.[4] They are not only well known for their activity as solid support for metal ions but their own active role towards chemical reactions have profound impact on heterogeneous catalysis also. Carbon materials such as charcoal, graphite, graphene oxide, carbon nanotube (CNT), fullerene *etc.* have also been used as inorganic solid supports as well as heterogeneous catalysts.[9] On the other hand, organic solid supports are generally polymers, ion-exchange resins, cellulose *etc*.[3] As organic supports, organic polymers such as polystyrene (PS) or that partially cross-linked (~1 to 2%) with divinylbenzene (DVB) remain the major choices except the uses of some other dendrimers.[3,1] Since, both adsorption and diffusion take place on the heterogeneous catalysis, the nature of solid surface like surface area as well as pore size distribution is one of the most important factors for determining the overall rate of catalysis. Most of the inorganic solid supports have surface area in the range of 100 to 1000 $>m^2/g$.

Porous materials have been classified according to the pore size by IUPAC nomenclature in three types: *microporous* having a diameter <2 nm, *mesoporous* having a diameter between 2 and 50 nm and *macroporous* with a diameter >50 nm.[11] Silica has been widely employed as main building block of mesoporous materials because it is inexpensive, thermally stable, chemically inert, harmless and abundant.[12] Due to such diverse nature, mesoporous silica,[13] have taken a major place in catalysis in comparison to other mesoporous materials like alumina,[14] carbon,[15] and transition metal oxides.[16] MCM-41, MCM-48, MCM-50 and SBA-15 are examples of ordered mesoporus silica widely used in heterogeneous catalysis. All these mesoporous silica materials are highly ordered, featuring large specific surface area, hexagonal array and uniform mesoporous channel.[17,18]

1.3.1. Amorphous silica

Silica is the major component of the earth's crust, made of two most abundant elements silicon and oxygen. Silica appears commonly in two forms; crystalline and amorphous. The most commonly used silica in catalysis is amorphous silica. The building blocks of silica are linked by SiO_4 tetrahedra, with each O atom bridging two Si atoms. Silica gel is a porous,

granular form of silica, synthetically manufactured from sodium silicate or silicon tetrachloride or substituted chlorosilane/orthosilicate solution. Silica gel is usually synthesized by the condensation polymerization of silicic acid [$Si(OH)_4$], joined by siloxane bridges (Si–O–Si) in its interior and it is amorphous in character with high porosity and mechanical strength. The commercial type silica have a specific surface area (300 to 800 m^2/g) with pore diameter of 20 to 150 Å containing impurities such as sodium, calcium, aluminium, Fe (III), and Ti (IV) in the order of 0.01–005%.[19]

- **Surface chemistry of silica**

Silica surface contains various active groups such as siloxane, several forms of silanol and absorbed water which was confirmed by several studies like FT–IR spectroscopy, atomic force microscopy (AFM), chemical analysis *etc*. Silanol groups are formed on the surface of silica in two ways; firstly, during the synthesis of silica by the condensation ploymerization of $Si(OH)_4$ and secondly, upon rehydroxylation of dehydrated silica with water or aqeous solution as shown in Figure I.1. In the polymerization of silicic acid, the polymeric form of silicic acid changes into spherical colloidal particles containing Si–OH groups on the surface. Subsequently, upon dehydrating this type of hydrogel is converted to the final product xerogel which retains some or all of silanol groups on its surface.

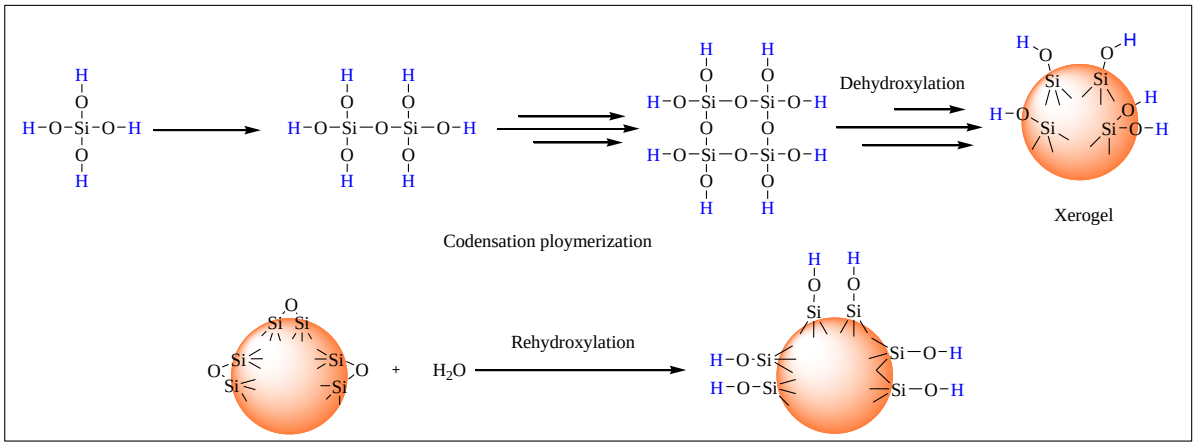

Figure I.1. The formation of silanol groups on the silica surface: (a) Condensation polymerization; (b) Rehydroxylation.

Hence, the presence of such silanol groups on the surface influences the excellent adsorbent property of silica. The presence of excess silanol groups make silica hydrophilic in nature, however after drying it becomes hydrophobic. Three types of silanol groups are present on the surface of silica; isolated (free silanols)≡SiOH, geminal (silane diols), $–Si(OH)_2$ and vicinal or bridged where –OH groups are bound through hydrogen bond. In

addition, siloxane groups or (≡Si–O–Si≡) bridges are also present on the surface as well as internal silanol groups do exist inside the silica (Figure I.2).

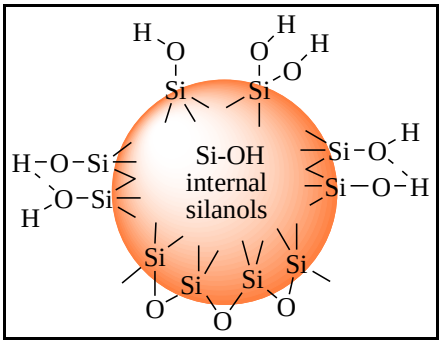

Figure I.2. Various types of silanol groups and siloxane bridges present on the surface of amorphous silica along with internal silanol groups.

Zuravlev's physico-chemical model for amorphous silica surface can give a very clear idea about the concentration and the distribution of different types of silanol and siloxane groups and make easier to characterize the energetic heterogeneity of the silica surface as a function of pre-treatment of temperature on SiO_2 samples.[20] The whole process involves dehydration (the removal of physically adsorbed water), dehydroxylation (the removal of silanol groups from the silica surface) and rehydroxylation (the resotoration of hydroxyl covering). This model represents the surface chemistry of amorphous silica and also makes it possible to determine the kind of chemisorptions of water (rapid, weakly activated or slow, strongly activated) under the restoration of the hydroxyl coverage and also to consider the –OH groups present inside the skeleton of silica and is found to be very useful in the field of adsorption, catalysis, chromatography, chemical modification, *etc*.

- **Modification of silica surface**

Chemical modification of the surface of silica has garnered huge interest to material chemists since this process allows researchers to regulate and change the adsorption properties and to alter the chemical properties of silica gel as well. This modification can be done either by 'physical treatment' (thermal or hydrothermal) that leads to change in ratio of silanol and siloxane concentration of the silica surface or by 'chemical treatment' that leads to change in chemical characteristics of silica surface. The most convenient way to develop a chemically modified surface is simple immobilization (or fixing) of the group on the surface by adsorption or electrostatic interaction or H–bond formation or other type of interaction.[21]

Silica gel surface can be modified by two distinct processes: organofunctionalization, where the modifying agent is an organic group and inorganofunctionalization, in which the group anchored on the surface can be an organometallic composite or a metallic oxide.

- **Application of amorphous silica in diverse organic reactions**

Silica gel which is non-toxic, non-flammable and stable, generally used as an effective adsorbent in chromatography for the separation of organic compounds. Owing to its very high surface area (~ 500m^2/g), high porosity and high mechanical strength also act as an effective catalyst support.[22] Again; silica gel can also act as a mild acid catalyst, an accelerator, or a reaction media along with its easy separation from the products after the reaction.[23] Chemical reactions catalyzed or promoted by silica gel are not only simple in work-up and isolation procedure than corresponding homogeneous reactions but also proceed under mild conditions with high chemo-, regio-, and stereoselectivity.

Accordingly, silica gel has taken an important part in solid-phase organic synthesis and a plenty of diverse organic transformation are promoted by unsupported silica gel exploiting its mild acidic behaviour as well as well as its high adsorption efficiency (Scheme I.1).[22]

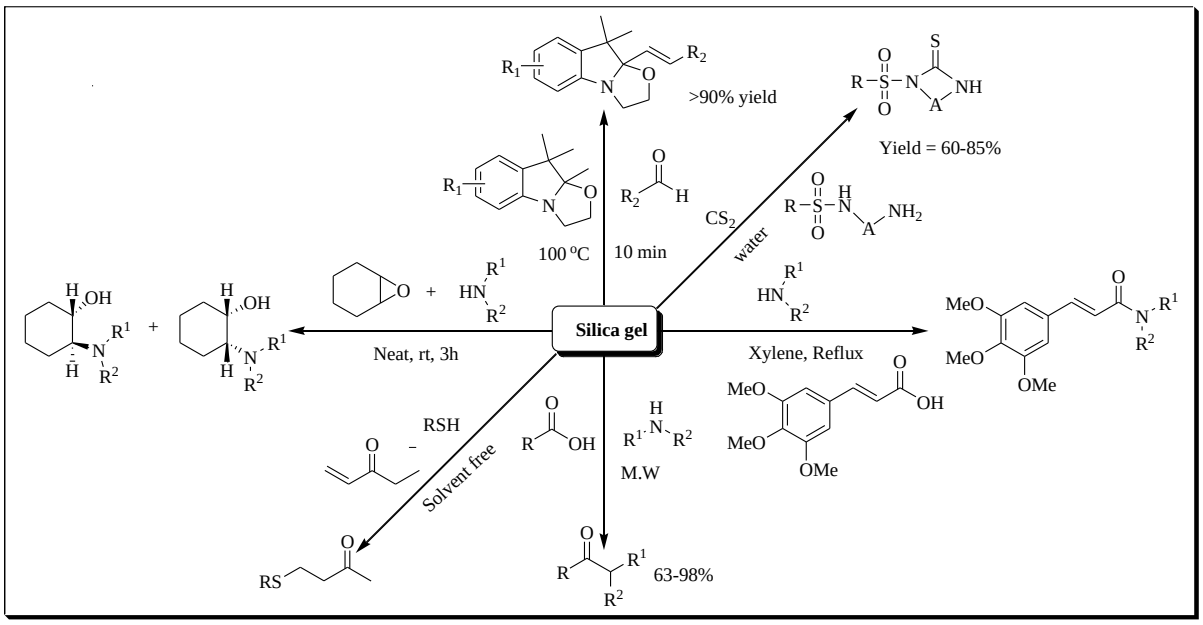

Scheme I.1. Silica gel promoted various organic transformations.

The Bronsted or Lewis acidic nature of silica gel has been also utilized for the synthesis of 2-bromobenzoates (Scheme I.1) *via* Diels-Alder reaction of furans with methy-3-bromopropiolate followed by a ring-opening aromatization in one pot.[23]

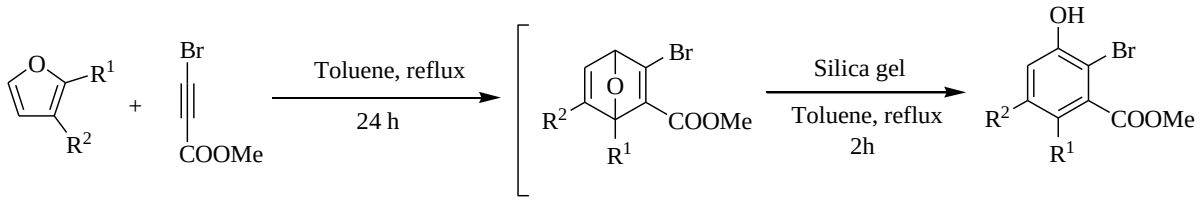

R^1 = *n* -C_5H_{11}, -OMe, 4-MeO-C_6H_4 , Ph, Mesityl, Me
R^2 = H, Me

Scheme I.2. Synthesis of 2-bromobenzoate in the one-pot method catalyzed by silica gel.

I.3.2. Ordered mesoporous silica

MCM-41

In 1992, a new family of highly ordered mesoporous silica was synthesized by Mobil Corporation Laboratories,[24] and designated as M41S (Mobil Crystalline of Materials) depending on their pore size. The synthesis of such mesoporous materials is based on the combination of two major sciences, sol-gel science and surfactant (templating) science. Three different mesoporous silica materials, MCM-41, MCM-48 and MCM-50 are the most well-known mesoporous silica in M41S family.[25] They have different techniques of synthesis and applications, which are based on instability and limitation of mesoporous structure.[26,27] Structurally, MCM-41 is hexagonal packed rod-shaped micelle whereas MCM-48 is cubic and MCM-50 is lamellar in shape.[25] MCM-41 has attracted the major attention of scientists compared to other two mesoporus silica materials due to its elevated specific surface area, hydrophobic and acidic nature, possibility of controlling its pore size, high thermal as well as hydrothermal stability. The diameter of hexagonal channels of MCM-41 varies from 15 to100 Å. Due to such exceptional characteristics, MCM-41 plays a dual role, both as a catalyst or a catalyst support,[27] and is found to be very useful in industrial processes such as adsorption,[28] ion- exchange,[29] and environmental control.[30]

SBA-15

In 1998, Stucky and his co-workers have discovered an another type of mesoporous silica, Santa Barbara Amorphous no. 15 (SBA-15) to overcome the weak hydrothermal stability encountered by M41S materials. SBA-15 is made of thermally stable thick walls and hexagonal mesopores (4-10nm).[31] The main difference between the M41S family and SBA-15 is that former is synthesized under basic conditions,[32] while SBA-15 is obtained in acidic media.[33] The synthesis of SBA-15 requires the use of triblock copolymer (typically non-ionic triblock copolymer) as a structure directing agent and various orthosilicates like tetramethyl

orthosilicate (TMOS), tetraethyl orthosilicate (TEOS) and tetrapropyl orthosilicate (TPOS) as one of the silica sources.[33a,34-37] Zhao *et al.* have synthesized the first synthetic mesoporous silica materials of SBA-type by using various non-ionic triblock polymers as templating agent.[33a,35,36] SBA-15 and SBA-16 were synthesized by using triblock copolymer surfactants Pluronic P123 (PEO20PPO70PEO20),[33a] and Pluronic F127 (PEO106PPO70PEO106),[33b] respectively in acidic media. Owing to large surface area, well-defined pore structure, inert framework, non-toxicity, high biocompatibility,[38] thermal and hydrothermal stability,[35] SBA-15 has attracted intense interests of material scientists. This type of mesoporus silica materials are found to be extensively used in catalysis,[39,40] adsorption,[41-43] chemical sensing,[44] immobilization,[45] drug delivery systems[46,47] and separation by chromatographic techniques such as high performance liquid chromatography (HPLC).[48–50]

I.3.3. Carbon materials

For the sake of sustainability as well as to reduce the metal dependency in catalysis, carbon materials have become more convenient alternatives due to their renewable resources and economic consideration. From ancient times, carbon materials with large surface area such as activated carbons, charcoal, carbon blacks, carbon powders have been considered as solid supports to deposit transition metals for their catalytic use. “Carbcatalysis” is based on the metal-free catalysis where catalysts are predominantly made of carbons. After the successful application of graphene-based materials as carbocatalysts in various organic transformations by Bielawski *et al.*,[51] the way of thinking to conventional metal-based catalysis has been drastically changed towards metal-free “carbocatalysis”. In recent years, graphene-based materials like graphene oxide (GO) and reduced graphene oxide (rGO) have been explored as excellent carbocatalysts almost in every field of science because of their sustainabilty and low-cost preparation.

1.3.3.1. Graphene-based materials and their catalytic applications in diverse organic reactions

Graphene

Graphite is the most common allotropic form of carbon. It is made of sp^2 hybridised carbon layers, which are stacked together by weak Vander Waals forces. The flat single layer of carbon atoms of graphite is known as graphene. It is the most “thinnest” material having 2D honeycomb-like crystalline lattice structure. The name ‘graphene’ was first given by Boehm, Setton and Stumpp in 1994.[52]

Graphene is also known as the basic building unit of all other carbon allotropes such as zero-dimensional (0D) fullerene, one-dimensional (1D) carbon nanotubes, or three-dimensional (3D) graphite (Figure I.3).[53]

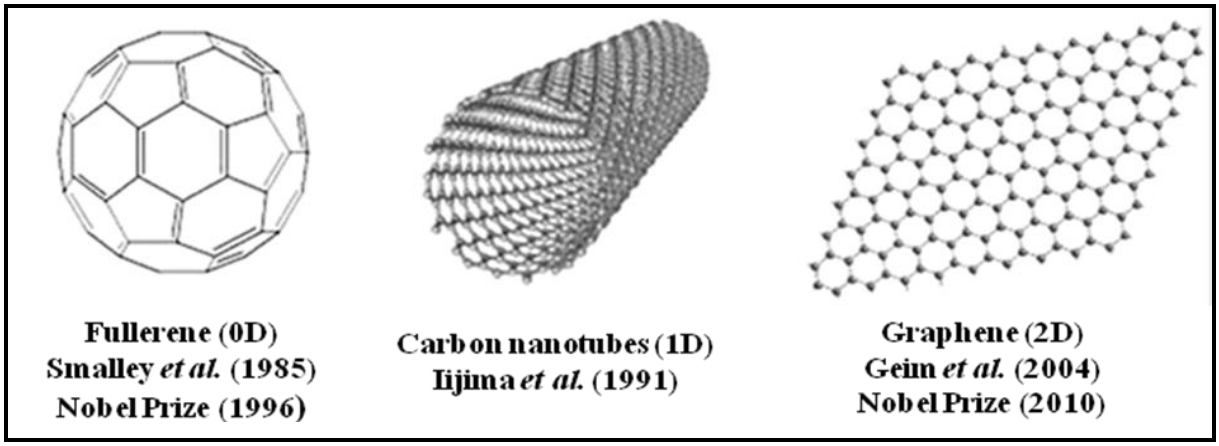

Figure I.3. Graphene, (2D) building material wrapped up into (0D) buckyballs, rolled into (1D) nanotubes or stacked into (3D) graphite.

Due to extraordinary electronic, thermal, optical, chemical and mechanical properties graphene has great potential for the use in energy-storage materials, nano-electronics, calatysis, biomedical and other fields.[54] The exciting properties of graphene are high electron charge mobility (230,000 cm^2/Vs),[53] high thermal conductivity (3000 W/mK),[55] high strength (130 GPa),[56] and high theoretical specific surface area (2600 m^2/g).[57] Moreover, graphene exhibits a half-integer quantum hall effect (QHE) even at ambient temperature (minimum hall conductivity 4 e^2/h, even at zero carrier concentration).[53]

- **Preparation methods**

It was impossible to think about the thermodynamic stability of two-dimensional crystals before the successful synthesis of monolayer graphene. In 2004, Geim and Novoselov first reported that monolyer graphene can be isolated by means of peeling the graphite through micromechanical cleavage (scotch tape method) on silicon oxide.[53a] As a result in 2010, they have awarded with the Nobel Prize in physics for their groundbreaking experiment regarding the two-dimensional material graphene. After that numerous number of methods have been developed to produce graphene, which are divided into different categories depending on the chemical or physical routes. The highest quality graphene is obtained by physical methods such as mechanical exfoliation of graphite,[58] chemical vapour deposition (CVD) on metal surface,[59] and arc discharge,[60] but the main drawback of all these methods is the low scale production of graphene. The most general procedure for the

preparation of graphene in large scale is the chemical oxidation of graphite to graphite oxide and subsequent reduction by chemical or thermal process (Scheme I.3).[61]

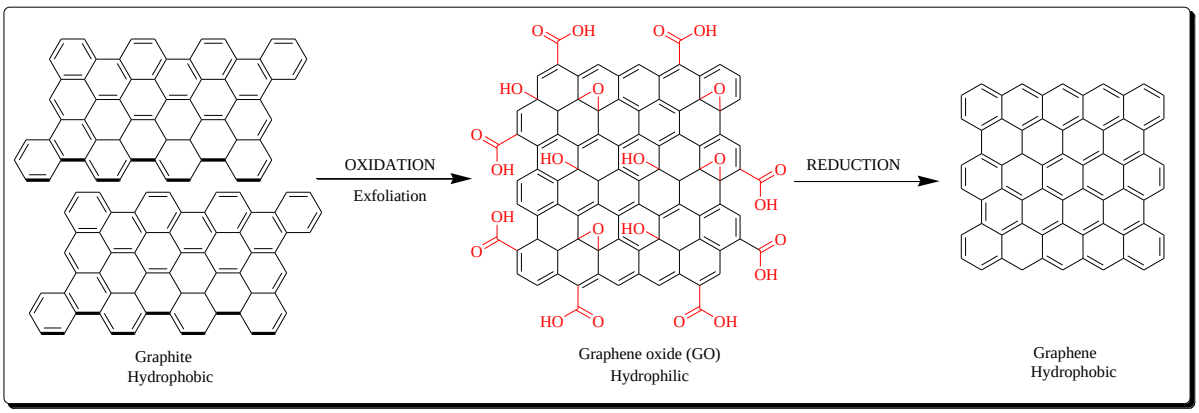

Scheme I.3. A schematic presentation for the preparation of suspended graphene sheets through consecutive graphite oxidation, exfoliation to GO and its eventual reduction to graphene.

The reduction of graphite oxide using chemical reagents has been considered as an effective route to synthesize graphene sheets due to its simplicity, reliability, ability for large-scale production and economic consideration.[62] A vast number of reagents like hydrazine hydrate, dimethylhydrazine, hydroquinone, aluminum powder, sodium borohydride, sulfur containing compounds, hexamethylenetetramine, polyelectrolyte, ethylenediamine (EDA), sodium citrate, carbon monoxide *etc.* have been employed for the reduction of GO.[63]

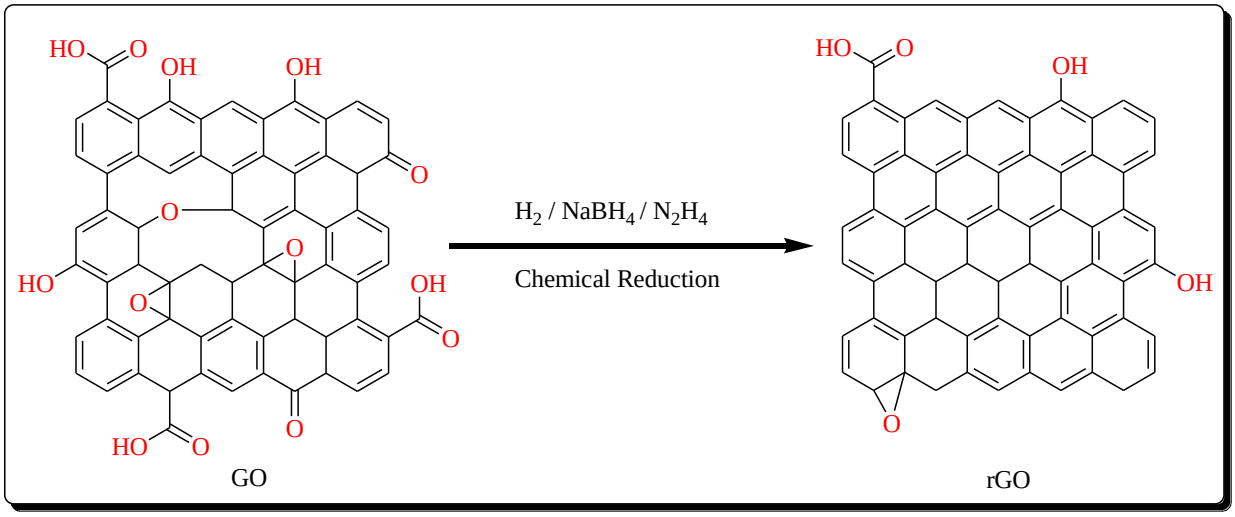

Scheme I.4. Chemical reduction of GO to rGO by means H_2, $NaBH_4$ or N_2H_4.

In recent years, various bio-sources like biomolecules, proteins, amino acids, plant extracts, microbes *etc.* are employing as green reducing sources for the reduction of GO to avoid the hazardous nature of chemical reagents.[64] Chemically converted graphene (CCG) or

reduced graphene oxide (rGO) has been found to contain some residual oxygen groups and some defects on the surface.

- **Catalytic applications**

Due to the high surface area and presence of different active sites on graphene and graphene-based materials such as GO, rGO have been widely used both as catalysts or catalyst supports in various organic transformations.

Mesoporous graphene (meso-G) which was obtained by chemical vapour deposition (CVD) of methane using MgO as a template has been used as an efficient catalyst for the selective oxidation of cyclohexane to cyclohexanol and cyclohexanone (Scheme I.5) *via* radical pathway where cylohexyl hydro peroxide (CyOOH) is used as an initiator.[65]

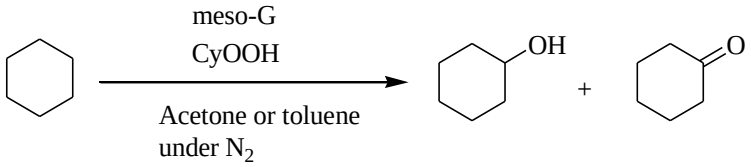

Scheme I.5. Graphene–catalyzed oxidation of cyclohexane.

Doping heteroatom's on the surface of graphene can effectively modulate the electrical properties and surface physico-chemical features of graphene and facilitate their catalytic activity towards the aerobic oxidation of hydrocarbons. *N*-doped graphene nanosheets (N)-rGO-T (T = 800 to 1000^{o}C) prepared by the high temperature nitridation with NH_3 gas can catalyze the oxidation of benzyl alcohol (Scheme I.6).[66]

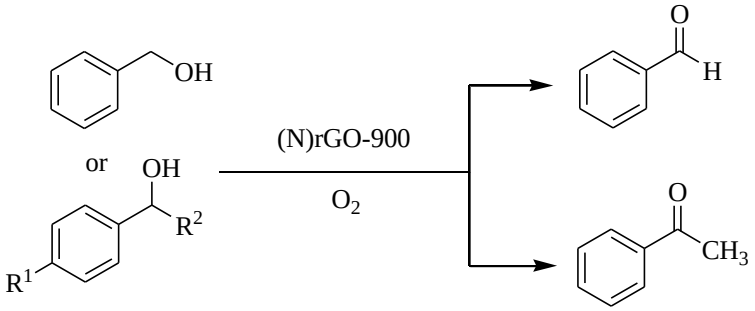

R^1 = H, -NO_2, -OMe, F
R^2 = H, CH_3

Scheme I.6. *N*-Doped graphene–catalyzed oxidation of alcohols.

The chemically converted graphene (CCG) prepared by the reduction of GO using hydrazine hydrate has been found to be used as an efficient catalyst for the direct, one-step hydroxylation of benzene to phenol (Scheme I.7) using H_2O_2 as oxidant.[67]

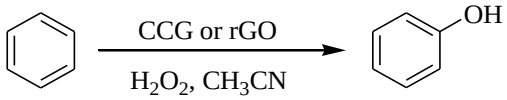

Scheme I.7. CCG–catalyzed oxidation of benzene to phenol.

Graphene supported KOH composite has been reported as an efficient and reusable catalyst for the synthesis of 9-fluorenone derivatives in high yield by aerobic oxidation of *9H*-fluorenes at room temperature in DMF (Scheme I.8).[68]

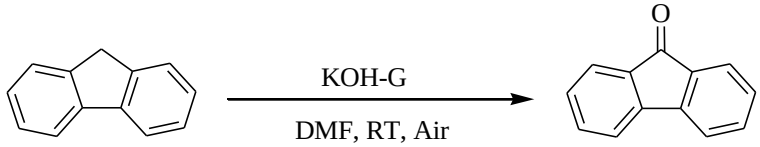

Scheme I.8. KOH–G catalyzed aerobic oxidation of *9H*-fluorene to 9-fluorenone.

Bai *et al.*[69] have reported that the rGO obtained by using hydrazine hydrate can act as an efficient and reusable carbocatalyst for the aerobic oxidative dehydrogenation of various hydrazo compounds to their corresponding azo compounds (Scheme I.9). According to them, electrons present in the holes and the edges are the main sources to activate O_2 to $O_2^{\cdot}$ radical resulting in the oxidation of hydrazo compounds to azo compounds.

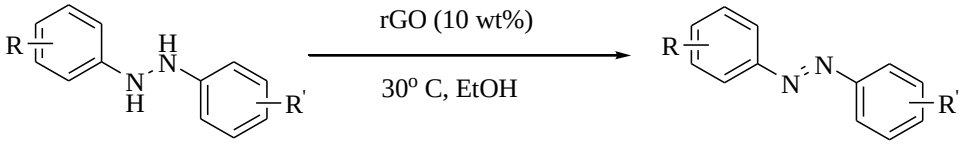

R=R'= H, p-OMe, *o*-Cl, *p*-Cl etc.

Scheme I.9. Reduced graphene oxide(rGO)–catalyzed dehydrogenation of various hydrazo compounds.

Sulfonated reduced graphene oxide (rGO-SO_3H) has been found to be used as solid acid catalyst to synthesize furfural from biomass (Scheme I.10).[70]

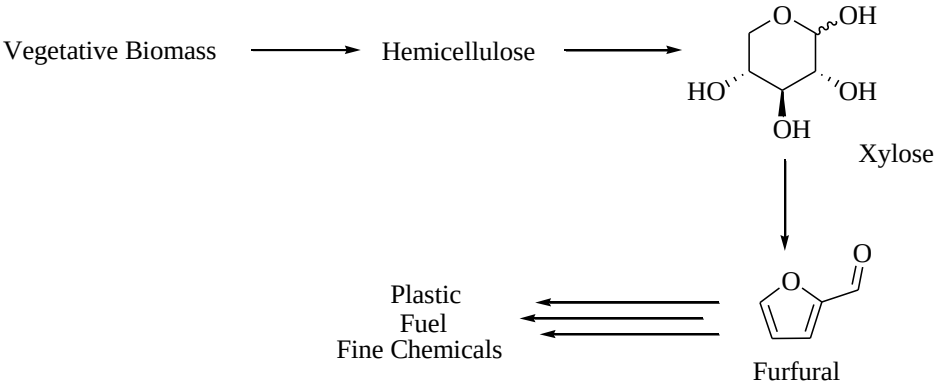

Scheme I.10. Conversion of hemicellulosic materials to xylose and then furfural.

The rGO is also found to be used as catalyst for the preparation of bis(aminothiocarbonyl)disulfides from various secondary amines and CS_2 under mild conditions (Scheme I.11).[71]

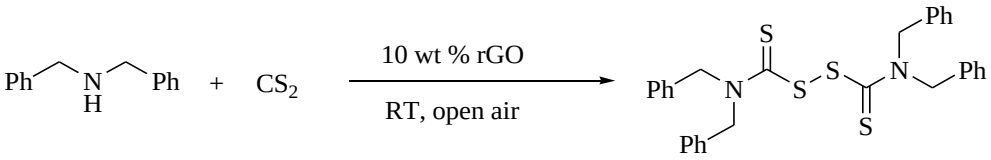

Scheme I.11. Reduced graphene oxide (rGO)–catalyzed disulfiram formation from dibenzylamine and CS_2.

The rGO grafted with polystyrene sulfonic acid (rGO-PSSA) has also been used as solid acid catalyst for the synthesis of isoamyl benzoate (Scheme I.12).[72]

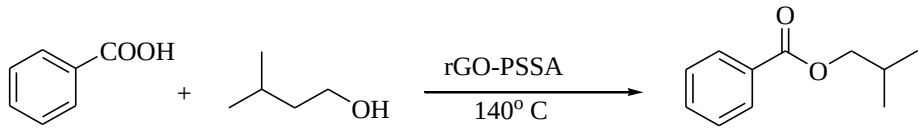

Scheme I.12. Preparation of isoamyl benzoate using rGO-PSSA.

Tan *et al.*[73] reported that both GO and rGO can be used as carbocatalysts for the electrochemical polymerization of 3-amino-phenylboronic acid (ABA) (Scheme I.13).

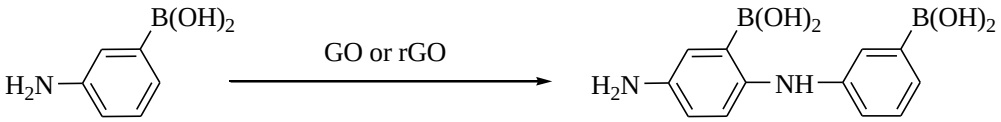

Scheme I.13. Polymerization of 3-amino-phenylbpronic acid catalyzed by GO or rGO.

It is also reported the zigzag edges and defects present on the surface of rGO are responsible for its catalytic acitivity towards reduction of nitrobenzene (Scheme I.14).[74]

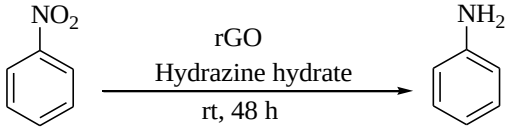

Scheme I.14. Reduction of nitrobenzene catalyzed by rGO.

Graphene oxide

Graphene oxide (GO) is one of the most imortant graphene-based materials and also known as the primary precursor of graphene. For the preparation of GO, there are five methods which were reported by Brodie,[74] Staudenmaier,[76] Hoffman,[77] Hummers,[78]and Tour.[89] From the comparison between these five methods as in Table I.1, it is found that the first method given by Brodie has been actually modified with time by others.[80]

Table I.1. Comparison of various synthetic methods for the preparation of GO

Method	Reagents for Oxidation	Carbon-to-oxygen ratio[a]	Raman spectral I_D/I_G ratio[a]	Charge-transfer resistance (R_{ct})[a]($k\Omega$)	Notes
Brodie	$KClO_3$,Fuming HNO_3 and Conc. H_2SO_4	–	–	–	Addition of $KClO_3$ was stepwise rather than at once
Staudenmaier	$KClO_3$, Fuming HNO_3	1.17	0.89	1.74	–
Hoffman	$KClO_3$, Non-fuming HNO_3	1.15	0.87	1.68	–
Hummers'	$KMnO_4$, $NaNO_3$ and Conc. H_2SO_4	0.84	0.87	1.98	The method can be modified by eliminating the use of $NaNO_3$[a]
Tour	$KMnO_4$,Conc. H_2SO_4 and Conc. H_3PO4	0.74	0.85	2.15	–

[a] Data's are taken from reference no. 82.

Among the five methods, Hummers' method is the most widely used method which is modified through several modification to reach the higher extent of oxidation.[80] The latest modified Hummers' method was reported by Tour *et al.*[79] After the oxidation of graphite, graphene layers become highly decorated with various oxygenated functional groups like hydroxyl (–OH), carboxylic (–COOH), epoxy (C–O–C) or ether and carbonyl (–C=O) *etc.* Due to the presence of such functional groups GO shows very high acidic nature (pH = 4.5 for 0.1mg/ml).[81] The characterization and analysis of chemical functionalization of GO surface can be performed by UV-Vis, Raman, FT–IR-spectroscopy, X–ray photoelectron spectroscopy (XPS), thermo gravimetric analysis (TGA), powder XRD and the morphological behaviour of the surface can be performed by TEM and SEM studies.[82] The number of oxygenated functional groups present on the surface of GO depends on degree of oxidation concluding, higher the oxidation higher will be the percentage of O than C in GO.

- **Structure of graphene oxide**

The chemical structure of GO contains a variety of oxygenated functional groups depending on the degree of oxidation. According to the presence of such functional groups several structural models (Figure I.4) for GO were prescribed by Dekany,[83] Scholz-Bohem,[84] Hoffman,[85] Nakajima-Matsuo,[86] Ruess,[87] Lerf and Klinowski.[88] The most accepted model was

given by Lerf and Klinowski,[88] which contains hydroxyl and epoxide groups on the basal planes and carboxylic groups edges of GO.

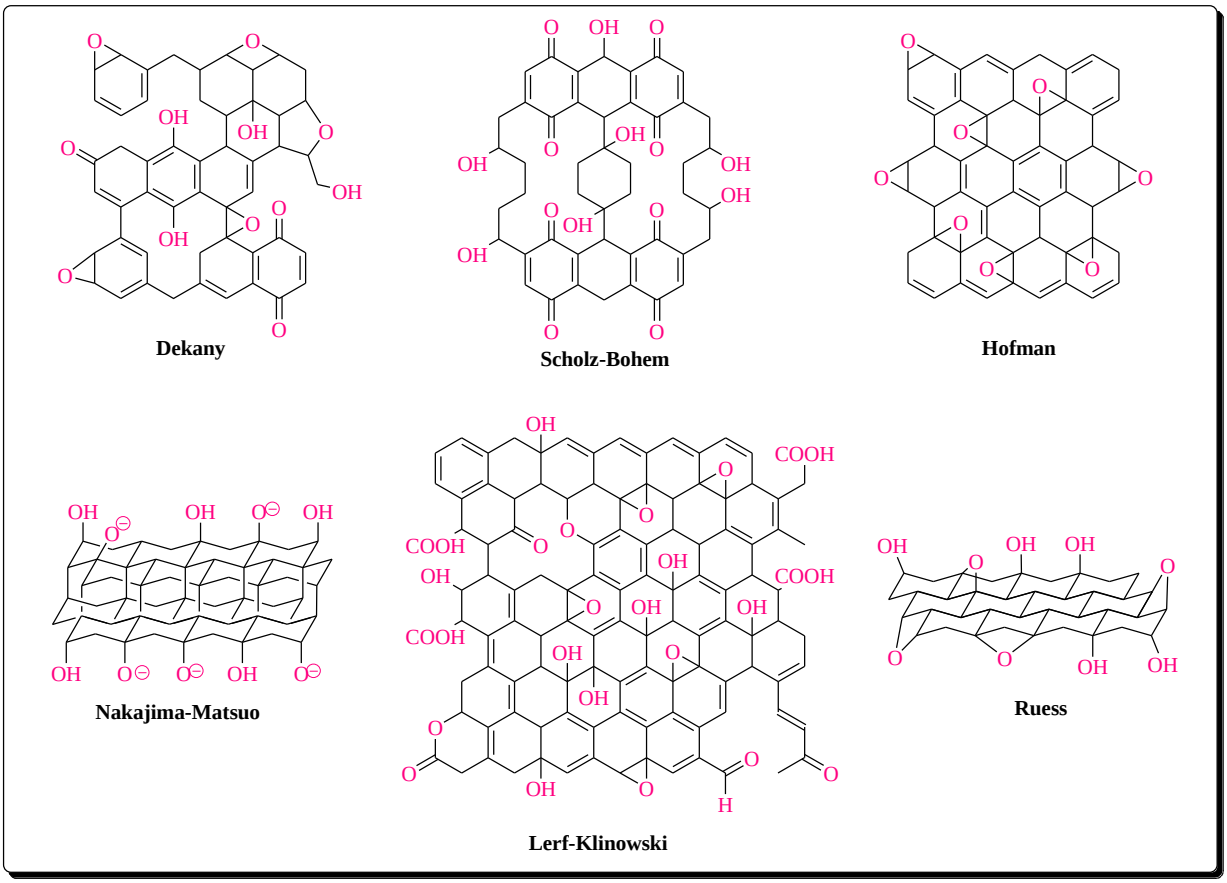

Figure I.4. Various structural models of graphene oxide.

- **Catalytic applications**

Graphene oxide has been found to be act as an efficient oxidant for a broad range of organic reactions, including the oxidation of olefins to their respective diones, methyl benzenes to their respective aldehydes, diarylmethanes to their respective ketones and various dehydrogenations (Scheme I.15).[89]

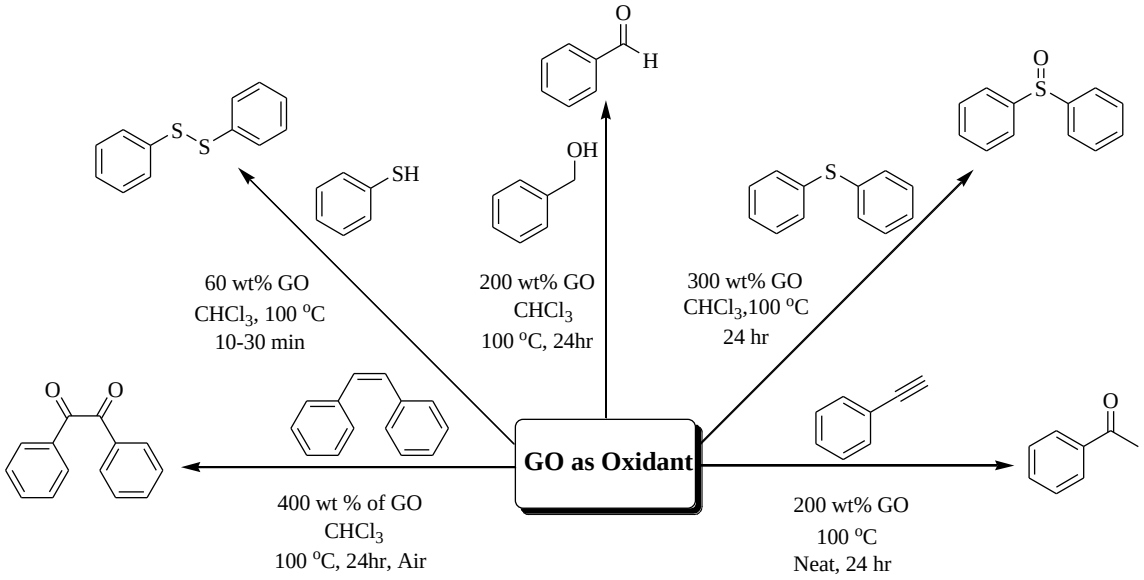

Scheme I.15. GO as an efficient oxidant for various organic transformations.

Additionaly, the high acidic nature of GO (pH 4.5 at 0.1 mg mL^{-1}),[83] make it as an effective solid acid catalyst to facilitate the Friedel-Craft addition of α,β-unsaturated ketones to indoles,[90] the conversion of polysaccharides (*e.g.*, fructose, sucrose and inulin) to 5-ethoxymethylfurfural,[91] and various dehydrative or cationic addition polymerizations (Scheme I.16).[92]

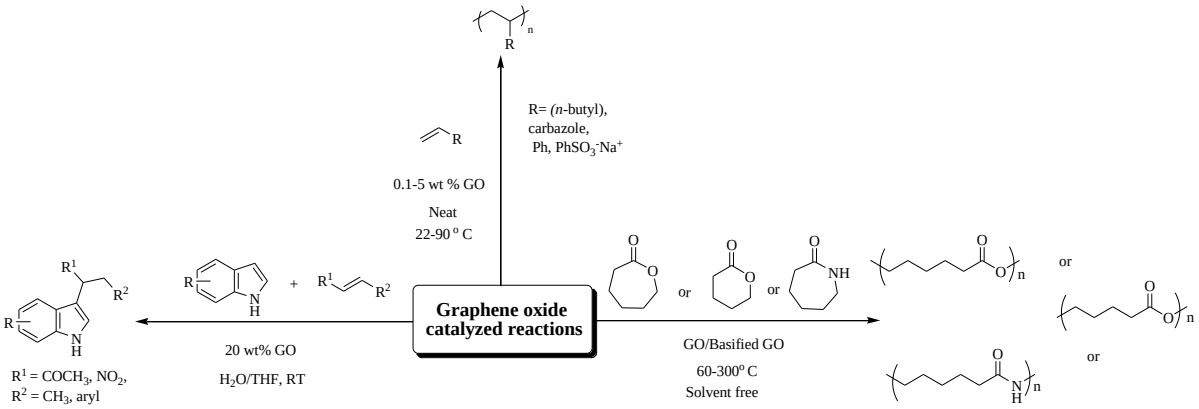

Scheme I.16. GO–catalyzed various organic transformations.

I.4. Organic polymers

After the pioneering work on solid-phase peptide synthesis (SPPS) by Merrifield, considerable research have been done on the use of polymers as solid supports, reagents and catalysts in worldwide laboratories.[93] The polymeric supports are mainly cross-linked polystyrene resin which are divided into two types according to their degree of cross-linking: gel-type microporus resin and macroporous resin. The gel-type microporous resins are lightly cross-linked (1-2%) polystyrene resin and the most commonly used resins for solid-phase

organic synthesis. On the other hand, macroporous resins are highly cross-linked (>5%) porous polystyrene which allow reagent diffusion through pore network within the beads, rather than through the spaces between beads in a swollen polymer gel.

I.4.1. Microporous gel-type resins

In solid-phase synthesis three types of commercially available microporous gel-type resins are mostly used: polystyrene resin (PS), poly (ethylene glycol)-polystyrene resins (PEG−PS), hydrophilic PEG-based resins.

I.4.1.1. Polystyrene (PS) resins

Polystyrene resins are the most widely used organic polymers employed as solid supports for the synthesis of peptides and small molecules. Polystyrene resins are obtained by the suspension polymerization of styrene and divinybenzene (DVB).[94] The first synthetic PS was prepared by Merrifield (Scheme I.17). Various physical characteristics, such as solvent swelling, chemical stability of PS depends on the degree of cross-linking and hence on the proportion of DVB. Generally, microporous PS resins containing 1-2% DVB cross-linking, have greater swelling capacity than the higher cross-linked macroreticular resins (> 5% DVB). The improvement of properties of such polystyrene resins for their use in organic synthesis can be possible by several strategies as following:

- Using heterogeneous cross-linked polystyrene in different polymers or preparing the polymer in such a way that the functional groups are concentrated toward the surface of the resins.
- Using cross-linker other than divinylbenzene to heterogenize polystyrene in order to modulate the physical and chemical properties of resins.
- Adding functional groups to polystyrene backbone that provide desired properties.
- Grafting polystyrene onto a heterogeneous support and the use of graft as point of substrate/reagent/catalyst attachment in order to reduce the importance of resins swelling.

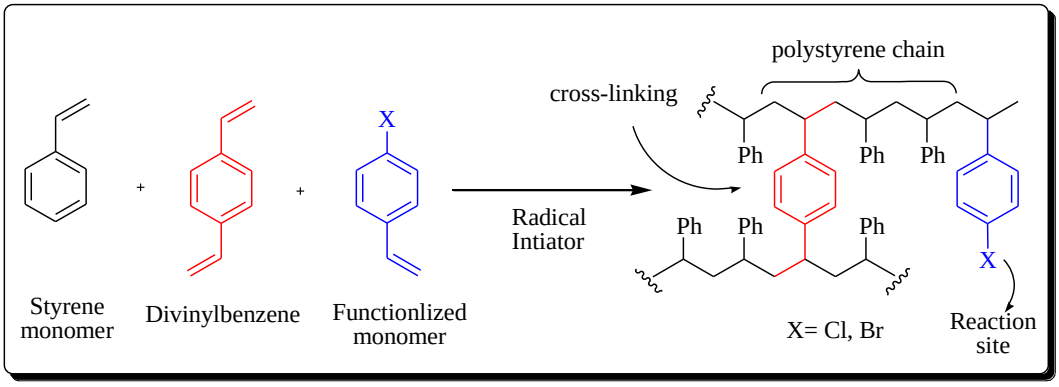

Scheme I.17. The formation of Merrifield's polystyrene resin.

I.4.1.2. Poly (ethylene glycol)-polystyrene resins (PEG–PS)

PEG-grafted polystyrene is an another class of microporous polystyrene resin uesd in soild-phase organic synthesis (SPOS). Such PS can be synthesized either by the reaction of preformed oligooxyethylenes with aminomethylated polystyrene beads (PEG–PS) or by graft polymerization on polystyrene beads. The first PEG–PS resin was developed with the idea of combining a hydrophobic PS core with hydrophilic PEG chains on the same support. In addition, the PEG unit might act as a spacer, separating the starting point of the solid-phase synthesis from the PS core in some of the aforementioned PEG-PS resins.[132] Due to unique conformational flexibility of PEG chains, PEG–PS resins are compatible with both polar and nonpolar solvents.[95] The high degree of swelling provides the beads with a firmer and flow-stable character and makes these resins physically stable in flow systems. The content of PEG varies significantly between distinct resins and therefore their swelling properties can differ markedly. But the drawback of using such resins is in the treatment with trifluoro acetic acid (TFA) which causes several lose of PEG. TentaGel, ArgoGel and NovaGel are the most widely used PEG-grafted polymers.

I.4.1.3. Hydrophilic PEG-based resins

In 1980, another type of PEG-based resins was introduced having polyacrylamide resin as their roots and used in solid-phase peptide synthesis using fluorenylmethoxycarbonyl (Fmoc)-tert-butyl(tBu) strategy.[96] They were developed following the concept that the insoluble support and peptide backbone should have comparable polarities. Polyacrylamides cross-linked with PEG (PEGA),[97] PEG cross-linked ethoxylate acrylate resin (CLEAR), [98] and cross-linked PEG (ChemMatrix),[99] are the most widely used hydrophilic PEG-based resins in SPOS. PEGA resin is obtained by inverse suspension radical polymerization of

various sizes of linear *bis*- and branched *tris*-2-aminopropyl-PEG samples with acryloyl chloride. The uniform beads swelled in all solvents, ranging from toluene to aqueous buffers.

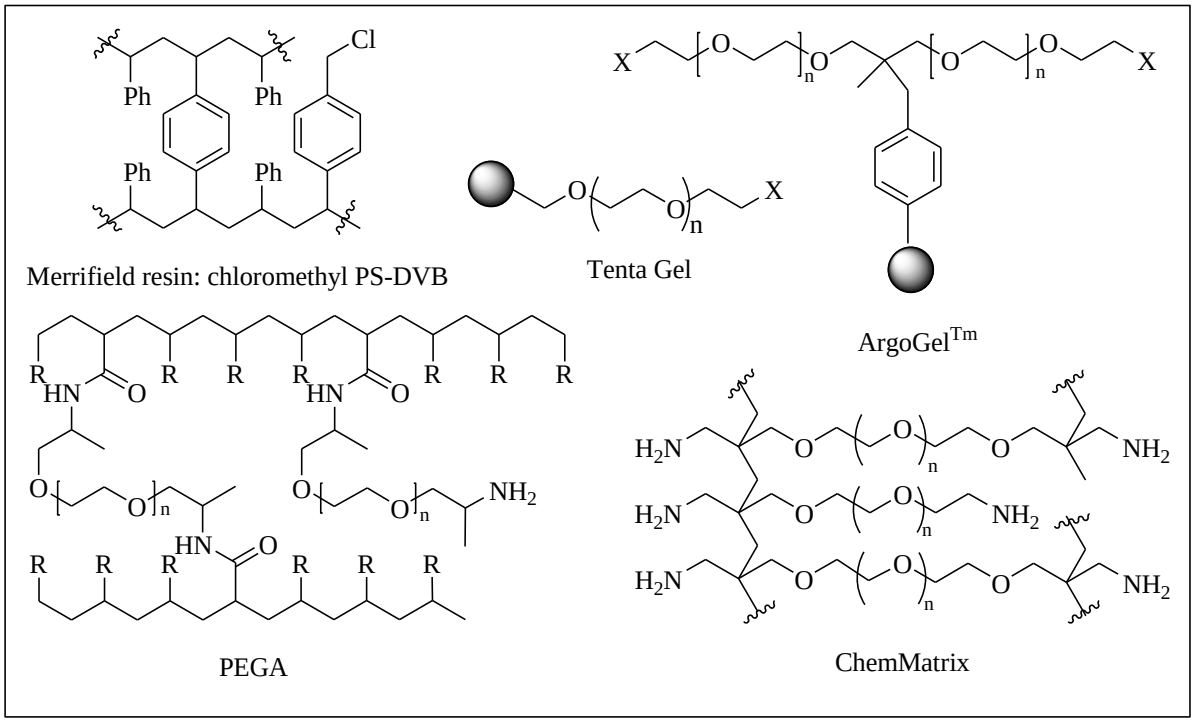

Figure.I.5. Structures of some common polymeric resins.

The ChemMatrix resin, developed by Côté,[99] consists of primary ether bonds. Because of its highly cross-linked matrix, ChemMatrix has greater mechanical stability than other PEG resins. Due to high swelling behaviour of such resins in almost every common solvents, they have broad utility on solid-phase organic synthesis. ChemMatrix resin performs extremely well compared to PS resins for the solid-phase synthesis of hydrophobic, highly structured, poly-arg peptide, ®- amyloid, (1-42) RANTES-a complex aggregated chemokine and HIV protease.[99-102] The CLEAR family, developed by Kempe and Barany,[98] based on the co-polymerization of branched PEG-containing cross-linkers such as trimethylolpropane ethoxylate triacrylate and contains various ethylene oxide units with amino-functionalized monomers such as allylamine or 2-aminoethylmethacrylate.

I.4.2. Macroporous resins

Macroporous resins are highly cross-linked (>8% DVB cross-linker) organic polymers having permanent porous structure and functionalization on the surface of a bead.[103] Because of the rigid open pore structure, these resins facilitate the fast diffusion of reagents to reaction sites. In addition, the choice of solvent is less critical for functionality of the support due to

non-swelling behaviour of such resins. Similarly, fast removal of excess reagents, solvents and by-products from resin in washing steps make them efficient support for the large scle automated SPOS.[104] They have been applied especially as ion-exchange resins,[105-106] and other applications include solid-phase extraction, scavenger resins, and heterogeneous catalysis.[107]

I.4.2.1. Ion-exchange resins

Ion exchange resins are usually insoluble polymeric materials manufactured by a suspension polymerisation using styrene and divinylbenzene (DVB) that carry ion exchangeable functional groups. The ion-exchange resins are mainly prepared as spherical (beads) either as conventional resin with a polydispersed particle size distribution from ~0.3 mm to ~1.2 mm (50–16 mesh) or as uniform particle sized (UPS) resin with all beads in a narrow particle size range. The first synthetic ion-exchange resins were prepared by the condensation of phenol and formaldehyde.[108] The basic requirements of ion-exchange resin beads are insolubility, bead size and resistance to fracture. The relative strength and also the porosity of bead depends on the amount of used cross-linking DVB polymer. Porosity and particle size can be controlled by the conditions of polymerization and uniform particle size manufacturing technology.

- **Types of ion-exchange resins**

Ion-exchange resins are divided into four types based on the charge on the exchangeable counterion (cation exchanger or anion exchanger) and the ionic strength of the bound ion (strong exchanger or weak exchanger).

These ion-exchange resins are:

i. Strong cation exchange resins, containing sulfonic acid ($–SO_3H$) groups or the corresponding salts.

ii. Weak cation exchange resins, containing carboxylic acid (–COOH) groups or the corresponding salts.

iii. Strong anion exchange resins, containing quarternary ammonium groups. Strong base anion exchange resins can be categorized as Type I or Type II depending on the nature of the functional groups/type of amine used during the chemical activation process. Type I resins contain trialkyl ammonium chloride or hydroxide and Type II resins contain dialkyl 2-hydroxyethyl ammonium chloride or hydroxide.

iv. Weak anion exchange resins, containing tertiary amine functional groups.

- **Applications of ion-exchange resins in various fields**

The selectivity or affinity of ion-exchange resins is influenced by properties of the bead, the exchangeable ions and the solution in which the ions are present. Water is an essential component of ion-exchange resins. Based on the desired quantity of water required, the resins are selected for the application in industry. The broad applications of ion-exhange resins are water softening, dealkalisation, demineralization, water purification, nuclear power plants, precious metal recovery and pharmaceuticals *etc*.

- **Application of ion-exchange resins in diverse organic reactions**

Organic polymers have not only used as catalyst support but also as a catalyst itself. As rule of solid-phase organic synthesis substrates, reagents and catalysts are generally immobilized onto the polymer surface through covalent bonding, entrapment and ion-pairing where cations or anions are bound to complementary resin sites.[108]

Microencapsulation is an another method for the immobilization of catalysts onto the surface of polymers using physical involvement by polymer backbones and interaction between π–electrons of benzene rings of the polystyrenes and vacant orbitals of the catalysts. Kobayashi *et al.*[109] have first prepared microencapsulated Sc, Os, Pd and Ru catalysts successfully and applied in various organic transformations (Scheme I.18).

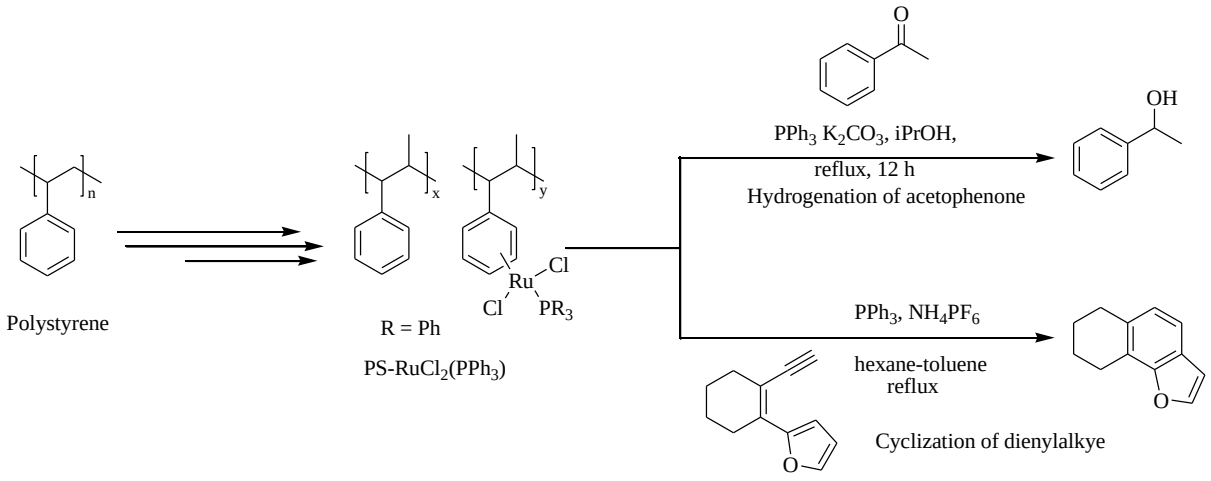

Scheme I.18. Microencapsulated PS-$RuCl_2$ (PPh_3) catalyzed organic transformations.

According to our laboratory report, Amberlyst A-26(OH) can efficiently promote the smooth conversion of disulfides from alkyl and acyl methyl thiocyanates in good to excellent yields (Scheme I.19).[110]

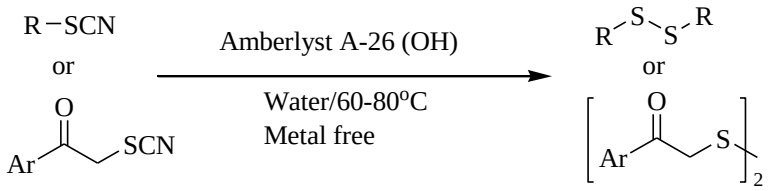

Scheme I.19. Amberlyst A-26 catalyzed disulfide formation.

Amberlyst-15, have been widely used as heterogeneous acid catalyst in various organic transformation as shown in Scheme I.20.[111]

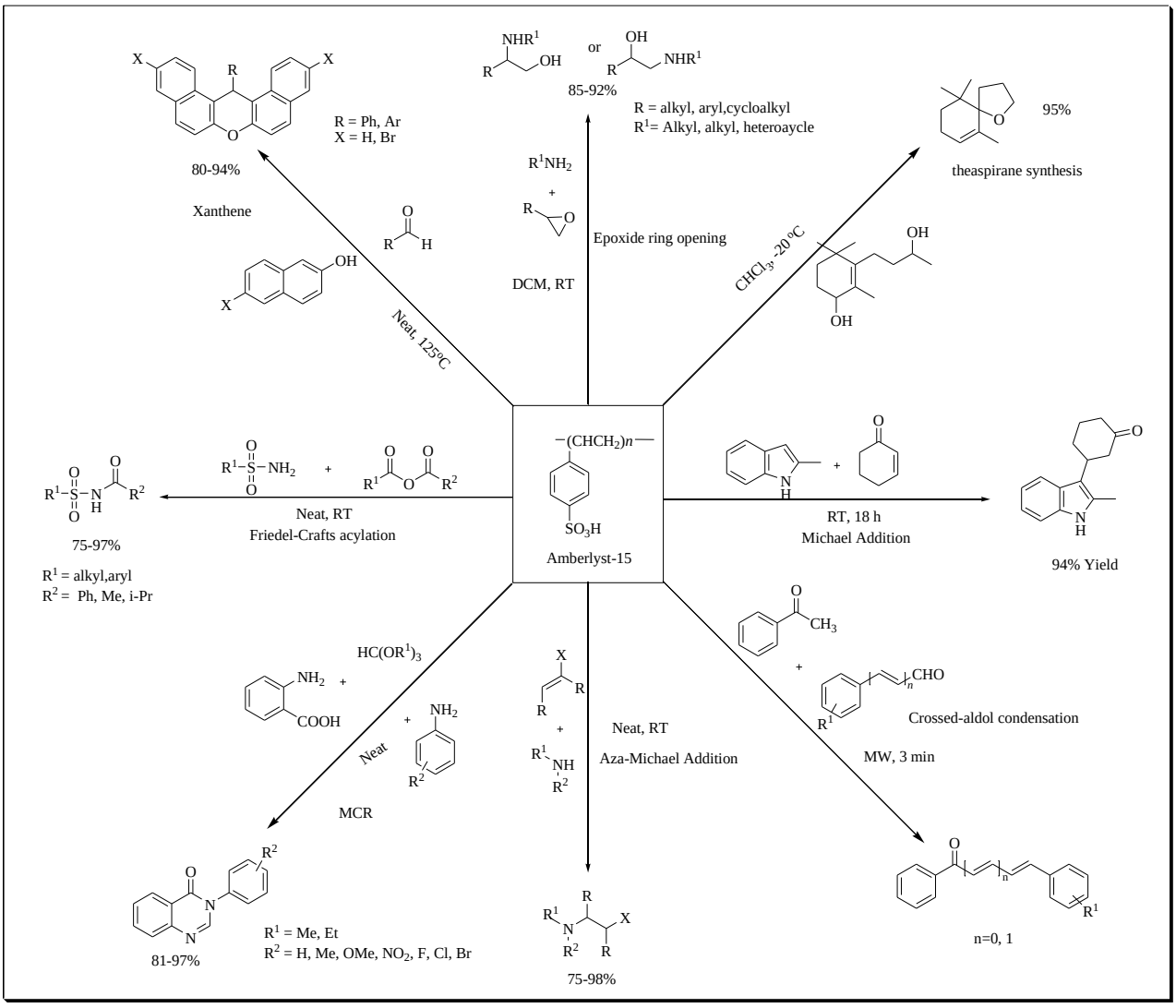

Scheme I.20. Amberlyst-15 catalyzed various organic transformations.

In heterogeneous catalytic hydrogenation, several molecules such as hydrocarbons, primary, secondary alcohols, formic acid and its salts have been employed as hydrogen source. Amberlite IRA–420 anion (chloride form) which has exchangeable chloride anion can easily be exchanged with formate anion ($HCOO^-$). This poly-ionic resin was designated as

amberlite resin formate (ARF) by our laboratory and applied as an excellent hydrogen source in Pd–catalyzed catalytic transfer hydrogenation (CTH) for several alkenes, imines and nitroarenes also. (Scheme I.21).[112] The advantages of using ARF are the stability in the open air and also the recyclability. A number of works for the formation of monometallic as well as bilmetallic nanocomposites of different transition metals such as Pd, Cu using ARF as a solid support have been reported from our laboratory which have broad application towards C–C bond forming reactions.[113]

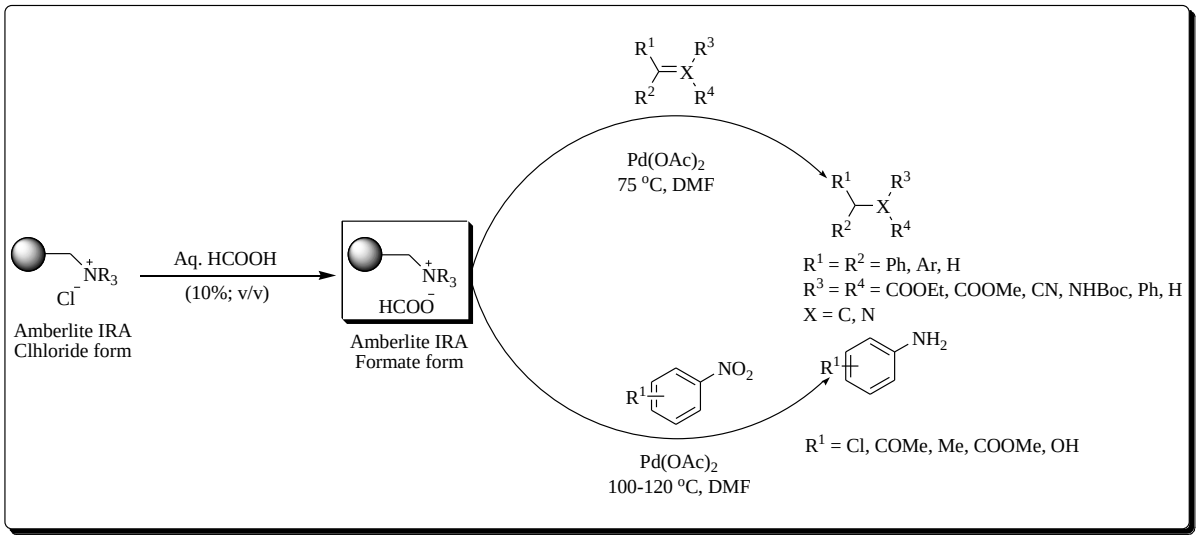

Scheme I.21. Synthesis of ARF and Pd–catalyzed catalytic transfer hydrogenation of alkenes, imines and nitroarenes.

ARF–Pd catalyst has been applied excellently for the C–C cross coupling reactions like Heck–Mizoroki, Suzuki–Miyaura and Sonogashira reactions (Scheme I.22).[113a] The high catalytic efficiency, selectivity and reusability of ARF–Pd make it a viable heterogeneous catalyst for these C–C bond forming reactions.

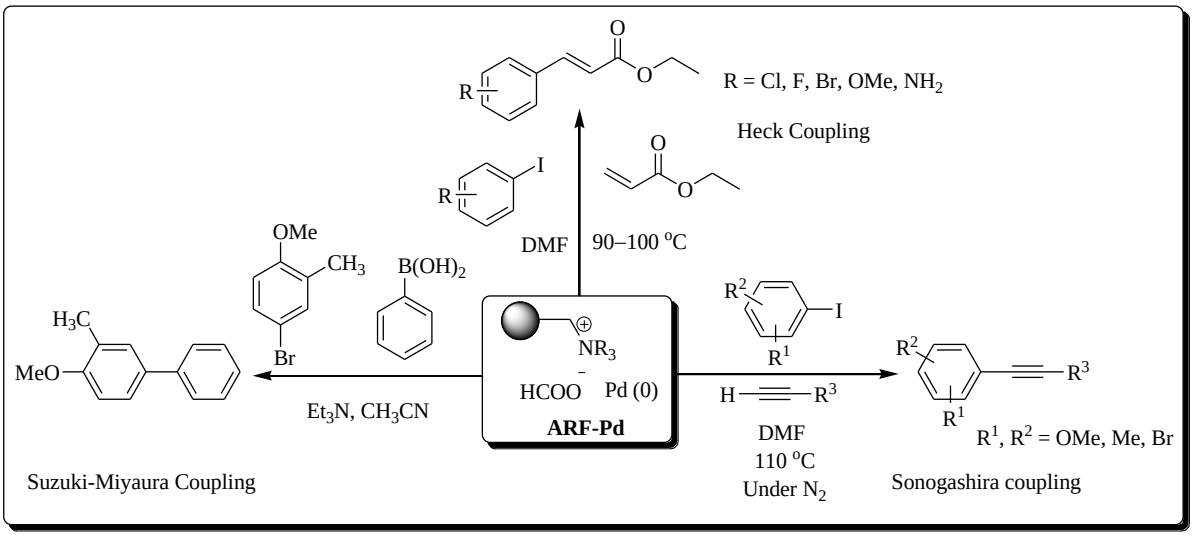

Scheme I.22. ARF–Pd catalyzed various C–C cross coupling reactions.

According to our previous laboratory report poly-ionic resin supported CuO NPs (CuO@ARF) have excellent catalytic effect for C−S coupling reaction under ligand-free and 'on-water' conditions. It is also applied for the chemoselective synthesis of bioactive heterocyclic scaffold phenothiazine (Scheme I.23).[114]

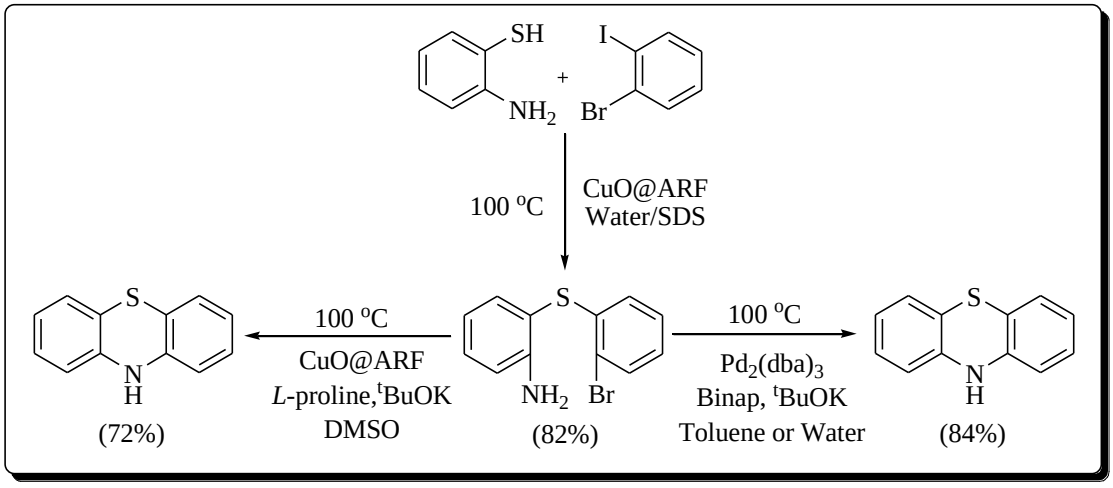

Scheme I.23. Synthesis of phenothiazine using poly-ionic resin supported CuO NPs.

Further application of poly-ionic resin bound reagents and/or catalysts has been established when an ion-exchange resin-supported organoborate species is derived as a heterogeneous phenylating agent. Amberlite ion-exchange resins (chloride form) have exchanged with tetraphenylborate anion (Ph_4B^-) by continuous rinsing with an aqueous solution of $NaBPh_4$ and have been used directly for the Suzuki coupling reaction in the presence of 2 mol% $Pd(OAc)_2$ affording unsymmetrical biphenyl in 90 % yield (Scheme I.24).[115]

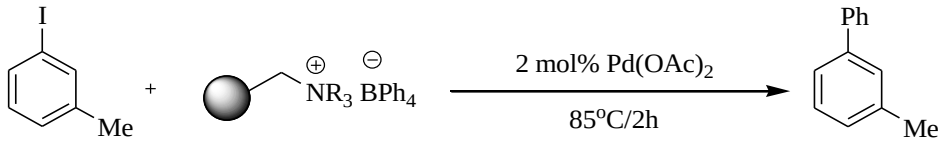

Scheme I.24. Amberlite supported tetraphenylborate as a phenylating agent for Suzuki reaction.

I.5. References

References are given in **BIBLIOGRAPHY** under **CHAPTER I**. (pp. 163−170).

CHAPTER II

Silica: An efficient inorganic solid support to promote one-pot regioselective synthesis of dithioethers

II.1. Introduction

Over the last decade, organic synthesis has taken a major turn towards developing reaction conditions that are environment-friendly, sustainable and amenable to industries.[1] In this respect, solid-phase organic reactions mediated by various solid supports as well as solid supported catalysts have played a significant role in combinatorial synthesis of small molecules of pharmaceutical interest.[2] Mesoporous inorganic oxides like silica, alumina, zeolite *etc.* are not only considered as suitable solid surfaces to facilitate various organic reactions but also to promote eco-friendly chemical processes.[3] On the other hand, organic reactions with a high selectivity under eco-friendly and sustainable conditions have attractive features in terms of the concept of green chemistry. Due to the high surface area (5–800 $m^2 g^{-1}$) and high porosity of silica gel, which is generally used in chromatography plays an important role in catalysis not only as a solid support but also as an active catalyst.[4] The high chemo-, regio- and stereoselectivity, simplification of product work-up, separation and isolation under mild conditions are the major advantages of silica gel promoted chemical reactions over conventional homogeneous reactions. A huge number of works have been already reported in literature based on chemical reactions catalyzed by silica gel.[5]

Diorganyl sulfides or thioethers are essential building blocks of various biologically active organosulfur compounds,[6] which play important role in both biological and chemical processes such as pharmaceutical, polymer, pesticide and food-processing industries.[7] In addition, dithioethers have employed as bridging ligands in the construction of metal-organic coordination complexes.[8] The flexibility and spacer length of these organic bridging ligands play fundamental role in determining the structure types of final assemblies and the luminescence properties of metal-organic framework (MOF). Figure II.1 represents few examples of flexible dithioether bridging ligands which are mainly used for the formation of coordination complexes with various metals like Ag, Cu, Pd, Rh, Ir, Pt etc.

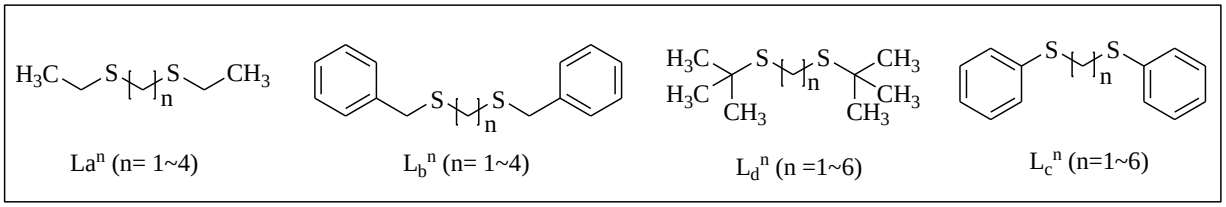

Figure II.1. Some flexible dithioether ligands involved in the formation of metal-organic coordination complexes.

The involvement of thioether ligands in bio-inorganic systems like copper containing metalloenzymes makes huge interests to the development of copper complexes containing thioether ligands to explore the role of sulphur-based donors in both biological process,[9] like blue copper proteins.[10] Recently, thioether ligands have been recognized as copper traffickers.[11] Moreover, the presence of sulfur donors around copper centres can modulate the redox potential of the Cu^{2+}/Cu^{+} couple, resulting in high redox potentials for sulfur-rich coordination complexes. Thioether-based copper complexes like $[\{Cu(\mu_2\text{-}I)_2Cu\}\{\mu\text{-}PhS(CH_2)_3SPh\}_2]_n$, $[Cu_4I_4\{\mu\text{-}PhS(CH_2)_3Ph\}_2]_n$, $[\{Cu(\mu_2\text{-}Br)_2Cu\}\{\mu\text{-}PhS(CH_2)_3SPh\}_2]_n$, $[Cu_4I_4\{\mu\text{-}PhS(CH_2)_5Ph\}_2]_n$, $[Cu_4I_4\{\mu\text{-}p\text{-}TolS(CH_2)_5STol\text{-}p\}_2]_n$, have structural diversities like 1D, 2D and 3D as in Figure II.2 which have potential applications in catalysis. It has been also postulated that the spacer length and also the nature of the thioether ligands have crucial role on composition as well as on topology of the co-ordination polymers. Hence, such structural variation of thioether ligands affect the mean distance of Cu···Cu resulting in the influence on their luminescence properties.[8c]

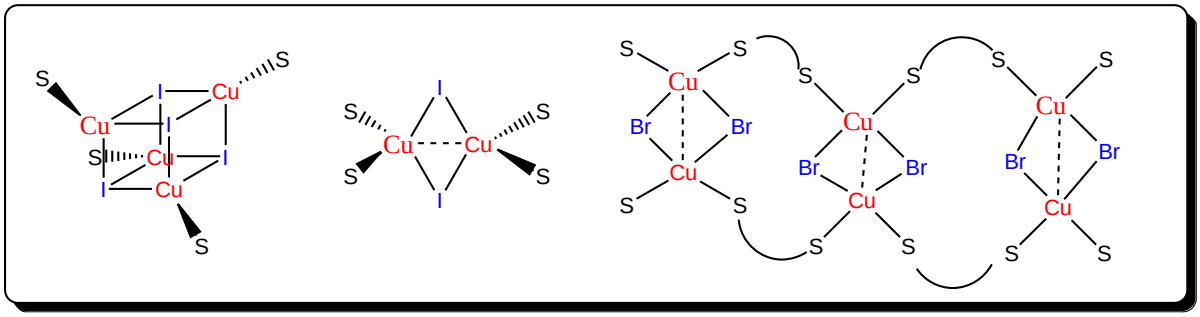

Figure II.2. Structural variation of thioether-based copper complexes.

Vicinal dithioethers are also used as bridging ligands which have diverse applications *e.g.* vicinal dithioether-based zirconium and titanium complexes have been used in the polymerization and hydroamination of alkenes.[12-15] Iridium-complexes prepared using chiral dithioethers also have been employed in asymmetric hydrogenation.[16] Because of their versatile applications, a great number of procedures have been developed to synthesize *bis*-thioethers with varying success and limitations.[7a,17] But in literature, synthesis of dithioethers mostly involved the metal-catalyzed addition of disulfides to alkenes,[17c,18] and conventional nucleophilic substitution of 1,2-dihalides with thiols/thiolate.[7a,19] Therefore, the synthesis of dithioethers in green and straightforward way still need to be explored.

Here, we have demonstrated a distinct protocol to synthesize either 1,2 or 1,3-dithioether *via* one-pot, solvent-free substitution and regioselective addition of allyl halides

with thiols using commercially available, inexpensive and no-corrosive silica gel as catalyst by following both Maronikov and Anit-Markonikov pathways.

II.2. Present Work: Background and objectives

The traditional method for the formation of thioethers is the addition of thiols to C=C double bonds *via* an electrophilic addition either protic,[20] or Lewis acids,[21] or a free-radical chain pathway.[19] On the other hand, vicinal dithioethers are generally synthesized either by metal-catalyzed addition of disulfides to alkenes,[17c,18] or by traditional nucleophilic substitution of 1,2-dihalides with suitable thiols/thiolate.[7a,19] They are also prepared *via* consecutive hydrothiolation of alkynes, both under nucleophilic or radical-induced conditions.[7a,19] In addition, 1,3-dithioethers can be prepared by nucleophilic substitution of compounds bearing suitable leaving groups at 1,3-positions of alkyl chain.[18] Several number of synthetic procedures have been already reported for the synthesis of *bis*-thioethers.

S. Poulain *et al.* have synthesized vicinal dithioethers by the sulfuration of norbornene derivatives with elemental sulphur using a catalytic amount of a nickel complex $[Ni(NH_3)_6]Cl_2$ in two step; first sulfuration by S_8 to double bond to afford selectively trithiolanes followed by further reduction and alkylation of the isolated trithiolanes to produce the desired 1,2-dithioethers (Scheme II.1).[13a]

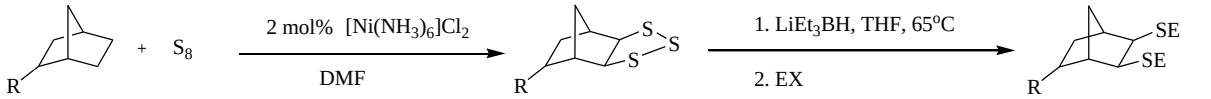

R = H, -CH=CH$_2$, -COCH$_3$ E = -H, -Me, -CH$_2$Ph

Scheme II.1. $[Ni(NH_3)_6]Cl_2$–catalyzed vicinal dithioethers of norbornene derivatives *via* S_8 activation.

Disubstitution of either 1,2-dibromoethylene or 1,1-dibromoethylenic compounds in an aprotic solvent such as 1,2-dimethoxyethane and toluene regioselectively produce corresponding ketene thioacetals (Scheme II.2) in good yields by using of *o*-phenylene-bis(diphenylphosphino) nickel(II) bromide complex as a catalyst.[22]

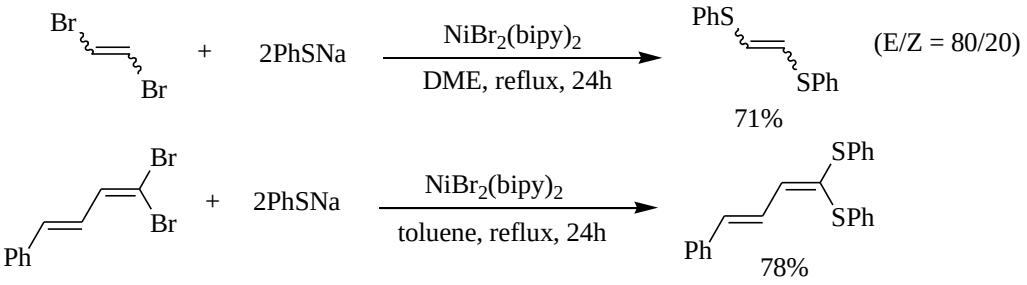

Scheme II.2. Bis(bipyridine)nickel(II) bromide complex catalyzed synthesis of alkenyl sulfides and ketene thioaetals.

Kondo *et al*.[23] have reported that the addition of disulfides to 2-norbornene can easily provide corresponding vicinal dithioethers in high yields using Cp*RuCl(cod) complex as a catalyst (Scheme II.3). The overall reaction involves stereoselective *cis*-thioruthenation of alkenes, followed by reductive elimination with retention of the stereochemistry to give the products. Ethylene and a variety of terminal alkenes bearing functional groups have been used to synthesize their corresponding dithioethers.

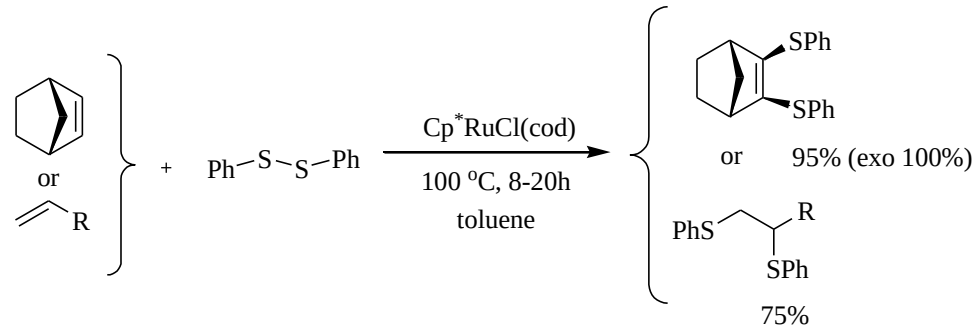

Scheme II.3. Cp*RuCl(cod)–catalyzed stereoselective synthesis of *vicinal* dithioethers.

K. Oshima and his co-workers have demonstrated the use of gallium trichloride for the highly selective disulfidation of terminal alkynes with to give (*E*)-1,2-dithio-1-alkenes (*E/Z* > 20/1) (Scheme II.4). They have also used alkenes to form their *trans* adducts under this reaction condition.[24]

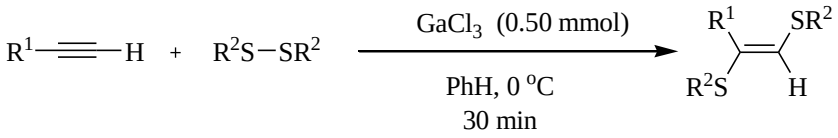

R^1 = *n*-Bu, *i*-Pr, *t*-Bu, Ph, p-$CF_3C_6H_4$, *p*-$MeOC_6H_4$, *n*-C_6H_{13}
R^2 = Ph, *p*-Tol, *n*-Bu

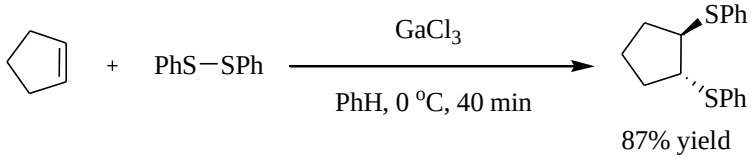

87% yield

Scheme II.4. $GaCl_3$–catalyzed disufidation of alkynes and alkenes.

The stereoselective addition of aromatic disulfides to terminal alkynes is also possible by using a palladium complex resulting in excellent yield (100%) of *Z*-isomer, (*Z*)-1,2-*bis*(arylthio)-1-alkenes are formed (Scheme II.5).[25]

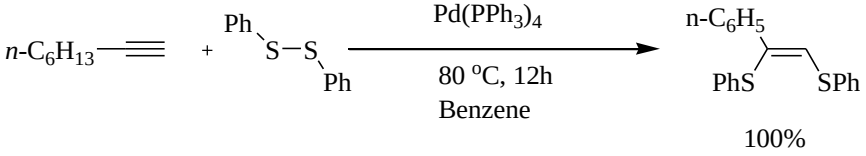

Scheme II.5. $Pd(PPh_3)_4$–catalyzed stereoselective addition of aromatic disulfides to terminal alkynes.

In such addition, the presence of carbon monoxide can undergo one-pot multicomponent carbonylative addition of disulfides to alkynes (Scheme II.6).[25]

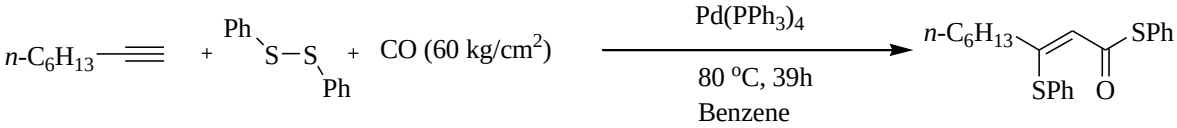

Scheme II. 6. $Pd(PPh_3)_4$–catalyzed one-pot carbonylative addition of disulfides to alkynes.

Moreover, the *syn*-addition of bis(triisopropylsilyl)disulfide to terminal alkynes in benzene (Scheme II.7) can afford good to excellent yield of their corresponding insertion products by using a catalytic amount of $Pd(PPh_3)_4$.[26]

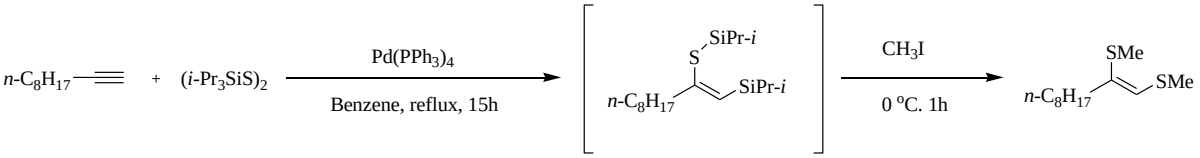

Scheme II.7. $Pd(PPh_3)_4$–catalyzed *syn*-addition of bis(triisopropylsilyl)disulfide to alkynes in benzene at 80 °C.

Very recently, a new method is developed for the formation of *S*-styryl/ *S*-aryl dithioethers by the tandem elimination/ring-opening of 2-benzyl-1,3-dithianes with subsequent cross coupling of the pendent thiol with various aryl bromides using a $Pd(OAc)_2$/xantphos catalytic system (Scheme II.8).[27]

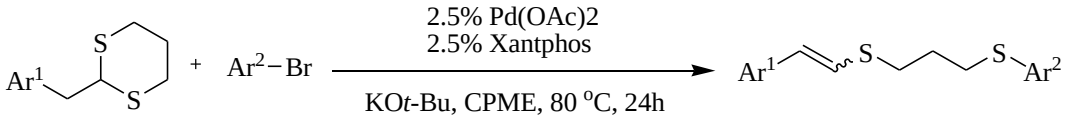

Ar^1 = Ph
Ar^2 = Aryl/ Heteroaryl

66–99%
E:*Z* upto 99:1

Scheme II.8. Synthesis of disubstituted dithioethers by $Pd(OAc)_2$/Xantphos promoted tandem elimination/ring opening/C−S cross coupling of 1,3-dithianes.

N. Yamagiwa *et al.*[28] have utilized very common Lewis acids like $FeCl_3/AlCl_3$ for catalytic disulfenylation reaction of alkenes to their corresponding vicinal dithioethers (Scheme II.9). In this method, the transformations were much faster and provide excellent yields by using $AlCl_3$ compared to $FeCl_3$.

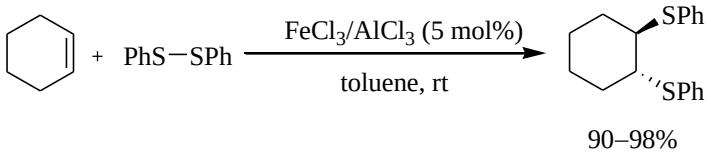

Scheme II.9. $FeCl_3$/ $AlCl_3$ catalyzed disulfenylation of cylohexene with aromatic sulphide.

A green and atom-economical "on water" synthesis of vicinal dithioethers from alkynes and thiols in metal-free condition (Scheme II.10) has been developed by Hammond *et al.* This method is not only applicable for terminal alkynes but can be also used for non-terminal propargyl alcohols to produce highly regio- and stereoselective monohydrothiolation product (*E*)-alkenyl thioether.[29]

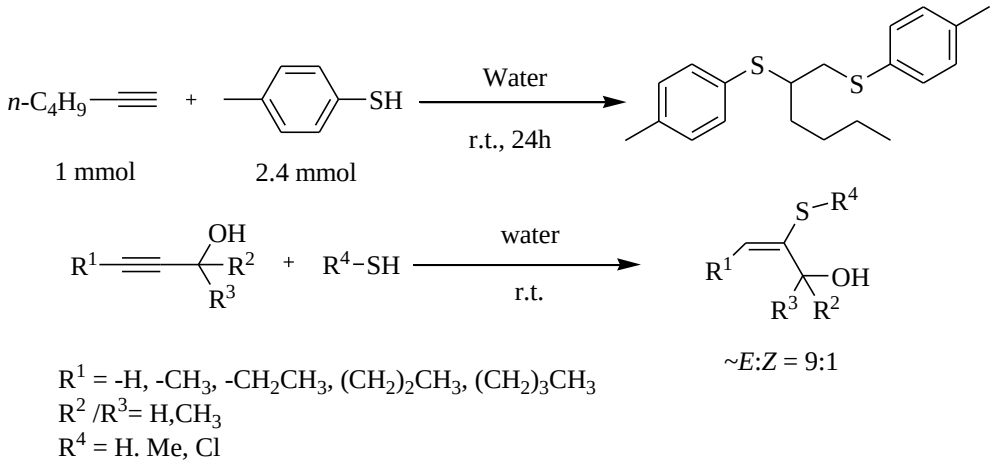

Scheme II.10. "On water" synthesis of vicinal dithioethers from alkynes and thiols and regio and stereoselective monohydrothiolation of propargyl alcohols.

Mesoporous inorganic oxide like silica having high surface area (>800 m^2/g) as well as high porosity has taken a widespread attention towards its application in chemical reactions. Banerjee and his co-workers have utilized silica nanoparticles (NPs) as a reusable catalyst for the synthesis of thioethers *via* the 1,2 addition of thiols to alkenes and 1,4 addition to conjugated alkenes at room temperature (Scheme II.11).[30]

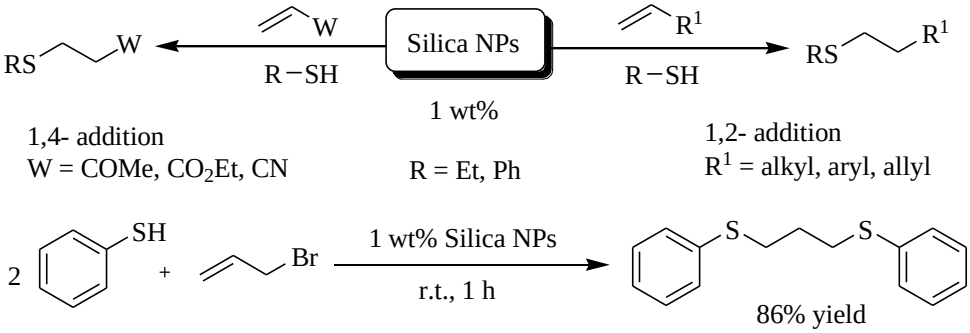

Scheme II.11. Silica NPs catalyzed anti-Markonikov addition of thiols to alkenes/allyl halides and also the synthesis of 1,3-dithioether.

They have also reported one example for the synthesis of 1,3-dithioether by anti-Markonikov addition reaction of allyl bromide and excess benzenethiol using silica NPs (Scheme II. 11).

Previous report from our laboratory depicts that commercially available silica gel can act as an efficient heterogeneous surface for promoting various organic transformations like Aza-Michael addition of amines to electron deficient alkenes,[31] and also in selective N and S-alkylation/acylation from amines or thiols respectively (Scheme II.12).[32,33] We have also utilized silica gel as an excellent solid support for the synthesis of Pd NPs and applied successfully in Suzuki and Heck coupling (Scheme II.12).[34]

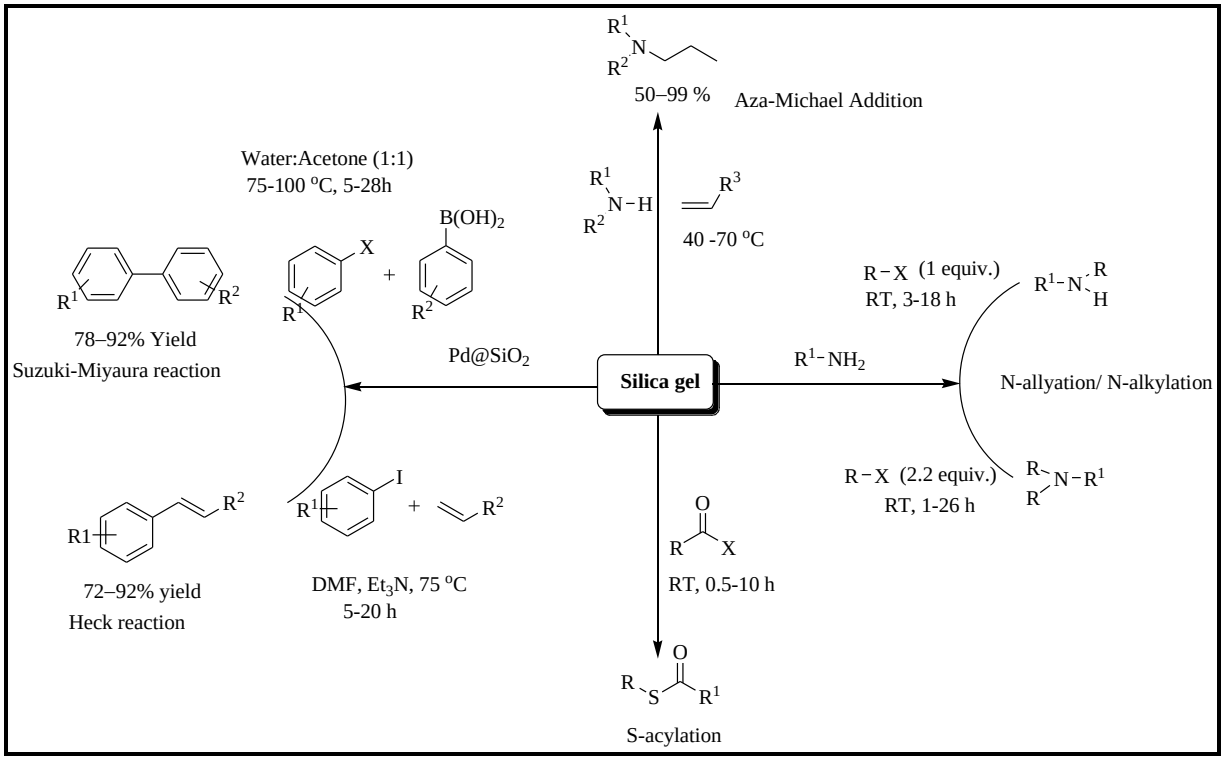

Scheme II.12. Silica gel promoted various organic transformations.

We observed that an equimolar mixture of a benzenethiol and allyl bromide on treatment with silica can produce allyl(phenyl)sulfane in excellent yield (Scheme II.13).[33]

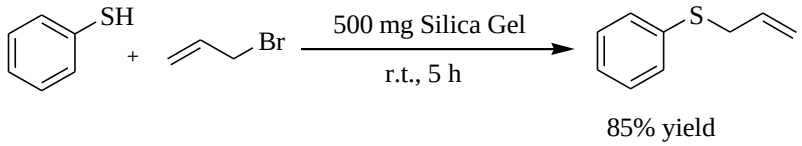

Scheme II.13. S-allylation of thiohenols promted by silica gel surface at room temperature.

Since, alkenes are known to undergo 'click' addition with thiols,[35] excess use of thiols could effectively produce dithioethers and based on a regioselective addition one could achieve either vicinal or 1,3-dithioethers in one-pot consecutive substitution hydrothiolation processes as represented in Scheme.II.14.

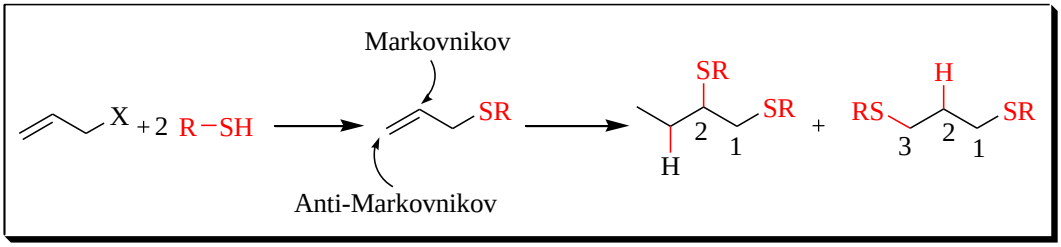

Scheme II.14. Sequential substitution-addition reactions of thiols with allyl halides leading to the formation of 1,2- or 1,3-dithioethers.

Although both reactions are well known, a critical search in the literature surprisingly revealed no general one-pot protocols for the preparation of dithioethers from allylic substrates. Banerjee *et al.* have only reported one example for the synthesis of 1,3-dithioether by anti-Markonikov addition reaction of allyl bromide and excess benzenethiol using silica NPs (Scheme II. 11).[30] The reaction was carried out in the presence of silica NPs under solvent free condition and found that silica NPs have significant influence in directing anti-Markonikov addition of thiols to different alkenes.

However, there is no report on the metal-free hydrothiolation of allylic substrates in a Markonikov way to produce 1,2-dithioethers in one-pot reactions. In addition, according to Banerjee *et al*. silica NPs can afford selectively anti-Markonikov product (100%) under solvent free condition without the formation of any Markonikov product.

Here, we have demonstrated that silica surface can have tuning behaviour depending on the physically adsorbed water and the presence of various silanol groups on its surface. Hence, using such tuning behaviour of silica gel surface under pre-calcined and moistened state we become successful to produce 1,2- or 1,3-dithioethers regioselectively in one-pot way.

II.3. Present work: Results and discussion

II.3.1. Optimization of reaction conditions

To begin our study, we have first activated silica gel (directly from the container, commercially available) by heating under vacuum at 150 ^{o}C until bubbling ceased, and then cooled to room temperature under vacuum following our previous laboratory method.[32,33] Then following the same method we first attempted the magnetic stirring of a mixture of allyl bromide and benzenethiol in a 1:2.5 ratio by using pre-calcined silica gel at room temperature that indeed led to the formation of 1,2-dithioether in 91% yield (Table II.1, entry 2).

Table II.1. Optimization of one-pot sequential substitution-hydrothiolation of allylic substrate with excess benzenethiol over silica at room temperature

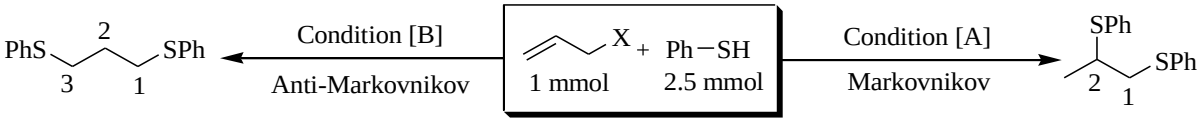

Entry	CH_2=CH-CH_2-X	Conditions[a]	Time (h)	Product[b] / Yield (%)[c]
1	X = Br	[A]	6	1,2-Dithioether / 77
2	X = Br	[A]	11	1,2-Dithioether / 91
3	X = Br	[B]	20	1,3-Dithioether / 83
4	X = I	[A]	12	1,2-Dithioether / 89
5	X = I	[B]	20	1,3-Dithioether / 85
6	X = Cl	[A]	15	1,2-Dithioether / 57
7	X = Cl	[B]	30	Diphenyldisulfide / 83
8	X = OAc	[A]	24	Diphenyldisulfide / 90
9	X = OTs	[A]	8	1,2-Dithioether / 75
10	X = OTs	[B]	22	1,3-Dithioether / 68
11[d]	X = SPh	[A]	5	1,3-Dithioether / 83
12[d]	X = SPh	[B]	12	1,3-Dithioether / 80
13[d]	X = OPh	[A]	6	3-Phenoxythioether/89
14[d]	X = OPh	[B]	14	3-Phenoxythioether/82
15	X = Br	Neat	20	No dithioether is formed

[a]Conditions: [A] allylic compound and PhSH (1:2.5 mmol) over pre-calcined dry silica gel (0.5g); [B] allylic compound and PhSH (1:2.5 mmol) over moist silica gel (0.5g). [b]In each case 5-10% diphenyldisulfide was formed except Entries 6, 7 and 8. [c]Yield refers to isolated pure product and no other constitutional isomer was detected. [d]Thiol (1.2 mmol) was used for Entries 11-13. [Entries no 2-6, 10, 13, 14, 15 were performed by the present author and others were performed by one of my co-author S. Kundu].

On the other hand, when we moistened silica gel with a few drops of water for the same reaction, then surprisingly we obtained regioselective anti-Markovnikov addition product, i.e. 1,3-dithioether, [1-(3-(phenylthio)propylthio)benzene] in 83% yield. In both cases, a minimal

amount of diphenyldisulfide (5–10%) was formed,[36] which was easily separable from the reaction mixture by column chromatography. Since the choice of silica led to the production of highly regioselective products, we wanted to optimize both conditions to establish them as general protocols. Table II.1 represents the optimization of the reactions of different allylic substrates with benzenethiol. Pre-calcined silica gel was used for the conditions A or moist with water (0.1 mL water for 0.5 g of silica) for use under conditions B. It was observed that allyl bromide or allyl iodide underwent sequential substitution-addition reactions entirely regioselectively with comparable yields (Table II.1, entries 1–5), whereas allyl chloride showed varying results under conditions A or B, and allyl acetate did not undergo any desired reaction, but merely produced the disulfide from oxidative dimerization of the thiol (Table II.1, entries 6–8). Allyl tosylate, however, produced the desired thioethers in a regioselective manner, but with relatively low yields (Table II.1, entries 9 and 10). Interestingly, allylphenylsulfane or allyl phenyl ether entirely followed an anti-Markovnikov addition, under both conditions, A and B (Table II.1, entries 11–14).

II.3.2. Applications of our optimized reaction conditions in one-pot tandem reactions of allyl bromide with a variety of thiols

By taking these two distinct conditions in our hand, we examined the scope of these one-pot tandem reactions of allyl bromide with a variety of thiols under both conditions. The results are presented in Table II.2. Arylthiols bearing different functional groups like CH_3, OCH_3, Cl or F were reacted with allyl bromide in the presence of pre-calcined and dry silica affording good to excellent yields of the corresponding 1,2-dithioethers (Table II.2, entries 1, 3, 5, 7, 9, 11 and 17). 2-Naphthylthiol also underwent a similar regioselective Markovnikov addition, resulting in the corresponding 1,2-dithioether in 82% yield (Table II.2, entry 18). Extending the protocol to aliphatic thiols, such as *n*-pentylthiol and cyclohexylthiol also afforded regioselective dithioether in good yields (Table II.2, entries 13 and 15). In all the cases, we observed 100% Markovnikov addition products and no anti- Markovnikov products were detected. We now turned our attention to the other conditions [B] – the use of moist silica gel. Again, a variety of aromatic thiols, including those that were used for the conditions [A], were employed to react with allyl bromide in the presence of silica moist with a few drops of water, and we isolated entirely regioselective 1,3-dithioethers (Table II.2, entries 2, 4. 6, 8, 10 and 12). The same selectivity was observed in the reaction of aliphatic thiols (acyclic or alicyclic) *viz. N*-pentane-1-thiol and cyclohexanethiol, with allyl bromide to

afford the corresponding 1,3-dithioethers in 71% and 67% yield, respectively (Table II.2, entries 14 and 16). In these cases, we did not detect any Markovnikov addition products. Thus, moistened silica gel turns out to be effective for sequential substitution reactions, and entirely anti-Markovnikov addition, while pre-calcined dry silica gel could efficiently give rise to only Markovnikov addition products. Interestingly, it was found that the reactions over dry silica gel appear to be faster than the procedure using moist silica. Moreover, the 1,2-dithioethers are formed in slightly better yields than the corresponding 1,3-analogues. We also experienced that aromatic thiols, under both conditions [A] and [B], give better yields than aliphatic thiols.

Table II.2. Regioselective one-pot synthesis of 1,2- and 1,3-dithioethers using dry (pre-calcined) or moist silica gel at room temperature

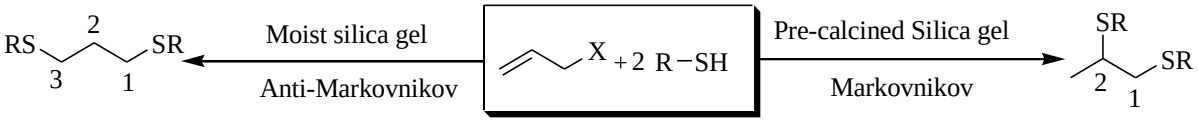

Entry	Thiol	Conditions[a]	Time (h)	Product	Yield[b](%)
1	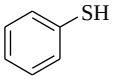	[A]	10	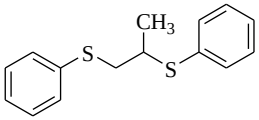	91
2	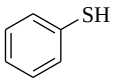	[B]	22	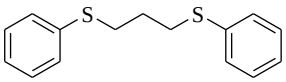	81
3	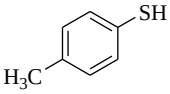	[A]	6	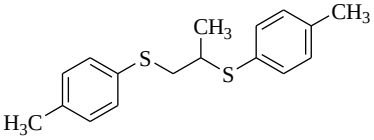	87
4	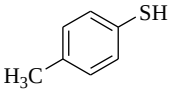	[B]	20	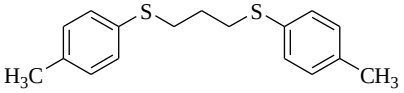	78
5	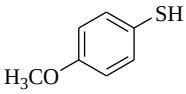	[A]	6.5	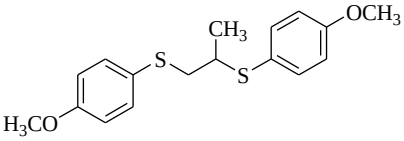	78
6	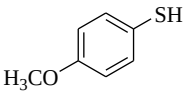	[B]	18	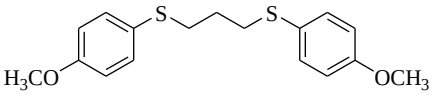	76
7	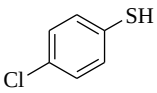	[A]	6	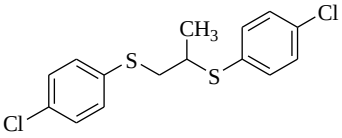	83

8	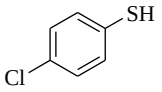	[B]	15	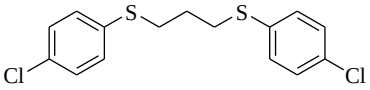	87
9	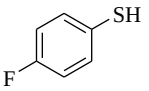	[A]	8	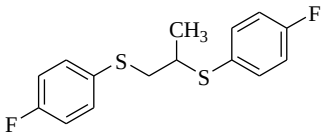	80
10	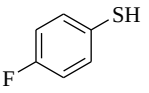	[B]	16	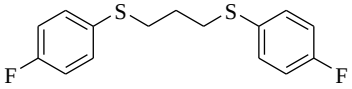	84
11	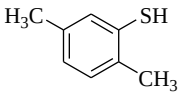	[A]	8	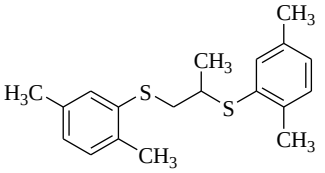	74
12	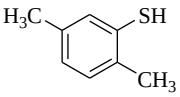	[B]	20	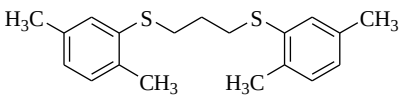	77
13	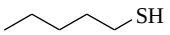	[A]	9	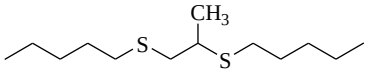	67
14	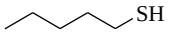	[B]	16	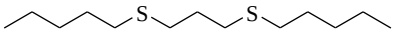	71
15	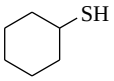	[A]	10	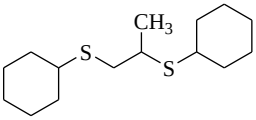	65
16	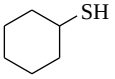	[B]	18	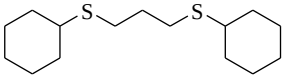	67
17	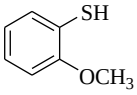	[A]	7	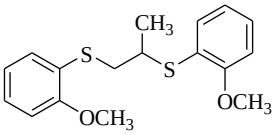	71
18	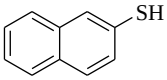	[A]	9	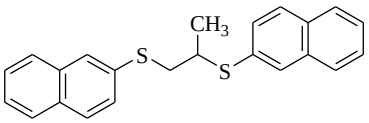	82
19[c]	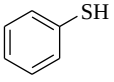	[B]	22	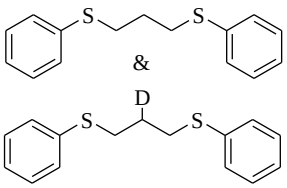	-
20	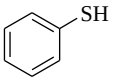	[A][d]	15	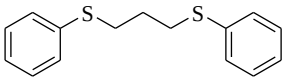	82

[a]Conditions: [A] allylic compound and PhSH (1:2.5 mmol) over pre-calcined dry silica gel (0.5g); [B] allylic compound and PhSH (1:2.5 mmol) over moist silica gel (0.5g). [b]Yield

refers to isolated pure product; in each case 5-10% dipheneyldisulfide was formed and isolated. [c]D_2O (0.5 mL for 0.5 g silica gel) was used instead of H_2O. [d]Mixture of silica and sodium silicate (1:1 w/w; 0.5 g for 1 mmol of allyl bromide) was used after drying under vacuum. [Entries 1, 3, 5, 7, 9-10, 1, 12, 17, 18 were performed by the present author and other by my co-author and every examples were checked carefully by both authors]

II.3.3. Mechanism

Mechanistically, we presume that the nature of the silica surface and its possible interactions with thiols is responsible for the notable regioselectivity in the hydrothiolation of allylsulfane. It is well known that amorphous or mesoporous silica consists of silanol groups and siloxane bridges that determine its surface properties, and the concentration of these –OH groups depends mostly on the actual process of calcinations.[37–39]

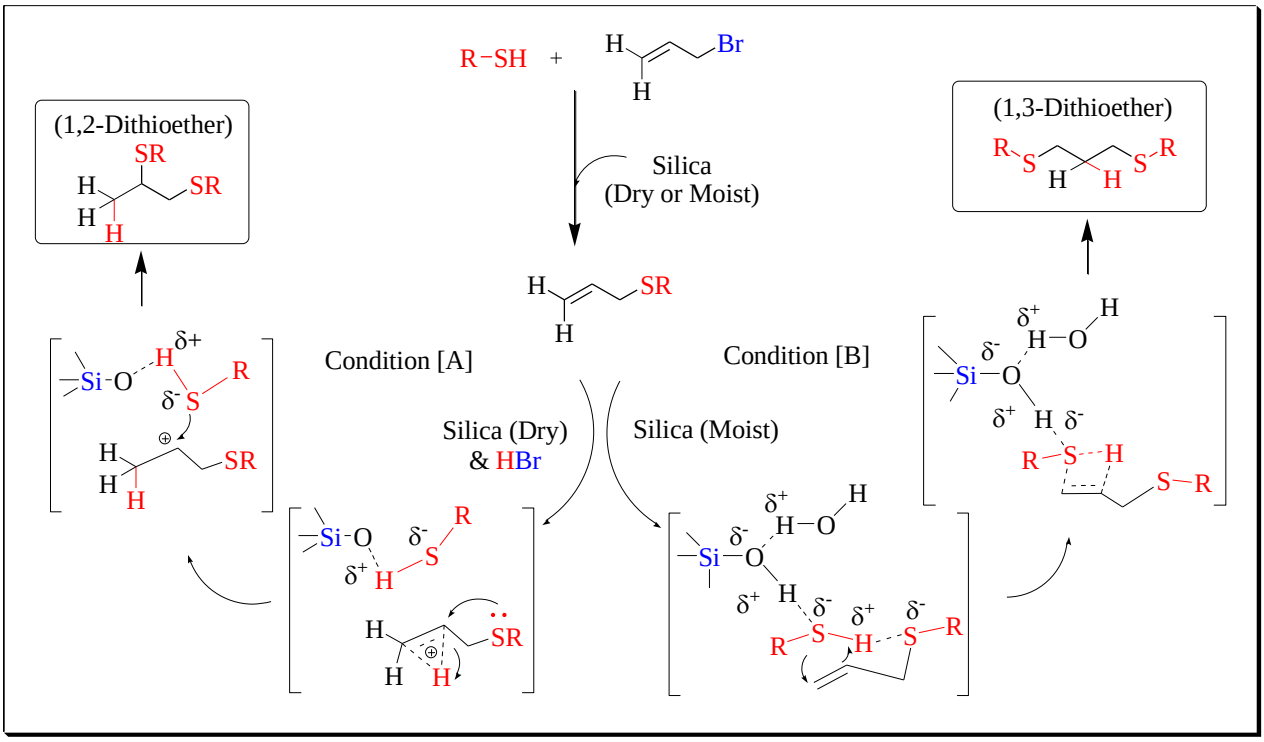

Scheme II.15. Plausible mechanisms for the regioselective formation of vicinal and 1,3-dithioethers in the presence of dry or moist silica gel.

Based on Zhuravlev's physicochemical model of silica surface,[37] it may be presumed that the moistened silica surface is covered with a single layer or multilayer of adsorbed water, which might disappear during the calcination process. Since, allylphenylsulfane on hydrothiolation affords the anti-Markovnikov product under both conditions [A] and [B] (Table II.1, entries 11 and 12), we presume that there might be an influence of the generated acid in the first step under dry conditions [A]. In the absence of water, the generated HBr in the first step might

activate the double bond and subsequent assistance by the neighbouring sulfur atom coupled with the stability of the secondary carbocation lead to the Markovnikov addition resulting in the exclusive formation of 1,2-dithioether (Scheme II.11, conditions [A]).

On the other hand, the moist silica consisting of a single layer or multilayered adsorbed water promotes thiols to bind with allylsulfane, and the subsequent addition takes place in an anti-Markovnikov approach (Scheme II.15, conditions [B]). The influence of water was also reported by Ranu *et al.*[40] for the regioselective anti-Markonikov addition of thiols to unactivated alkenes where water promotes the reaction through H–bond formation with sulfhydryl hydrogen of thiol which increases the nucleophilicity of the thiolate ion. Then, the addition of thiolate anion to the C=C bond takes place in a concerted manner with steric factors controlling the regioselectivity leading to anti-Markonikov product.

When the reason behind the anti-Markonikov addition was well understood we further went through few experiments to diagonise the exact role of in situ produced HBr as well as physically adsorbed water for the formation of 1,2-dithioether and 1,3-dithioether respectively. In order to find evidence for the role of silica adsorbed water, we conducted the following experiments:

(i) First the reaction was carried out under conditions [A] using allylphenylsulfane as starting substrate in the presence of an exogenous base (sodium silicate; see Experimental section), which leads to the formation of anti-Markovnikov product only (1,3-dithioether) (Table II.2, entry 20).

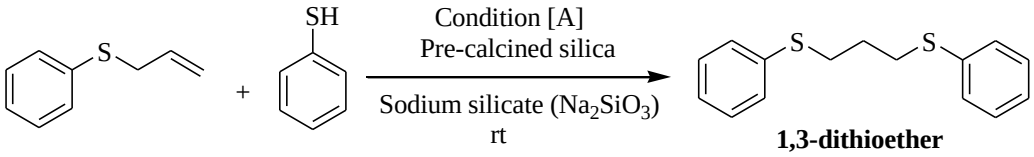

Scheme II.16. Addition of thiophenol to allylphenylsulfane with thiophenol in the presence of an exogenous base.

(ii) Secondly, two reactions were carried out using moistened silica gel under conditions [B] with varying quantities of H_2O (0.5 mL and 1.0 mL) but did not observed any significant changes producing only 1,3-dithioethers in quantities.

(iii) To confirm the role of HBr produced in first step of the reaction, we have performed another experiment. We passed dry HCl gas through pre-calcined silica and then performed hydrothiolation of allylphenylsulfane, exclusively yielding an Markovnikov addition product (1,2-dithioether).

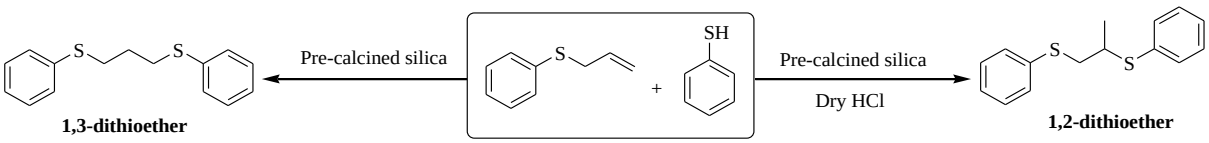

Scheme II.17. Reaction of allylphenylsulfane with thiophenol in the presence of dry HCl gas.

(iv) Last experiment was carried out with silica moistened with D_2O (Table II.2, entry 19), which afforded a mixture of 1,3-bis(phenylthio)propane and [2-D]1,3-dithioether as seen from the 1H NMR spectrum of the mixture and calculated to be in the ratio of 1:3.9. In the ^{13}C NMR spectrum, the deuterated carbon appeared as a triplet at δ 27.96, J = 20 Hz (see the experimental section, Figure II.2).This observation supports our proposed mechanism for conditions [B] which might occur through an initial thiol proton exchange with D_2O (PhS–H → PhS–D) as following Scheme II.18.

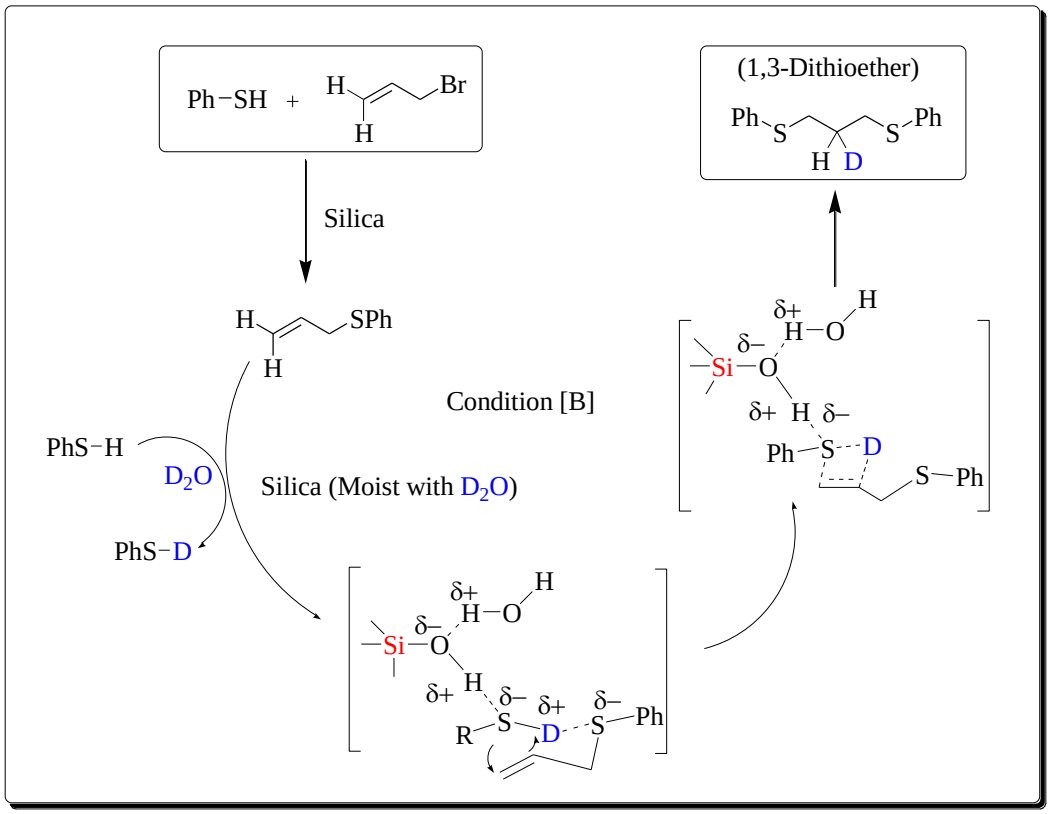

Scheme II.18. Plausible mechanism for the formation of 2-D-1,3-dithioether following condition [B]. [All experiments were performed by both the present author and my co-author as well as reproduced 2 times by both of us].

II.3.4. Recyclability of the catalyst

We have also checked the recyclability of the silica gel for both conditions [A] and [B]. We first performed the reaction between allyl bromide and thiophenol (1:2.5 ratio) under both

condition [A] and [B] and then the catalyst silica (0.5g) was separated by simple filtration using a filter paper and after washing with water followed by acetone, dried under vacuum for half an hour and then re-used for the next cycle. After 7th consecutive runs no catalytic loss of silica gel was found and so it might be possible to use it for the next cycles. The results are summarised in Figure II.3.

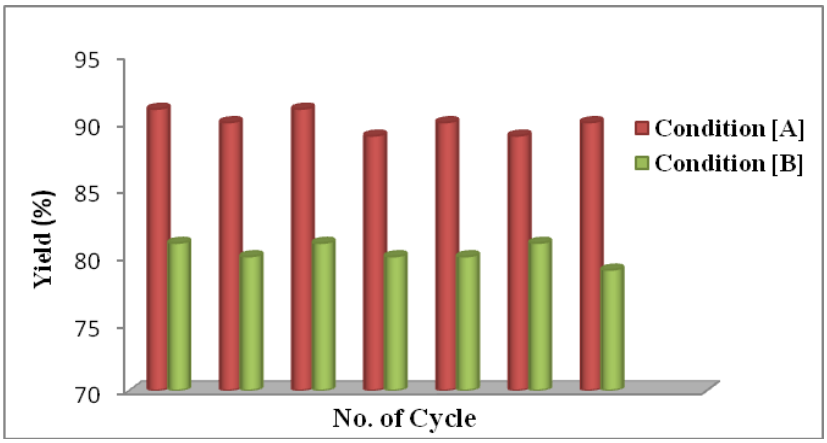

Figure II.3. Recyclability of silica gel for the one-pot regioselective addition of thiophenols to allyl bromide under pre-calcined silica (Condition [A]) and moistened silica (condition [B]). [Recylability of the catalyst was observed by the present author]

II.4. Conclusion

Based on the above discussions, we can conclude that the choice of commercially available silica gel, either dry or moistened, could lead to highly selective pathways for the preparation of different dithioethers. Interestingly, no such modification of silica gel surface was needed to promote the reaction rather its recyclability can influence its use in broaden way. In addition, the sequential reactions in one-pot protocols are robust, neutral, metal-free and notably selective with a broad range of substrates. The diverse reactivity of silica gel in the formation of vicinal or 1,3-dithioethers might not only spur the adaptation of existing procedures for selective dithioether preparation but also attract novel applications. Finally, such an alternative 'green' reaction methodology can make us more beneficial for further utilizations of the diverse reactivity of inexpensive and non-corrosive silica gel in solid-phase organic synthesis.

II.5. Experimental Section

II.5.1. General Information

All chemicals were purchased from commercial suppliers and used without further purification. IR spectra were recorded on an FTIR spectrophotometer (8300 Shimadzu) using

Nujol mulling for liquid compounds and KBr pellets for solid compounds. NMR spectra were recorded on a Varian AV–300 spectrometer with $CDCl_3$ as a solvent. Chemical shifts (δ) are reported in ppm and referenced to TMS for ^1H NMR spectra and residual solvent signals for ^{13}C NMR spectra as internal standards. Coupling constants (*J*) are reported in Hertz (Hz). Standard abbreviations indicating multiplicity were used as follows: s = singlet, d = doublet, t = triplet, q = quartet, qnt = quintet, m = multiplet. Melting points were determined by heating in an open capillary tube. High resolution mass spectra (HRMS) were performed in a Micromass Q-TOF Spectrometer under ESI (positive mode) by the services at the Indian Association for the Cultivation of Science, Kolkata.

Calcination: Commercially available silica gel (Merck, India; Grade: TLC; HF_{254}) was heated under vacuum at 150 °C for 1 h, cooled, and then be used for the reaction or stored in a glass-stoppered flask for at least two weeks.

Moistened silica: Commercially available silica gel (Merck, India; Grade: TLC; HF_{254}) was mixed with water and used for the reactions. For column chromatography: silica (60–120 μm) (Thomas Baker, India), and for TLC, Merck plates coated with silica gel 60, F_{254} were used.

II.5.2. General procedure for the preparation of 1,2- and 1,3-dithioethers (Table II.2, Route A & B)

Route [A]: A mixture of allyl bromide (1 mmol) and thiol (2.5 mmol) was intimately mixed with pre-calcined dry silica gel (Table II.2, for Entries 1, 3, 5, 7, 9, 11, 13, 15, 17 and 18) and stirred magnetically using a spin bar for several hours as listed in Table II.2.

Route [B]: A mixture of allyl bromide (1 mmol) and thiol (2.5 mmol) was intimately mixed with silica gel (0.5 g) moist with two-drops of water, (Table II. 2, for Entries 2, 4, 6, 8, 10, 12, 14 and 16) and stirred similarly as route [A] using a spin bar for hours as listed in Table II.2.

Both the reactions were monitored by tlc, and after completion, the silica gel was separated by simple filtration for both route and the products were isolated using diethyl ether/DCM as solvent and purified by column chromatography over silica gel. Elution with light petroleum furnished the desired dithioether. All products were characterized by IR, ^1H-, ^{13}C-NMR and HRMS data.

II.5.3. Procedure for the reaction using a mixture of silica and sodium silicate under condition [A] (Table II.2, Entry 20)

Equal quantities of silica gel and sodium silicate (1 g each) were intimately mixed, dried under vacuum at 100 ^{o}C for 1 h, then cooled and used for the reaction. The mixture (500 mg) was stirred in water (10 mL) and its pH was measured to be 12.7. A mixture of allyl bromide (1 mmol) and benzene thiol (2.5 mmol) was thoroughly mixed with the mixture of dry silica gel and sodium silicate (500 mg) and stirred the solid reaction mixture for 10 h at room temperature. After the reaction, the product was purified by column chromatography and characterized as 1-(1-(phenylthio)propan-2-ylthio)benzene (1,3-dithioether) in 82% yield.

II.5.4. Physical properties and spectral data of compounds (Table II.2, Entries 1-19)

Entry 1

1-(1-(phenylthio)propan-2-ylthio)benzene

The compound was obtained as a pale yellow liquid.

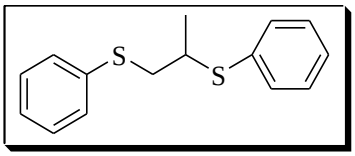

IR (Nujol) 1581.5, 740.6, 690.5 cm^{-1}; ^{1}H **NMR (CDCl$_3$, 300 MHz):** δ 1.40 (d, *J* = 6.2 Hz, 3H, CH_3), 2.72-2.80 (m, 1H, CH), 3.19-3.29 (m, 2H, CH_2), 7.11-7.33 (m, 10H, ArH).
^{13}C NMR (CDCl$_3$, 75 MHz): δ 19.2, 40.4, 42.3, 126.1, 127.2, 128.8, 129.5, 132.5, 133.9, 135.6.
HRMS (ESI) calcd for $C_{15}H_{16}KS_2$ 299.0330; found 299.0331.

Entry 2

1-(3-(phenylthio)propylthio)benzene

The compound was obtained as a colourless liquid.

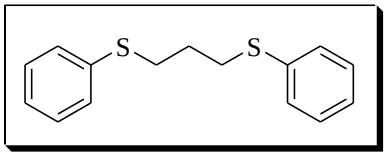

IR (Nujol) 690.5, 736.8 cm^{-1}.
^{1}H NMR (CDCl$_3$, 300 MHz): δ 1.93 (quintet, *J* = 6.9 Hz, 2H, CH_2), 3.02 (t, *J* = 6.9 Hz, 4H, $2CH_2$), 7.12-7.17 (m, 2H, ArH), 7.21-7.31 (m, 8H, ArH).

^{13}C NMR ($CDCl_3$, 75 MHz): δ 28.2, 32.3, 126.0, 128.8, 129.2, 135.9.
HRMS (ESI): calcd for $C_{15}H_{16}KS_2$ 299.0330; found 299.0331.

Entry 3
1-(2-(*p*-tolylthio)propylthio)-4-methylbenzene
The compound was obtained as a pale yellow liquid.

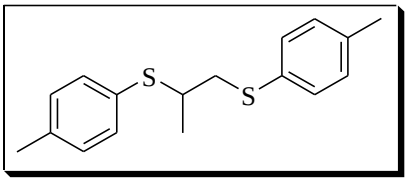

IR (Nujol): 1492.8, 802.3, 721.3 cm^{-1}.
^{1}H NMR ($CDCl_3$, 300 MHz): δ 1.36 (d, *J* = 6.9 Hz, 3H, CH_3), 2.27 (s, 3H, $ArCH_3$), 2.30 (s, 3H, $ArCH_3$), 2.70-2.74 (m, 1H, CH), 3.17-3.24 (m, 2H, CH_2), 6.98-7.22 (m, 6H, ArH), 7.21 (d, *J* = 8.1 Hz, 2H, ArH).
^{13}C NMR ($CDCl_3$, 75 MHz): δ 19.2, 20.9, 21.0, 41.0, 42.5, 129.5, 130.0, 130.1, 132.0, 133.0, 136.1, 137.2.
HRMS (ESI) calcd for $C_{17}H_{20}KS_2$ 327.0643; found 327.0645.

Entry 4
1-(3-(*p*-tolylthio)propylthio)-4-methylbenzene
The compound was obtained as a colourless liquid.

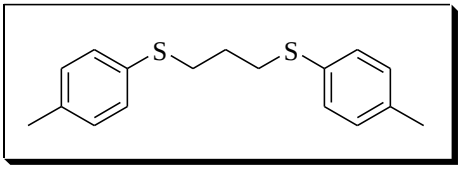

IR (Nujol): 1492.8, 1091.6, 1018.3, 802.3, 721.3, 505.3 cm^{-1}.
^{1}H NMR ($CDCl_3$, 300 MHz): δ 1.83 (qnt, *J* = 6.9 Hz, 2H, CH_2), 2.26 (s, 6H, $2ArCH_3$), 2.92 (t, *J* = 6.9 Hz, 4H, $2CH_2$), 7.02 (d, *J* = 7.8 Hz, 4H, ArH), 7.17 (d, *J* = 8.4 Hz, 4H, ArH).
^{13}C NMR ($CDCl_3$, 75 MHz): δ 21.0, 28.4, 33.1, 129.6, 130.2, 132.1, 136.2.
HRMS (ESI) calcd for $C_{17}H_{20}KS_2$ 327.0643; found 327.0644.

Entry 5
1-(1-(4-methoxyphenylthio)propan-2-ylthio)-4-methoxybenzene
The obtained was compound appeared as a colourless liquid.

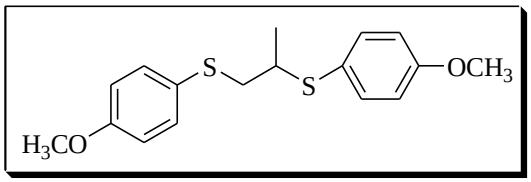

IR (Nujol): 1593.1, 1492.8, 1284.5, 1245.9, 1176.5, 1099.3, 1033.8, 1006.8, 825.5, 640.0, 524.6 cm^{-1}.

^{1}H NMR ($CDCl_3$, 300 MHz): δ 1.35 (d, *J* = 6.6 Hz, 3H, CH_3), 2.63-2.71 (m, 1H, CH), 3.00-3.16 (m, 2H, CH_2), 3.78 (s, 3H, OCH_3), 3.79 (s, 3H, OCH_3), 6.75-6.82 (m, 4H, ArH), 7.17-7.22 (m, 2H, ArH), 7.25-7.30 (m, 2H, ArH).

^{13}C NMR ($CDCl_3$, 75 MHz): δ 19.2, 42.2, 43.2, 55.2, 114.3, 114.5, 123.9, 125.9, 132.9, 135.6, 158.8, 159.5.

HRMS (ESI): calcd for $C_{17}H_{20}O_2KS_2$ 359.0542; found 359.0543.

Entry 6

1-(3-(4-methoxyphenylthio)propylthio)-4-methoxybenzene

The compound was obtained as colourless liquid.

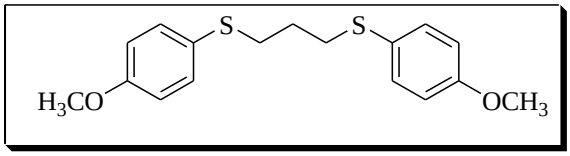

IR (Nujol): 1593.1, 1492.8, 1284.5, 1242.1, 1176.5, 1033.8, 825.5, 620.0, 525.0 cm^{-1}.

1H NMR ($CDCl_3$, 300 MHz): δ 1.80 (qnt, *J* = 6.9 Hz, 2H,CH_2), 2.90 (t, *J*= 6.9 Hz, 4H, $2CH_2$), 3.78 (s, 6H, $2OCH_3$), 6.78-6.83 (m, 4H, ArH), 7.25-7.32 (m, 4H,ArH).

^{13}C NMR ($CDCl_3$, 75 MHz): δ 28.5, 34.4, 55.2, 114.5, 125.9, 133.4, 158.9.

HRMS (ESI): calcd for $C_{17}H_{20}O_2KS_2$ 359.0542; found 359.0540.

Entry 7

1-(2-(4-chlorophenylthio)propylthio)-4-chlorobenzene

The compound was obtained as a pale yellow liquid.

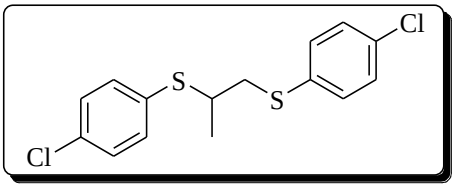

IR (Nujol): 1176.5, 1095.5, 1010.6, 817.8, 744.5, 550.0, 493.7 cm^{-1}.

^{1}H NMR ($CDCl_3$, 300 MHz): δ 1.37 (d, *J* = 6.6 Hz, 3H, CH_3), 2.71-2.79 (m, 1H, CH), 3.12-3.19 (m, 2H, CH_2), 7.10 (d, *J* = 8.4 Hz, 2H, ArH), 7.17 (d, *J* = 8.4 Hz, 2H, ArH), 7.21 (s, 4H, ArH).
^{13}C NMR ($CDCl_3$, 75 MHz): δ 19.2, 40.8, 42.7, 128.9, 129.0, 131.0, 132.3, 133.5, 133.8, 134.0.
HRMS (ESI): calcd for $C_{15}H_{14}Cl_2KS_2$ 366.9551; found 366.9557.

Entry 8
1-(3-(4-chlorophenylthio)propylthio)-4-chlorobenzene
The compound was obtained as a no-viscous colourless liquid.

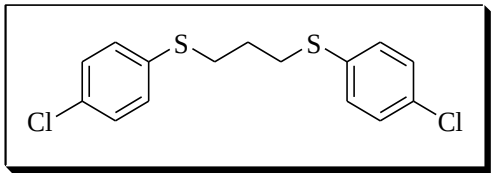

IR (Nujol): 1249.8, 1095.5, 1010.6, 813.9, 744.5, 540.0, 489.9 cm^{-1}.
^{1}H NMR ($CDCl_3$, 300 MHz): δ 1.89 (quintet, *J* = 6.9 Hz, 2H, CH_2), 2.99 (t, *J* = 6.9 Hz, 4H, $2CH_2$), 7.22 (s, 8H, ArH).
^{13}C NMR ($CDCl_3$, 75 MHz): δ 28.0, 32.5, 129.0, 130.7, 132.1, 134.3.
HRMS (ESI): calcd for $C_{15}H_{14}Cl_2KS_2$ 366.9551; found 366.9549.

Entry 9
1-(1-(4-fluorophenylthio)propan-2-ylthio)-4-fluorobenzene
The compound was obtained as a pale yellow liquid.

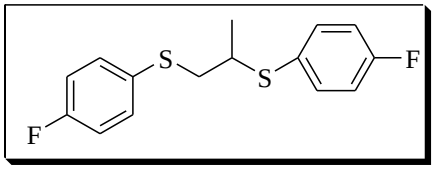

IR (Nujol) 1589.2, 1488.9, 1230.5, 1157.2, 1091.6, 1006.0, 980.0, 825.5, 620.0, 513.0 cm^{-1}.
^{1}H NMR ($CDCl_3$, 300 MHz): δ 1.37 (d, *J* = 6.6 Hz, 3H, CH_3), 2.73-2.78 (m, 1H, CH), 3.06-3.15 (m, 2H, CH_2), 6.90-7.00 (m, 4H, ArH), 7.18-7.29 (m, 4H, ArH),.
^{13}C NMR ($CDCl_3$, 75 MHz): δ 19.2, 41.7, 41.8, 43.1, 115.8, 115.82, 116.09, 116.1, 128.7, 128.8, 130.5, 130.54, 132.5, 132.6, 135.3, 135.4, 160.2, 160.8, 163.4, 164.1.
HRMS (ESI): calcd for $C_{15}H_{14}F_2KS_2$ 335.0142; found 335.0144.

Entry 10
1-(3-(4-fluorophenylthio)propylthio)-4-fluorobenzene
The isolated liquid compound was pale yellow in colour.

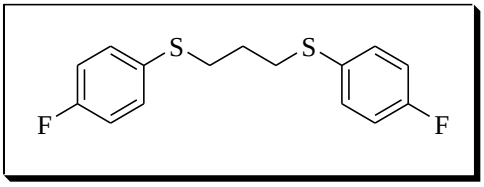

IR (Nujol) 1589.2, 1488.9, 1226.6, 1157.2, 1091.6, 1014.5, 825.5, 628.8, 513.0 cm^{-1}.
^{1}H NMR ($CDCl_3$, 300 MHz): δ 1.85 (quintet, *J* = 6.9 Hz, 2H, CH_2), 2.96 (t, *J* = 6.9 Hz, 4H, $2CH_2$), 6.94-7.00 (m, 4H, ArH), 7.28-7.33 (m, 4H, ArH).
^{13}C NMR ($CDCl_3$, 75 MHz): δ 28.3, 33.7, 115.8, 116.1, 130.6, 130.7, 132.5, 132.6, 160.2, 163.4. **HRMS (ESI)** calcd for $C_{15}H_{14}F_2KS_2$ 335.0142; found 335.0143.

Entry 11

2-(1-(2,5-dimethylphenylthio)propan-2-ylthio)-1,3-dimethylbenzene

The compound was obtained as a colourless liquid.

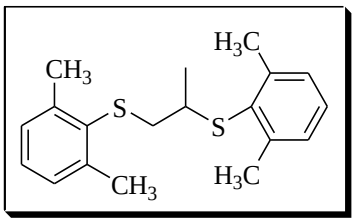

IR (Nujol): 1600.8, 1558.4, 1485.1, 1176.5, 1064.6, 1041.5, 1006.8, 879.5, 810.0, 690.0, 550.0, 451.3 cm^{-1}.
^{1}H NMR ($CDCl_3$, 300 MHz): δ 1.45 (d, *J* = 6.6 Hz, 3H, CH_3), 2.20 (s, 3H, $ArCH_3$), 2.23 (s, 3H, $ArCH_3$), 2.29 (s, 3H,$ArCH_3$), 2.35 (s, 3H, $ArCH_3$), 2.71-2.80 (m, 1H, CH), 3.21-3.26 (m, 2H, CH_2), 6.88-7.09 (m, 6H, ArH).
^{13}C NMR ($CDCl_3$, 75 MHz): δ 19.4, 19.9, 20.3, 20.77, 20.8, 39.9, 41.6, 126.9, 128.2, 129.5, 130.1, 130.3, 133.1, 133.3, 134.4, 135.0, 135.9, 137.0.

Entry 12

2-(3-(2,5-dimethylphenylthio)propylthio)-1,3-dimethylbenzene

The compound was obtained as a colourless liquid.

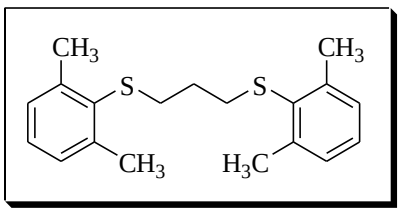

IR (Nujol) 1600.8, 1060.8, 806.2 cm^{-1}.

^{1}H NMR ($CDCl_3$, 300 MHz): δ 1.99 (quintet, *J* = 6.9 Hz, 2H, CH_2), 2.28-2.32 (s, 12H, $4CH_3$), 3.03 (t, *J* = 6.9 Hz, 4H, $2CH_2$), 6.89 (d, *J* = 6.9 Hz, 2H, ArH), 7.03-7.07 (m, 4H, ArH).
^{13}C NMR ($CDCl_3$, 75 MHz): δ 19.9, 21.0, 28.2, 31.9, 126.6, 128.7, 130.0, 134.5, 135.0, 135.9.
HRMS (ESI) calcd for $C_{19}H_{24}K_2S_2$ 394.0594; found 394.0597.

Entry 13
1-(2-(pentylthio)propylthio)pentane
The compound was obtained as a pale yellow liquid.

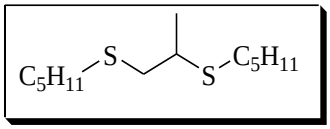

IR (Nujol): 1168.8 cm^{-1}.
^{1}H NMR ($CDCl_3$, 300 MHz): δ 0.88-0.92 (m, 6H, $2CH_3$), 1.29-1.39 (m, 8H, $4CH_2$), 1.35 (d, *J* = 6.9 Hz, 3H, CH_3), 1.54-1.61 (m, 4H, $2CH_2$), 2.50-2.58 (m, 5H, CH & 2 S-CH_2), 2.82-2.88 (m, 2H, S-C<u>H</u>$_2$-CH).
^{13}C NMR ($CDCl_3$, 75 MHz): δ 13.9, 20.2, 22.2, 29.3, 29.4, 30.6, 30.9, 31.1, 33.9, 39.6, 39.8;
HRMS (ESI): calcd for $C_{13}H_{28}KS_2$ 287.1269; found 287.1271.

Entry 14
1-(3-(pentylthio)propylthio)pentane
The compound was obtained as a colourless liquid.

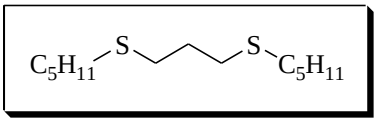

IR (Nujol): 1253.6 cm^{-1}; ^{1}H NMR ($CDCl_3$, 300 MHz): δ 0.90 (t, *J* = 6.9 Hz, 6H, $2CH_3$), 1.29-1.41 (m, 8H, 4CH2), 1.56-1.61 (m, 4H, $2CH_2$), 1.86 (quintet, *J* = 6.9 Hz, 2H, CH_2), 2.51 (t, *J* = 7.2 Hz, 4H, $2CH_2$), 2.59-2.62 (m, 4H, $2CH_2$).
^{13}C NMR ($CDCl_3$, 75 MHz): δ 14.0, 22.3, 29.3, 29.4, 31.0, 31.1, 32.1.
HRMS (ESI): calcd for $C_{13}H_{28}KS_2$ 287.1269; found 287.1270

Entry 15
(1-(cyclohexylthio)propan-2-ylthio)cyclohexane
The compound obtained as a pale yellow liquid.

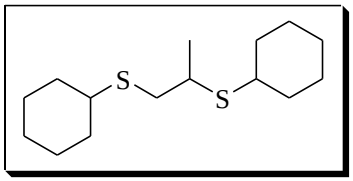

IR (Nujol) 1265.2, 995.2, 887.2, 817.8, 721.3 cm^{-1}.
^{1}H NMR ($CDCl_3$, 300 MHz): δ 1.29-1.32 (m, 10H, CyH), 1.34 (d, *J* = 6.6 Hz, 3H, CH_3), 1.62 (s, 2H, CyH), 1.76 (s, 4H, CyH), 1.95 (s, 4H, CyH), 2.49-2.75 (m, 3H, 2CyH, CH), 2.84-2.97 (m, 2H, CH_2).
^{13}C NMR ($CDCl_3$, 75 MHz): δ 20.7, 25.6, 25.9, 25.94, 33.5, 33.6, 33.7, 33.9, 37.8, 38.2, 42.4, 44.2.
HRMS (ESI): calcd for $C_{15}H_{28}KS_2$ 311.1269; found 311.1271.

Entry 16
(3-(cyclohexylthio)propylthio)cyclohexane
The compound obtained as a colourless liquid.

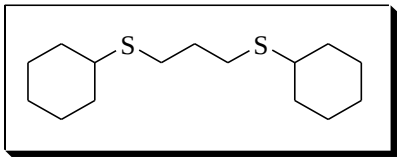

IR (Nujol): 1203.5, 999.1, 883.3, 817.8, 717.5 cm^{-1}.
^{1}H NMR ($CDCl_3$, 300 MHz): δ 1.24-1.41 (m, 11H, Cy-H), 1.60-1.99 (m, 12H, Cy-H & CH_2), 2.63 (t, *J* = 7.2 Hz, 4H, 2 S-CH_2), 2.97-2.99 (m, 2H, 2 S-CH).
^{13}C NMR ($CDCl_3$, 75 MHz): δ 25.7, 25.8, 25.9, 26.1, 29.0, 30.1, 33.66, 33.7, 37.8, 33.9, 43.4, 43.5, 44.7, 49.3.
HRMS (ESI): calcd for $C_{15}H_{28}KS_2$ 311.1269; found 311.1270.

Entry17
1-(1-(2-methoxyphenylthio)propan-2-ylthio)-2-methoxybenzene
The compound obtained as a pale yellow liquid.

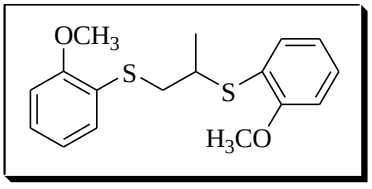

IR (Nujol):1577.7, 1296.1, 1272.9, 1242.1, 1180.4, 1130.2, 1072.3, 1026.1, 833.2, 794.6, 748.3, 721.3, 675.0, 525.0 cm^{-1}.

^{1}H NMR ($CDCl_3$, 300 MHz): δ 1.42 (d, *J* = 6.9 Hz, 3H, CH_3), 2.64-2.72 (m, 1H, CH), 3.24-3.37 (m, 2H, CH_2), 3.70 (s, 3H, OCH_3), 3.71 (s, 3H, OCH_3), 6.74-6.84 (m, 4H, ArH), 7.07-7.23 (m, 4H, ArH).
^{13}C NMR ($CDCl_3$, 75 MHz): δ 18.8, 38.7, 39.8, 55.2, 110.2, 110.4, 120.49, 120.5, 121.8, 123.1, 127.3, 128.4, 130.3, 133.2, 157.4, 158.4.
HRMS (ESI): calculated for $C_{17}H_{20}O_2NaS_2$ 343.0802; found 343.0801.

Entry 18
2-(1-(naphthalene-6-ylthio)propan-2-ylthio)naphthalene
The compound obtained as a white crystalline solid with melting point 91–93 ^oC.

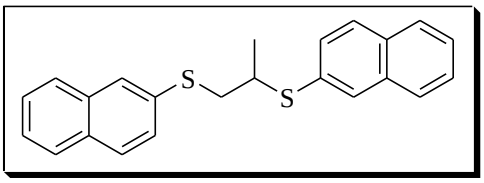

IR (KBr): 817.8, 740.6, 478.3 cm^{-1}.
^{1}H NMR ($CDCl_3$, 300 MHz): δ 1.47 (d, *J* = 6.9 Hz, 3H, CH_3), 2.82-2.90 (m, 1H, CH), 3.37-3.44 (m, 2H, CH_2), 7.23 (d, *J* = 8.4 Hz, 1H, ArH), 7.33-7.44 (m, 6H, ArH), 7.48-7.55 (m, 3H, ArH), 7.61 (d, *J* = 8.4 Hz, 1H, ArH), 7.67-7.74 (m, 3H, ArH).
^{13}C NMR ($CDCl_3$, 75 MHz): δ 19.2, 40.5, 42.4, 125.7, 126.1, 126.4, 126.43, 127.0, 127.3, 127.5, 127.57, 127.6, 128.38, 128.4, 129.7, 130.9, 131.5, 131.7, 132.2, 132.9, 133.5, 133.55.
HRMS (ESI): calculated for $C_{23}H_{20}KS_2$ 399.0643; found 399.0645.

Entry 19
1-(3-(phenylthio)propylthio)benzene and its 2-Deuterated product
The mixture containing both isomer was obtained as a colourless liquid mixture.

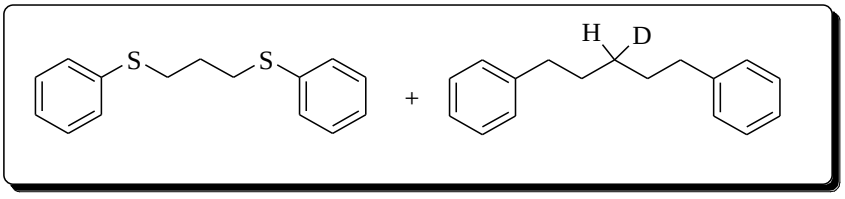

^{1}H NMR ($CDCl_3$, 300 MHz): δ 1.90-1.99 (m, CHD & CH_2), 3.03-3.07 (m, $2CH_2$, each from the mixture), 7.14-7.33 (m, 10 ArH, each from the mixture).
^{13}C NMR ($CDCl_3$, 75 MHz): δ 27.9 (t, *J* = 20 Hz, CHD), 28.3, 32.3, 32.4, 126.1, 128.9, 129.4, 136.0.

^{1}H NMR and ^{13}C NMR spectra of the mixture of Entry 19 (Table II.2) in $CDCl_3$

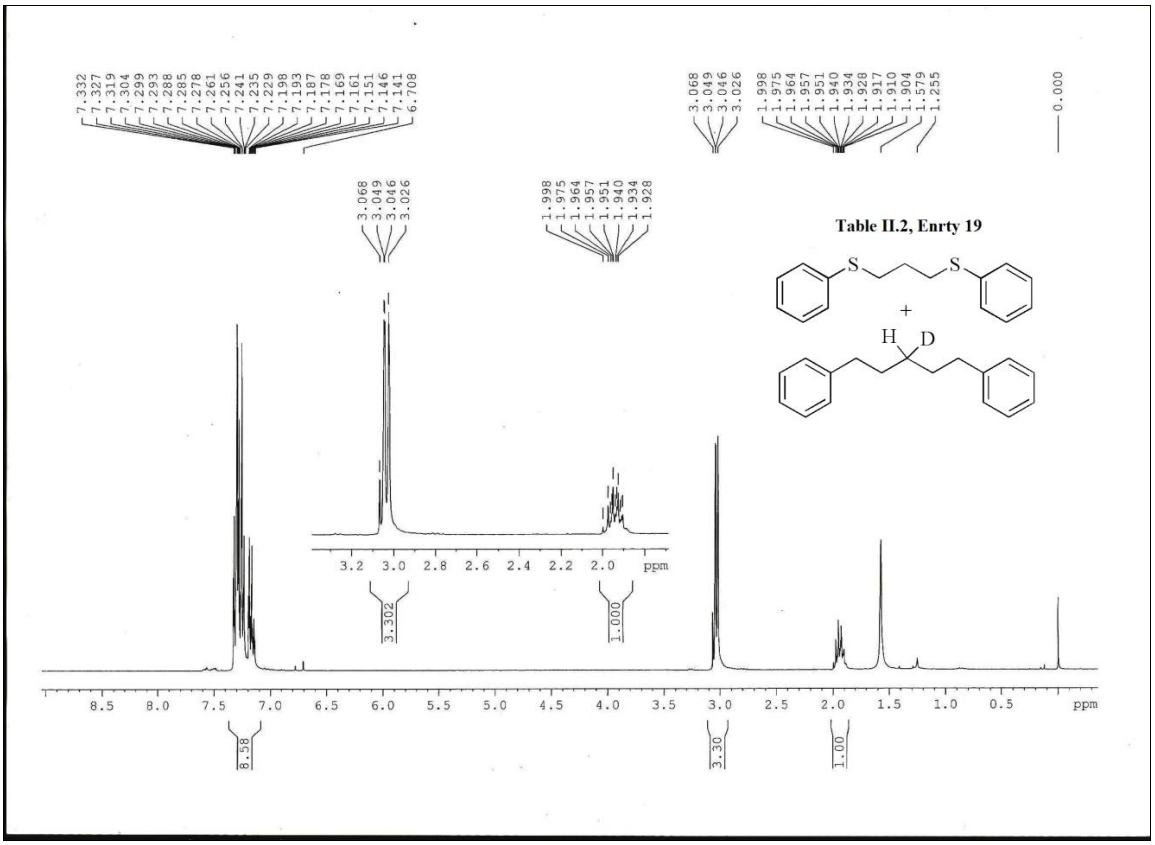

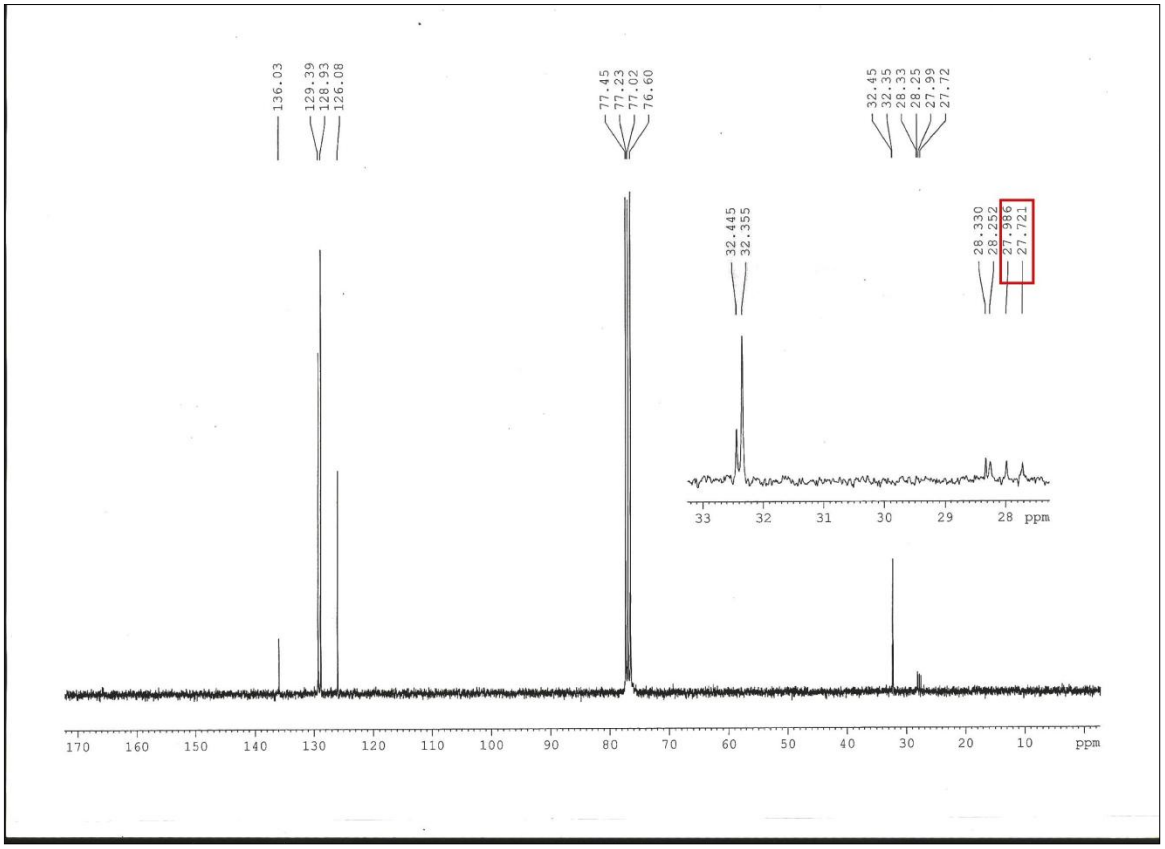

II.6. References

References for chapter II are given in **BIBLIOGRAPHY** under **CHAPTER II** (page 170–173).

CHAPTER III
Section A

Graphene oxide (*GO*): *A* convenient metal-free "Carbocatalyst" for diverse organic reactions

III.A.1. Introduction

After the remarkable synthesis of monolayer graphene,[1] graphene-based materials have became most focused arena of research in material science because of their involvement in multidisciplinary field like physics, chemistry, biology, applied science and engineering. Owing to high surface area, conductivity, presence of different active sites, such carbonaceous materials are considered as a new class of catalysts called "carbocatalysts".[2] Recently, graphene-based materials have widely explored as metal-free catalysts or as supports,[3] for immobilizing active species to facilitate a number of useful synthetic transformations and are now considered as a greener alternative for metal-based catalysts.[2] After the first synthetic application of graphene-based materials such as graphene oxide (GO) as heterogeneous carbocatalysts by Bielawski and his co-workers,[4] the concept of "carbocatalysis" is considered as an fascinating new direction in chemistry and materials science. Furthermore, due to large surface area, conjugated domains, rich active sites like acidic and basic sites, π-electron domain of carbon, oxygen debris, holes, defects, armchair and zigzag edges as in Figure III.A.1, graphene oxide and its derivatives have been widely accepted as excellent carbocatalysts for various organic transformations.[2]

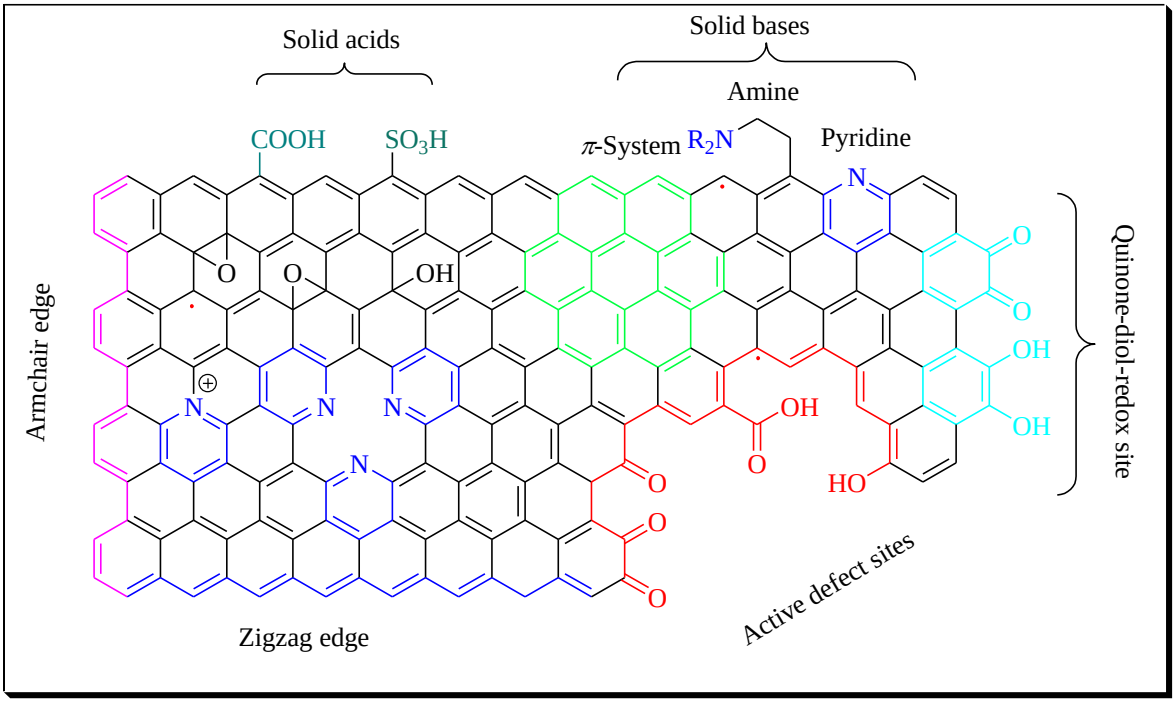

Figure III.A.1. Various active sites present in the graphene-based materials like GO and rGO.

Among other derivatives of graphene-based materials, GO has been most extensively cultivated in carbocatalysis due to its highly acidic nature (pH 4.5 at 0.1mg/ml),[5] as well as

highly decorated surface with myriad of different oxygen functionalities. GO mostly utilized as an oxidant in various organic reactions[6] and a very few number of synthetic application are there exploiting its acidic behaviour.[7]

The present chapter represents a brief review on carbocatalysis by GO along with its catalytic application towards thioacetalization of carbonyl compounds.

III.A.2. Present Work: Background and Objectives

GO has been widely explored as an efficient heterogeneous carbocatalyst for the various well known organic transformations (Scheme III.A.1) and is considered as an excellent alternative for old traditional non-carbonaceous metal-based catalysts. [2,3,5,8]

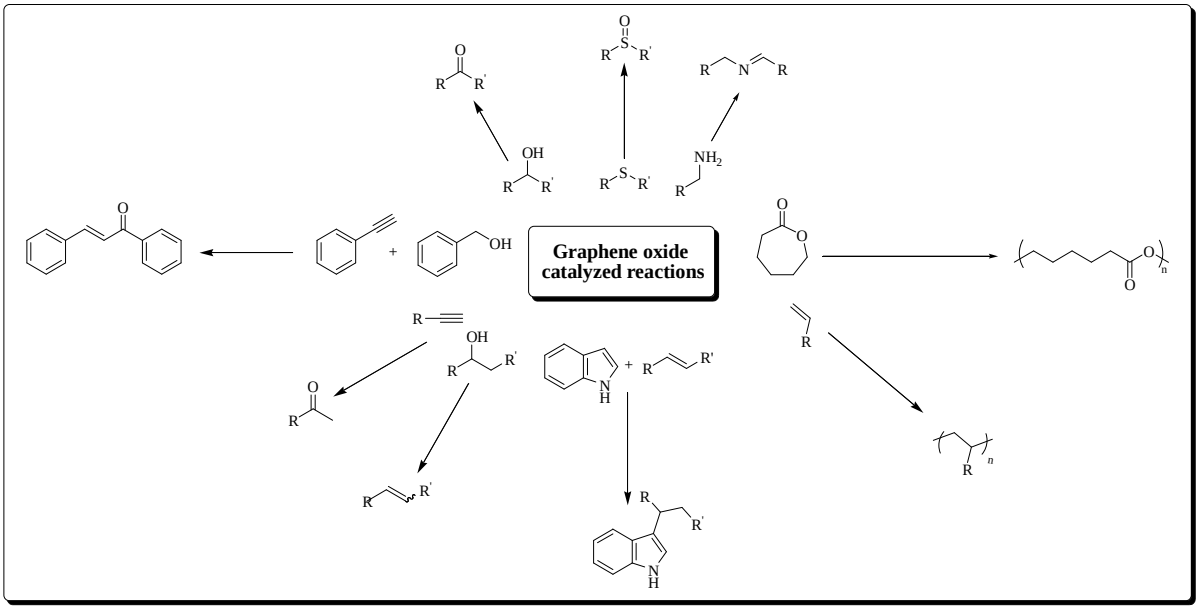

Scheme III.A.1. GO–catalyzed various organic transformations.

Lee *et. al.*[9] has reported that GO having high surface area containing various oxygenated functional groups can hold metal cations of any size by forming a metal-centered intercalated structure like GO-metal-GO layers and can act as an efficient recyclable phase transfer catalyst (GO-PTC). They have employed this GO-PTC for the Michael addition between *trans*-β-nitrostyrene and 2,4-pentanedione at room temperature (Scheme III.A.2).

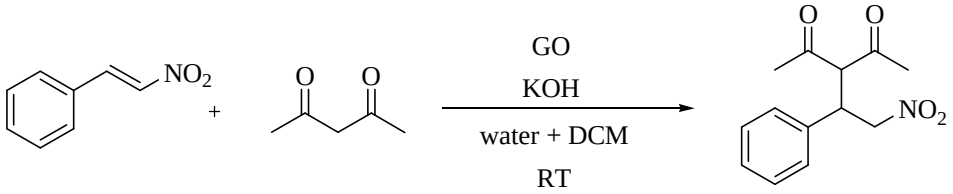

Scheme III.A.2. Michael addition reaction of *trans*-β-nitrostyrene and 2,4-pentanedione.

Using GO as an acid catalyst, the Aza-Michael addition of various amines to electron deficient olefins forming various amino-substituted compounds is found to proceed under mild conditions with excellent product yield and with shorter time (Scheme III.A.3).[10]

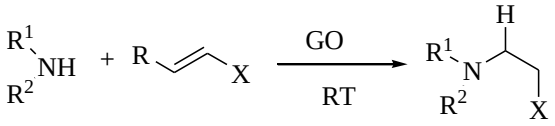

R= H, CH_3
R^1= Et, *n*-Bu, *n*-Pr, Bz
R^2= Et, *n*-Bu, *n*-Pr, Bz
X= CN, $CONH_2$, $COOCH_3$

Scheme III.A.3. GO-catalyzed Aza-Michael addition reaction.

GO has been used as solid catalyst for the synthesis of dipyrromethanes and calix[4]pyrroles both in organic and aqueous solvent at room temperature (Scheme III.A.4).[11] In this context, it has been reported that GO materials give better yield in comparison to Zeolite-HY, H-ZSM and Amberlyst^{TM}–15 under the same reaction condition.

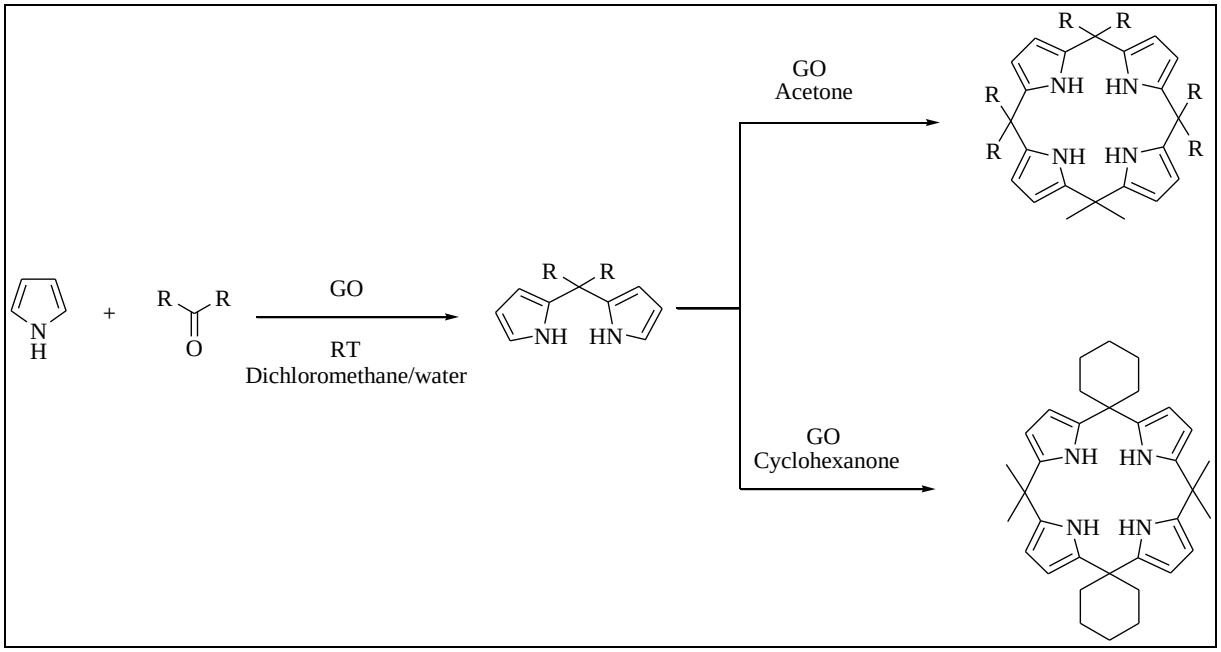

Scheme III.A.4. GO–catalyzed synthesis of dipyrromethane and calix[4]pyrrole.

From our laboratory, it is reported that GO can act as an efficient and a mild carbocatalyst for the one-pot sequential dehydration-hydrothiolation reaction to give unsymmetrical thioethers from a mixture of secondary aryl alcohols and thiols under metal-free condition (Scheme III.5).[12]

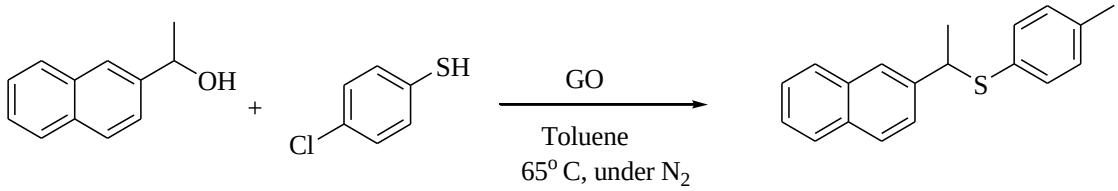

Scheme III.A.5. One-pot sequential dehydration-hydrothiolation catalyzed by graphene oxide.

GO has been found to act as an oxidising agent for the oxidation of additive NaI to liberate I_2 and also as a recoverable and reusable catalyst for the synthesis of biologically important motifs imidazo[1,2-*a*]pyridines and 3-sulfenylimidazo[1,2-*a*]pyridines (Scheme III.A.6) *via* one-pot multi-component reactions (MCR).[13]

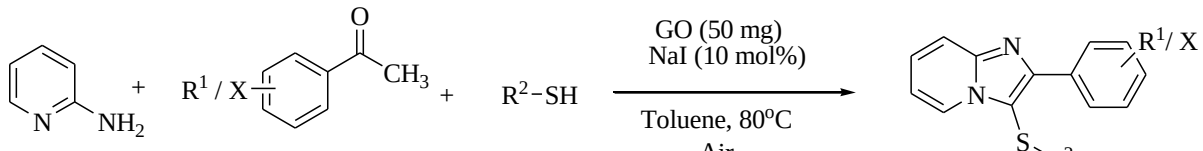

R^1= aryl/ naphthyl
X= Cl, Br, I
R^2= Aryl/alkyl

Scheme III.A.6. GO–catalyzed one-pot multi-component synthesis of 3-sulfenylimidazo[1,2-*a*]pyridines.

The excellent catalytic behaviour of graphene oxide as carbocatalyst has been utilized in the aerobic oxidation of 5-hydroxymethylfulfural (HMF) to 2,5-diformylfuran (DFF) using TEMPO (2,2,6,6-tetramethylpiperidin-1-oxyl) as co-catalyst (Scheme III.A.7).[14]

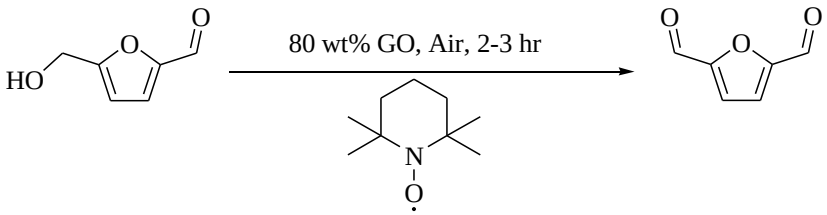

Scheme III.A.7. GO/TEMPO–catalyzed aerobic oxidation of 5-hydroxymethylfulfural to 2,5-diformylfuran.

Primarily, it was believed that various carboxylic groups or other oxygenated functional groups present on the surface of GO are mainly responsible for GO's acidity.[15a] But, in 2013, Eigler and his co-workers,[16] reported that during the oxidation of graphite by Hummers' method results in the formation of cyclic organosulfates on the surface of GO, which are susceptible to hydrolysis during the aqueous workup (Scheme III.A.8). These sulfate groups (estimated to be present at approximately one sulfate per twenty carbon atoms) are now also supposed to be the source of GO's acidity (pKa 3–4 in water).

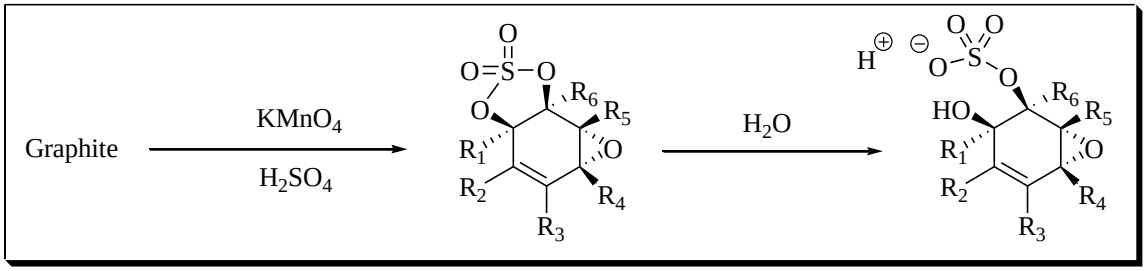

Scheme III.A.8. Organosulfates present in GO prepared *via* the Hummers' method; susceptible to hydrolysis, leading to the formation of acidic sulfate species in the final product.

Garcia *et al.*[17] reported that minor hydrogen sulfate groups introduced on the surface of GO during its preparation by Hummers' method renders this material as a highly efficient, recyclable acid catalyst for the ring opening of epoxides with methanol and other primary alcohols as nucleophile (Scheme III.A.9). In their method, only 5 mg of GO has been used to catalyse the ring opening of styrene oxide in methanol *via* S_N1 mechanism to form 2-methoxy-2-phenyl ethanol.

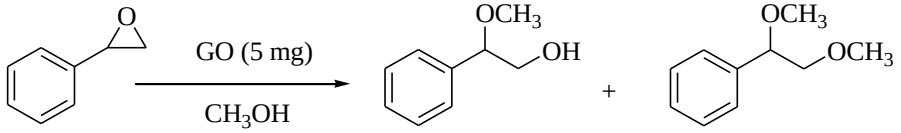

Scheme III.A.9. GO–catalyzed ring opening of styrene oxide in methanol.

Dakshinamoorthy *et al.*[18] also reported GO can act as a metal free and highly efficient heterogeneous catalyst for the acetalalization of various aromatic and aliphatic aldehydes in methanol (Scheme III.A.10). They have shown that sulfate groups introduced on GO spontaneously during Hummers are responsible for catalysis.

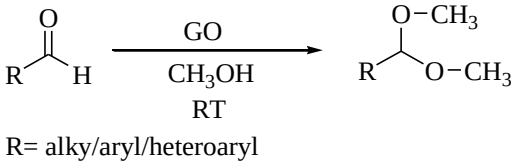

Scheme III.A.10. Acetalization of aldehydes at room temperature using GO as a solid acid catalyst.

This work of Garcia *et al.* motivated us to exploit the acidic nature of GO for the thioacetalization of carbonyl compounds.

On the other hand, in the multistep synthesis of natural and non-natural products, protection of carbonyl compounds is a basic need for such synthetic steps.[19]

Dithioacetalization is one of the most useful way to protect carbonyl compounds forming their dithioacetals due to their inherent stability under both acidic and basic conditions.[20] In addition, dithioacetals can also be used as nucleophilic acylating agents, masked methylene functions in the C-C bond.[20,21] Generally, thioacetals are formed as the results of Brønsted and Lewis acid catalyzed condensation reactions of aldehydes and ketones with thiols or dithiols and a vast number of methods are available in the literature.[22] Due to various advantages of heterogeneous catalysts over homogeneous catalyst like ease of separation, simple work-up procedure and also reusability a myriad of heterogeneous acid catalysts,[23] have been employed for the preparation of thioacetals forming reactions over the past decade.

As a heterogeneous solid acid catalyst Preyssler-type heteropoly acid ($H_{14}NaP_5W_{30}O_{110}$) has been used as a new, mild and efficient catalyst for protection of a variety of carbonyl compounds with 1,3-propane dithiol (Scheme III.A.11).[24]

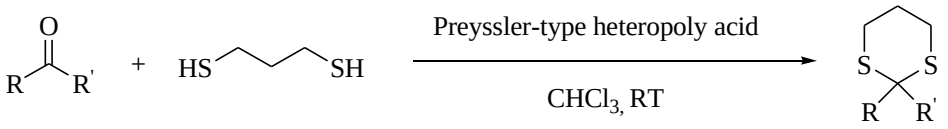

Scheme III.A.11. Hetero poly acid catalyzed dithioacetalization.

A catalytic amount of *p*-toluenesulfonic acid and silica gel has been utilized for the protection of carbonyl compounds (Scheme III.A.12).[25]

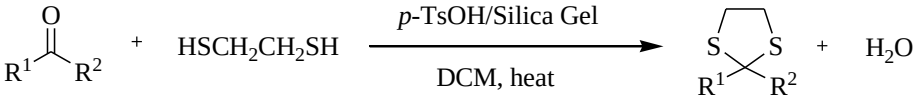

R^1 = Alkyl, aryl
R^2 = H, Alkyl, Aryl

Scheme III.A.12. Dithioacetalization of carbonyl compounds using *p*-toluenesulfonic acid and silica gel.

Montmorillonite K-10 clay has been found to be a mild and efficient solid catalyst for the protection of a variety of carbonyl compounds, such as oxathiolanes, with 2-mercaptoethanol in good to excellent yields (Scheme III.A.13).[26]

R^1 = Alkyl, aryl, allyl, heterecyclic
R^2 = H, alkyl

Scheme III.A.13. Montmorillonite K-10 clay catalyzed oxathioacetalization of carbonyl compounds.

Silica sulphuric acid (SSA) has been found to act an efficient and reusable catalyst for chemoselective dithioacetalization of aldehydes over ketones in excellent yields (Scheme III.A.14).[27]

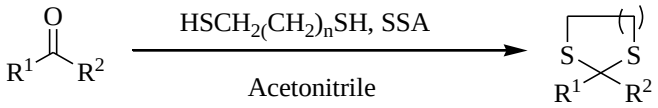

R 1= alkyl, aryl or cycloalkyl
R2 = H

Scheme III.A.14. Silica sulphuric acid catalyzed dithioacetalization of aldehydes.

A solid supported, odourless reagent prepared by the combination of dimercaptoalkane equivalents and acid immobilized as dithianylium or dithiolanylium tetrafluoroborate salt on solid supports allows the conversion of aldehydes into dithianes or dithiolanes with high yields and purities often without the need for purification (Scheme III.A.15).[28]

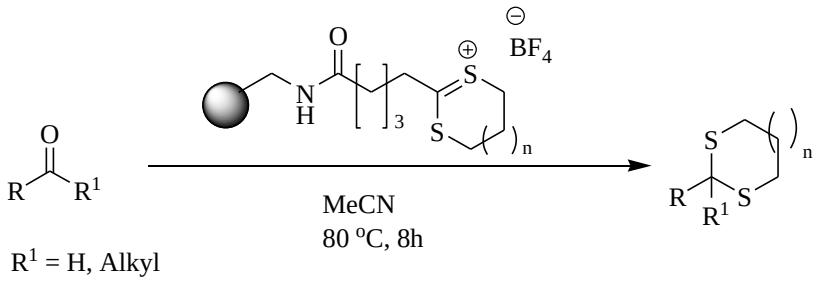

R1 = H, Alkyl

Scheme III.A.15. Dithioacetalization of aldehydes and ketones by resin-bound reagents.

However, moisture sensitivity and reactivity of thioacetals towards acidic sources for reversible reactions cause a great limitation for their preparation in high yield. Again, most of the methods are very often unsuitable for use in large-scale applications. Moreover, while in most cases the catalyst is not recoverable, heterogeneous acid catalysts often do not find wide applicability to various substrates.

We herein report an efficient and practical method for the preparation of dithioacetals from aryl/alkyl aldehydes with the aid of catalytic amount graphene oxide (GO). The reaction is highly selective to aldehydes and can be carried out under solvent-free and mild conditions. In addition, the reaction is also applicable to a variety of aryl and alkyl aldehydes including hetero-aryl aldehydes with diverse aromatic/aliphatic thiols. Further extension of this reaction using GO has been continued for the preparation of unsymmetrical dithioacetals resulting in excellent yields by using two different aliphatic thiols (Scheme III.A.16).

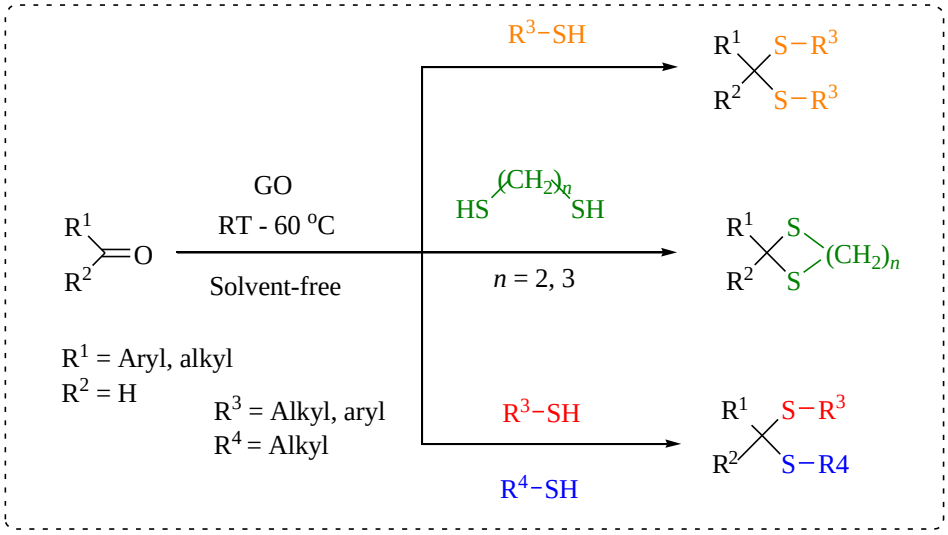

Scheme III.A.16. GO–catalyzed diverse dithioacetals formation.

Although GO is commonly used as an oxidation catalyst[5] and thiols can produce disulfides *via* oxidative coupling in the presence of GO,[5a] we demonstrate here that the catalytic role of GO can be varied and tuned by changing its loading and reaction conditions.

III.A.3. Present Work: Results and Discussion

III.A.3.1. Preparation and characterization of graphene oxide

We have started our investigation by preparing GO from graphite powder following modified Hummers' method.[29b] To an ice-cold concentrated sulfuric acid (46 mL) was slowly added sodium nitrate (0.1 g) and then graphite powder (2 g) with vigorous magnetic stirring. After the complete addition of graphite powder, potassium permanganate (6 g) was added to the reaction mixture very slowly, keeping the temperature within 0–5 ^{o}C to avoid any possible explosion. The mixture was allowed to stir at room temperature for 6 h forming a thick paste. It was diluted with distilled water (92 mL) under stirred condition. The temperature of the solution was raised to about 90 ^{o}C and the mixture was allowed to stir for 30 min. Finally, 280 mL water was added followed by slow addition of 3 mL H_2O_2 (30%). The colour of the solution changes from dark brown to yellowish brown. The overall solution was exfoliated under sonication followed by centrifuged at 5000 rpm to collect the solid mass at the bottom. This process was continued for several times until the pH of the supernatant aqueous part becomes neutral (using pH paper). Finally, the brown mass was collected and dried at 60 ^{o}C under vacuum to obtain solid graphene oxide.

The characterization of GO was done by FT–IR spectroscopy and compared with reported FT–IR spectrum. GO exhibits a broad peak around 3360 cm^{-1}, which was assigned

to O−H stretching vibrations. The other stretching vibration bands at 1719, 1618, 1412 and 1218 cm^{-1} are assigned respectively for COOH, C=C, O−H, and C−O (epoxy) groups, respectively.[30] The peak at 1052 cm^{-1} was assigned to SO_3−H stretching vibration bands.[18,30]

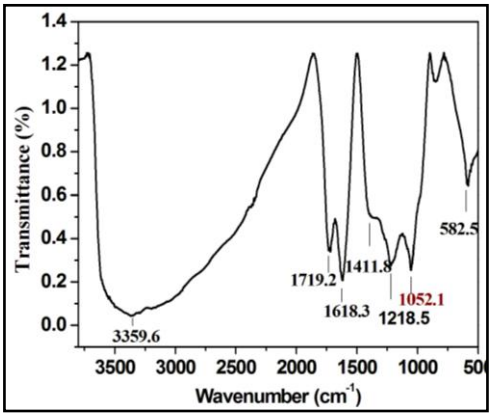

Figure III.A.2. FT–IR spectra of GO.

We investigated our optimization of the GO-catalyzed thioacetalization by taking *p*-anisaldehyde and *n*-pentanethiol (1: 2.2 ratios) as the model case and the results are shown in Table III.A.1. Initially, a mixture of the aldehyde and mercaptan (in 1:2.2 ratios) was gently stirred in neat at room temperature in the presence of GO (10 mg $mmol^{-1}$ of the aldehyde) under aerobic condition. Monitoring the reaction by tlc at intervals showed the presence of the starting aldehyde along with the desired dithioacetal even after 24h. The reaction was stopped and the desired dithioacetal obtained in 51% yield (entry 1). Increasing the quantity of GO (50 mg $mmol^{-1}$ of the aldehyde) revealed that nearly complete conversion of the aldehyde to dithioacetal could be achieved at room temperature within 3h under aerobic condition (entry 3). Significantly, there was no detectable amount of disulfide formed under the aerobic condition. A control experiment was performed in the absence of the GO under similar reaction condition, which did not produce any dithioacetal even after 24h (entry 4). In order to see any faster conversion, the reaction was also carried out at 60 ^oC. This however resulted in partial conversion of the mercaptan into the corresponding disulfide along with the desired dithioacetal in relatively lower yield (entry 5). Moreover, the same reaction at 60 ^oC and under a blanket of N_2 did not stop the formation of disulfide (entry 6). Conducting the experiments in a solvent (THF, toluene or water) showed rather a negative effect affording the desired dithioacetal in relatively lower yields (entries 7−9). To scale up the reaction, one set of reaction was performed (in 5 mmol) using the same quantity of catalyst (GO = 50 mg).

Excellent yield of the dithioacetal was realized in this case as well signifying that the minimum quantity of the catalyst can promote the reaction in a longer time (entry 10).

Table III.A.1. Optimization of dithioacetal formation from *p*-anisaldehyde and *n*-pentane thiol.[a]

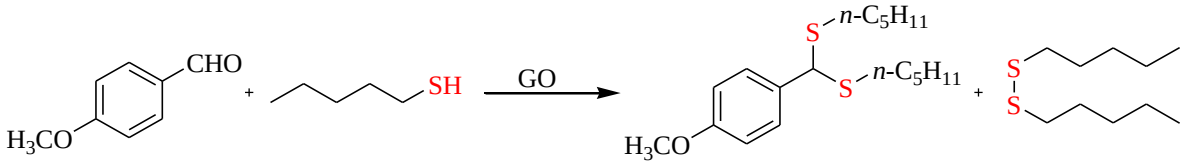

Entry	GO (in mg mmol^{-1})	Reaction medium	Time (h) / Temp(^{o}C)	Dithioacetal (%)[b]	Disulfide (%)[b]
1	10	Neat	24 / RT	51	Not observed
2	25	Neat	24 / RT	65	Not observed
3	**50**	**Neat**	**3 / RT**	**95**	**Not observed**
4	Nil	Neat	24 / RT	Not observed	Not observed
5	50	Neat	3 / 60	61	10
6[c]	50	Neat	3 / 60	57	8
7	50	THF	20 / RT	35	trace[d]
8	50	PhMe	12 / RT	68	Not observed
9	50	H_2O	12 / RT	55	trace[d]
10[e]	50	Neat	16 / RT	91	trace[d]

[a]*p*-Anisaldehyde (1 mmol), *n*-pentanethiol (2.2 mmol), [b]Isolated yield. [c]Reaction carried out under N_2. [d]Detected only on tlc, not isolated. [e]*p*-Anisaldehyde (5 mmol), pentanethiol (11 mmol). [All optimisation experiments were performed by both the present author as well as one of my co-author]

With this mild and solvent-free optimized condition at our hand, we became interested to explore the general applicability of the reaction. A variety of aryl aldehydes were subjected to the reaction in the presence of thiols, are presented in Table III.A.2. It can be seen that aryl aldehydes bearing different functional groups react easily with aliphatic thiols in the presence of catalytic amount of GO under solvent-free aerobic condition. The reactions were completed in 3–8 h and the products were realized in excellent yields (Table III.A.2, entries 1–5). Higher temperature was required for α-naphthaldehyde and *p*-chlorobenzaldehyde, which caused partial formation of disulfide (~5–8%) (entries 6, 7). However, the reaction with *p*-nitrobenzaldehyde needed much longer time and higher temperature, and gave the dithioacetal in relatively lower yield along with disulfide (Table III.A.2, entry 8). Trying the reaction with aromatic thiols afforded the desired dithioacetal in 80–85% yields but achieved

only at higher temperature (60 ^{o}C) and was associated with the formation of diaryl disulfides in 5–12% isolated yields (entries 9–11). In the case of using 1,2- and 1,3-dithiol, corresponding cyclic thioacetals were obtained in excellent yields (95-98%) and the reaction was also successful with aliphatic cyclohexyl aldehyde (entries 12–15). However, there was no such formation of dithioketals from a ketone under the GO-catalyzed reaction condition (entry 16). So, there is excellent chemoselectivity observed between the aldehyde and keto-carbonyl groups.

Table III.A.2. GO–catalyzed thioacetalization of aldehydes with different thiols.[a]

Entry	Aldehyde	Thiol	Time (h)	Temp	Product	Yield[b] (%)
1	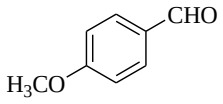	*n*-C_5H_{11}−SH	3	RT	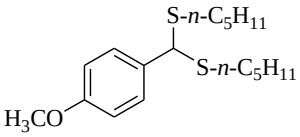	95
2	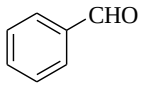	*n*-C_5H_{11}−SH	5	RT	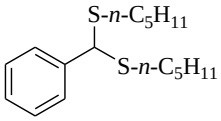	91
3	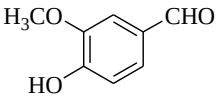	*n*-C_7H_{15}−SH	5	RT	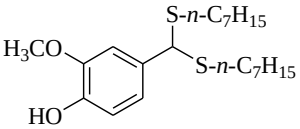	95
4	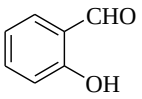	*n*-C_5H_{11}−SH	8	RT	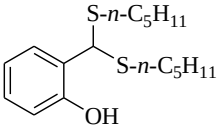	89
5	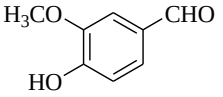	Bu^t−SH	5	RT	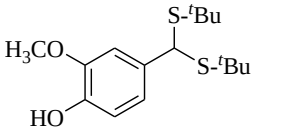	93
6[c]	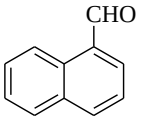	*n*-C_7H_{15}−SH	3	60^{o}C	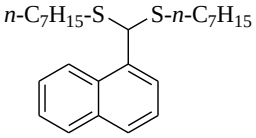	87
7[c]	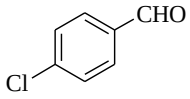	CySH	5	60^{o}C	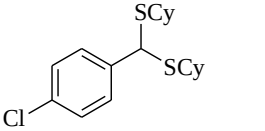	90
8[c]	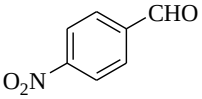	*n*-C_5H_{11}−SH	14	60^{o}C	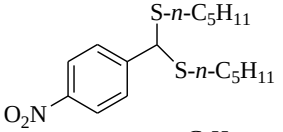	68
9[c]	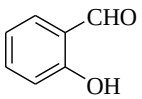	C_6H_5−SH	10	60^{o}C	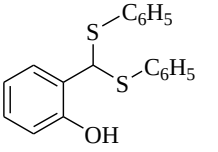	80

10[c]	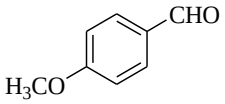	C_6H_5-SH	10	60°C	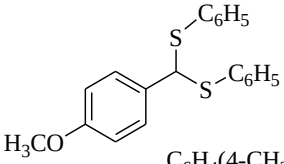	85
11[c]	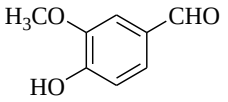	$(H_3C\text{-}4)C_6H_4-SH$	10	60°C	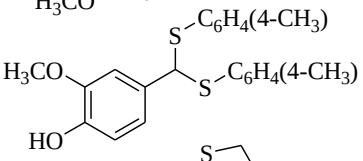	82
12[d]	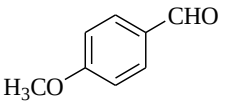	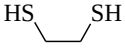	5	RT	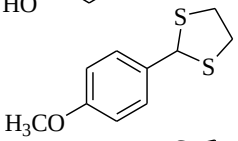	98
13[d]	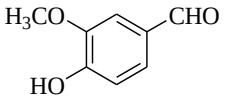	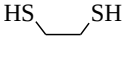	5	RT	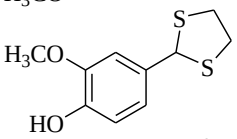	98
14[d]	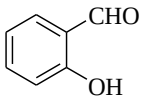		5	RT	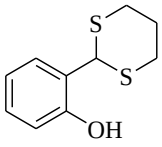	98
15[d]	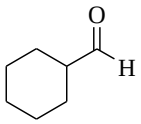		5	RT	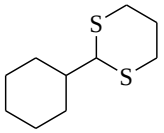	95
16	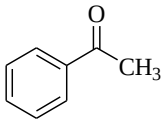	$n\text{-}C_5H_{11}-SH$	24	RT/ 60°C	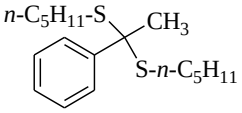	Not observed

[a]Aldehyde : thiol : GO (1 mmol : 2.2 mmol : 50 mg) and reactions were performed at room temperature. [b]Isolated yield. [c]Corresponding disulfides (5-12%) were formed. [d]Aldehyde : thiol : GO (1 mmol : 1.1 mmol : 50 mg). [Entries 1, 2, 3, 4, 5, 6, 7, 8, 9, 10, 11, 12, 13, 14 & 15 were isolated by the present author and others by one of my co-author]

Heteroaryl compounds often exhibit promising pharmacological activities and open chain dithioacetals of heteroaryl aldehydes such as thiophene-based dithioacetals are important scaffolds for design and discovery of new medicines.[31] Since, the reaction conditions are mild and solvent-free, we were interested to extend the GO–catalyzed dithioacetalization to thiophene aldehydes and also of other heteroaryl aldehydes. Indeed, 5-bromothiophene-2-carbaldehyde and furfural result in the formation of corresponding dithioacetals with variety of aliphatic and benzenethiol without any difficulty (Table III.A.3, entries 1–5). Other heteroaryl aldehyde indole-3-carbaldehyde also produces corresponding dithioacetals with long chain aliphatic thiols without any difficulty and in excellent yields (Table III.A.3, entry 6). Cyclic dithioacetals of furfural and indole-3-carbaldehyde were obtained in excellent yields under mild conditions (entries 7, 8).

Table III.A.3. GO-catalyzed thioacetalization of heteroaryl aldehydes.[a]

Entry	Aldehyde	Thiol	Time(h)	Product	Yield (%)[b]
1	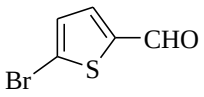	Bu^t-SH	8	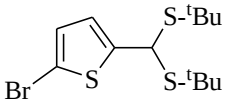	89
2[c]	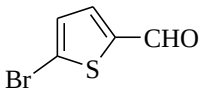	C_6H_5-SH	10	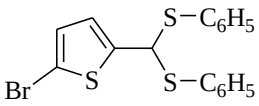	81
3	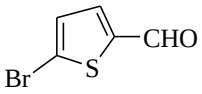	n-$C_7H_{15}-SH$	8	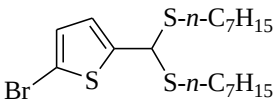	89
4	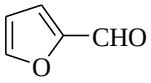	n-$C_5H_{11}-SH$	3	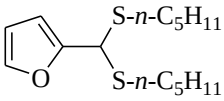	92
5	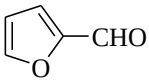	CySH	3	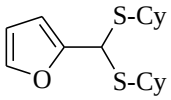	88
6	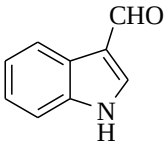	n-$C_7H_{15}-SH$	8	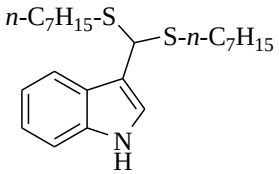	85
7[d]	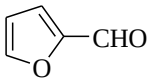		3	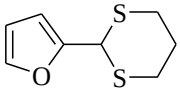	90
8[d]	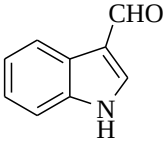	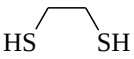	5	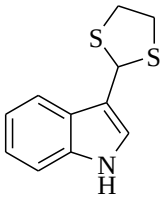	93

[a]Aldehyde : thiol : GO (1 mmol : 2.2 mmol : 50 mg) and reactions were performed at room temperature. [b]Isolated yield. [c]Isolated yield of disulfide was ~ 5%. [d]Aldehyde : thiol : GO (1 mmol : 1.1mmol : 50 mg). [Entries 1, 2, 3, 4, 6, 7 & 8, were isolated by the present author and others by one of my co-author]

In order to further broaden the scope of the reaction, we attempted synthesis of unsymmetrical dithioacetal using two different thiols. Gratifyingly, the reactions of *p*-anisaldehyde or vanillin with two different aliphatic thiols (*n*-pentyl- and *n*-heptyl thiols) resulted in the formation of unsymmetrical dithioacetals as the only product in 85-88%

isolated yields (Table III.A.4, entries 1, 2). HPLC analysis of the crude product (before column chromatographic purification) showed the unsymmetrical thioether as the sole product. On the other hand, use of one aliphatic and one aromatic thiol gave rise to a mixture of all three possible products in varying proportions, as seen from the analysis of the crude product mixture by HPLC (Table III.A.4, entry 3). This might be attributable to the difference in reactivity between aliphatic or aromatic thiols as the thioacetal from benzenethiol was formed in highest quantity amongst the three products.

Table III.A.4. Unsymmetrical thioacetals from aryl aldehydes using two different thiols.[a]

Entry	Aldehyde	Thiol (A)	Thiol (B)	Time	Product	Yield (%)
1	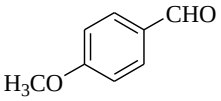	*n*-C_5H_{11}-SH	*n*-C_7H_{15}-SH	5	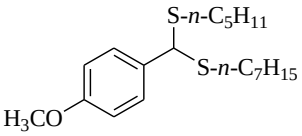	88[b]
2	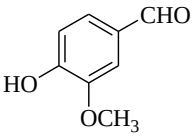	*n*-C_5H_{11}-SH	*n*-C_7H_{15}-SH	5	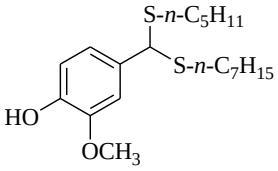	85[b]
3[c]	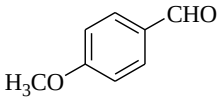	*n*-C_5H_{11}-SH	C_6H_5−SH	10	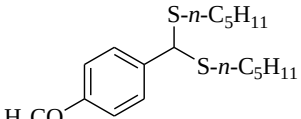	13[d]
					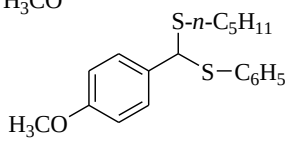	39[d]
					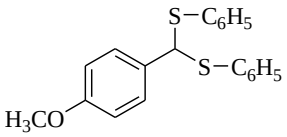	48[d]

[a]Thiol (A):thiol (B):GO (1.1 mmol:1.1 mmol:50 mg) for 1 mmol of aldehyde and the reaction was done at RT for entries 1 and 2; [b]Isolated yield; [c]Reaction performed at 60 ^oC; [d]Product ratios are from HPLC analysis. [Entries 1 & 2 were isolated by the present author and the other one was analysed by both the present author and one of my-co author]

As regard to the plausible mechanism for the reaction, we wanted to probe the nature of active sites present in GO. In the recent years, the acidic nature of GO has been attributed mostly to the organosulfate group being originated during the oxidation of graphite using Hummers method in the presence of sulphuric acid,[16,18, 32] though previous measurements of acidic pH were attributable to the presence of surface attached carboxylic functions.[4] The FT–IR spectrum of GO showed the presence of carboxyl (1719 cm^{-1}; COOH stretching) and

sulphate functional groups (1052 cm^{-1}; SO_3–H stretching), which are comparable with that reported in the literature.[18,30] In this case we measured the pH of the GO in aqueous suspension (pH = 3.9; 50 mg in 50 ml 0.5M aqueous NaCl solution), and found it in fair agreement with previous observations.[4] The pH of GO remains fairly similar when measured after the reaction and also of a mixture of *n*-pentane thiol and GO in water. On the other hand, thioacetal formation is greatly retarded when the reaction is carried out in water or in other organic solvents (Table III.A.1, entries 7, 8 and 9). GO also gave positive Carius test and Lassaigne's test signifying qualitatively the presence of S-containing functional groups.

The above results suggest that GO is an acid catalyst and we tend to believe that the acidity of GO might be originating from a combination of both carboxyl and organosulfate groups, which is more pronounced in neat. Mechanistically, surface active acidic functional groups of GO facilitate activation of the aldehyde carbonyl group, more effectively in neat condition, and subsequent nucleophilic attack by the thiol results in the eventual formation of thioacetal.

The reusability of the GO as heterogeneous acid catalyst was examined with the combination of reactants: *p*-anisaldehyde and *n*-pentanethiol in 1:2.2 ratios at room temperature. The GO was recovered from the first batch of reaction by centrifugation and washed with diethyl ether, dried and reused for subsequent four batches of reactions. In all recycling experiments carried out at room temperature, appreciable conversions were achieved (Figure III.A.3).

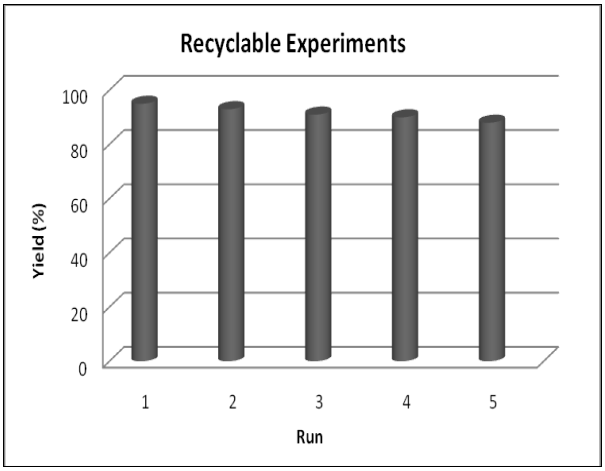

Figure III.A.3. Recyclability of GO in the thioacetalization of *p*-anisaldehyde and *n*-pentanethiol.

A comparison of the FT–IR spectra of the GO before and after use does not indicate any changes of the absorption bands, signifying that the catalyst remain same after the reaction (Figure III.A.4).

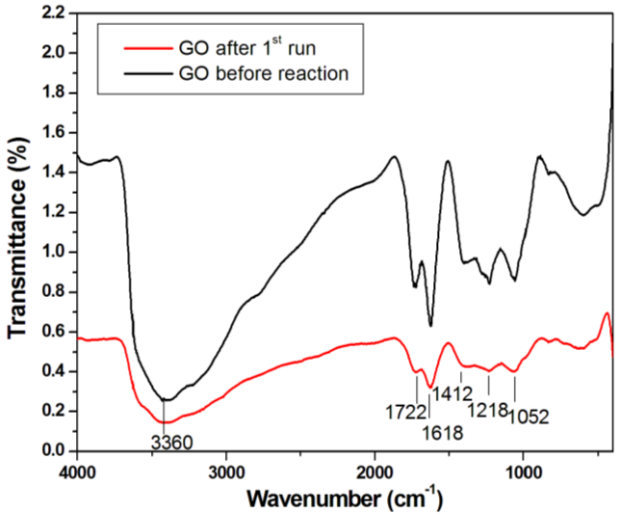

Figure III.A.4. Comparative FT–IR spectra of GO before and after 1st use in the reaction between *p*-anisaldehyde and *n*-pentanethiol under neat condition.

III.A.4. Conclusion

In summary, GO was found to catalyze the formation of thioacetal from a neat mixture of aldehyde and thiol under mild, solvent-free and aerobic conditions. Notable features of the methodology described herein are: operational simplicity, nil or negligible quantity of disulfide formation, applicability to a large variety of aryl/heteroaryl aldehydes, chemoselectivity, recyclability and environmental compatibility. Moreover, low-cost facial preparation and sustainability of GO make it a convenient metal-free carbocatalyst for such dithioacetalization. Thus it provides a practical approach for the preparation of open chain, cyclic and unsymmetrical dithioacetals. The present method also demonstrates that controlled loading of GO in combination with reaction conditions could lead to the diversity in reaction types as well as the formation of the products, and is likely to spur more catalytic applications.

III.A.5. Experimental Section

III.A.5.1. General Information

All chemicals were purchased and used directly and futher details are same as in chapter II (see, chapter II.5. General Information). HPLC analyses were carried out using HPLC (Agilent Technologies, 1260 Infinity), Column: ZORBAX Rx–SIL (4.6 x 150 mm, 5

μm), eluent: *n*–hexane (flow rate 3 mL min^{-1}). High resolution Mass Spectra (HRMS) were performed in Micromass Q-TOF Spectrometer under ESI (positive mode), by the services at the Indian Association for the Cultivation of Science, Kolkata.

III.A.5.2. General procedure for the preparation of dithioacetals

To a mixture of aldehyde (1 mmol) and thiol (2.2 mmol), 50 mg of graphene oxide was added and stirred the reaction mixture at room temperature for hours as mentioned in the Tables (2-4). After completion of reaction, diethyl ether (5 mL) was added, stirred gently and then allowed to stand. The supernatant liquid was carefully collected in another flask and this process was repeated three times more. The liquid part was concentrated and the residue was purified through column chromatography over silica gel. Elution with light petroleum or ethyl acetate-light petroleum (2:98) affords the pure dithioacetal (% Yield as mentioned in the Tables). All products were characterized by ^{1}H, ^{13}C NMR data and compared with the reported melting points for known solid compounds.

III.A.5.3. HPLC analysis

After completion of reaction the mixture was allowed to cool at room temperature and 5 mL methanol was added, filtered and HPLC analysis was done. HPLC analysis of this crude mixture revealed that the area percentage of product (sum of three peaks) and that of starting aldehyde is in the ratio 59:41, i.e. about 59% conversion was occurred. Among these three (product) peaks two corresponds to symmetrical dithioacetals, confirmed from their respective retention times (Figure III.A.5) and the rest one could be the unsymmetrical dithioacetal. Area parentages of all three components (products) are shown in Figure III.A.6.

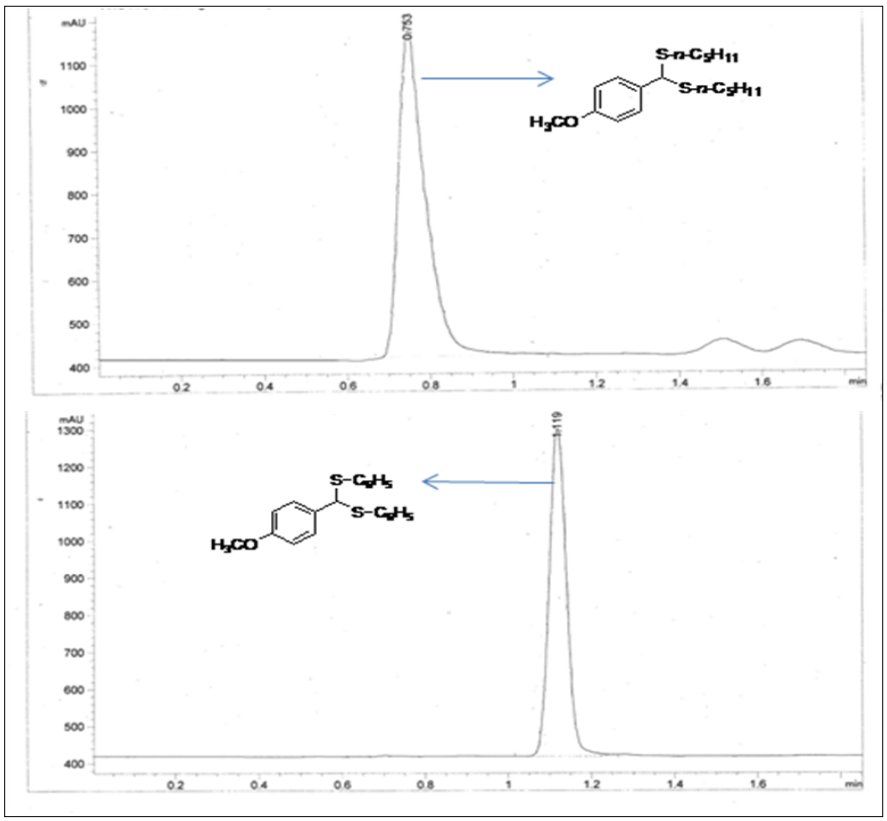

Figure III.A.5. HPLC analysis showing retention times of two different symmetrical dithioacetals (Table III.A.2, entry 1 and entry 10)

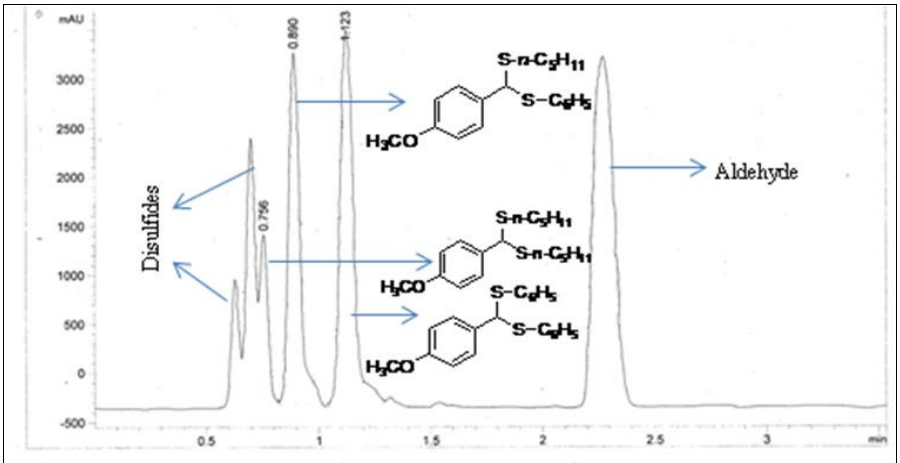

Area Percent Report

Sorted By : Signal
Multiplier : 1.0000
Dilution : 1.0000
Use Multiplier & Dilution Factor with ISTDs

Signal 1: VWD1 A, Wavelength=250 nm

Peak #	RetTime [min]	Type	Width [min]	Area [mAU*s]	Height [mAU]	Area %
1	0.756	VB	0.0381	4303.72949	1722.77527	12.9847
2	0.890	BB	0.0568	1.27964e4	3568.77368	38.6078
3	1.123	BV	0.0671	1.60444e4	3810.33032	48.4074
Totals :				3.31445e4	9101.87927	

Figure III.A.6. HPLC analysis showing area percentage of three possible dithioacetals obtained from *p*-anisaldehyde, *n*-pentanethiol and benzenethiol (Table III.A.4, entry 3).

III.A.5.4. Physical properties and spectral data of dithioacetals

All products were characterized by ^{1}H and ^{13}C NMR spectra and compared with those reported melting points for known solid compounds. The HRMS data supported the structures for the unsymmetrical dithioacetals.

Table III.A.2; Entry 1
1-(bis(pentylthio)methyl)-4-methoxy benzene
The compound was obtained as a colourless oil.

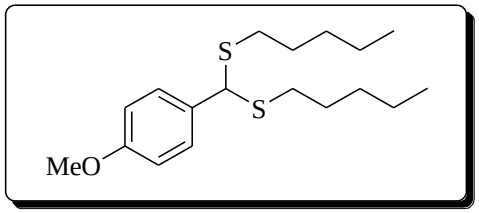

^{1}H NMR ($CDCl_3$, 300 MHz): δ 0.86 (t, *J* = 6.9 Hz, 6H, CH_3), 1.36-1.23 (m, 8H, CH_2), 1.58-1.49 (m, 4H, CH_2), 2.58-2.43 (m, 4H, CH_2), 3.74 (s, 3H, OCH_3), 4.86 (s, 1H, CH), 6.84-6.80 (m, 2H, ArH), 7.37-7.33 (m, 2H, ArH).
^{13}C NMR ($CDCl_3$, 75 MHz): δ 14.0, 22.3, 28.9, 31.1, 32.2, 52.6, 55.1, 113.7, 128.8, 132.6,159.

Table III.A.2; Entry 2
1-(bis(pentylthio)methyl)benzene
The compound was obtained as a colourless oil.

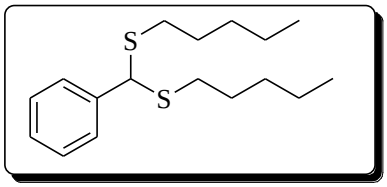

^{1}H NMR ($CDCl_3$, 300 MHz): δ 0.86 (t, *J* = 6.9 Hz, 6H, CH_3), 1.34-1.23 (m, 8H, CH_2), 1.57-1.49 (m, 4H, CH_2), 2.59-2.44 (m, 4H, CH_2), 4.88 (s, 1H, CH), 7.32-7.22 (m, 3H, ArH), 7.45-7.32 (m , 2H, ArH).
^{13}C NMR ($CDCl_3$, 75 MHz): δ 14.0, 22.3, 28.9, 31.1, 32.2, 53.2, 127.7, 128.4, 140.7.

Table III.A.2; Entry 3
4-(bis(heptylthio)methyl)-2-methoxyphenol
The compound was obtained as a colourless oil.

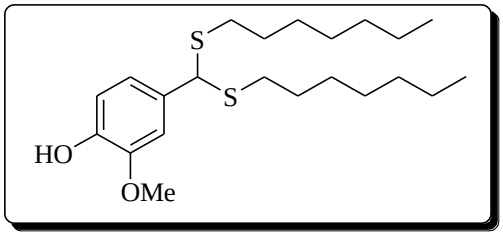

^{1}H NMR ($CDCl_3$, 300 MHz): δ 0.89-0.84 (m, 6H, CH_3), 1.36-1.21 (m, 16H, CH_2), 1.57-1.49 (m, 4H, CH_2), 2.56-2.47 (m, 4H, CH_2), 3.94 (s, 3H, OCH_3), 4.82 (s, 1H, CH), 6.83 (dd, *J* = 2.1 and 12.9 Hz, 2H, ArH), 7.04 (d, *J* = 1.8 Hz, 1H, ArH).
^{13}C NMR ($CDCl_3$, 75 MHz): δ 13.9, 22.5, 28.7, 29.1, 31.6, 32.3, 53.0, 55.8, 109.8, 113.6, 120.7, 132.4, 145.2, 146.6.

Table III.A.2; Entry 4
2-(bis(pentylthio)methyl)phenol
The compound was obtained as a colourless oil.

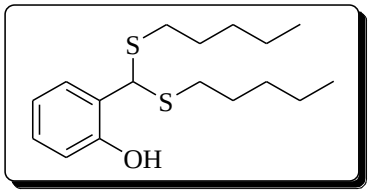

^{1}H NMR ($CDCl_3$, 300 MHz): δ 0.88-0.84 (m, 6H, CH_3), 1.34-1.24 (m, 8H, CH_2), 1.58-1.51 (m, 4H, CH_2), 2.57-2.51 (m, 4H, CH_2), 5.08 (s, 1H, CH), 6.90-6.83 (m, 2H, ArH), 7.03 (s, 1H, OH), 7.22-7.17 (m, 2H, ArH).
^{13}C NMR ($CDCl_3$, 75MHz): δ 13.8, 22.1, 28.7, 30.8, 32.4, 50.0, 117.6, 120.2, 123.5, 129.4, 129.6, 154.9.

Table III.A.2; Entry 5
4-(bis(tert-butylthio)methyl)-2-methoxyphenol
The compound was obtained as a white solid and its melting point was in the range of 78-80 ^{o}C.

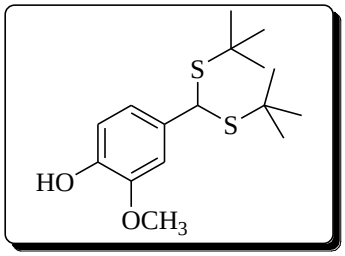

^{1}H NMR ($CDCl_3$, 300 MHz): δ 1.31 (s, 18H, CH_3), 3.90 (s, 3H, OCH_3), 5.00 (s, 1H, CH), 5.60 (s, 1H, OH), 6.80 (d, *J* = 8.1 Hz, 1H, ArH), 6.86 (dd, *J* = 2.1 and 8.1 Hz, 1H, ArH), 7.08 (d, *J* = 1.8 Hz, 1H, ArH).

^{13}C NMR ($CDCl_3$, 75 MHz): δ 31.2, 45.6, 48.8, 56.0, 110.4, 113.8, 120.0, 135.7, 145.0,146.8.

Table III.A.2; Entry 6

1-(bis(heptylthio)methyl)naphthalene

The compound appeared as a colourless oil.

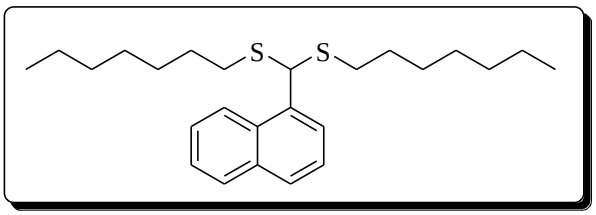

^{1}H NMR ($CDCl_3$, 300 MHz): δ 0.87-0.83 (m, 6H, CH_3), 1.60-1.21 (m, 20H, CH_2), 2.69-2.47 (m, 4H, CH_2), 5.66 (s, 1H, CH), 7.57-7.48 (m, 3H, ArH), 7.87-7.75 (m, 3H, ArH), 8.24 (d, *J* = 7.8 Hz, 1H, ArH).

^{13}C NMR ($CDCl_3$, 75 MHz): δ 14.0, 22.5, 28.8, 29.1 31.6, 32.3, 32.5, 123.3, 125.0, 125.6, 125.8, 126.0, 126.2, 128.5, 128.9, 130.4, 134.0, 135.2.

Table III.A.2; Entry 7

1-(bis(cyclohexylthio)methyl)-4-chlorobenzene

The compound was isolated as a colourless oil.

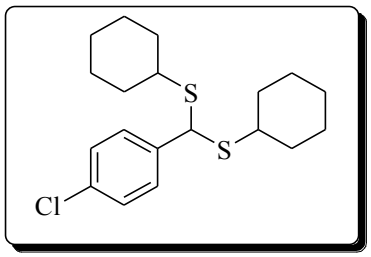

^{1}H NMR ($CDCl_3$, 300 MHz): δ 1.35-1.17 (m, 10H, CyH), 1.55 (d, *J* = 4.5 Hz, 2H, CyH), 1.74-1.70 (m, 4H, CyH), 1.92-1.85 (m, 4H, CyH), 2.74-2.67 (m, 2H, CyH), 4.96 (s, 1H, CH), 7.30-7.26 (m, 2H, ArH), 7.42-7.38 (m, 2H, ArH).

^{13}C NMR ($CDCl_3$, 75MHz): δ 25.6, 25.7, 33.2, 33.2 44.2, 48.9, 128.5, 129.0, 133.0, 139.9.

Table III.A.2; Entry 8

1-(bis(pentylthio)methyl)-4-nitrobenzene

The compound was obtained as a pale yellow oil.

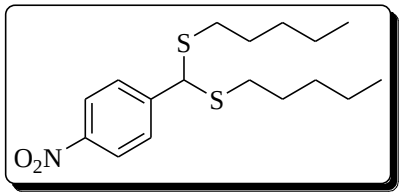

^{1}H NMR ($CDCl_3$, 300 MHz): δ 0.89 (m, 6H, CH_3), 1.36-1.25 (m, 8H, CH_2), 1.59-1.51 (m, 4H, CH_2), 2.62-2.49 (m, 4H, CH_2), 4.93 (s, 1H, CH), 7.64-7.61 (m, 2H, ArH), 8.20-8.17 (m, 2H, ArH),
^{13}C NMR ($CDCl_3$, 75 MHz): δ 13.8, 22.2, 28.7, 30.9, 32.3, 52.5, 123.7, 128.6, 147.2, 148.4.

Table III.A.2; Entry 9
2-(bis(phenylthio)methyl)phenol
The compound was obtained as a colourless oil.

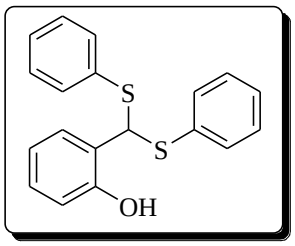

^{1}H NMR ($CDCl_3$, 300 MHz): δ 5.73 (s, 1H, CH), 6.39 (s, 1H, OH), 6.83-6.73 (m, 2H, ArH), 7.25-7.09 (m, 8H, ArH), 7.39-7.35 (m, 4H, ArH).
^{13}C NMR ($CDCl_3$, 75 MHz): δ 56.4, 117.0, 120.7, 128.0, 128.8, 129.5, 129.6, 132.5, 133.6.

Table III.A.2; Entry 10
1-((4-methoxyphenyl)(phenylthio)methylthio)benzene[33]
The compound was obtained as a white solid, mp 71-73 ^{o}C.

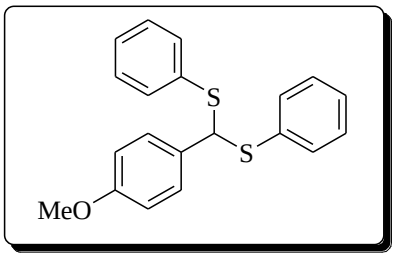

^{1}H NMR ($CDCl_3$, 300 MHz): δ 3.73 (s, 3H, OCH_3), 5.42 (s, 1H, CH), 6.77 (d, *J* =8.7 Hz, 2H, ArH), 7.34-7.20 (m, 12H, ArH).
^{13}C NMR ($CDCl_3$, 75 MHz): δ 55.1, 59.6, 113.7, 127.5, 128.7, 129.0, 131.5, 132.2, 134.6, 159.1.

Table III.A.2; Entry 11

4-(bis(p-tolylthio)methyl)-2-methoxyphenol

The compound was obtained as a white solid, mp 70-72 ^{o}C.

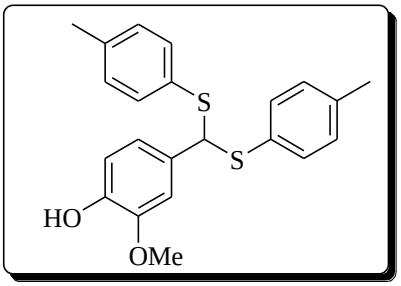

^{1}H NMR ($CDCl_3$, 300 MHz): δ 2.29 (s, 3H, CH_3), 3.79 (s, 3H, OCH_3), 5.28 (s, 1H, CH), 5.60 (s, 1H, OH), 6.76 (d, *J* = 0.9 Hz, 2H, ArH), 6.86 (s, 1H, ArH), 7.04 (d, *J* = 8.1 Hz, 4H, ArH), 7.24-7.22 (m, 4H, ArH).

^{13}C NMR ($CDCl_3$, 75 MHz): δ 21.1, 55.8, 60.9, 110.2, 113.9, 121.0, 129.5, 130.9, 131.7, 133.0, 137.9, 145.2, 146.3.

Table III.A.2; Entry 12

2-(4-methoxyphenyl)-1, 3-dithiolane[23g]

The compound was obtained as a white solid, mp 58-60 ^{o}C.

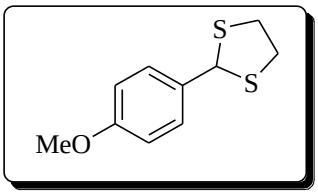

^{1}H NMR ($CDCl_3$, 300 MHz): δ 3.37-3.29 (m, 2H, CH_2), 3.52-3.44 (m, 2H, CH_2), 3.78 (s, 3H, OCH_3), 5.63 (s, 1H, CH), 6.83 (dd, *J* = 2.1 and 6.6 Hz, 2H, ArH), 7.44 (dd, *J* = 2.1 and 6.6 Hz, 2H, ArH).

^{13}C NMR ($CDCl_3$, 75 MHz): δ 40.1, 55.2, 55.9, 113.7, 129.0, 131.7, 159.3.

Table III.A.2; Entry 13

4-(1, 3-dithiolan-2-yl)-2-methoxyphenol

The compound was isolated as white solid, mp 81-83 ^{o}C.

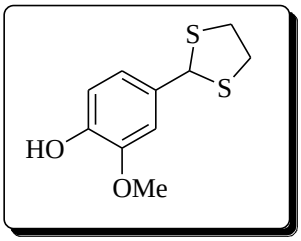

^{1}H NMR ($CDCl_3$, 300 MHz): δ 3.35-3.27 (m, 2H, CH_2), 3.50-3.41 (m, 2H, CH_2), 3.85 (s, 1H, OCH_3), 5.61 (s, 1H, CH), 6.81 (d, *J* = 8.1 Hz, 1H, ArH), 6.98 (dd, *J* = 2.1 and 8.1 Hz, 1H, ArH), 7.08 (d, *J* = 2.1 Hz, 1H, ArH).
^{13}C NMR ($CDCl_3$, 75 MHz): δ 39.9, 55.8, 56.5, 110.2, 113.9, 120.9, 131.1, 145.4, 146.3.

Table III.A.2; Entry 14
2-(1,3-dithian-2-yl)phenol[34]
The compound was obtained as a white crystalline solid, mp 131-133 ^{o}C.

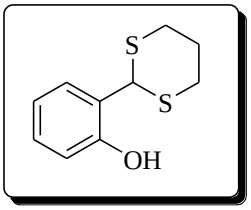

^{1}H NMR ($CDCl_3$, 300 MHz) : δ 1.96-1.92 (m, 1H, CH_2), 2.18-2.11 (m, 1H, CH_2), 2.92-2.84 (m, 2H, CH_2), 3.09-2.99 (m, 2H, CH_2), 5.44 (s, 1H, CH), 6.55 (s, 1H, OH), 6.90-6.84 (m, 2H, ArH), 7.33-7.15 (m, 2H, ArH).
^{13}C NMR ($CDCl_3$, 75 MHz): δ 24.9, 31.7, 47.0, 117.1, 120.8, 123.9, 129.1, 130.0, 154.2.

Table III.A.2; Entry 15
2-cyclohexyl-1, 3-dithiane[35]
The compound was obtained as a white solid, mp 49-51 ^{o}C.

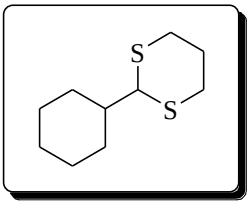

^{1}H NMR ($CDCl_3$, 300 MHz): δ 2.12-1.21 (m, 13H, CyH), 2.88-2.82 (m, 4H, CH_2), 4.04-3.99 (m, 1H, CH).
^{13}C NMR ($CDCl_3$, 75 MHz): δ 26.1, 26.1, 26.3, 30.3, 30.8, 43.0, 55.2.

Table III.A.; Entry 1
2-(bis(tert-butylthio)methyl)-5-bromothiophene
The compound was obtained as a white crystalline solid, mp 68-70 ^{o}C.

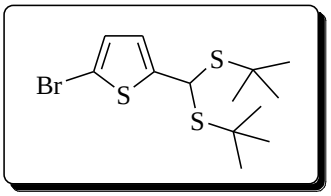

^{1}H NMR ($CDCl_3$, 300 MHz): δ 1.33 (m, 18H, CH_3), 5.17 (s, 1H, CH), 6.82 (s, 2H, ArH).
^{13}C NMR ($CDCl_3$, 75 MHz): δ 31.0, 43.4, 46.2, 111.8, 124.5, 129.0, 151.1.

Table III.A.3; Entry 2
2-(bis(phenylthio)methyl)-5-bromothiophene.
The compound was obtained as a pale yellow oil.

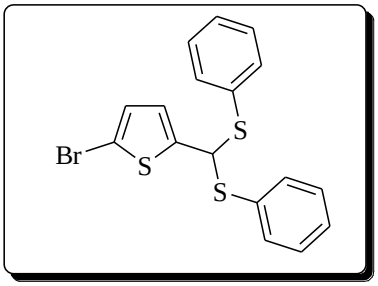

^{1}H NMR ($CDCl_3$, 300 MHz): δ 5.55 (s, 1H, CH), 6.66 (d, *J* = 3.6 Hz, 1H, ArH), 6.76 (d, *J* = 3.9 Hz, 1H, ArH), 7.29-7.21 (m, 6H, ArH), 7.41-7.35 (m, 4H, ArH).
^{13}C NMR ($CDCl_3$, 75MHz): δ 55.7, 112.8, 126.8, 128.3, 129.0, 129.3, 129.4, 132.8,133.7,145.5.

Table III.A.3; Entry 3
2-(bis(heptylthio)methyl)-5-bromothiophene
The compound was obtained as a colourless oil.

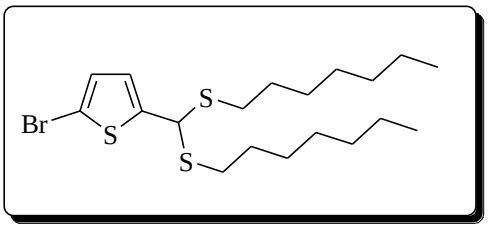

^{1}H NMR ($CDCl_3$, 300 MHz): δ 0.89-0.84 (m, 6H, CH_3), 1.37-1.24 (m, 16H, CH_2), 1.59-1.51 (m, 4H, CH_2), 2.67-2.54 (m, 4H, CH_2), 5.04 (s, 1H, CH), 6.85-6.81 (m, 2H, ArH).
^{13}C NMR ($CDCl_3$, 75 MHz): δ 14.0, 22.5, 28.8, 28.8, 29.0, 31.6, 32.1, 48.6, 112.3, 125.9, 129.1, 147.1.

Table III.A.3; Entry 4

2-(bis(pentylthio)methyl)furan

The compound was obtained as a pale yellow liquid.

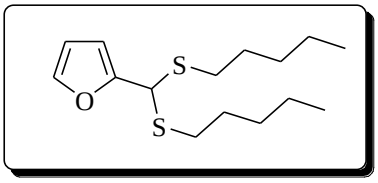

^{1}H NMR ($CDCl_3$ 300 MHz): δ 0.90-0.85 (m, 6H, CH_3), 1.37-1.26 (m, 8H. CH_2), 1.60-1.50 (m, 4H, CH_2), 2.70-2.50 (m, 4H, CH_2), 4.99 (s, 1H, CH), 6.31 (d, *J* = 1.5 Hz, 2H, ArH), 7.36 (t, *J* = 1.5 Hz, 1H, ArH).

^{13}C NMR ($CDCl_3$, 75 MHz): δ 13.8, 22.1, 28.7, 31.0, 31.4, 45.8, 107.5, 110.3, 142.0, 152.3.

Table III.A.3; Entry 5

2-(1, 3-dicyclohexylpropan-2-yl) furan

The compound was obtained as a colourless oil.

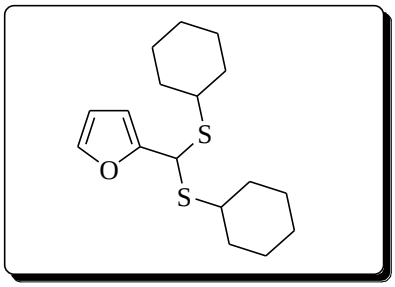

^{1}H NMR ($CDCl_3$, 300 MHz): δ 1.37-1.22 (m, 10H, CyH), 1.93-1.55 (m, 10H, CyH), 2.82-2.80 (m, 2H, CyH), 5.09 (m, 1H, CH), 6.34-6.29 (m, 2H, ArH), 7.35-7.34 (m, 1H, ArH).

^{13}C NMR ($CDCl_3$, 75 MHz): δ 25.6, 25.7, 25.7, 33.2, 33.3, 42.7, 43.9, 107.1, 110.2, 141.7, 153.1.

Table III.A.3; Entry 6

3-(bis(heptylthio)methyl)-1H-indole

The compound was obtained as a colourless oil.

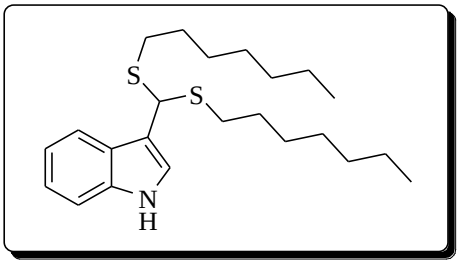

^{1}H NMR ($CDCl_3$, 300 MHz): δ 0.88-0.83 (m, 6H, CH_3), 1.35-1.22 (m, 16H, CH_2), 1.65-1.51 (m, 4H, CH_2), 2.69-2.48 (m, 4H, CH_2), 5.28 (s, 1H, CH), 7.26-7.11 (m, 4H, ArH), 7.84-7.80 (m, 1H, ArH), 8.00 (s, 1H, NH).
^{13}C NMR ($CDCl_3$, 75 MHz): δ 13.9, 22.5, 28.7, 28.8, 29.1, 31.6, 31.9, 45.7, 111.2, 114.9, 119.5, 119.6, 122.3, 123.0, 125.5, 136.4.

Table III.3; Entry 7
2-(1, 3-dithian-2-yl)furan[36]
The compound was obtained as a colourless oil.

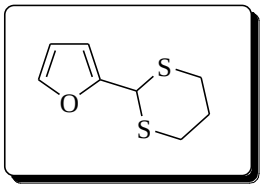

^{1}H NMR ($CDCl_3$, 300 MHz): δ 2.02 -1.96 (m, 1H, CH_2), 2.16-2.10 (m, 1H, CH_2), 3.00-2.93 (m, 4H, $2CH_2$), 5.22 (s, 1H, CH), 6.40-6.33 (m, 2H, ArH), 7.37-7.26 (m, 1H, ArH).
^{13}C NMR ($CDCl_3$, 75 MHz): δ 25.2, 30.2, 42.0, 107.8, 110.5, 142.2, 151.7.

Table III.A.3; Entry 8
3-(1, 3-dithiolan-2-yl)-1H-indole
The compound was obtained as a pale yellow solid, mp 121-123 ^oC.

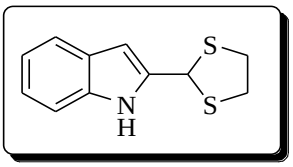

^{1}H NMR ($CDCl_3$, 300 MHz): δ 3.50-3.31 (m, 4H, CH_2), 6.03 (s, 1H, CH), 7.32 - 7.11 (m, 4H, ArH), 7.81 (d, *J* = 7.2 Hz, 1H, ArH), 8.00 (s, 1H, NH).
^{13}C NMR ($CDCl_3$, 75 MHz): δ 39.4, 48.9, 111.4, 114.9, 119.7, 122.5, 123.1, 125.8, 136.8.

Table III.A.4; Entry 1
1-(bis(pentylthio)methyl)-4-methoxybenzene
The compound was obtained as a colourless oil.

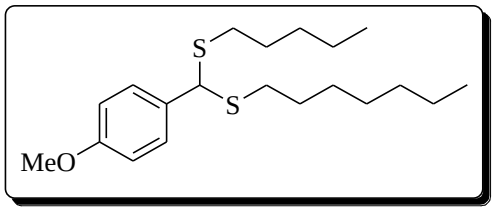

^{1}H NMR ($CDCl_3$, 300 MHz): δ 0.89-0.84 (m, 6H, CH_3), 1.35-1.24 (m, 12H, CH_2), 1.56-1.51 (m, 4H, CH_2), 2.58-2.46 (m, 4H, CH_2), 3.78 (s, 3H, OCH_3), 4.85 (s, 1H, CH), 6.84 (dd, *J* = 2.1 and 6.6 Hz, 2H, ArH), 7.36 (dd, *J* = 2.1 and 6.6 Hz, 2H, ArH).
^{13}C NMR ($CDCl_3$, 75 MHz): δ 13.8, 13.9, 22.1, 22.5, 28.7, 28.7, 29.0, 30.9, 31.6, 32.1, 52.5, 55.1, 113.6, 128.7, 132.5, 158.9.
ESI-HRMS: for $C_{20}H_{34}KOS_2$, **calculated** 393.1688; **observed** 393.1676.

Table III.A.4; Entry 2
4-(bis(pentylthio)methyl)-2-methoxyphenol
The compound was obtained as a pale yellow oil.

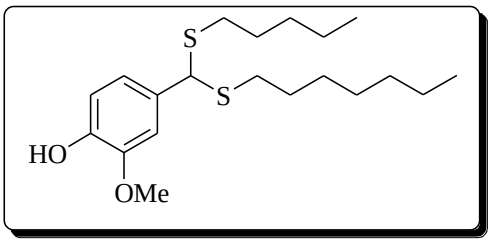

^{1}H NMR ($CDCl_3$ 300 MHz): δ 0.89 0.84 (m, 6H, CH_3), 1.35-1.24 (m, 12H, CH_2), 1.57-1.50 (m, 4H, CH_2), 2.58-2.48 (m, 4H, CH_2), 3.89 (s, 3H, OCH_3), 4.82 (s, 1H, CH), 5.70 (s, 1H, OH), 7.04 (d, *J* = 2.1 Hz, 1H, ArH).
^{13}C NMR ($CDCl_3$, 75 MHz): δ 13.8, 13.9, 22.1, 22.5, 28.7, 28.8, 29.1, 30.9, 31.6, 32.3, 32.3, 53.0, 55.8, 109.8, 113.7, 120.7, 132.4, 145.2, 146.6.
ESI-HRMS: for $C_{20}H_{34}O_2S_2Na$, calculated 393.1898; observed 393.1898.

^{1}H NMR spectra of the mixture of of Table III.A.4; Entry 1 in $CDCl_3$

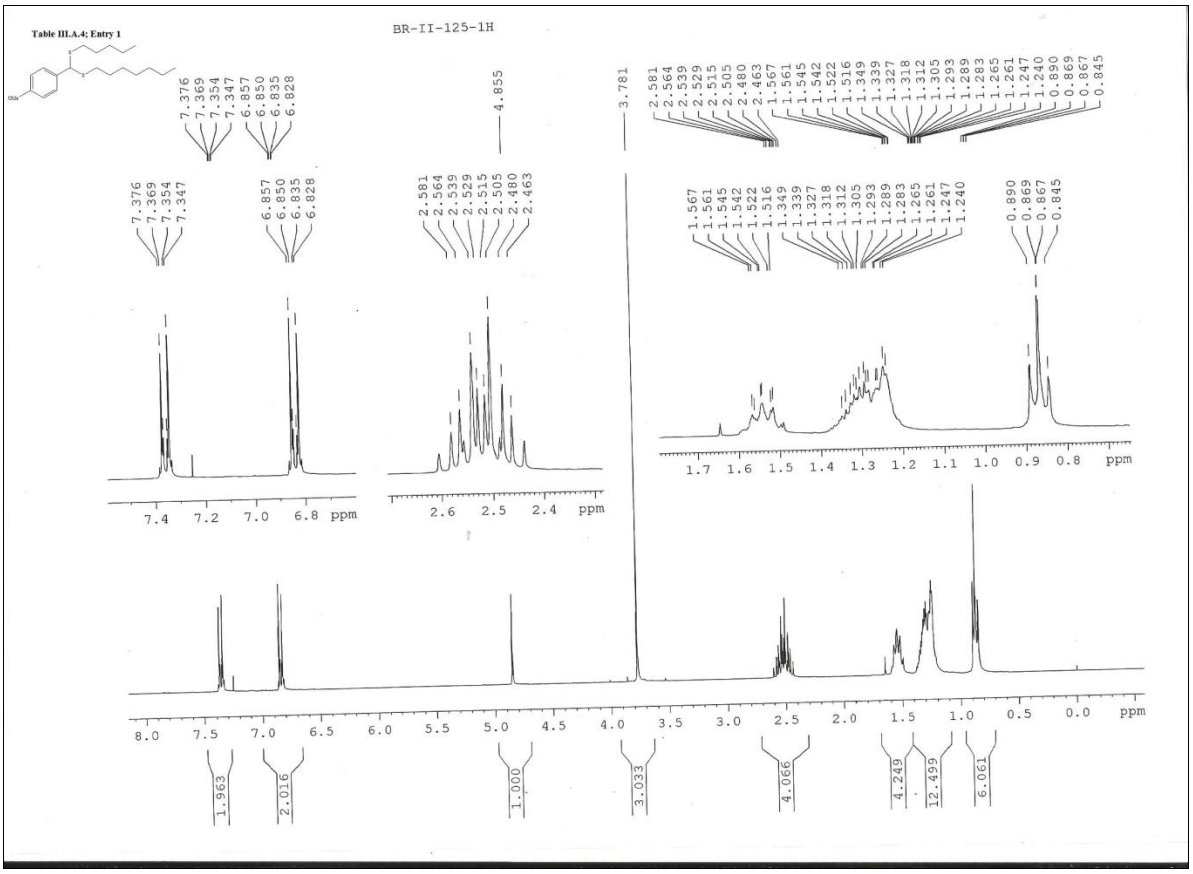

^{13}C NMR spectra of the mixture of of Table III.A.4; Entry 1 in $CDCl_3$

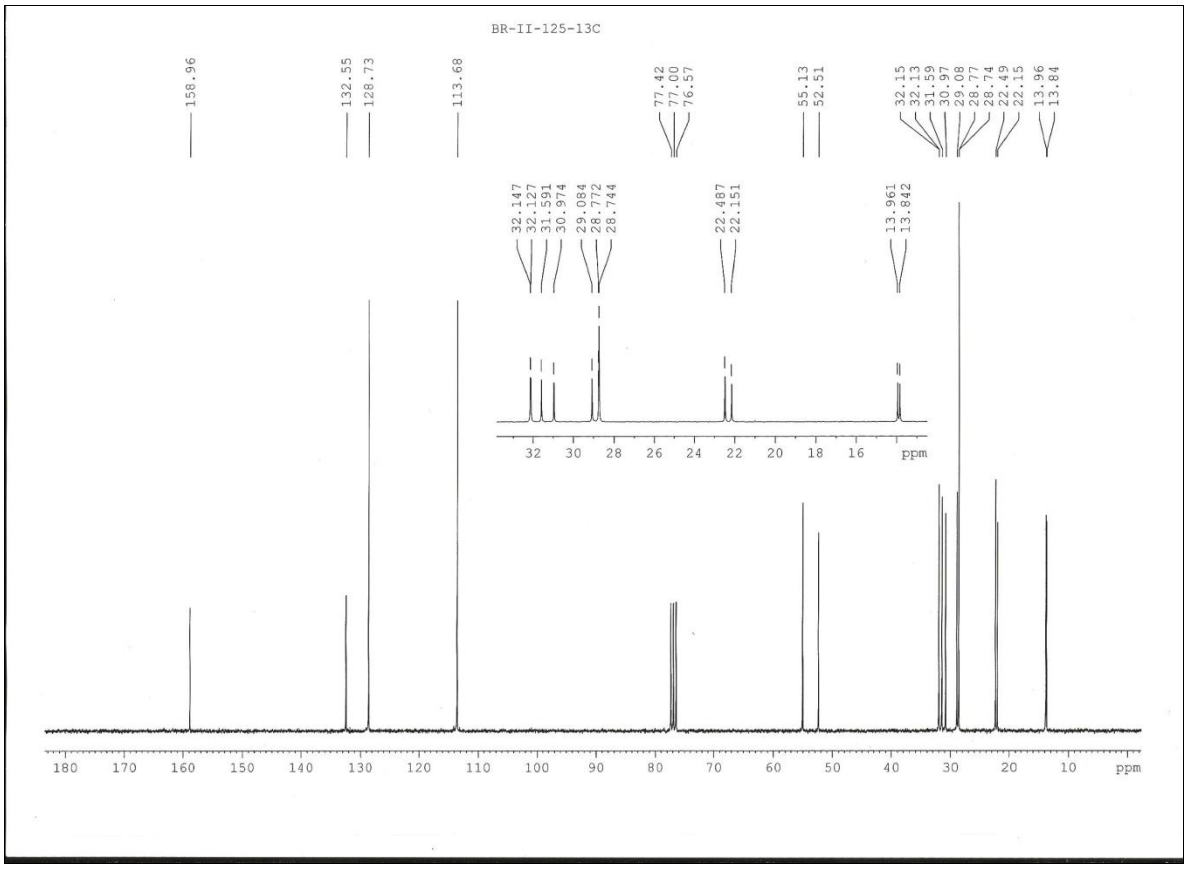

^{1}H NMR spectra of oTable III.A.4; Entry 2 in $CDCl_3$

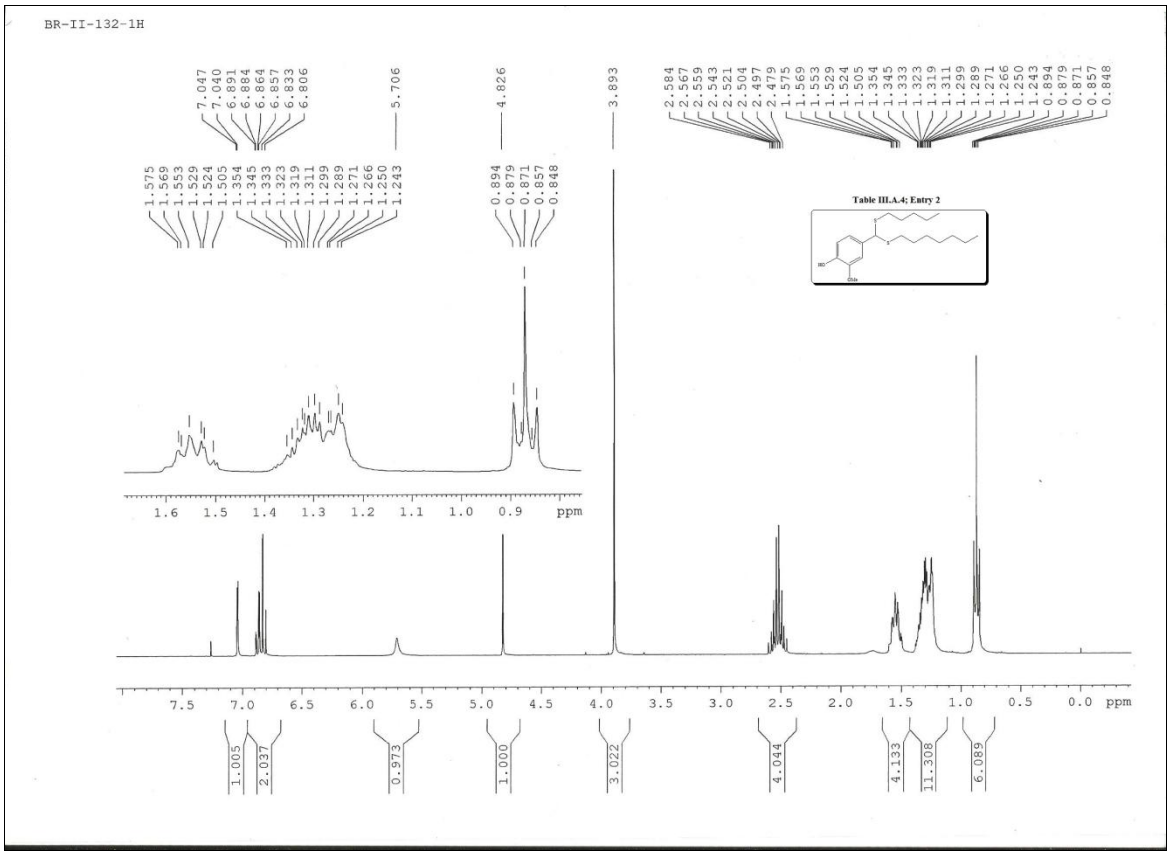

^{13}C NMR spectra of oTable III.A.4; Entry 2 in $CDCl_3$

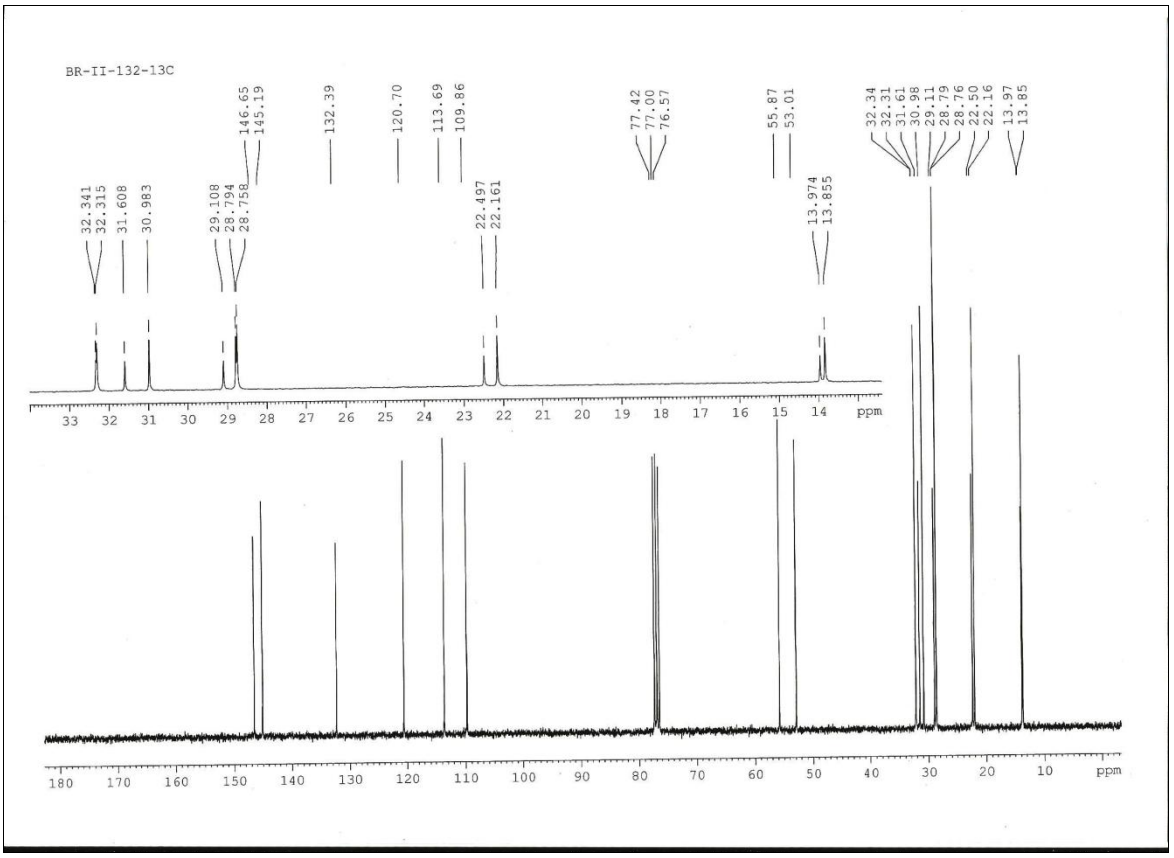

III.A.6. References

References are given in **BIBLIOGRAPHY** under **CHAPTER III, Section A**. (page 173–186).

CHAPTER III
Section B

Graphene oxide (*GO*) or reduced graphene oxide (r*GO*): Efficient catalysts for one-pot metal-free synthesis of quinoxalines from 2-nitroaniline

III.B.1. Introduction

Heterocyclic compounds are ubiquitous in nature.[1] Among different *N*-heterocyclic compounds, quinoxaline and its congeners have broad spectrum of biological activities such as antiviral, anti-inflammatory, antitumour, antibacterial, anthelmintic, kinase inhibitory, anti-HIV and anticancer activities.[2] Some important quinoxaline moieties which have been widely used as drug are shown in Figure III.B.1. Quinoxalines are also widely applied to other technical such as in the preparation of dyes,[3] metal complexes,[4] organic semiconductors,[5] cavitands,[6] luminescent materials[7] and chemically controllable switches.[8]

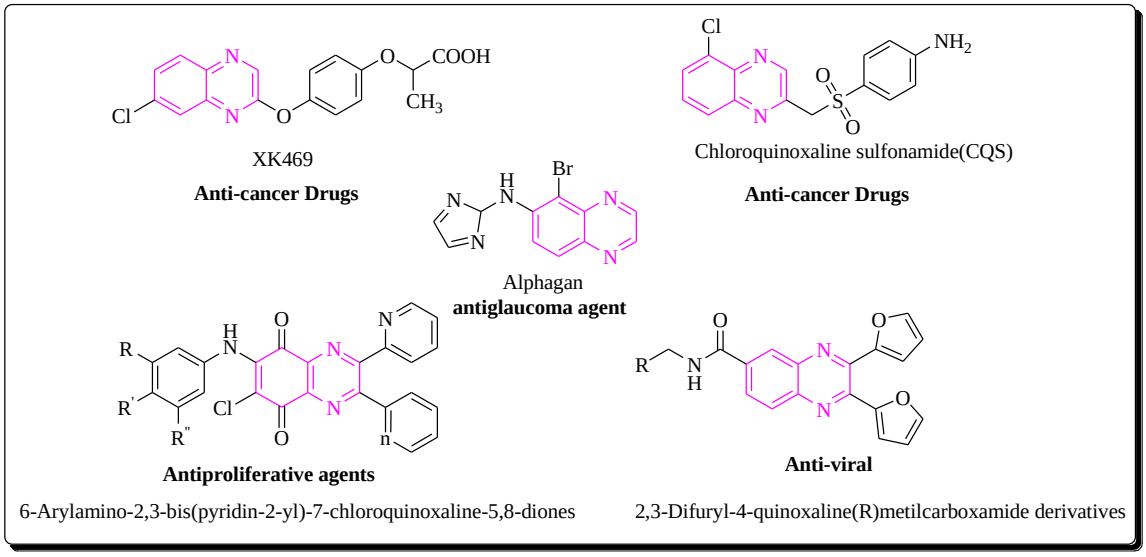

Figure III.B.1. Some important drugs containing quionxaline moieties.

Due to diverse therapeutic and technical interests, the incorporation of quinoxline moieties has become a field of intensive research. Myriads of designs and synthetic strategies have been developed for the creation of these "privileged structures". [9] To address the ever-increasing ecological hazards and economic demands, chemists have been driven towards developing synthetic processes by following the demands of green chemistry. In this regard, solid-phase synthesis of small organic molecules has emerged as an important tool in drug discovery.[10] The solid-phase synthetic method has helped in both expediting the preparation and increasing the diversity of the molecules.[11]

In recent years, the utilization of sustainable carbonaceous materials as metal-free catalysts or catalyst supports for diverse organic transformations has taken a major attraction towards chemical community.[12,13] Among graphene-based materials, graphene oxide (GO) and reduced graphene oxide (rGO) have been widely explored as carbocatalysts for a numerous number of useful synthetic transformations.[13] Previously, we have utilized GO as a

metal-free carbocatalyst for a several number of important organic reactions.[14] In continuation of our interests towards the utilization of GO as convenient metal-free carbocatalyst for diverse organic reactions, we demonstrated herein an alternative and viable one-pot metal-free procedure for the synthesis of quinoxalines directly from 2-nitroaniline.

III.B.2. Present Work: Background and Objectives

Owing to vast and outstanding applications, several synthetic strategies have been developed for the synthesis of quinoxalines over the years.[15] The most common method involves the condensation of an aryl 1,2-diamine with 1,2-dicarbonyl compound.[16] In view of green chemistry, solid phase synthesis of such heterocyclic compounds using various solid supported reagents and catalysts have some advantages over their traditional synthesis like simple work up, simple isolation procedure and recyclability of catalysts.[17]

The first solid-phase synthesis of quinoxalines on SynPhase™ Lanterns has been reported by Wu *et al.*[18] in which a Synphase™ Lanterns bound *o*-pheneyldiamine was reacted with a-bromoketones in DMF at 60 °C to give quinoxaline in good purity and yield after the cleavage of solid support using trifluoro acetic acid (TFA) (Scheme III.B.1).

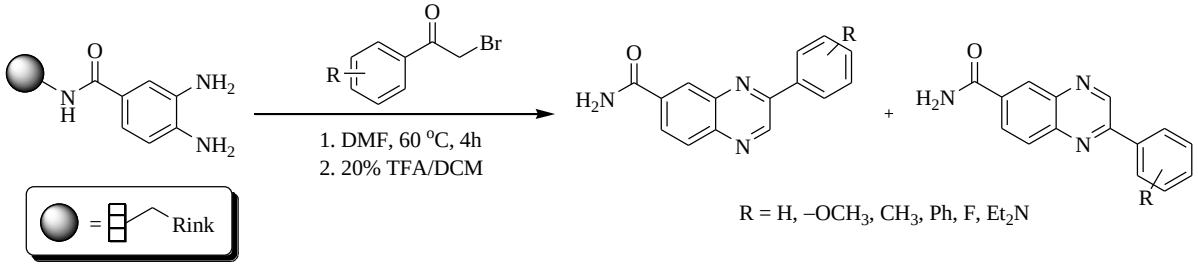

Scheme III.B.1. Solid-phase synthesis of quinoxaline on SynPhase™ Lanterns.

Another one-pot biomimetic approach to the quinoxaline synthesis has been developed by Kakulapati *et al.*[19] using recyclable ruthenium on charcoal (Ru/C) as a catalyst and randomly methyalted β-cyclodextrin in water under neutral condition (Scheme III.B.2).

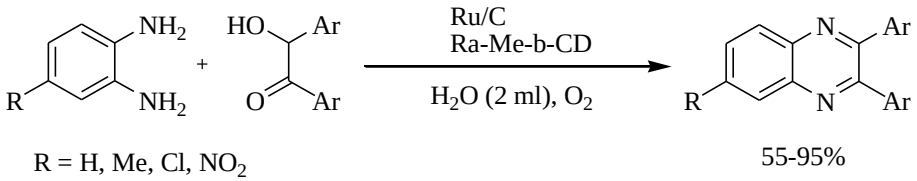

Scheme III.B.2. Ru/C–catalyzed one-pot synthesis of quinoxalines.

A remarkable use of heterogeneous basic surface of KF/alumina for the synthesis of a library of quinoxalines *via* tandem oxidation-condensation reaction has been developed in our laboratory (Scheme III.B.3).[20]

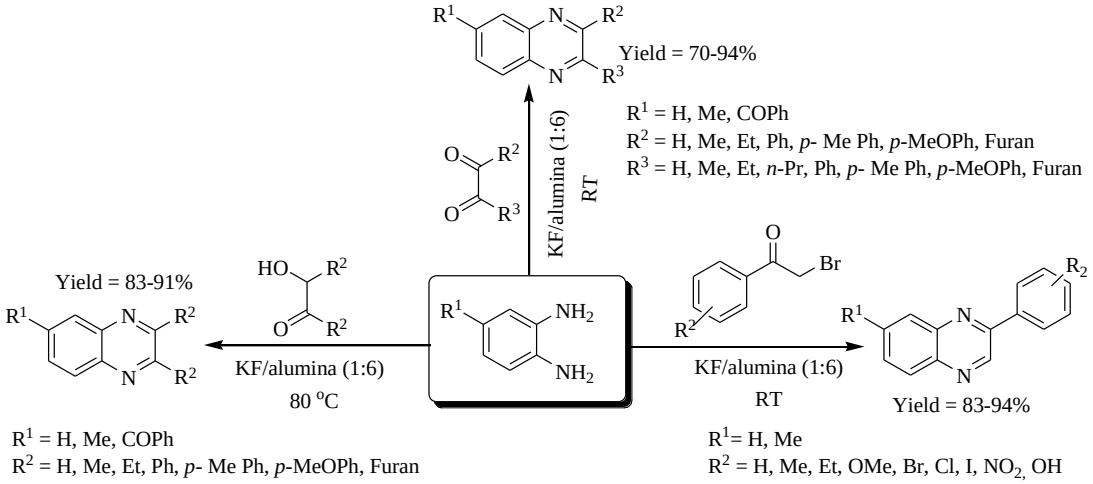

Scheme III.B.3. Quinoxaline synthesis on heterogeneous KF/Alumina basic surface.

Graphite has been also used as a cheap, benign and recyclable catalyst for the synthesis of quinoxalines derivatives starting from diketones (substituted benzils, phenanthrene-9,10-dione) and also benzoins and aromatic diamines in 71-93% yields at room temperature in ethanol (Scheme III.B.3).[21]

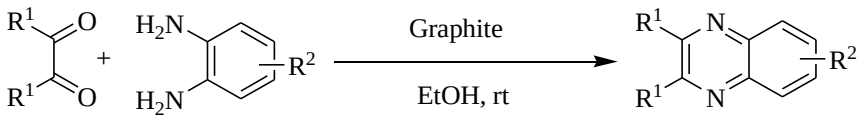

R^1 = Ph, 4-$OMeC_6H_4$, 4-$OMeC_6H_4$, furyl
R^2 = H, 4-MeC_6H_4, 4-COPh, NO_2

Scheme III.B.4. Graphite–catalyzed quinoxalie synthesis.

It is worth to mention that 1, 2-diamines are most common substrates generally used for the quinoxaline synthesis but practically it is reported that aryl 1,2-diamines are carcinogenic and relatively unstable than its precursor nitro compounds.[22] Therefore, there becomes a need to develop more efficient methodologies for such heterocyclic compounds quinoxalines using nitro-compounds. But a very few number of methods are reported for the quinoxline synthesis directly from 2-nitroaniline.[22, 23]

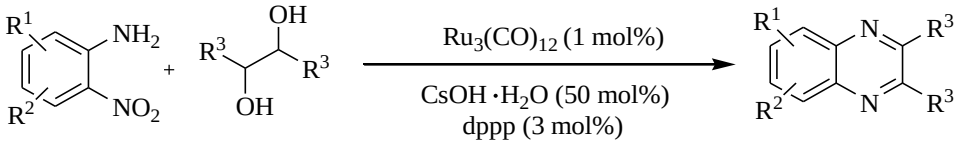

R^1 = H, 4-Me, 4-OMe, 4-Cl, 4-F
R^2 = H, 5-Me
R^3 = H, Me, Ph

upto 87% yield

Scheme III.B.5. Ruthenium catalyzed quinoxaline synthesis from various nitroanilines and symmetrical vicinal diols.

Xie *et al.*[22] reported a one-pot method for efficient synthesis of quinoxalines (Scheme III.B.5) from 2-nitroanilines and biomass-derived vicinal diols using ruthenium-catalyzed hydrogen transfer strategy.

Go *et al.*[23a] have utilized indium with an appropriate acid such as acetic acid or indium(III) chloride for the synthesis of a variety of quinoxaline derivatives in moderate to excellent yield by the one-pot reduction-cyclization of 2-nitroanilines and 1,2-diketones (Scheme III.B.6).

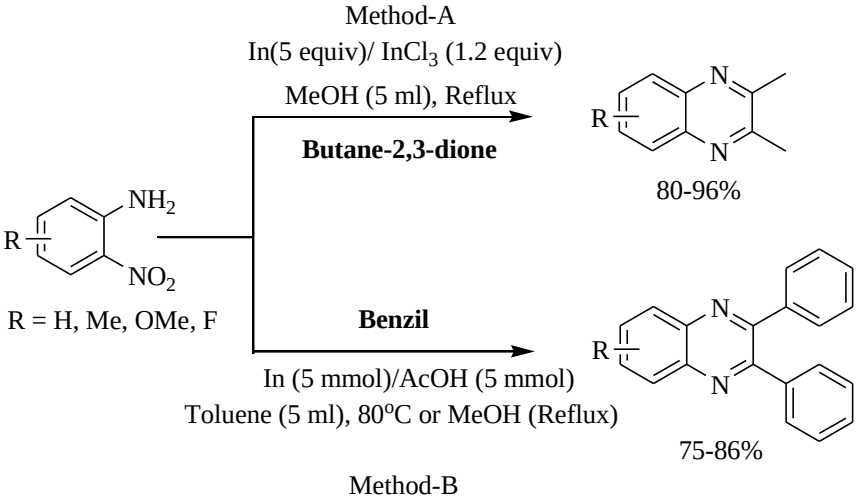

Scheme III.B.6. Synthesis of 2,3-dimethylquinoxalines and 2,3-diphenylquinoxaline in the presence of indium and $InCl_3$ in different condition.

A catalytic amount of iron sulfide generated in situ from nontoxic $FeCl_3 \bullet 6H_2O$ and elemental sulfur was found to act as an efficient catalyst for the redox condensation reaction between *o*-nitroanilines and 2-arylethylamines under solvent free conditions which constitutes a new atom-, step-, and redox-economical route to 2-arylquinoxalines (Scheme III.B.7).[23b]

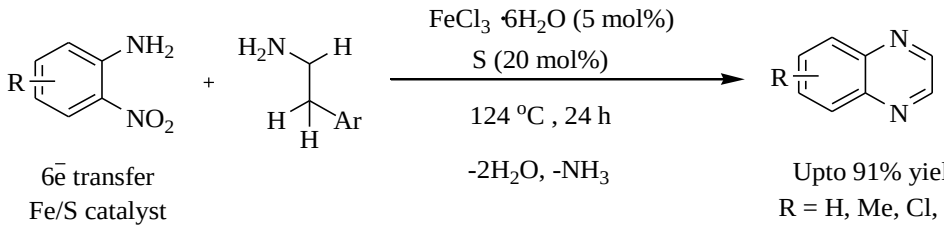

Scheme III.B.7. Fe/S–catalyzed redox condensation reaction of 2-arylethylamines with various *o*-nitroanilines.

Gold nanoparticles supported on nanoparticulated ceria (Au/CeO2) or hydrotalcite (Au/HT) have been reported as efficient catalysts for the one-pot three-step synthesis of 2-methylquinoxaline starting from 1,2-dinitrobenzene and 1,2-propanediol (Scheme III.B.8).[23c]

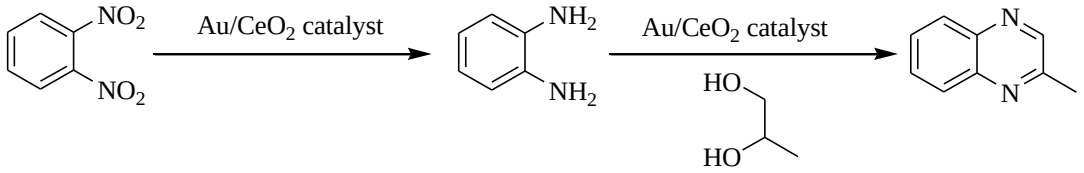

Scheme III.B.8. Au/CeO_2 catalyzed one-pot three-step synthesis of quinoxaline derivatives.

D.-Q. Shi *et al.*[23d] reported the role of stannous chloride as both reductive agent and catalyst for the synthesis of various quinoxaline derivatives by the reaction of 1,2-diketones and 2-nitroaniline. This method has the advantages of accessible starting materials, convenient manipulation, short reaction time and high yields (Scheme III.B.9).

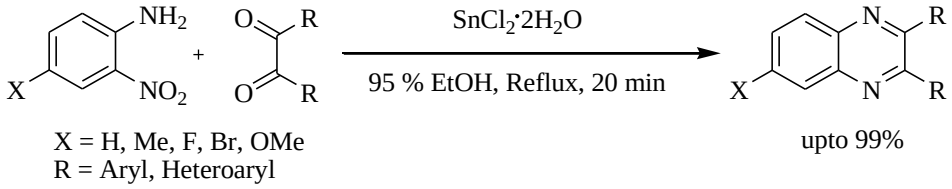

Scheme III.B.9. The synthesis of quinoxalines by the reaction of 2-nitroanilines and 1,2-dicarbonyl compounds mediated by $SnCl_2 \cdot 2H_2O$.

Although all these methods have enough efficiency for the synthesis of quinoxaline derivatives but the problem is in the involvement of expensive metals to carry out the reduction of nitro compounds to amine. On the other hand, the primary demands of green synthesis include minimization of steps, that is, one-pot tandem reactions as well as catalytic processes under metal-free conditions.[24] Since, there is no method developed for the one-pot and metal-free tandem synthesis of quinoxalines from nitroaniline or dinitrobenzene, we were interested to develop an alternative metal-free greener process for the synthesis of quinoxalines directly from 2-nitroaniline. The biomass derived carbon materials has been considered as potential catalyst for diverse organic reactions.[25] Since the seminal report by

Bielawski *et al.*[26e] in 2010, the use of graphene oxide (GO) as the 'carbocatalyst' in organic reactions has evolved enormous interests among the synthetic organic chemists.[25,26] While searching the literature, we find that reduced graphene oxide (rGO) in combination with large excess of hydrazine hydrate can perform the reduction of nitrobenzene to aniline, which is as good as commonly used noble metal catalyst like Pt/SiO_2.[27]

In connection with our interest to harness the utilization of sustainable carbonaceous materials in catalyzing diverse organic reactions,[28] we envisioned that GO or rGO could serve as an eco-friendly alternative catalyst for the synthesis of quinoxaline through the metal-free tandem reduction-condensation in one-pot protocol. Although the reported procedure using rGO for the reduction of nitroaniline is quite useful, further one-pot condensation with 1,2-dicarbonyl compound might lead to multifarious results due to the presence of excess hydrazine in the reaction mixture. In our strategy, it was therefore necessary to find out an optimized condition that could avoid the excess use of the reducing source hydrazine.

We report herein our findings that finally established a practical and clean procedure for the synthesis of quinoxalines directly from 2-nitroaniline *via* one-pot reduction-condensation reactions under metal-free condition. There was no other by-product detected by analysis of the crude product, the conversion was high (observed through HPLC) and the isolation of the desired quinoxaline was achieved in excellent yield. A large variation of functional groups attached with the aromatic rings of either of the condensing partners was observed with excellent conversions to quinoxalines (Scheme III.B.10).

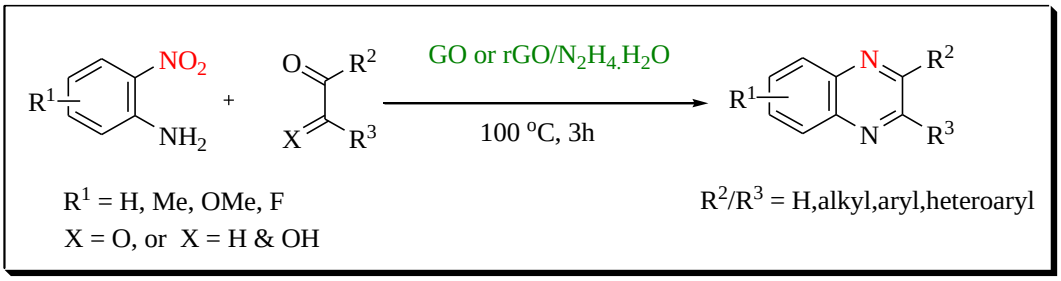

Scheme III.B.10. One-pot reduction of nitro compounds and subsequent condensation resulting quinoxalines.

III.B.3. Present Work: Results and Discussion

III.B.3.1. Preparation and characterization of graphene oxide

Initially, we have prepared GO according to the modified Hummer's method,[29] as following:

To an ice-cold concentrated sulfuric acid (46 mL) sodium nitrate (0.1 g) and then graphite powder (2 g) were slowly added with vigorous magnetic stirring. After the complete addition of graphite powder, potassium permanganate (6 g) was added to the reaction mixture very slowly, keeping the temperature within 0-5 ^{o}C to avoid any possible explosion. The mixture was allowed to stir at room temperature for 6 h forming a thick paste. It was diluted with double distilled water (92 mL) under stirred condition. The temperature of the solution was raised to about 90 ^{o}C and the mixture was allowed to stir for 30 min. Finally, 280 mL water was added followed by slow addition of 3 mL H_2O_2 (30%). The colour of the solution changes from dark brown to yellowish brown. The overall solution was washed using deionized and distilled water repeatedly *via* ultrasonication and centrifugation at 5000 rpm until the pH of the solution become 7 (using pH paper) to make it free from acid. Finally, the product was filtered off and the brown mass was collected and dried at 60 ^{o}C under vacuum to obtain solid graphene oxide prepared GO by using modern Hummers' method,[29] and properly characterized by FT–IR spectroscopy (Figure III.B.2).

GO was characterized by FT–IR spectroscopy in KBr, which was comparable with literature data.[30, 31]

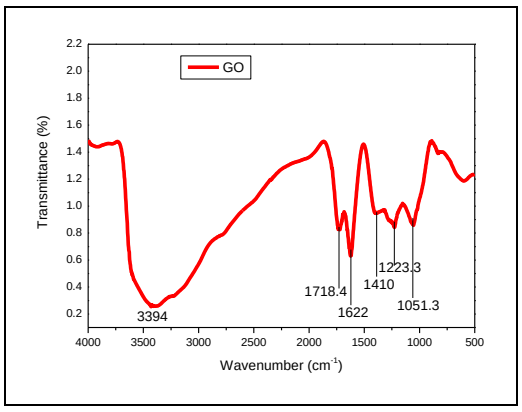

Sl. No.	Functional groups of GO	Wave number (cm^{-1})	
		Observed	Literature[3]
1	–OH	3394	3368
2	–COOH	1718.4	1719
3	–C=C–	1622	1624
4	–C–OH	1410	1373
5	C–O–C (epoxy)	1223	1228
6	C–O–C (alkoxy)	1051.3	1050

Figure III.B.2. The FT–IR Spectra of GO.

II.B.3.2. DLS study of GO

To know the particle size we have performed the dynamic light scattering (DLS) analysis of graphene oxide. For this we have prepared 50 mL GO dispersion (0.1mg/mL) in DI water which was sonicated for one hour. Then we go through the DLS study of the dispersion of GO. The average size of GO particles in the dispersion of water was found to be 544 ± 37 nm which is comparable with the literature report (Figure III.B.3).[32]

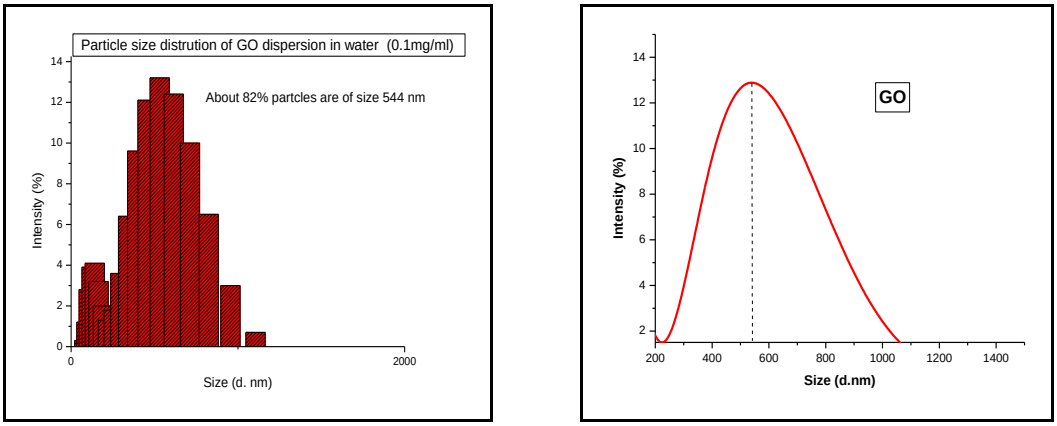

Figure III.B.3. Particle size distribution plot of graphene oxide obtained from dynamic light scattering (DLS).

III.B.3.3. AAS study of GO

Since, a large quantity of $KMnO_4$ was used for the preparation of GO, we presumed that few ions of manganese can exist as metal impurities. To confirm the presence of manganese in graphene oxide we performed atomic absorption spectroscopy (AAS) study. For this purpose, 50 mg of GO was first digested with 25 mL concentrated HNO_3 on a hot plate. Then GO was separated through filtration and the remaining acid extract was diluted to 100 ml to performe AAS. The amount of manganese estimated was 0.16 mg per 100 mg of GO.

III.B.3.4. Optimization of reaction conditions

After that our studies began with the reaction of 2-nitroaniline and benzil in the presence of GO and hydrazine hydrate. Since benzil can also react with hydrazine to form hydrazone,[33] we set up the reaction by adding the reacting components in a step-wise manner and not in the multi-component reaction approach.[34] Thus a neat mixture of 2-nitroaniline (1 mmol), graphene oxide (5 mg), and hydrazine hydrate (6 mmol) was heated at 100 ^{o}C for 3 h (tlc monitoring showed complete disappearance of the nitroaniline), and then benzil (1 mmol) was added to the reaction mixture. After stirring for another 3h at 100 ^{o}C, tlc showed complete disappearance of benzil on tlc plate. Ethyl acetate was added to the reaction mixture and the catalyst GO was separated out by centrifugation. HPLC analysis of the crude mixture showed the ratios of quinoxaline and dihydrazone derivative of benzil (prepared separately for comparison) in 70:30 mixtures. Separation of the crude mixture by column chromatography over silica gel afforded the quinoxaline (68%). The observation is presented in Table III.B.1 (entry 1). Further optimization of the reaction conditions by changing the

quantity of GO and/or hydrazine hydrate led us to achieve only quinoxaline as the sole product in 92% isolated yield (entries 2–7). However, as in entry 7, there was un-reacted benzil (6%) observed by HPLC analysis of the crude reaction mixture. Decreasing the temperature of the reaction furnished the hydrazone again (entry 8). Use of solvents like water, methanol or ethyl acetate however resulted in significant quantity of the hydrazone (entries 9–11). Further examination of the second step, that is, the condensation reaction carried out at room temperature was not favorable but the same at 60 ^{o}C afforded the quinoxaline in isolated yield (93%) (entries 12 and 13).

Table III.B.1. Optimization of reaction conditions for GO–catalyzed one-pot reduction and heterocyclization of 2-nitroaniline (1 mmol) and benzil (1 mmol)

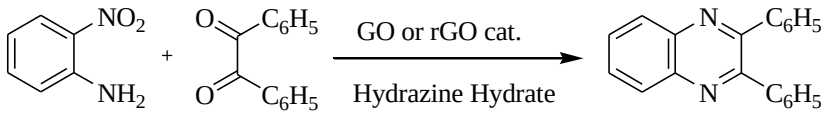

Entry no.	GO (mg)	Temp (^{o}C)	Solvent	Hydrazine hydrate ($N_2H_4.H_2O$) (mmol)	Time (h) (Reduction & Condensation)	Conversion (%)[a]	
						Quinoxaline (% Yield)	Hydrazone[a]
1	5	100	No	6	(3 & 2)	70 (68)	30
2	10	100	No	4	(3 & 2)	78 (76)	22
3	15	100	No	4	(3 & 2)	80 (78)	20
4	15	100	No	3	(3 & 2)	87 (85)	13
5	15	100	No	2.5	(3 & 2)	90 (88)	10
6	15	100	No	2.2	(3 & 2)	91 (89)	09
7[b]	20	100	No	2.2	(3 & 2)	94 (92)	No
8	20	80	No	2.2	(3 & 2)	87 (81)	13
9	20	100	Water	2.2	(4 & 2)	75 (71)	25
10	20	100	MeOH	2.2	(4 & 2)	71 (68)	29
11	20	100	EtOAc	2.2	(4 & 2)	75 (68)	25
12[c]	20	100	No	2.2	(3 & 12)	83 (81)	17
13[d]	**20**	**100**	**No**	**2.2**	**(3 & 3)**	**95 (93)**	**No**
14[e]	20	100	No	2.2	(3 & 3)	93 (91)	07
15[f]	No	100	No	2.2	(6 & 3)	09	65
16[g]	50	100	No	11	(4 & 3)	88	No

[a]Conversion was checked by HPLC and yield of quinoxaline (in the parenthesis) represents the isolated product after column chromatography. [b]Un-reacted benzil (6%). [c]Condensation with benzil was performed at room temperature. [d]Condensation with benzil was performed at 60 ^{o}C and un-reacted benzil. [e]rGO was used instead of GO and condensation with benzil was performed at 60 ^{o}C. [f]Un-reacted benzil (26%). [g]Reaction carried out with 2-nitroaniline (5 mmol). [Entries 1-5, 9-11, 13, 16 were performed by the present author and the remaining

optimization experiments were performed by one of my co-author S. Ghosh and entries 13 and 6,7, 14, 15 were repeated by both of author for 2 times]

Since hydrazine can also reduce the GO to reduced GO (rGO), we had separately prepared rGO using hydrazine,[30] and used it for the same one-pot reaction. It was observed that the rGO is also an equally effective catalyst for the reduction of 2-nitroaniline and subsequent condensation with benzil (entry 14). The control experiment without using GO did provide only trace amount of quinoxaline (≤10%) signifying the catalytic role of the graphene oxide (entry 15). In another experiment, the reaction was scaled up using 2-nitroaniline (5 mmol) and the catalyst GO (50 mg), which afforded finally the quinoxaline in 88% isolated yield (entry 16). Thus the optimized condition was found to be the reaction of 2-nitroaniline (1 mmol), hydrazine hydrate (2.2 mmol) and GO (20 mg), stirring the mixture in neat at 100 ^{o}C for 3h, then benzil (1 mmol) was added and further stirring at 60 ^{o}C for 3h.

III.B.3.5. Applications of our optimized condition in a variety of 2-nitroanilines and benzil derivatives

With the optimized condition at our hand (as in Table III.B.1, entry 13), we examined its practical applications with a variety of nitroanilines and benzil derivatives. The results are presented in Table III.B.2. It can be seen that different nitroanilines undergo one-pot reduction and condensation with benzils gave rise to the formation of corresponding quinoxalines in excellent yields (Table III.B.2, entries 1–8). Since the present reducing condition is metal-free, it was interesting to examine whether halogen substituents could survive the overall reaction conditions. We employed 4,4′-dibromobenzil as the condensing partner and indeed the corresponding bromosubstituted quinoxalines were isolated in 90–95% yields (entries 9–11). Heteroaromatic benzils like a-furil also yielded corresponding furyl-containing quinoxaline derivatives in isolated yield (>90%) (entries 12–14). Further studies with glyoxal, aliphatic 1,2-diketones, and phenylpropane-1,2-dione also resulted in the formation of quinoxaline in good to excellent yields (entries 15–19). Thus, functional groups like methyl, methoxyl, furyl, or bromide being present with either nitroaniline or dicarbonyl compounds as well as the ketone or aldehyde functions worked without any difficulty yielding the final quinoxalines in excellent yields. We then examined similar reactions using 2-nitroaniline bearing an electron-withdrawing group such as F or –COPh (entries 20 and 21) as well as with 1,2-dinitrobenzene (entry 22). While 4-fluoro-2-nitroaniline resulted in the formation of the desired quinoxaline in excellent yield, 4-benzoyl-2-nitroaniline gave rise to a

mixture of four spots on tlc and one of those was matched with the authentic sample [(phenyl(2,3-diphenylquinoxalin-6-yl) methanone)].[16b] However, the desired quinoxaline could not be separated and its actual yield was not obtained. Possibly, the benzoyl group suffers from reaction with hydrazine causing an inseparable mixture of products. In the case of 1,2-dinitrobenzene, similar reaction was sluggish and the desired quinoxaline was isolated in 48% yield. Since GO is known by its intriguing properties as an oxidizing agent, dual role of GO might be expected if α-hydroxy ketone is used as the condensing partner instead of 1,2-diketone. Acyloins are often considered as the precursor of diketo equivalent compounds. The reaction with benzoin indeed resulted in the formation of quinoxaline in isolated yield (91%) (entry 23). Substituted nitroanilines and other variety of acyloin such as furoin also gave rise to the formation of quinoxaline in 86–92% yields (entries 24–28).

Table III.B.2. GO-catalyzed reduction of various 2-nitroanilines and subsequent heterocyclization with 1,2-dicarbonyl compounds or with α–hydroxy ketones[a]

Entry	2-Nitro aryl amine	1,2-Dicarbonyl compound/ a-Hydroxy ketone	Temp (°C) (Reduction & Codensation)	Time (h) (Reduction & Codensation)	Product	Yield (%)[b]
1	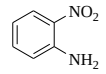	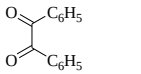	100 & 60	3 & 3	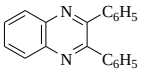	93
2	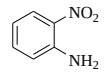	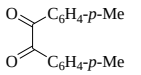	100 & 60	3 & 3	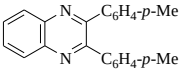	91
3	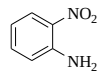	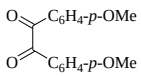	100 & 60	3 & 3	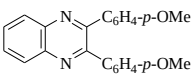	92
4	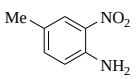	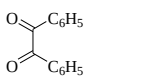	100 & 60	4 & 3	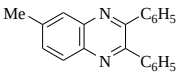	89
5	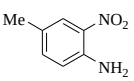	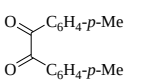	100 & 60	4 & 3	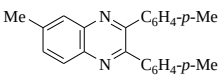	91
6	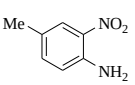	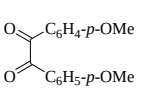	100 & 60	4 & 3	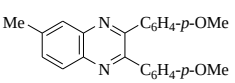	90
7	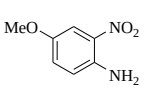	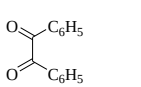	100 & 60	4 & 3	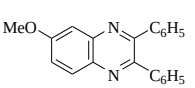	90
8	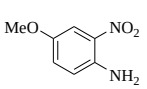	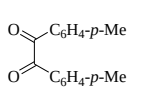	100 & 60	4 & 3	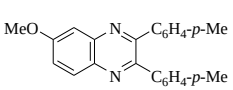	88
9		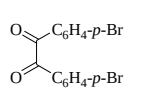	100 & 60	3 & 3.5	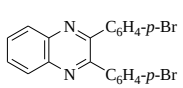	95

10	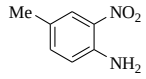	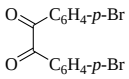	100 & 60	4 & 3.5	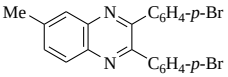	92
11	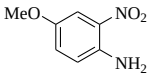	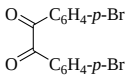	100 & 60	4 & 3	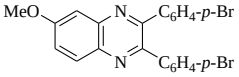	90
12	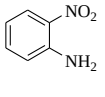	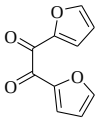	100 & 60	3 & 3	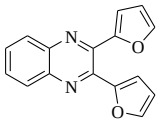	91
13	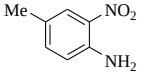	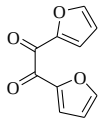	100 & 60	4 & 3	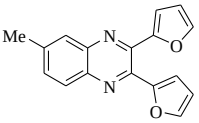	90
14	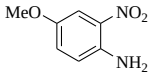	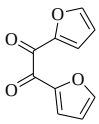	100 & 60	4 & 3	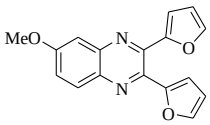	89
15	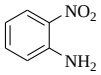		100 & 60	3 & 2		85
16	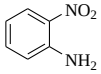		100 & 60	3 & 3	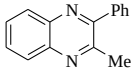	84
17	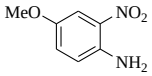		100 & 60	4 & 2	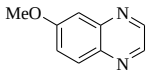	87
18	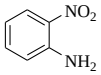		100 & 60	3 & 2.5	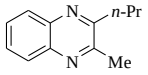	83
19	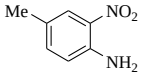		100 & 60	4 & 3	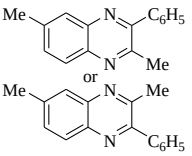	88
20	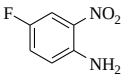		100 & 60	4 & 4	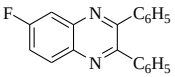	87
21[c]	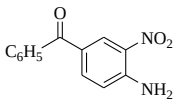		100 & 60	5 & 4	Inseparable mixtures of different products	–
22[d]	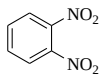		100 & 60	4 & 3	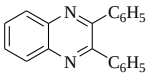	48
23	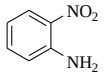	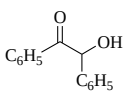	100 & 80	3 & 1.5		91
24			100 & 80	4 & 2		90

25	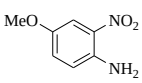	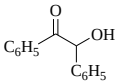	100 & 80	4 & 2	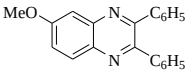	92
26		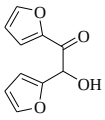	100 & 80	3 & 2	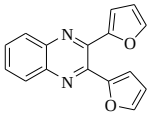	87
27	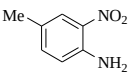	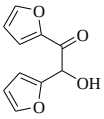	100 & 80	4 & 2	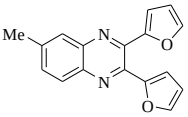	88
28	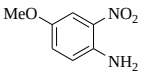	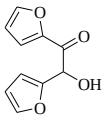	100 & 80	4 & 2	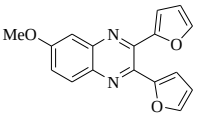	86

[a] Reaction conditions: a mixture of 2-nitro aryl amine (1 mmol), hydrazine monohydrate (2.2 mmol) and GO (20 mg) was heated in a sealed tube with magnetic stirring for hours and then 1,2-dicarbonyl compound or a-hydroxy ketone (1 mmol) was added to the reaction mixture and stirred. [b]Isolated yield after column chromatography. [c]The reaction furnished a non-separable mixture of compounds.[d] The reaction was carried out using 4.4 mmol of hydrazine hydrate. [Entries 1−4, 8−13, 18−19, 22, 27−28 were performed by the present author]

III.B.3.6. Recyclability of the catalyst

We have also tested the reusability of the catalyst GO. The catalyst was recovered from the reaction mixture as follows: The reaction mixture was taken in water (2 mL), subjected to the centrifugation (5000 rpm) and removed the supernatant liquid. The residue was washed with ethyl acetate followed by acetone. Drying under vacuum furnished the free-flowing powder, which is visibly blackish as compared to the first-time used GO.

After the first run, the recovered catalyst by weight was low, which could possibly be attributed to the removal of several oxygenated functional groups. It was then used in the second run with nearly equal catalytic efficiency in the reduction and subsequent condensation producing the quinoxaline product in 91% isolated yield. In the third and fourth runs, the quantity of the recovered catalyst by weight was nearly equal (from the second run) and indeed found to be significantly active with appreciable conversions. The results are presented in the Table III.B.3.

Table III.B.3. Recycling of the catalyst tested with 2-nitroaniline and benzil in one-pot reactions

Entry[a]	Recovered Catalyst (mg)	Catalyst used (mg)	Time (h) (Reduction & Condensation)	Yield (%)[b]
1st run	–	40	3 & 3	93
2nd run	28	20	3 & 3	91
3rd run	16	15	4 & 3	85
4th run	14	10	5 & 3	84

[a]First experiment was performed with 2-nitroaniline (2 mmol), hydrazine hydrate (4.4 mmol), benzil (2 mmol) and GO (40 mg), and subsequently in 1, 0.75 and 0.5 mmol scales. [b]Isolated product after column chromatography.

III.B.3.7. Characterization of the recovered catalyst after 1st run of the reaction and also the hydrazine reduced GO

Owing to the colour change from brownish to totally blackish of the recoverd catalyst as well as the weight loss of the catalyst after the 1st run of the reaction, we assume that the recovered catalyst may be the reduced graphene oxide (rGO), which was confirmed by comparison of the FT-IR spectroscopic characteristic absorption peaks as in Figure III.B.3.

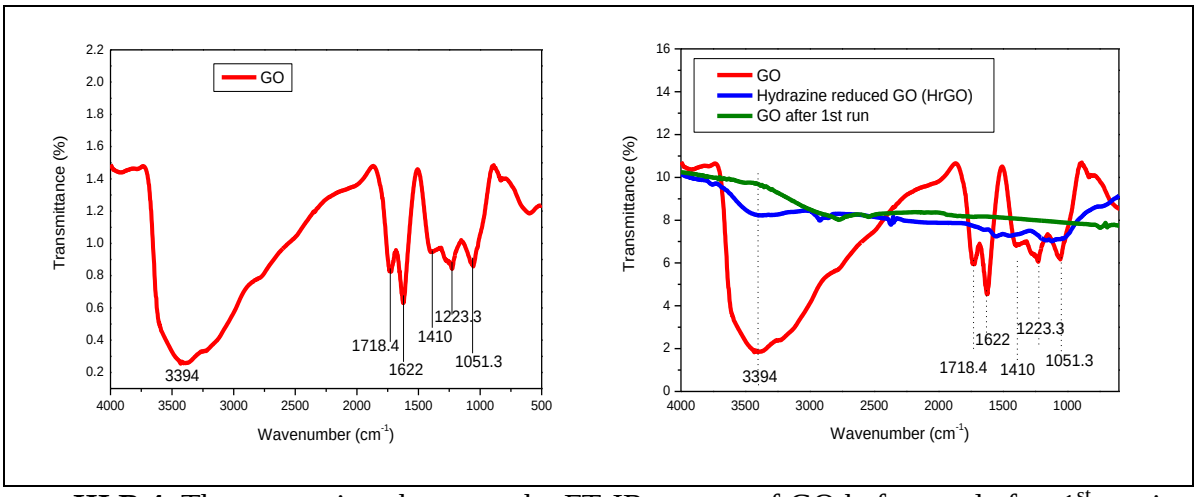

Figure III.B.4. The comparison between the FT-IR spectra of GO before and after 1st use in the one-pot reduction and heterocyclization reaction between 2-nitroaniline and benzil with hydrazine reduced GO (HrGO).

III.B.3.8. Mechanism

Mechanistically, carbon-catalyzed reduction of nitrobenzene to aniline by hydrazine is believed to involve four-electron process occurring through the formation of

phenylhydroxylamine.[35] While hydrazine is a two-electron reducing agent, the role of carbon materials such as graphite, GO or rGO might be to serve as an adsorbent as well as the conductor of electrons.[27, 35] In order to find out the possible involvement of GO or rGO in the second step of condensation, we performed few reactions starting from *o*-phenylenediamine, it was postulated that the attack of amine N-lone pair to the carbonyl group is facilitated by the presence of graphite.[21] At our hand, the condensation of *o*-phenylenediamine with benzil in neat in the absence of GO afforded only 30% conversion to quinoxaline after 3h at 60 ^{o}C, while the same reaction carried out in ethyl acetate resulted in >90% conversion to quinoxaline. Similarly, heating the neat reaction mixture of *o*-phenylenediamine, benzoin, and rGO at 80 ^{o}C gave nearly complete conversions after 2h (analyzed by HPLC).

The above observations suggest that the catalyst GO or rGO plays a positive role in promoting the second step of condensation as well as the oxidation of benzoin to benzil. Although the exact function of GO or rGO is not clearly understood, we tend to believe that GO is at first reduced to rGO and its electron-rich large surface area might act favourably as the conductor of electrons thereby facilitating release of hydrogen source from hydrazine that is finally responsible for the reduction of nitro group,[27,36] as well as assisting to promote the condensation between the diamine and diketone to form quinoxaline. Plausible mechanism is presented in Scheme III.B.11 indicating the role of GO or rGO.

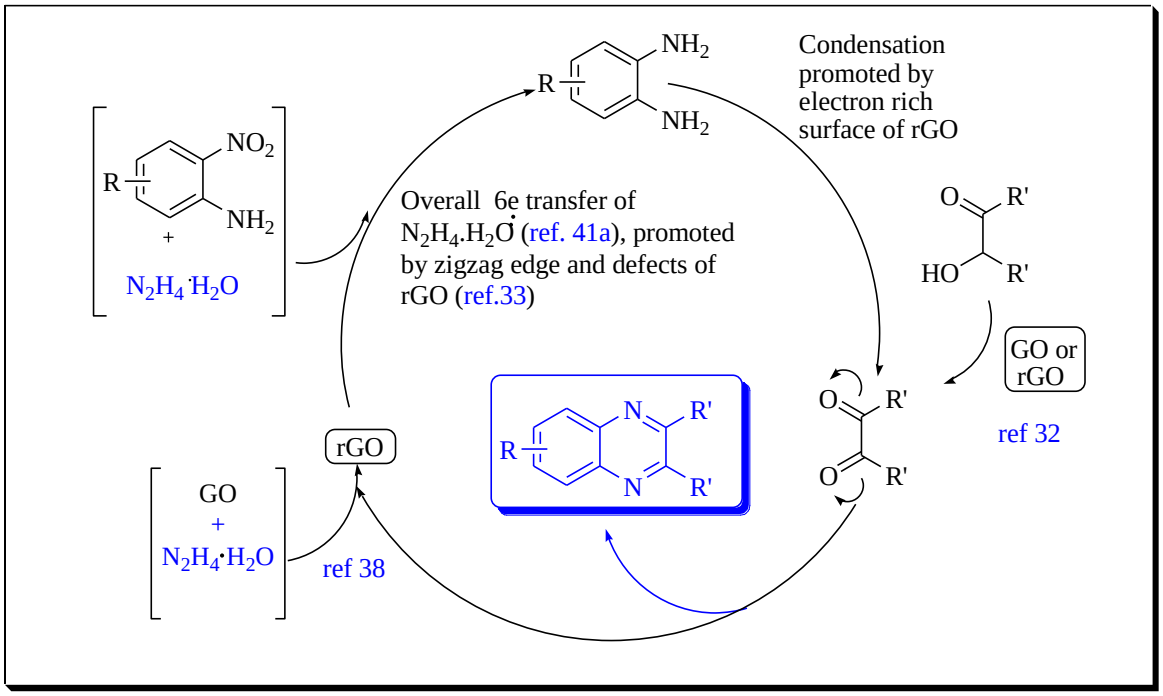

Scheme III.B.11. Plausible mechanism for the quinoxaline synthesis. [This mechanism was developed by present author as well as my co-author]

III.B.4. Conclusion

In summary, the present work demonstrates synthesis of bio-active scaffold quinoxalines directly from 2-nitroaniline via one-pot reduction-condensation reactions using hydrazine as the reductant and GO/rGO as the catalysts under complete metal free conditions. The conditions are straightforward, mild and no other side-products are obtained. Green process of preparation of quinoxalines from 2-nitroaniline is developed that could override existing metal-catalyzed reaction conditions. Finally, GO/rGO can have broad utility in various organic reactions under metal-free condition which will be attractive for further research.

III.B.5. Experimental Section

III.B.5.1. General Information

All the reagents were purchased from Sigma-Aldrich and used directly without further purification. Hydrazine monohydrate (80%) was purchased from SDFCL. The solvents were purchased from commercial suppliers and used after distillation. The other information related to column chromatography and FT–IR spectroscopy are same as described in the Chapter II (please, see the Chapter II.5. General Information). HPLC analyses were carried out using HPLC (Agilent Technologies, 1260 Infinity), Column: Poroshell 120 EC-C18 (4.6 x 50 mm, 2.7 μm), eluent: MeOH (flow rate 0.25 mL min^{-1}). Centrifugation was done in REMI R-8C DX (RPM 5250) centrifuge. AAS was measured by Varian SpectrAA 50B Atomic Absorption Spectrometer. DLS analysis was done by Malvern Zetasizer Nano-ZS90 instrument.

III.B.5.2. Preparation of reduced graphene oxide (rGO)

Reduced graphene oxide (rGO) was prepared according to Ruoff's method.[30] For the preparation of hydrazine hydrate reduced graphene oxide (HrGO), 100 mg of GO prepared by Hummers' method,[29] was taken in a 250 ml round bottom flask and 100 ml deionized water was added to make a dispersion of GO. This dispersion was then sonicated for 1 h to make a homogenous dispersion of graphene oxide. Then, 1 ml of hydrazine hydrate (80% in water) was added to this yellowish brown dispersion and heated in an oil bath at 100 ^{o}C under reflux for 24 h. When the overall dispersion would become black indicates the reduction have taken place. This product was then separated through centrifugation at 5000 rpm and washed for

three times using de-ionized (DI) water and finally with acetone. The solid black product was dried over vacuum pump.

III.B.5.3. General procedure for the preparation of quinoxaline derivatives

A mixture of 2-nitro aniline (1 mmol), hydrazine monohydrate (2.2 mmol) and GO (20 mg) was taken in a screw-capped glass tube and stirred the reaction mixture for 3-4 h at 100 ^{o}C temperature. After the complete reduction (as monitored by tlc and by the colour change of the reaction mixture from yellow to total black), 1,2-dicarbonyl compound (or α-hydroxy ketone) (1 mmol) was added to the reaction mixture and stirred for few hours at 60 ^{o}C (80 ^{o}C for α-hydroxy ketone), as mentioned in the Table 2. After completion of the reaction (checked by tlc), the reaction mixture was cooled to room temperature. Water and ethyl acetate were added to the reaction mixture and centrifuge (5000 rpm) the whole reaction mixture to separate the GO (which is now converted to rGO). This process was repeated for three times. The combined organic-aqueous part was then taken in a separating funnel and the organic layer was separated from aqueous layer, and finally dried over anhydrous Na_2SO_4. Evaporation of the solvent afforded the desired quinoxaline (satisfactorily pure), which was further purified by passing through a short column of silica gel and using the light petroleum ether:ethyl acetate (97:3) as the eluent. All products were characterized by ^{1}H, ^{13}C NMR data and compared with the reported melting points for known solid compounds.

III.B.5.4. HPLC analysis

After completion of the reaction the crude mixture was allowed to cool at room temperature, then a little of this crude reaction mixture was taken in a vial and then 5 ml of MeOH (HPLC grade) was added to it. Finally it was filtered and then HPLC analysis was performed. Fig. 3 signifies there was no formation of any hydrazone in our optimized condition.

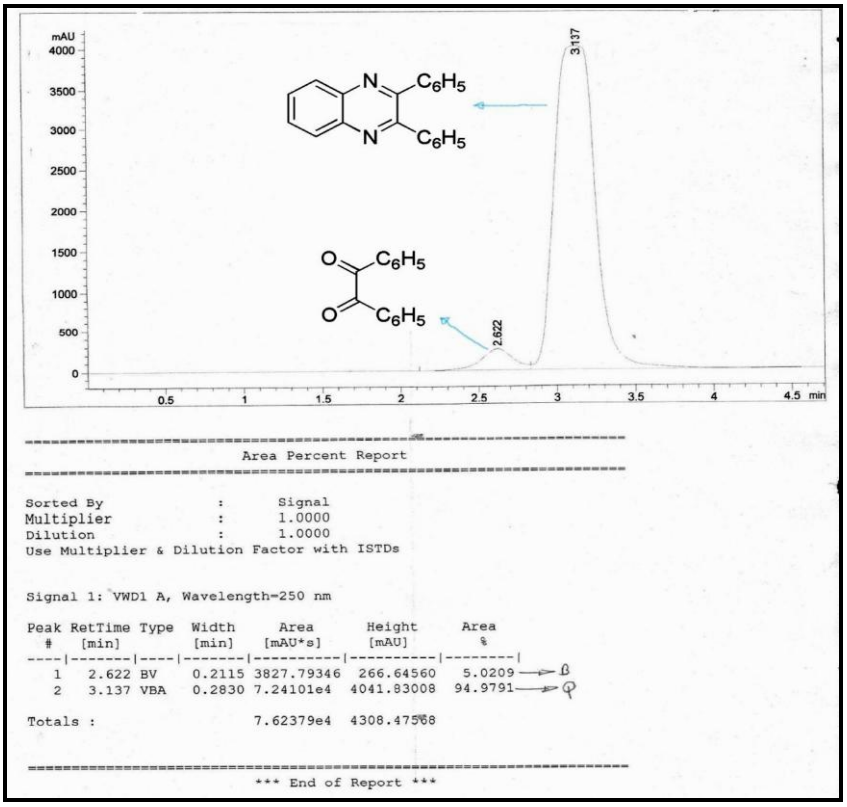

Area Percent Report

Sorted By : Signal
Multiplier : 1.0000
Dilution : 1.0000
Use Multiplier & Dilution Factor with ISTDs

Signal 1: VWD1 A, Wavelength=250 nm

Peak #	RetTime [min]	Type	Width [min]	Area [mAU*s]	Height [mAU]	Area %	
1	2.622	BV	0.2115	3827.79346	266.64560	5.0209	→ β
2	3.137	VBA	0.2830	7.24101e4	4041.83008	94.9791	→ Q

Totals : 7.62379e4 4308.47568

*** End of Report ***

Figure III.B.5. HPLC of crude reaction mixture (Table III.B.1, Entry 13 reaction), the area percentage of quinoxaline product and starting benzil is in the ratio of 95:5.

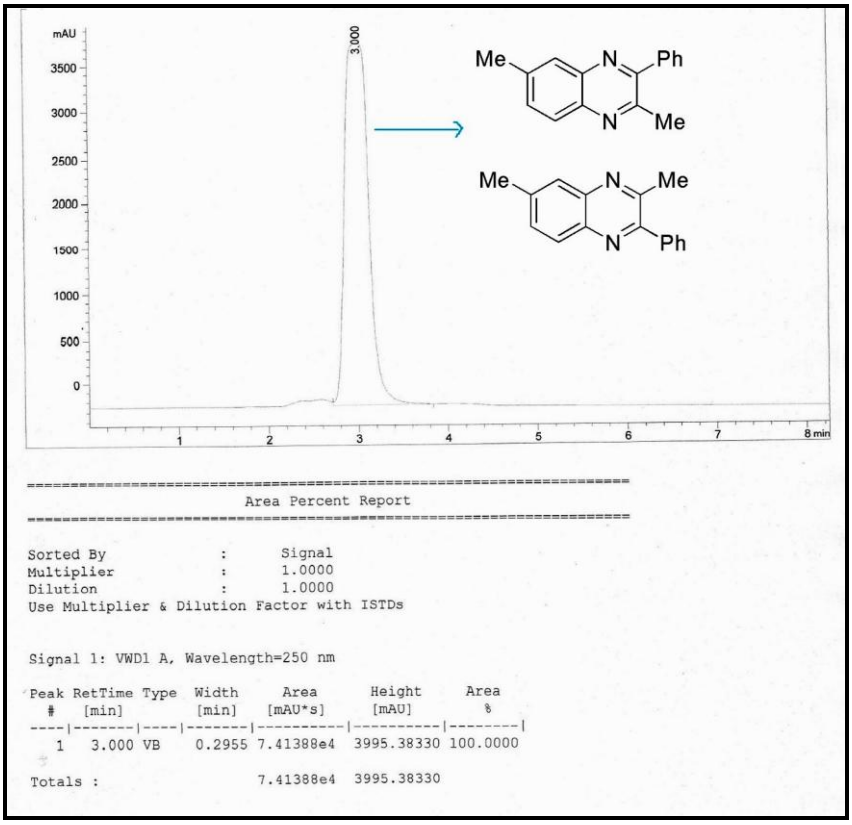

Area Percent Report

Sorted By : Signal
Multiplier : 1.0000
Dilution : 1.0000
Use Multiplier & Dilution Factor with ISTDs

Signal 1: VWD1 A, Wavelength=250 nm

Peak #	RetTime [min]	Type	Width [min]	Area [mAU*s]	Height [mAU]	Area %
1	3.000	VB	0.2955	7.41388e4	3995.38330	100.0000

Totals : 7.41388e4 3995.38330

Figure III.B.6. HPLC analysis of a pure mixture of two regioisomer (Table III.B.2, Entry 19).

III.B.5.5. Spectral data and melting points of quinoxaline compounds

Table III.B.2; Entry 1, 21 & 22

2,3-Diphenyl quinoxaline[37]

The product obtained as a white needles crystal, mp: 126–127 ^{o}C (lit. 125–127 ^{o}C)

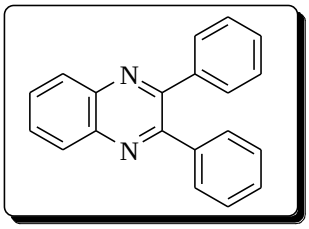

^{1}H NMR (CDCl$_3$, 300 MHz): δ 7.35-7.42 (m, 6H), 7.52-7.58 (m, 4H), 7.76-7.83 (m, 2H), 8.19-8.26 (m, 2H).

^{13}C NMR (CDCl$_3$, 75 MHz): δ 128.6, 128.8, 129.2, 129.89, 129.98, 139.1, 141.3, 153.5.

Table III.B.2; Entry 2

2,3-Di-*p*-tolyl quinoxaline[38]

The product obtained as a white crystalline solid, mp: 146-148 ^{o}C (lit. 148.5–149.7 ^{o}C).

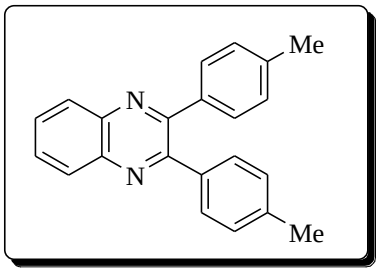

^{1}H NMR (CDCl$_3$, 300 MHz): δ 2.27 (s, 6H), 7.04 (dd, *J* = 2.1 & 6 Hz, 4H), 7.31-7.35 (m, 4H), 7.60-7.65 (m, 2H), 8.02-8.07 (m, 2H).

^{13}C NMR (CDCl$_3$, 75 MHz): δ 21.4, 129.0, 129.1, 129.7, 129.8, 136.4, 138.8, 141.2, 153.5.

Table III.B.2; Entry 3

2,3-Bis(4-methoxyphenyl) quinoxaline[39]

The product was obtained as pale yellow crystals, mp: 148-150 ^{o}C (lit. 148–150 ^{o}C)

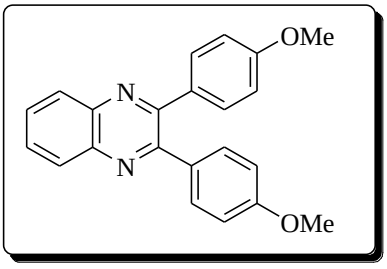

^{1}H NMR ($CDCl_3$, 300 MHz): 3.83 (s, 6H), 6.87 (d, *J* = 8.4 Hz, 4H), 7.49 (d, *J* = 8.7 Hz, 4H), 7.71 (dd, *J* = 3.6 & 6.3 Hz, 2H), 8.12 (dd, *J* = 3.6 & 6.3 Hz, 2H).
^{13}C NMR ($CDCl_3$, 75 MHz): δ 55.3, 113.8, 129.0, 129.6, 131.3, 131.8, 141.1, 153.0, 160.2.

Table III.B.2; Entry 4 & 23
6-Methyl-2,3-diphenyl quinoxaline[38]
The product was obtained as a white crystalline solid, mp: 116-118 ^{o}C (lit. 115.7–116.9 ^{o}C)

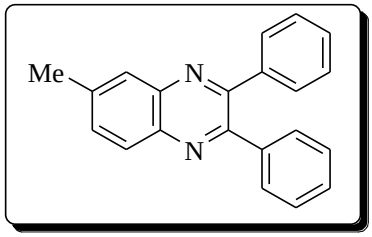

^{1}H NMR ($CDCl_3$, 300 MHz): δ 2.53 (s, 3H), 7.25-7.53 (m, 11H), 7.87 (s, 1H), 7.98 (d, *J* = 8.4 Hz, 1H).
^{13}C NMR ($CDCl_3$, 75 MHz): δ 21.9, 128.1, 128.2, 128.6, 128.7, 129.9, 132.3, 139.3, 139.7, 140.5,141.3,152.6,153.3.

Table III.B.2; Entry 5
6-Methyl-2,3-di-*p*-tolyl quinoxaline[40]
The product was obtained as a pale yellow solid, mp: 136-138 ^{o}C (lit. 137 ^{o}C)

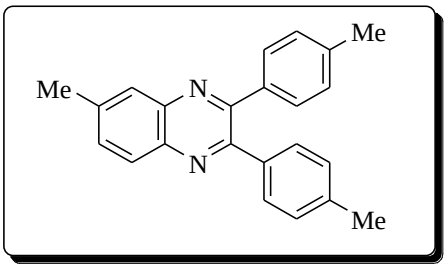

^{1}H NMR ($CDCl_3$, 300 MHz): δ 2.23 (s, 6H), 2.46 (s, 3H), 7.02-7.46 (m, 9H), 7.80 (s, 1H), 7.9-7.95 (m, 1H).
^{13}C NMR ($CDCl_3$, 75 MHz): δ 21.4, 21.9, 128.0, 128.7, 129.0, 129.8, 132.0, 136.6, 138.5, 138.6, 139.7, 140.1, 141.3, 152.6, 153.4.

Table III.B.2;Entry 6
2,3-Bis(4-methoxyphenyl)-6-methyl quinoxaline[41]
The product was obtained as a white crystalline solid, mp: 123-125 ^{o}C (lit. 125–127 ^{o}C)

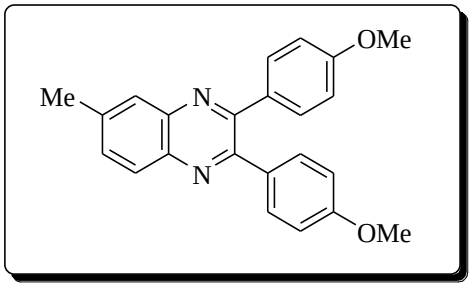

^{1}H NMR ($CDCl_3$, 300 MHz): δ 2.45 (s, 3H), 3.67 (s, 6H), 6.73 (d, *J* = 8.7 Hz, 4H), 7.34-7.41 (m, 5H), 7.77 (s, 1H), 7.88 (d, *J* = 8.4 Hz, 1H).
^{13}C NMR ($CDCl_3$, 75 MHz): δ 21.7, 55.1, 113.6, 127.7, 128.4, 131.0, 131.1, 131.7, 131.8, 139.4, 139.8, 141.0, 152.0, 152.7, 159.89, 159.94.

Table III.B.2; Entry 7 & 24
2,3-Diphenyl-6-methoxy quinoxaline[23d]
The product was obtained as a white solid, mp: 152-154 ^{o}C (lit. 154–156 ^{o}C)

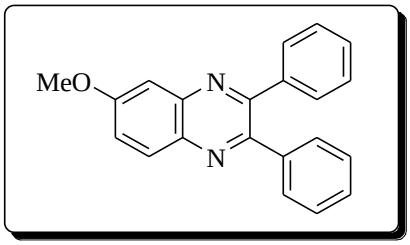

^{1}H NMR ($CDCl_3$, 300 MHz): δ 3.89 (s, 3H), 7.17-7.35 (m, 6H), 7.39-7.43 (m, 6H), 7.97 (d, *J* = 9 Hz, 1H).
^{13}C NMR ($CDCl_3$, 75 MHz): δ 55.9, 106.5, 123.4, 128.2, 128.3, 128.5, 128.7, 129.8, 130.2, 137.4, 139.2, 139.3, 142.8, 151.0, 153.4, 160.9.

Table III.B.2; Entry 8
6-Methoxy-2,3-di-*p*-tolyl quinoxaline
The product was obtained as a pale yellow solid, mp: 73-75 ^{o}C

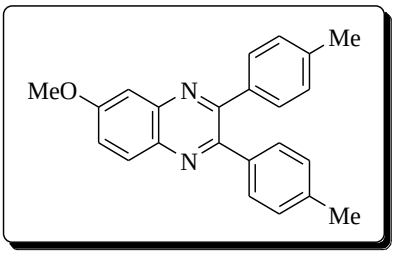

^{1}H NMR ($CDCl_3$, 300 MHz): δ 2.27 (s, 3H), 3.87 (s, 6H), 7.03-7.06 (m, 4H), 7.27-7.35 (m, 6H), 7.93 (dd, *J* = 3 & 9 Hz, 1H).

^{13}C NMR ($CDCl_3$, 75 MHz): δ 55.8, 106.5, 123.0, 129.0, 129.7, 129.72, 130.1, 136.5, 136.6, 137.3, 138.3, 138.6, 142.7, 151.0, 153.4, 160.7.

Table III.B.2; Entry 9

2,3-Bis(4-bromophenyl) quinoxaline

The product was obtained as a white crystalline solid, mp: 192–194 ^{o}C.

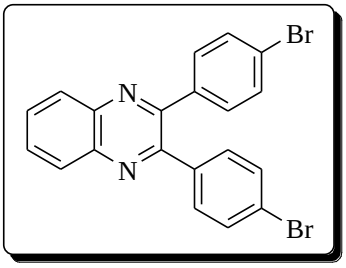

^{1}H NMR ($CDCl_3$, 300 MHz): δ 7.38 (d, *J* = 8.1 Hz, 4H), 7.48 (d, *J* = 8.4 Hz, 4H), 7.76 (dd, *J* = 3.3 & 6.3 Hz, 2H), 8.13 (dd, *J* = 3.3 & 6.3 Hz, 2H).
^{13}C NMR ($CDCl_3$, 75 MHz): δ 123.7, 129.1, 130.4, 131.4, 131.6, 137.6, 141.1, 151.8.

Table III.B.2; Entry 10

2,3-Bis(4-bromophenyl)-6-methyl quinoxaline[42,43]

The product was obtained as a white solid, mp: 174-176 ^{o}C (lit. 175–177 ^{o}C).

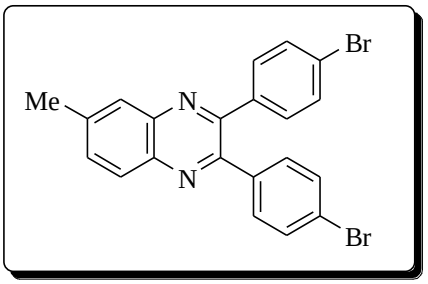

^{1}H NMR ($CDCl_3$, 300 MHz): δ 2.50 (s, 3H), 7.27 (d, *J* = 6.6 Hz, 4H), 7.37 (d, *J* = 6.3 Hz, 4H), 7.48-7.51 (m, 1H), 7.80 (s, 1H), 7.91 (d, *J* = 6.6 Hz, 1H).
^{13}C NMR ($CDCl_3$, 75 MHz): δ 22.0, 123.5, 123.6, 128.0, 128.7, 131.4, 131.6, 132.8, 137.8, 139.7, 141.1, 141.3, 151.0, 151.7.

Table III.B.2; Entry 11

2,3-Bis(4-bromophenyl)-6-methoxy quinoxaline

The product was obtained as a yellowish white solid, mp: 154–156 ^{o}C.

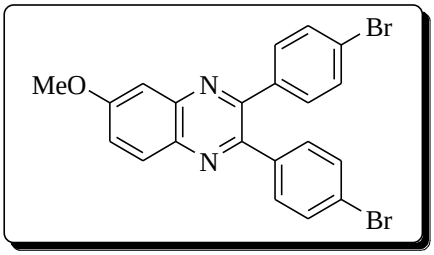

^{1}H NMR ($CDCl_3$, 300 MHz): δ 3.9 (s, 3H), 7.26-7.42 (m, 10H), 7.93 (d, *J* = 9.9 Hz, 1H).
^{13}C NMR ($CDCl_3$, 75 MHz): δ 55.9, 106.3, 123.3, 123.6, 124.0, 130.2, 131.4, 131.6, 131.7, 137.5, 137.8, 137.9, 142.9, 149.3, 151.8, 161.2.

Table III.B.2; Entry 12 & 25;
2,3-Di(furan-2-yl)-quinoxaline[38]
The product was obtained as a dark brown solid, mp 128–130 ^{o}C (lit. 131.3–131.6).

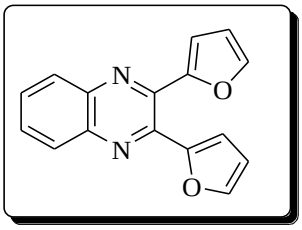

^{1}H NMR ($CDCl_3$, 300 MHz): 6.48-6.50 (m, 2H), 6.59 (d, *J* = 2.7 Hz, 2H), 7.55-7.57 (m, 2H), 7.65-7.70 (m, 2H) 8.04-8.09 (m, 2H).
^{13}C NMR ($CDCl_3$, 75 MHz): δ 111.9, 113.0, 129.1, 130.4, 140.7, 142.7, 144.2, 150.8.

Table III.B.2; Entry 13 & 26
2,3-Di(furan-2-yl)-6-methyl quinoxaline[44]
The product was obtained as a dark brown solid, mp: 116–118 ^{o}C (lit. 116–118 ^{o}C).

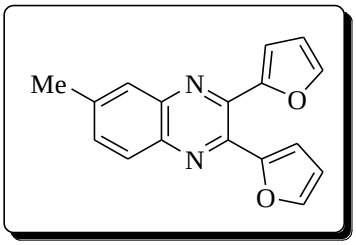

^{1}H NMR ($CDCl_3$, 300 MHz): δ 2.49 (s, 3H), 6.48-6.58 (m, 4H), 7.45-7.55 (m, 3H), 7.83-7.95 (m, 2H).
^{13}C NMR ($CDCl_3$, 75 MHz): δ 21.8, 111.81, 111.83, 112.5, 112.8, 127.9, 128.5, 132.7, 139.0, 140.6, 140.9, 141.7, 142.5, 143.9, 144.0, 150.9.

Table III.B.2; Entry 14 & 27

2,3-Di(furan-2-yl)-6-methoxy quinoxaline[45]

The product was obtained as a dark brown solid, mp: 93–95 ^{o}C.

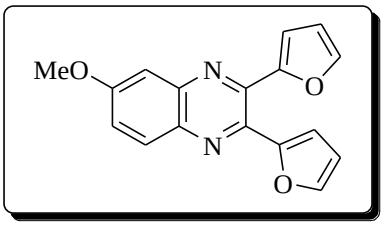

^{1}H NMR (CDCl$_3$, 300 MHz): δ 3.90 (s, 3H), 6.46-6.50 (m, 3H), 6.58-6.59 (m, 1H), 7.30-7.38 (m, 2H), 7.53-7.56 (m, 2H), 7.94 (d, *J* = 9 Hz, 1H).

^{13}C NMR (CDCl$_3$, 75 MHz): δ 55.9, 106.5, 111.78, 111.87, 111.94, 113.0, 123.9, 130.1, 136.7, 140.2, 142.4, 142.7, 143.6, 144.3, 150.8, 151.0, 161.4.

Table III.B. 2; Entry 15

Quinoxaline

The product was obtained as a brown liquid.

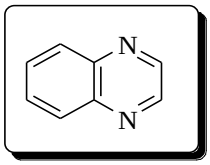

^{1}H NMR (CDCl$_3$, 300 MHz): δ 7.70-7.74 (m, 2H), 8.07-8.11 (m, 2H), 8.81-8.84 (m, 2H).

^{13}C NMR (CDCl$_3$, 75 MHz): δ 129.4, 130.0, 142.9, 144.9.

Table III.B.2; Entry 16

2-Methyl-3-phenyl quinoxaline[40]

The product was obtained as an orange solid, mp 54–56 ^{o}C (lit. 56 ^{o}C)

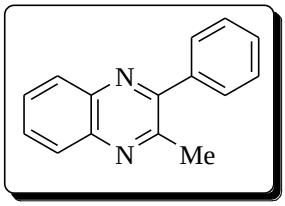

^{1}H NMR (CDCl$_3$, 300 MHz): δ 2.7 (s, 3H), 7.39-7.46 (m, 3H), 7.55-7.65 (m, 4H), 7.95-8.04 (m, 2H).

^{13}C NMR (CDCl$_3$, 75 MHz): 24.4, 128.3, 128.6, 128.9, 129.0, 129.2, 129.4, 139.0, 141.0, 141.2, 152.5, 154.9.

Table III.B.2; Entry 17

6-Methoxy quinoxaline[22]

The product was obtained as a brown solid, mp 56–58 °C (lit. 57–58 °C)

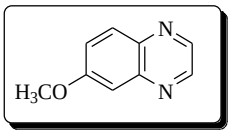

^{1}H NMR ($CDCl_3$, 300 MHz): δ 3.86 (s, 3H), 7.22-7.34 (m, 2H), 7.88 (d, *J* = 9.3 Hz, 1H), 8.59-8.66 (m, 2H).

^{13}C NMR ($CDCl_3$, 75 MHz): δ 55.7, 106.6, 123.4, 130.4, 139.2, 142.4, 144.6, 144.9, 160.7.

Table III.B.2; Entry 18

2-Methyl-3-propyl quinoxaline[46]

The product was obtained as pale yellow flakes, mp 62–64 °C (lit. 63–64 °C).

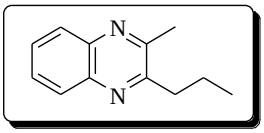

^{1}H NMR ($CDCl_3$, 300 MHz): δ 1.09 (t, *J* = 7.2 Hz, 3H), 1.81-1.91 (sext, *J* = 7.5 Hz, 2H), 2.77 (s, 3H), 2.98 (t, *J* = 7.5 Hz, 2H), 7.64-7.68 (m, 2H), 7.97-8.03 (m, 2H).

^{13}C NMR ($CDCl_3$, 75 MHz): δ 14.2, 21.5, 22.8, 37.8, 128.2, 128.5, 128.8, 128.9, 140.8, 141.1, 153.2, 156.7.

Table III.B.2; Entry 19

2,6-Dimethyl-3-phenyl quinoxaline & 2,7-Dimethyl-3-phenyl quinoxaline

A mixture of two regioisomers, not separable by column chromatography, was obtained as an yellow viscous oil.[10] The mixture was identified by both the NMR spectra as well as in HPLC in which separate product peak was not observed (see Figure III.B.6 & Figure III.B.7).

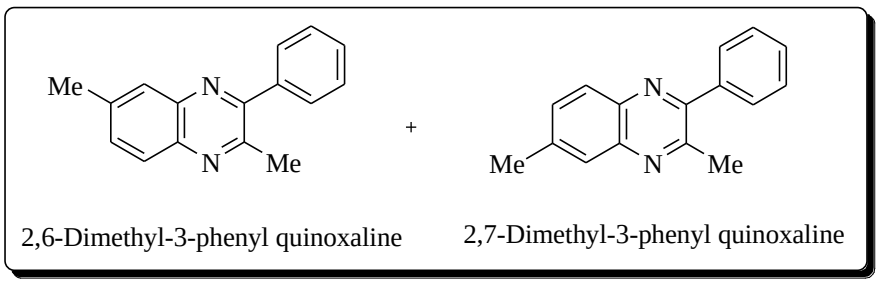

^{1}H NMR ($CDCl_3$, 300 MHz): δ 2.48 (s, 3H), 2.5 (s, 3H), 2.66 (s, 3H), 2.68 (s, 3H), 7.38-7.48 (m, 8H), 7.54-7.56 (m, 4H), 7.73-7.91 (m, 4H).

^{13}C NMR ($CDCl_3$, 75 MHz): δ 21.7, 21.8, 24.2, 24.3, 127.2, 127.8, 128.1, 128.5, 128.7, 128.83, 128.87, 128.96, 131.5, 132.0, 139.2, 139.5, 139.6, 139.7, 140.2, 141.1, 141.3, 151.5, 152.3, 154.0, 154.8.

^{1}H NMR spectra of the mixture of Entry 19 (Table III.B.2) in $CDCl_3$

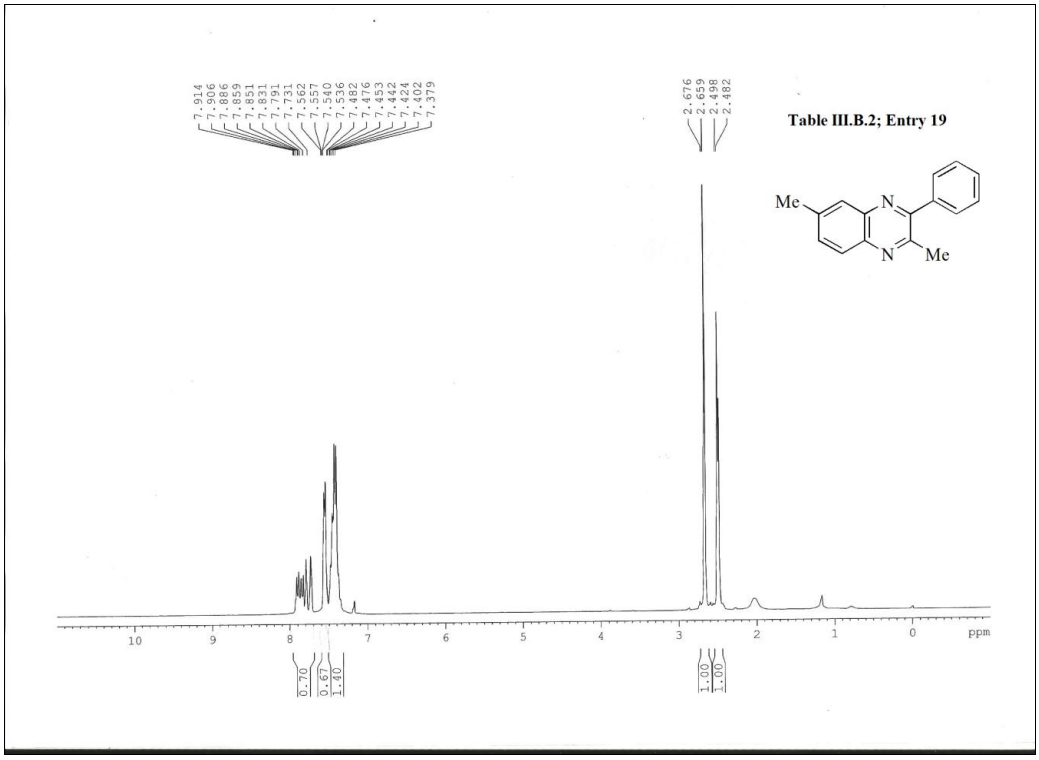

^{13}C NMR spectra of the mixture of Entry 19 (Table III.B.2) in $CDCl_3$

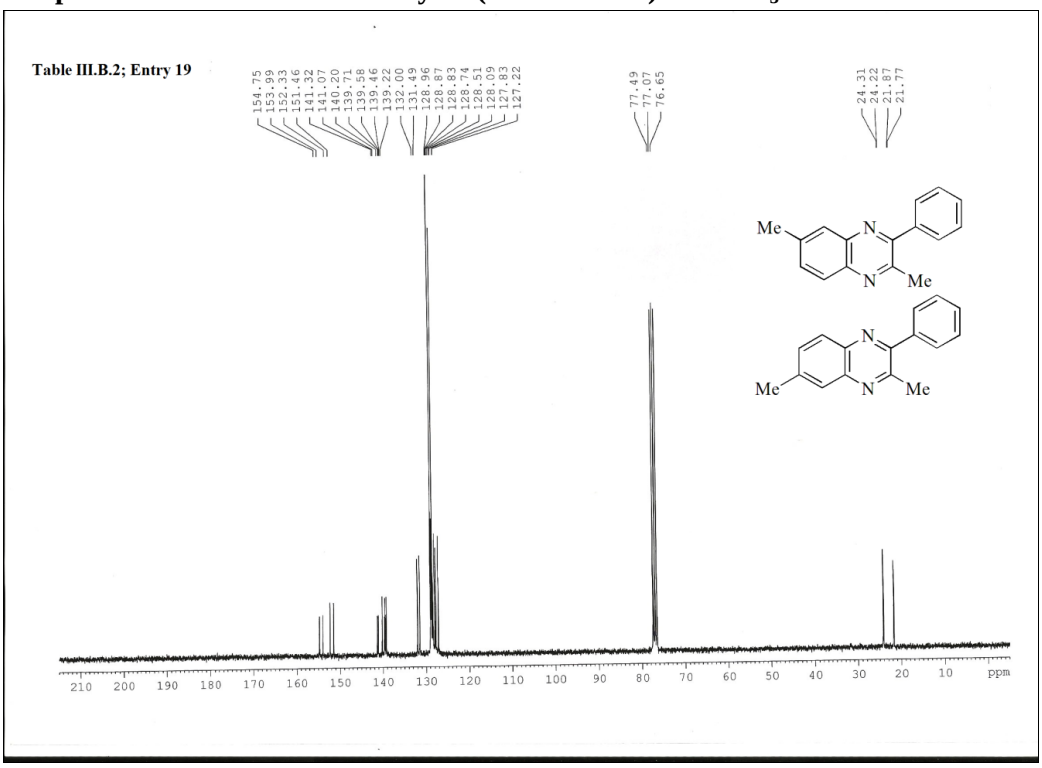

III.B.6. References

References are given in **BIBLIOGRAPHY** under **CHAPTER III**, **Section B** (pp. 177–186).

CHAPTER IV

Chemically and Biologically Reduced Graphene Oxides: Comparative Evaluation of Diverse Properties and Catalytic Activity

IV.1. Introduction

The remarkable synthesis of two–dimensional (2D) carbon nanomaterial graphene, made up of sp^2 hybridized carbon atoms intimately packed in a honeycomb crystal lattice,[1] has driven the scientific community towards developing new and practical applications of graphene and graphene-based materials.[2-3] The most common chemical method to obtain graphene in large quantity involves oxidation of graphite powder to graphite oxide, exfoliation and subsequent reduction by using hydrazine hydrate or sodium borohydride .[4–6] Beside broad applications of graphene nanosheets in diverse fields, graphene oxide (GO) and partially reduced graphene oxides (rGOs) have also attracted enormous interests to organic chemistry and material sciences.[7–9] This is basically due to the fact that GO, which is obtained commonly through the Hummers' method of oxidation of graphite powder, consists of diverse oxygen functionalities that in turn account for its high acidic and oxidizing properties.[10–12] Since the first report from Bielawaski *et al*. in 2010,[13] GO has been widely used as a "carbocatalyst" for different organic reactions.[13–20] GO has also been used to prepare more efficient and smart materials,[21–23] either through chemical modifications or *via* blending with polymers,[24–25] that find vast applications in material sciences.[26–27] On the other hand, rGO is known to be used as potential electron-rich surface for the immobilization of metal nanoparticles and subsequent uses as recyclable heterogeneous catalysts in variety of organic and inorganic reactions.[7,28] While several chemical reagents are used for the reduction of GO, [4–5,29–30] there is recent trend towards greener reducing sources from active components of biomolecules, microorganisms and plant extracts.[31–32]

The chemical reduction of GO to rGO is straightforward, however, the use of bio-sources for such reduction has two distinct advantages: (i) can eliminate toxic chemicals resulting in a greener process; and (ii) can resist irreversible aggregation of rGO possibly due to the presence of biomolecules.[33] Few studies have revealed that the rGO obtained by direct chemical reducing sources like hydrazine hydrate, (i.e. chemically reduced graphene oxide, crGO), and rGO obtained by using bio-available reducing sources (brGO) often provide or exhibit different quality and property. This might be due to the fact that the reduction or removal of the carbon–oxygen moieties in GO occurs differently based on the reducing source. However, there is no specific study, which can establish a greener process of obtaining rGO possessing various properties and catalytic activity as good as of crGO. In connection with our interests in making and finding catalytic applications of GO and rGO, we undertook a detail investigation on the preparation of rGOs from different reducing sources

and comparative evaluation of various properties as well as catalytic efficiency in organic reaction.

We report herein preparation of rGOs by using four different plant leave extracts *viz*. *Adathoda Vasika* (Malabar nut), *Azadirachta Indica* (Neem), *Camellia Sinensis* (Tea), *Moringa Oleifera* (Drumstick), and one fungi *Volvereilla Volvacea* (Edible Mushroom), all are edible to human beings, as well as rGO by hydrazine hydrate, characterize them through physiochemical and morphological studies, and finally compare their catalytic efficiency in the reduction of nitrobenzene to aniline. Our studies clearly revealed that diverse activity of rGO largely depend on the preparative procedure, nature of reducing sources and studies on textural aspects might not be enough to ensure its application in a specific area.

IV.2. Present Work: Background and Objectives

Owing to the exceptional electrical, thermal, optical and mechanical properties graphene has emerged as a most exciting material of the 21st century. Such high versatility of properties and diverse applications in every field of science and technology encouraged recent scientific community to develop efficient methods for graphene synthesis. Various attempts were made to synthesize graphene which are divided into two: the top-down and the bottom-up approaches. The bottom up approach was first applied by A. Geim and K. Novoselov in 2010 and termed as scotch tape method.[1] The top-down approaches include micromechanical cleavage,[34] chemical vapour deposition (CVD),[35] and mechanical exfoliation in solution.[36] Although all these methods produce high quality graphene but the major drawback is their limitations towards mass production. However, in terms of high yield and low cost, the top-down method *via* chemical oxidation of graphite followed by reduction has been considered as most effective route for the large-scale production of graphene. The graphene obtained by this method has been termed as reduced graphene oxide (rGO) due to the presence of some residual oxygenated functional groups on the surface of graphene. In the chemical oxidation of graphite, intermediate product graphene oxide (GO) acts as the main precursor of rGO or graphene nano sheet. Several approaches,[37–41] have been employed for the synthesis of GO but the most commonly used methods are Hummers',[40] and modified Hummers' method.[41] GO consists of several oxygenated functional groups such as hydroxyl groups (–OH), carboxyl groups (–COOH) and epoxy groups (C–O–C) and the reduction of GO mainly signifies the removal of all these functional groups from the surface of GO layers.

For the chemical reduction of GO, myriads of reducing agents have been reported in literature such as hydrazine hydrate, dimethylhydrazine hydroquinone pyrrole, aluminum

powder, Lithium aluminium hydride ($LiAlH_4$), sodium borohydride, sulfur containing compounds, hexamethylenetetramine, polyelectrolyte, ethylenediamine (EDA) etc.[29,42] under various conditions such as acid or base treatment, thermal treatment and others treatments such as laser, microwave, sonochemical, electrochemical, two-step reduction, and so on.[43] Although there are several advantages of chemical reduction method but few negative aspects such as tendency towards irreversible aggregation of rGO due to strong Vander Waals attractive forces among planes of GNS and high toxic nature of reducing agents like hydrazine hydrate, dimethylhydrazine, sodium borohydride, hydroquinone *etc*. make them not suitable for various applications. In addition, the existence of trace amounts of such toxic reagents in rGO could have detrimental effect particularly in bio-related application like in medicinal field and also in catalysis. In case of metal/acid or metal/alkali mediated reduction, there is a definite possibility for the presence of trace amounts of metals as impurities which might interfere in catalysis. To overcome all these inconvenience related to chemical reduction, biological approaches for the reduction of GO have taken a major attraction towards recent graphene scientific community because of their renewable resources, sustainability and biocompatibility compared to chemical reduction. Biomolecules such as proteins, amino acids, polysaccharides, hormones, alkaloids, polyphenolic compounds, enzymes and vitamins, microbes and plant extracts have been found to be highly effective for reduction of GO.[44]

Recently, different phyto extracts have been utilized as effective reducing sources for the reduction of GO.[44] It has been reported that extracts of different parts of plants such as leaf, root, peel etc. can play dual role both as reducing and capping agents in nanoparticle synthesis and received huge attention as a cost effective alternative for avoiding hazardous chemical synthesis of metal nanopartcles. Such reducing properties of various plant extracts make huge interests towards bio-reduction of graphene oxide among recent scientific community.

Thakur and Karak have been utilized aqueous leaf extracts of *Colocasia esculenta* and *Mesua Ferrea* Linn. and an aqueous peel extract of *citrus sinensis* (Orange) for the reduction of graphene oxide.[45] They have reported that leaves of *C. Esculenta*, *M. Ferrea* Linn. and orange peel extract mainly contain phytochemicals such as pectins, flavonoids, ascorbic acid, apigenin, luteolin and various other flavones which have high tendency to get oxidized to their corresponding quinone. To characterize their prepared GO and also rGO they have used UV-Vis spectroscopy, Raman spectroscopy and FT-IR Spectra and powder XRD analysis.

Firdouse and Lalitha,[46] have reported an eco-friendly process for the reduction of graphene oxide using an aqueous extract of *Amaranthus dubias* and well analysed by UV-Visible spectroscopy, X-ray diffraction (XRD) analysis, Raman spectroscopy, FT-IR analysis and SEM-EDAX analysis. They claimed that phytoconstituents present in the plant extract have essential role for the reduction of GO.

The reduction of aromatic and aliphatic aldehydes, ketones and esters using natural fluid derived from C. nucifera (*Cocos nucifera L.*) which is well known as coconut water has been reported by Lemos *et al.*[47] By taking motivation from this work, Katrick *et al.*[48] have developed a green protocol for the reduction of GO using coconut water (*Cocos nucifera L.*).

Haghighi and Tabrizi have used rose water as a green reducing and stabilizing agent for the preparation of reduced garphene oxide nanosheets (rGONs).[49] They proposed that the presence of natural antioxidants in rose water could have potential for the reduction.

Gurunathan *et al.*[50] have utilized *Ginkgo biloba* leaf extract as an efficient reducing and stabilizing agent for the reduction of graphene oxide and also evaluated the biocompatibility effect of as-prepared graphene in human breast cancer cells. They have presumed that flavanoids, glycosides and terpenoids present in *G. biloba* leaves are responsible for such reduction.

Various phytochemicals present in different plant leaves have vital role for the reduction of GO which is reported by Lee and Kim.[51]They have analysed and compared the reducing properties of seven plant leaf extracts (Cherry, Magnolia, Platanus, Persimmon, Pine, Maple, and Ginkgo) towards graphene oxide reduction. The highest reducing capacity was found for Cherry leaf extract (*Prunus serrulata*).

Ogale *et al.*[52] have demonstrated the deoxygenation of GO into graphene nanosheets using aqueous extract of four naturally occurring aquatic macrophytes of Nile Delta, namely, *Potamogeton pectinatus* L., (Po) *Ceratophyllum demersum* L. (Cer) *Lemna gibba*, (Le) and *Cyperus difformis* (Cy). They proposed that biomolecules already present in plant extract have major role for the reduction of GO as well as stabilizing the plant extract converted graphene nanosheets (PCGN).

Khan *et al.*[53] have reported that aqueous root extract of *Salvadora persica* (SP) L. (miswak) which contains various classes of phytochemicals such as alkaloids, flavanoids, saponins, terpenoids.[54] can act both as bio-reductant and stabilizer in reduction of graphene oxide and applied for the large-scale production of graphene nanosheets.

All these reported methods for the green reduction of GO to rGO are not only efficient but also noticeable that the textural aspects of all rGOs obtained by using different bio-

sources are more or less similar. Again, a very few of them have been utilized for their application in specific area like biomedical application as well as bio-sensor application. Owing to chemical reactivity of different rGOs, there is no specific study in literature which can specify the different catalytic activities of different rGOs.

In the present study, we have been aimed at making a comparative evaluation of diverse properties of reduced graphene oxides (rGOs), prepared by using chemical and biological reducing sources, and to establish specific reducing agent, in particular from greener sources, which might be more effective in exhibiting catalytic activity. We have used four different plants extracts viz. *Adathoda Vasika* (Malabar nut), *Azadirachta Indica* (Neem), *Camellia Sinensis* (Tea), *Moringa Oleifera* (Drumstick), and a fungi *Volvereilla Volvacea* (Mushroom), all are edible to human beings, and one chemical reductant (hydrazine hydrate) to obtain rGOs from GO.

Adathoda Vasika (Malabar nut), *Azadirachta Indica* (Neem), *Camellia Sinensis* (Tea), *Moringa Oleifera* (Drumstick) are well known traditional medicinal plants widely used by Asian people. They are indigenous in Sub-Himalayan countries like in India and Burma. *Adhatoda vasica* has been extensively used in Ayurvedic medicine, for the treatment of various diseases like bronchitis, leprosy, blood disorders, heart troubles, thirst, asthma, fever, vomiting, loss of memory, leucoderma, jaundice, tumors, mouth troubles, sore-eye, fever, and gonorrhea. Every part of *A. Vasika* plant such as leaves, bark, the root bark, the fruit and flowers are useful in the treatment of intestinal parasites. It is reported that major chemical constituent present in *A. Vasika* is vasicine derived mainly from leaves has various pharmacological activities including; antioxidant, anti-inflammatory and bronchodilatory activity. Other chemical constituents mainly alkaloids are vasicinone (from leaves, stem and also roots), vasicinol (stem and root), and deoxyvasicinone etc. are expected to be responsible for high pharmacological behaviour of *A. Vasaka.*[55]

A. Vasika has been also reported to be highly active reducing source for the synthesis of silver nanopartcles without using any capping agent.[56]

Moringa Oleifera leaves contain several phytochemicals; flavonoid pigments, such as kaempferol, rhamnetin, isoquercitrin and kaempferitrin, a group of the glycoside compounds such as glucosinolates and isothiocyanates as well as *beta*-sitosterol, glycerol-1-(9-octadecanoate),3-*O*-(6'-*O*-oleoyl-*beta*-*D*-glucopyranosyl),*beta*-sitosteroland betasitosterol- 3-*O*-*beta*-D-glucopyranoside, most of which have highly medicinal properties.[57] *Moringa Oleifera* leaf extracts have been also used both as reducing and stabilizing agent for the synthesis of silver nanopartcles.[58]

Azadirachta Indica (Neem), another important medicinal plant containing various phytochemicals such as isomeldenin, nimbin, nimbinene, 6-desacetylnimbinene, nimbandiol, nimocinol, quercetin, and beta-sitosterol has been widely used as reducing agent for the synthesis of Ag nanoparticles (AgNPs).[59]

On the other hand, green tea leaves contain mainly polyphenols which are responsible for their reducing properties. Such reducing properties of green tea leaf extracts have been widely exploited for the synthesis of metal nanoparticles such Pd, Ag, Au *etc*.[60] Green tea leaf extract also have been found to be highly efficient reducing source for the reduction of graphene oxide.[61]

It is well known that edible mushrooms are rich in proteins, amino acids and vitamins which have pharmacological activities like anti-inflammatory, antitumor, anti-oxidant and anti-cancer activities.[62] The aqueous extract of edible mushroom containing antioxidant and antitumor compounds have been also utilized as reducing and protecting agent for the synthesis of gold, silver and Au–Ag alloy nanoparticles.[63] Following the reducing properties of such plant extracts and also fungi like edible mushroom, we get motivated to exploit their reducing properties for the reduction of graphene oxide. For this purpose we collected all these bio-sources from the University of North Bengal region and applied in the reduction of graphene oxide.

However, rGOs obtained by different methods using different sources might exhibit different properties depending on the extent of residual oxygen–containing functional groups, though textural aspects of rGOs seem to be rather similar. But there is no such clear study in literature which can establish that rGOs obtained by different sources might have different properties. The present study has been aimed at making a comparative evaluation of various properties of reduced graphene oxides (rGOs), prepared by using chemical and biological reducing sources, and to establish specific reducing agent, in particular from greener sources, which might be more effective in exhibiting catalytic activity.

Each rGO was characterized by UV–Vis, FT–IR, Raman spectroscopic techniques, and surface morphological aspects were obtained by powder XRD, Scanning and Transmission electron microscopic images. The acidic nature (pH) of rGOs in aqueous suspension was measured with a pH meter and their cation-exchange capacity was calculated by potentiometric titration in the presence of an electrolyte. Further, the catalytic activity of rGOs was measured in a model reduction of nitrobenzene to aniline at room temperature and monitoring the progress by UV–Vis spectroscopy. While textural aspects of various rGOs are fairly similar, various physicochemical properties like pH, cation-exchange ability etc. are

found to be different for rGOs obtained by using different reductants. Moreover, there is significant variation observed in their catalytic activity in the reduction of nitrobenzene. By comparison, it was found that rGOs obtained by using plant leaf extract of *Adathoda Vasika,* (brGO–AV) and *Volvereilla Volvacea*, (brGO–VV) exhibit significantly better catalytic efficiency than others.

IV.3. Present Work: Results and Discussion

IV.3.1. Experimental

IV.3.1.1. Materials

For the preparation of graphene oxide, graphite powder (LobaChemie Pvt. Ltd., Mumbai, India) and other reagents $NaNO_3$, $KMnO_4$, H_2SO_4 and H_2O_2 (30%) were purchased from Merck and used directly.

IV.3.1.2. Preparation of plants and fungi extracts

Four different plants leaf extracts *viz. Adathoda Vasika* (Malabar nut), *Azadirachta Indica* (Neem), *Camellia Sinensis* (Tea), *Moringa Oleifera* (Drumstick), and a fungi extract of *Volvereilla Volvacea* (Mushroom) were chosen primarily from the local sub–Himalayan region, all are edible to human beings as well as have long been used as traditional medicines to combat with various diseases. The plant leaves were washed carefully with distilled water, kept in air oven at 80 ^oC for two days, and then the dry leaves were crushed to fine powder. The plant leaf–extracts were obtained by stirring a suspension of each type of finely grinded leaf powder (500 mg in 80 mL of DI water) overnight at room temperature. In the case of *Volvereilla Volvacea*, however, the water extract was obtained by stirring it in boiling water for 1h and then filtering the extract.

IV.3.1.3. Preparation of graphene oxide (GO)

In order to obtain GO, the finely grinded graphite powder was oxidized by using modified Hummers' method,[24,40] [For detail please see the Chapter III (Section A & B)]. In brief, after oxidation, the bright yellow suspension of graphite oxide in water was centrifuged several times and separated out. The dark brown dusty material was then washed with 5% aqueous HCl and then with distilled water repeatedly until the washing was neutral to pH paper. Again, the solution was tested for the presence of Cl^- and $SO4^=$ ions using $AgNO_3$ and $BaCl_2$ aqueous solutions respectively.

IV.3.1.4. General procedure for the preparation of different biologically reduced graphene oxides (brGOs)

The as prepared GO was then suspended in distilled water (50 mg in 100 mL) and sonicated in an ultrasonic bath for 1h. The resulting yellow–brown GO dispersion in water was then added to the plant extract and refluxed at 80 ^{o}C for 24 hours. Same procedure was followed for each type of plant extracts. During this period, the colour of the overall solution changes from brown to black and the aqueous suspension was centrifuged (10000 rpm) for 10 min and separated out the black mass. The process of centrifugation was repeated three times more (10 min each) and the combined black mass was washed with methanol (AR grade; 2 x 10 mL). Finally, the black mass was dried at 60 ^{o}C for 1 hr under vacuum to obtain free–flowing powder of different brGOs.

IV.3.1.5. Preparation of chemically reduced GO (crGO)

The crGO was prepared following the reported procedure from graphite powder and hydrazine hydrate (100 mg GO in 100 ml water and 1 ml hydrazine hydrate) at 100 ^{o}C under boiling conditions.[63] (For details, please see the Chapter III, Section B; content **III.B.5.2**.)

IV.3.2. Characterizations

Each brGO was denoted as brGO–AV, brGO–AI, brGO–CS, brGO–MO and brGO–VV, based on the abbreviation of sources, each material was characterized and compared with crGO in respect of various properties as well as the catalytic ability in the reduction of nitrobenzene to aniline.

The as-prepared GO, all five brGOs and crGO samples were characterized by various techniques such as UV–Visible spectroscopy (JASCO V–530 spectrophotometer), FT–IR spectroscopy (FT–IR–8300 Shimadzu spectrophotometer, Kyoto, Japan), X–ray diffraction patterns (Rigaku SmartLab, Shibuya–ku, Japan, 9kW diffractometer using CuKα radiation), Raman spectroscopy (Rigaku SmartLab, Renishaw In Via micro Raman spectrometer), Field emission scanning electron microscopy (FESEM) (Hitachi S–4800, Japan) and High-resolution transmission electron microscopy (HRTEM) (JEM–2100F microscope, JEOL, Japan). The pH of the all samples (aqueous suspension) was measured by using digital pH meter, Systronics, India. For centrifugation, REMI C–24 cooling centrifuge, India, was used at 10,000 rpm.

Each reduced graphene oxide (rGO) was characterized by UV–Vis, FT–IR, Raman spectroscopic techniques, and surface morphological aspects were studied by powder XRD,

Scanning and Transmission electron microscopic images (SEM and TEM). The acidic nature (pH) of each rGO in aqueous suspension as well as cation-exchange capacity was measured by potentiometric titration in the absence and presence of an electrolyte respectively. Finally, the catalytic ability was evaluated in a model reduction of nitrobenzene to aniline at room temperature monitored by UV–Vis spectrophotometer.

IV.3.2.1. UV–Vis spectroscopy

To investigate the reduction of GO in the presence of plant leaf extracts, we have taken UV–Vis spectra of water dispersion of GO and another bio-reduced rGOs (Fig. 1). The aqueous dispersion of GO shows an absorption peak at 231 nm, and a shoulder peak at 303 nm, which are attributed to the $\pi \rightarrow \pi^*$ transitions of C=C bond and $n \rightarrow \pi^*$ transitions for C=O bond respectively. After the reduction, bio-reduced GOs (brGOs) display $\pi \rightarrow \pi^*$ transitions at 269–273 nm (Figure. IV.1), clearly indicating greater conjugation of C=C bonds and removal of carbon–oxygen functions, which is in agreement with the literature report as well.[45,50–51,64–65]

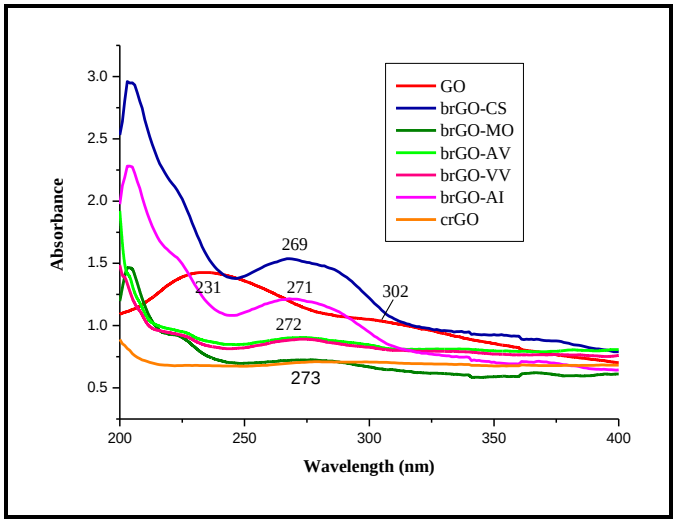

Figure IV.1. UV–Vis spectra of GO, brGO–CS, brGO–MO, brGO–AV, brGO–VV, brGO–AI, crGO (0.5 mg/ml in water).

Similarly, chemically reduced GO (crGO) obtained by using hydrazine hydrate and following Ruoff's method,[63] also showed UV absorption maxima at 273 nm, signifying that GO has been successfully reduced. Table IV.1 shows the UV–Vis absorption maxima at a glance and suggests for the changes attributable to restoration of π–electron networks in rGOs, not seen in the case of GO.

Table IV.1. UV–Vis spectra of GO, crGO and different brGOs

Materials	Wavelength (nm)
GO	231
brGO–CS	269
brGO–MO	273
brGO–AV	272
brGO–VV	272
brGO–AI	271
crGO	273

IV.3.2.2. FT–IR spectroscopy

The FT–IR spectra were recorded for GO, crGO and brGOs on KBr pellets and shown in Figure 2**.** The GO displays functional groups like hydroxyl (O−H), carbonyl (C=O of carboxylic group), tertiary (O−H), epoxy (C−O−C) and alkoxy (R−O), as seen by their stretching vibrations at 3370, 1719, 1412, 1224, and 1051 cm^{-1} respectively.[24,45, 50–51 64–70] On the other hand, FT–IR spectra of each brGOs and crGO did show absorption peaks for epoxy (C−O−C) and alkoxy (R−O) with lower intensity in addition to broader absorption peak in the range 1550–1560 cm^{-1}, attributed to skeletal vibration of graphene nanosheets.[67–71] However, absorptions for carbonyl (C=O of carboxylic group) and O−H stretching vibrations (*tert*–alcohol) did not appear suggesting restoration of π–electron networks in rGOs. A comparative chart of the absorption peaks for each type of functional groups for all samples are shown in Table IV.2, while Figure IV.2 represents the FT–IR spectra of all samples. The overall observations are however in agreement with the literature reports, [45, 50–51 64–70] and no major differences are observed in rGOs irrespective of the source of reducing agents.

Table IV.2. Comparative chart for FT–IR data of GO and various rGOs

Materials	O−H stretching vibrations (cm^{-1})	C=O stretching of COOH (cm^{-1})	C=C stretching (cm^{-1})	O−H stretching (*tert*–OH) (cm^{-1})	C−O−C (epoxy) stretching (cm^{-1})	C−O (alkoxy) stretching (cm^{-1})
GO	3370	1719	1622	1412	1224	1051
brGO–CS	–	–	1560	–	1200	1038
brGO– MO	–	–	1560	–	1213	1053
brGO–AV	–	–	1550	–	1208	1044
brGO–VV	–	–	1555	–	1218	1043
brGO–AI	–	–	1550	–	1199	1051
crGO	–	–	1552	–	1118	1051

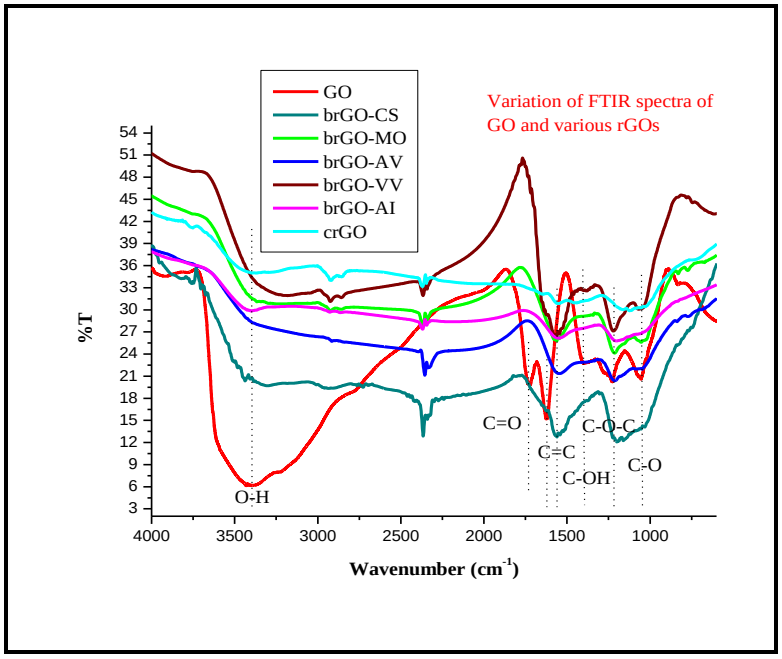

Figure IV.2. FT–IR spectra of GO, brGOs and crGO.

IV.3.2.3. Raman spectroscopy

The Raman spectroscopy is another fundamental approach for the determination of π electron dispersion on the surface of graphene and graphene-based materials and also to ascertain their electronic properties.[71–72] Raman spectrum of monolayer graphene is characterized mainly by two characteristic peaks – the G band arising due to first order scattering of the E_{2g} phonon of sp^2 carbon atoms at ~1580 cm^{-1} and the 2D band at 2700 cm^{-1}. Another peak at around 1350 cm^{-1} assigned to the breathing mode of *K* point phonons of A_{1g} symmetry becomes visible in case of a disordered graphene which is called disorder–induced D–band.[71–73] We recorded Raman spectra of as-synthesized GO and different rGOs and their respective characteristic spectral bands are shown in Figure IV.3. Since the reduction of GO to rGO brings about restoration of sp^2 hybridized carbon atoms with π electron networks, it is expected that both characteristic bands should resemble primarily to that of graphene surface. However, while crGO and some brGOs (*viz.* brGO–VV & brGO–AI) exhibit the D band close to that of graphene (monolayer), other three brGOs rather display the D band close to that of GO. On the other hand, among the G bands appeared for different rGOs only in one case (i.e. brGO–CS), it is nearly similar to that of graphene (monolayer). The decrease in the intensity ratios (I_D/I_G) ratio is indicative of the defects or disorder of graphene materials. We did observe increase in I_D/I_G for different brGOs except in one case (i.e., brGO–AV) with respect to that of GO, while the same is found to be increased for crGO (Table 3). The observation suggests lesser defects on the surface of most of the brGOs than crGO, [50–51, 71–74]

and is in agreement with previously reported reduction of GO using some other plant extracts,[51] or with Fe–based reduction,[64] as well as under solvo-thermal reduction.[73] The 2D band observed on graphite powder at 2700 cm^{-1}, [71–72] is an important Raman scattering band to differentiate between mono- or multi-layered graphene, and becomes broadened and shifted to the range of ~2712–2723 cm^{-1} for GO and all rGOs. This suggests that both GO and all different rGOs have multi-layer sheets. In fact, there are no significant changes observed among crGO and different brGOs.

Table IV.3. Raman peak position of D and G band and their intensity ratio

Carbon materials	D band (cm^{-1})	G band (cm^{-1})	I_D/I_G ratio	2D band (cm^{-1})
Graphite	~1332	~1585	–	~2700
Graphene	~1350	~1580	–	~2700
GO	~1364	~1613.4	1.00	~2720
brGO–CS	~1359.6	~1583.4	0.91	~2718
brGO–MO	~1362.6	~1598.3	0.95	~2712
brGO–AV	~1359.6	~1587.9	1.00	~2722
brGO–VV	~1351.9	~1595.3	0.95	~2723
brGO–AI	~1353.4	~1593.9	0.90	~2715
crGO	~1354.7	~1598.1	1.26	~2717

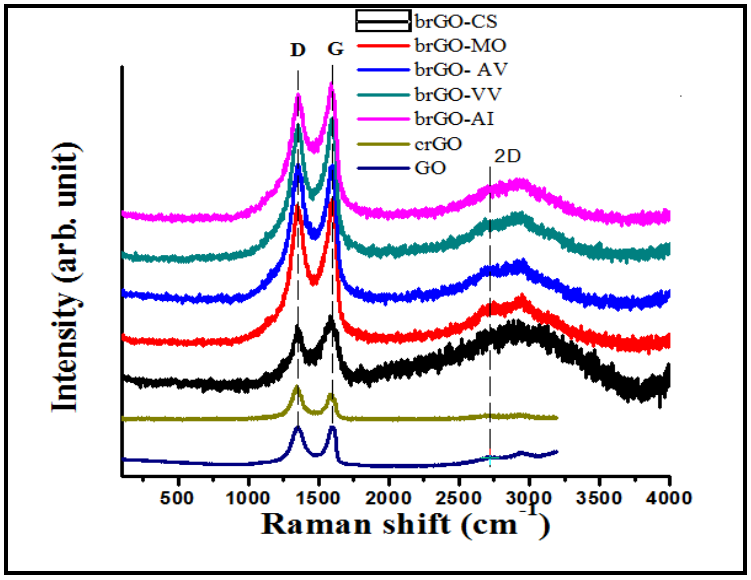

Figure IV.3. Raman spectra of GO and different rGOs

IV.3.2.4. Powder X–Ray diffraction patterns

The powder XRD patterns of GO and different rGOs are shown in Figure 4 and comparative data are presented in Table 4. Graphite powder gives X–ray diffraction peak (2θ) at 26.5^{o} with *d*–spacing 0.34 nm, while that for GO appeared at 10.5^{o} with *d*–spacing 0.84 nm. On the other hand, XRD patterns of different rGOs appeared in the range of (2θ) 23.6^{o}–25.36^{o} with *d*–spacing 0.37–0.35 nm thereby resembling mostly with the graphitic materials. In the case of GO, the *d*–spacing (0.84 nm) is attributed to the fact that the formation of various oxygenated functional groups and intercalation of water molecules between the graphite layers.[51] Broadening and shifting of XRD peaks both for crGO and brGOs and comparison with that of GO revealed that reduction can be carried out by chemically as well as by using biomolecules of different extracts, as also reported previously by some other groups.[33, 50–51, 64–65]

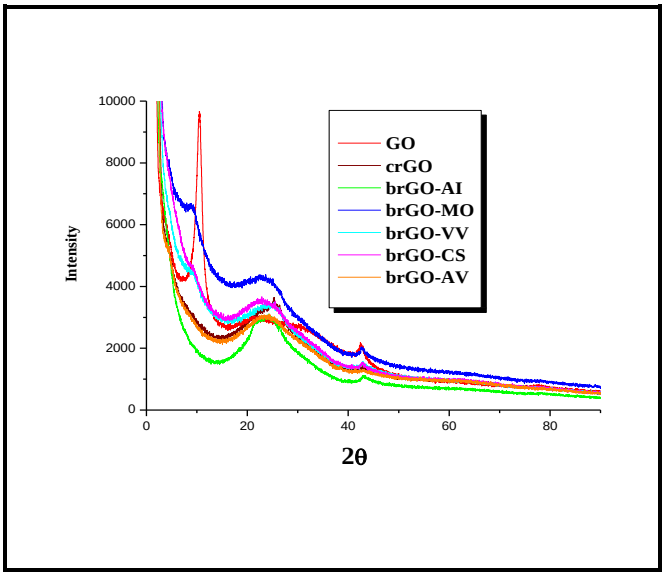

Figure IV.4. XRD patterns of GO and different rGOs

Table IV.4. XRD value of GO and different rGO's

Materials	2θ value (diffraction peak)	*d*–spacing
Graphite	2θ =26.50^{o}	0.34 nm
GO	2θ =10.50^{o}	0.84 nm
crGO	2θ =24.26^{o}	0.36 nm
brGO–CS	2θ =25.28^{o}	0.35 nm
brGO–MO	2θ =23.98^{o}	0.37 nm
brGO–AV	2θ =25.36^{o}	0.35 nm
brGO–VV	2θ =23.60^{o}	0.37 nm
brGO–AI	2θ =23.60^{o}	0.37 nm

IV.3.2.5. FESEM & HRTEM studies

The successful reduction using various plant leaf extracts can further be confirmed by the FESEM and HRTEM images of GO and different brGOs. Comparison of FESEM images of GO and brGOs suggests restacking of graphene sheets in brGOs, further curled and randomly aggregated than exfoliated GO (Figure IV.5). [75–77]

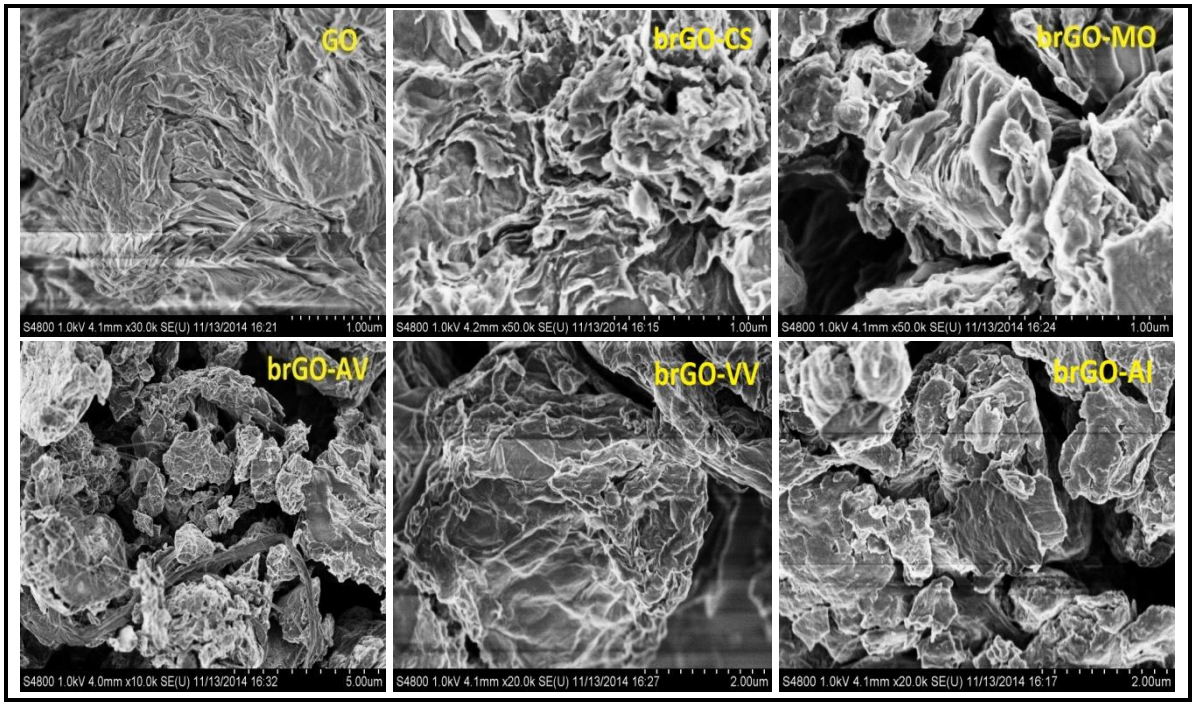

Figure IV.5. FESEM images of GO and different brGOs

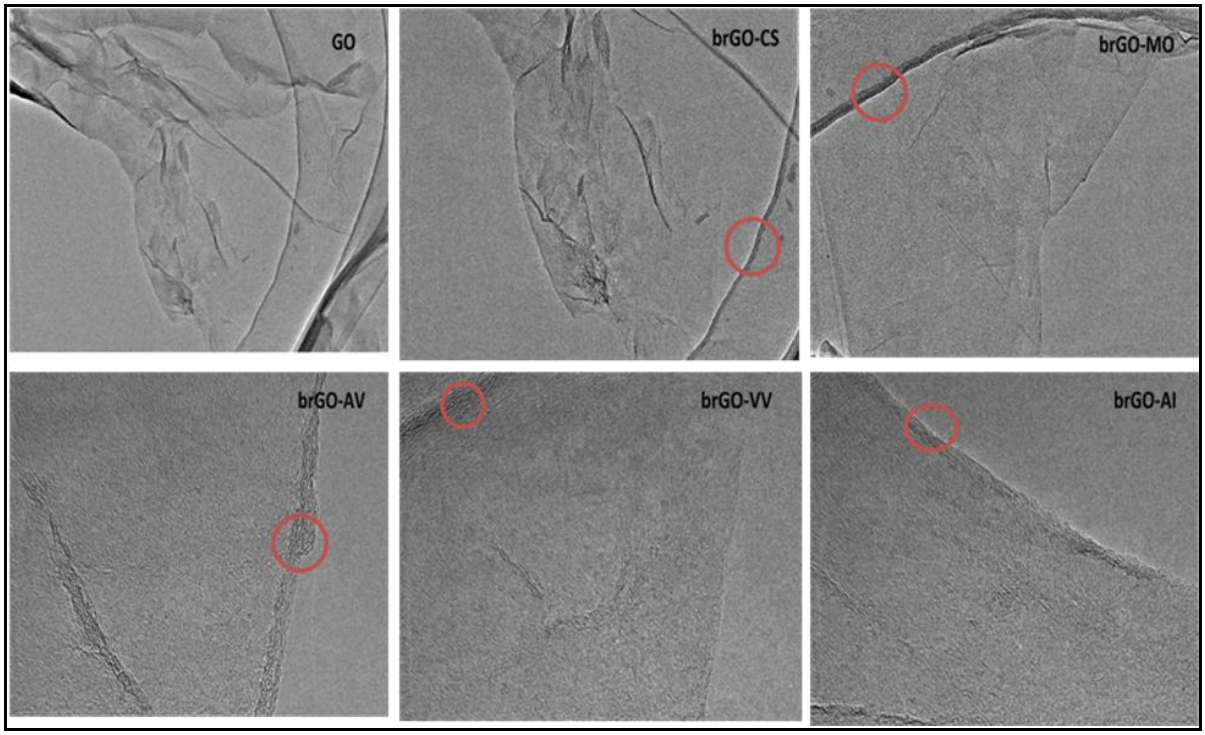

Figure IV.6. HRTEM images of GO, brGO–CS, brGO–MO, brGO–AV, brGO–VV, brGO–AI respectively.

In the case of HRTEM images of exfoliated GO, it looks like ultrathin layer sheet, while there are discontinued fringes observed across the sheet of different brGOs with corrugation and scrolling (Figure IV.6). The fringes are indicative of the re–stacking of graphene layers after the reduction.[45, 50.]

IV.3.2.6. The pH measurements

GO possesses several carboxylic functions primarily present on the edges of the basal plane and its acidic nature has been measured in aqueous suspension (pH ~ 4.5; 0.1 g/L).[78]We prepared GO by following Hummers' method and measured the pH in aqueous suspension (pH ~ 3.51; 1 mg/mL). Since the reduction of GO to rGO involves removal of the carboxyl functions, the pH measurements of different brGOs and crGO indeed showed decreasing acidity in the range of pH 6.40–6.85 (Table IV.5). The change of pH from acidic to neutral range ensured that the reduction had occurred successfully in all cases. The use of background electrolytes in the aqueous suspension of graphitic oxidized materials through intercalation of cationic species could alter the pH of the aqueous suspension.[78]Therefore, further pH measurements were performed taking each rGOs (50 mg) in 0.5 (M) aqueous NaCl solution (50 mL) and after sonication for 1h. The change of pH after adding the electrolyte (NaCl) is given in Table 5, which showed an increase of acidity of the aqueous suspension in the range of 5.35–6.35 signifying the exchange of intercalated acidic protons with cationic species. However, the increase in acidity of different rGOs varies from pH 0.30 (for crGO) to pH 1.32 (for brGO–AI) indicating that the reduction ability of different reducing sources for conversion of GO to rGO is not similar. Thus, the plant leaf extract from *Azadirachta Indica* (Neem) has presumably least reducing capacity, whereas extracts of *Adathoda Vasika* (Malabar nut), and *Camellia Sinensis* (Tea) show better reducing ability but not as good as hydrazine hydrate. In order to confirm further, we performed acid–base titration potentiometrically for the GO and rGOs in the presence of Na^+ ion and corresponding curves are given in Figure 6. From the inflection point of these curves, we measured the cation-exchange capacity (CEC) of GO and all rGOs. It is reported that GO is a very weak acidic cation exchanger and its CEC largely depends on the pH and salt concentration of the aqueous suspension.[78–79]Titration of each aqueous suspension of GO and rGOs (50 mg in 0.5 (M) aqueous solution of NaCl) with 0.1(M) NaOH solution revealed noticeable changes in the CEC values for GO and other rGOs, as presented in Table 5. While GO has highest CEC (1.92 mmol/g), which might be due to the presence of more exchangeable protons with Na^+ ions, rGOs display considerable decrease in CEC and in the

range of 0.36–0.84 mmol/g. This experiments again confirm that the reduction of GO had occurred in different extents and residual presence of acidic functional groups varies mainly with respect to the reducing source.

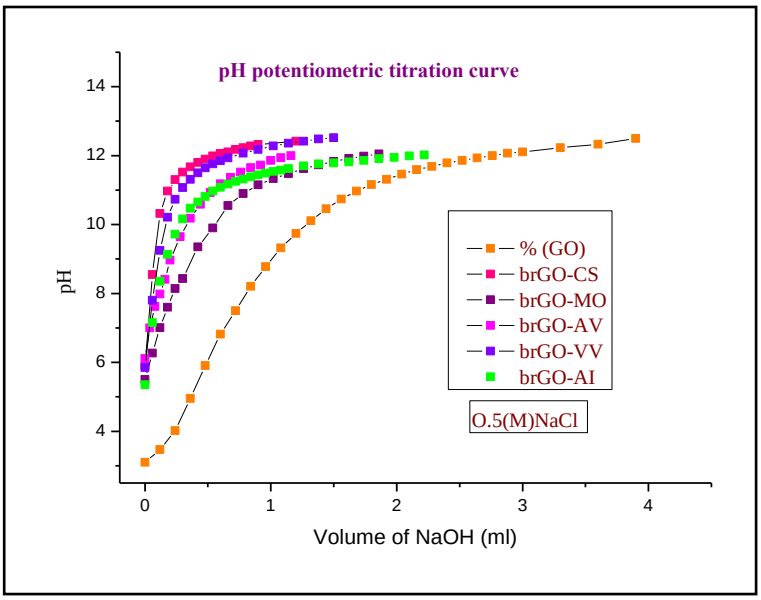

Figure IV.7. Titration curves for GO and different brGO in aqueous NaCl with (0.1 M) NaOH solution.

Table IV.5. pH variation of GO and different brGO and their cation exchange capacity

Materials	Strength of NaOH aq. solution	Cation–exchange capacity mmol/gm	pH (50 mg carbon materials in 50 ml water)	pH of the solution after adding NaCl electrolyte (0.5M)
GO	0.1 M	1.92	3.51	3.10
brGO–CS	0.1 M	0.36	6.55	5.90
brGO–MO	0.1M	0.84	6.40	5.50
brGO–AV	0.1M	0.56	6.75	6.11
brGO–VV	0.1M	0.48	6.85	5.85
brGO–AI	0.1 M	0.72	6.67	5.35
crGO	0.1M	0.60	6.65	6.35

IV.4. Catalytic applications

Apart from studies on textural aspects and chemical behaviours (pH measurements before and after cation exchange), we also explored the catalytic ability of different rGOs in the reduction of nitrobenzene to aniline at room temperature in the presence of hydrazine hydrate (Scheme IV.1).[80] For this study, we used nitrobenzene (1 mmol), 2 ml hydrazine

hydrate (2 mL) and the brGOs (10 wt %) in 1:1 MeOH and water. The progress of the reaction was monitored by UV–Vis spectroscopy.[81–82] The standard UV spectral data for nitrobenzene and aniline are shown in Figure IV.8 and spectral decay along with their plot of $\ln(C_t/C_0)$ *vs.* reduction time are given in Figures IV.10–15. Since the reduction of nitrobenzene follows the first-order law, we considered the apparent rate constants (k) from the slope of the straight lines for all brGO samples, which however are not sharp in all cases because of very slow conversion rate. It was observed that the catalytic efficiency of different brGOs and crGO differ considerably, and found that brGO–AV and brGO–VV exhibit better catalytic performance as compared to other brGOs. Further comparison revealed that the order of catalytic efficiency is in the order of brGO–AV>brGO–VV>crGO. Table 6 represents the rate constants for the reduction of nitrobenzene to aniline in the presence of different rGO samples under identical conditions clearly establishing the difference in their catalytic ability.

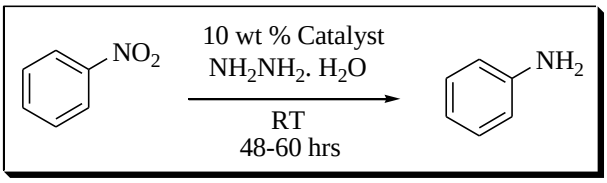

Scheme IV.1. Reduction of nitrobenzene using brGO as a catalyst.

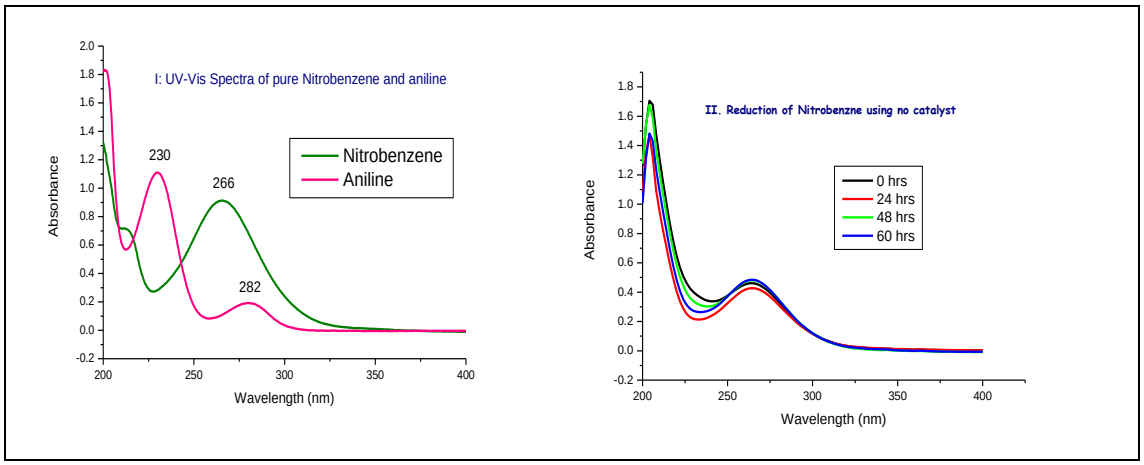

Figure IV.8. UV–Vis absorption spectra of pure nitrobenzene and aniline (I) and of the reduction of nitrobenzene without catalyst (II).

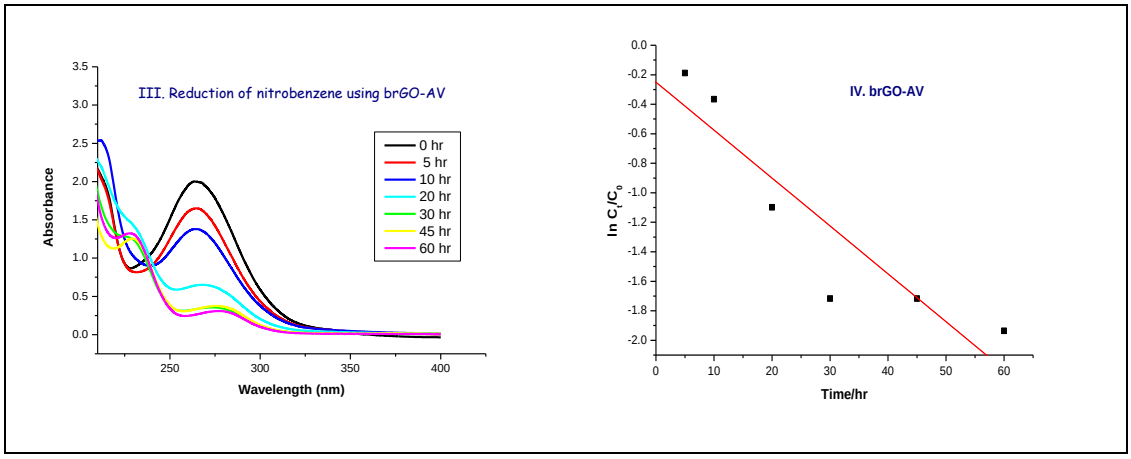

Figure IV.9. Spectral decay at different time intervals using brGO–AV (III) and plot of ln (C_t/C_0) *vs.* reduction time (IV).

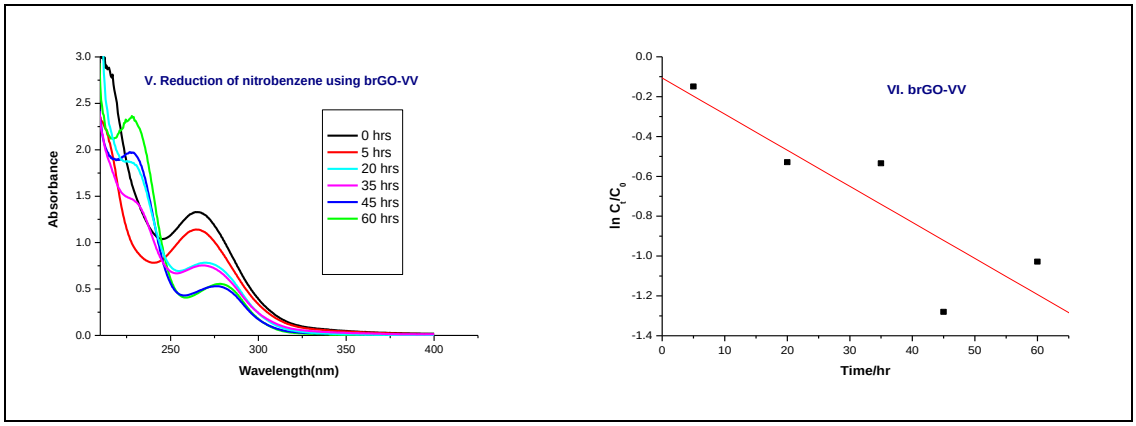

Figure IV.10. Spectral decay at different time intervals using brGO–VV (V) and plot of ln (C_t/C_0) *vs.* reduction time (VI).

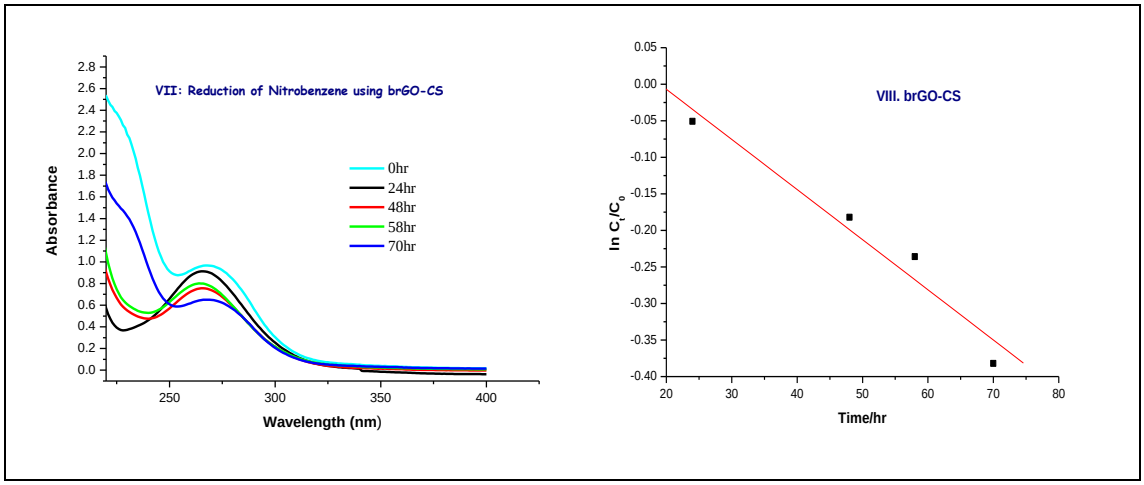

Figure IV.11. Spectral decay at different time intervals using brGO–CS (VII) and plot of ln (C_t/C_0) *vs.* reduction time (VIII).

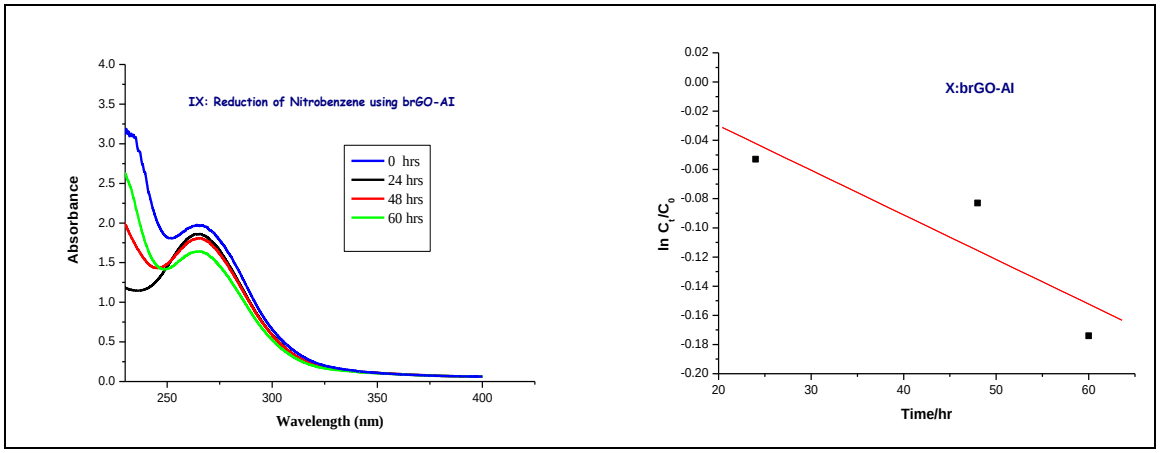

Figure IV.12. Spectral decay at different time intervals using brGO–AI (IX) and plot of ln (C_t/C_0) *vs.* reduction time (X).

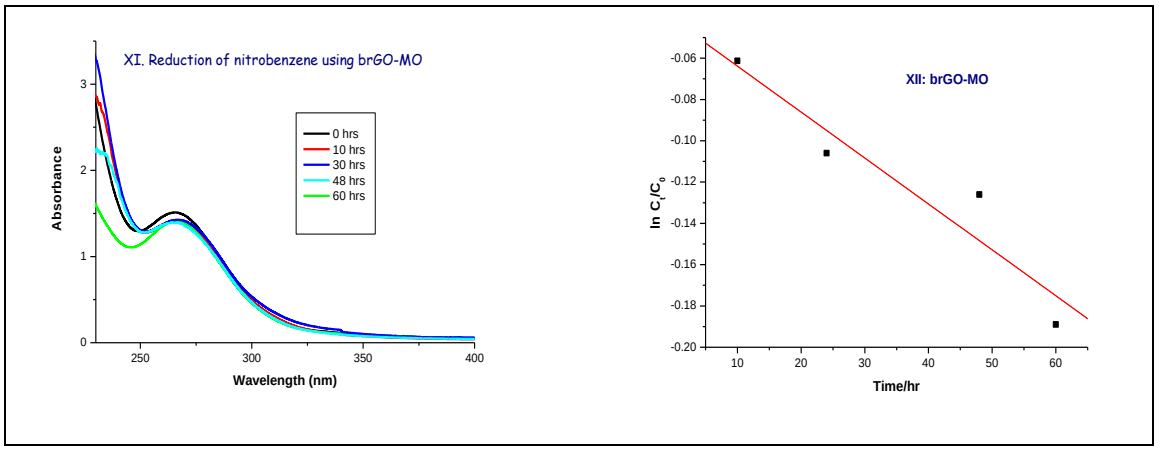

Figure IV.13. Spectral decay at different time intervals using brGO–MO (XI) and plot of ln (C_t/C_0) *vs.* reduction time (XII).

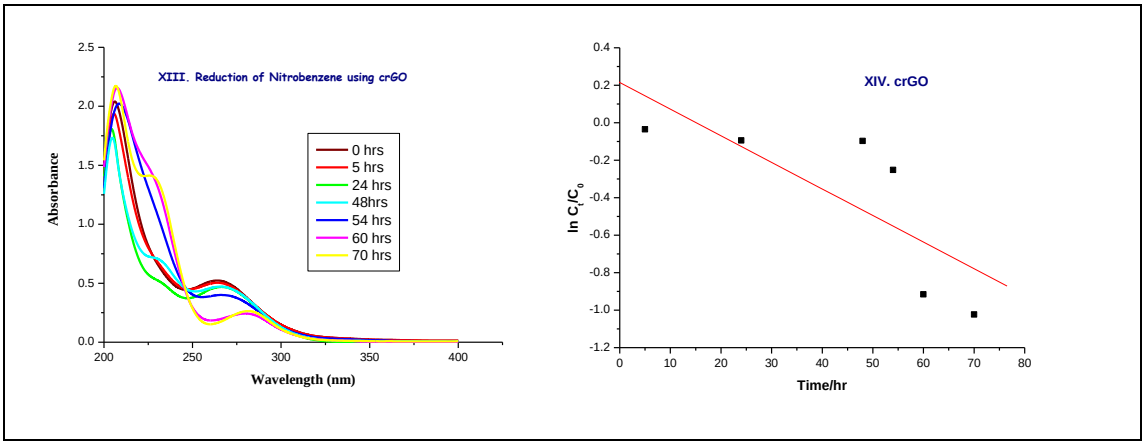

Figure IV.14. Spectral decay at different time intervals using crGO (XIII) and plot of ln (C_t/C_0) *vs.* reduction time (XIV).

Table IV.6. Rate constants of different rGO samples for the reduction of nitrobenzene to aniline.

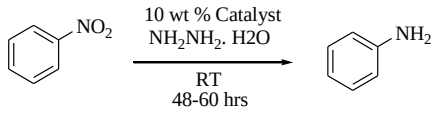

Entry	rGO samples	Rate constants	Figures
1	brGO–AV	3.45×10^{-2}	9
2	brGO–VV	1.91×10^{-2}	10
3	brGO–CS	5.2×10^{-3}	11
4	brGO–AI	3.06×10^{-3}	12
5	brGO–MO	2.22×10^{-3}	13
6	crGO	1.42×10^{-2}	14

IV.5. Conclusion

In summary, we prepared rGOs from GO by using different plant leaf/fungi extracts as well as a common chemical reductant hydrazine hydrate and then characterized morphologies of each graphitic species by spectroscopic and microscopic tools. A comparison of textural data of each species revealed in general fairly similar observations. However, comparison of the acidity of aqueous suspensions of GO and different rGOs in the absence or presence an electrolyte, measured with the aid of pH meter as well as by potentiometric titrations, revealed that all rGOs are not rather alike. The difference is even more prominent in their catalytic performance in the reduction of nitrobenzene to aniline, which is systematically studied for the first time. Major facets from the above studies are: (i) some plant leaf extracts are equally efficient for the reduction of graphene oxide (GO) to rGO so as to avoid the use of toxic and hazardous chemical reagents, (ii) some properties and catalytic ability of reduced graphene oxide (rGO) could reasonably vary depending on the reducing sources and preparative procedures; and (iii) the textural features of rGOs obtained by spectroscopic and microscopic tools might not be enough about their purity and characteristic properties.

IV.6. References

References are given in **BIBLIOGRAPH**Y under **CHAPTER IV** (pp. 181−186).

CHAPTER V

Poly-ionic resins embedded with Pd/Cu bimetallic NPs: Applications in Suzuki–Miyaura and Mizoroki–Heck Coupling reactions

V.1. Introduction

The use of transition-metal nanoparticles (NPs) in catalysis has attracted huge interest because of their excellent selectivity, efficiency and recyclability, which are regarded as most important requirements in "green chemistry". Metal nanoparticles are generally stabilized by immobilizing or grafting onto inorganic or organic polymer supports,[1] depending on the steric bulk of their framework and also on their weak binding to the NP surface by the heteroatom which make them able to play the role of ligands.

On the other hand, among noble metal catalysts Pd–based catalysts have taken major attention in organic synthesis because of its ability to selectively carry out the C–C and C–heteroatom bond formation reactions.[2] Moreover, palladium-catalyzed reactions have taken a central part in organic synthesis as one of the most powerful and versatile tool for the preparation of fine chemicals, pharmaceutical intermediates, active pharmaceutical ingredients, and also bioactive drugs.[3]

Owing to high catalytic activity and selectivity, monometallic Pd nanoparticles have become most widely used catalysts in modern synthetic chemistry. These NPs have been extensively used in various coupling reactions such as Stille, Heck, Suzuki, Sonogashira, Kumada, Negishi, Nozaki–Hiyama, Buchwald–Hartwig, and Tsuji–Trost employed for the formation of C–C or C–heteroatom bonds.[4-5] But the growing concern towards limited resource and also the high cost of noble metals take attention of materials scientists towards developing alternative catalyst to replace monometallic NPs. Bimetallic nanoparticles, which are prepared by mixing of two metal-components, recently, have taken more attention than monometallic nanoparticles because of their multiple functionalities and prominent catalytic activity, selectivity, and stability over monometallic nanomaterials. In material science, introduction of a second metal in the precious metal to generate intermetallic compounds has proven to improve the catalytic activity as well as the durability of bimetallic nanoparticle catalysts.[6] This improvement of catalytic activity occurs due to the electronic exchange (cooperative/synergic interaction) between two metal atoms which modify the surface electronic properties leading to the interaction of reactants, stabilization of intermediates, and the product release.[7] Moreover, the catalyst stability in adverse conditions such as in high or low pH, water or oxygen environment can be enhanced by the presence of a second metal and therefore enhance the catalyst recyclability and recovery which is an important criteria for industrially important catalysts.[8]

Palladium–catalyzed Suzuki–Miyaura and Mizoroki–Heck cross-coupling reactions are most fundamental synthetic tools for C–C bond formation reactions in both industry and academia.[9] In last few decades, a large number of bimetallic alloy nanoparticles such as Au/Pd,[10] Ru/Pd,[11] Pd/Rh,[12]Pd/Cu,[13] Cu/Ni,[14]Pd/Ni,[15] Pd/Ag,[16] Pd/Co[17] and Fe/Pd[18] have been employed for C–C bond forming reactions like Suzuki–Miyaura and Mizoroki–Heck reactions. The noble metal gold has been most extensively utilized for preparation of bimetallic nanoparticles with Pd due to the excellent intermetallic atomic level mixing of Au and Pd. In addition, the high electronegative nature of Au causes the flow of electronic charge transfer from Pd to Au resulting in negatively populated Au centre which enhances the catalytic effect of Pd–Au bimetallic form.

Khashab *et al.* have synthesised four different Au–Pd core-shell NPs with the help of emulsion phase surrounding the Au core NPs at room temperature and investigated these catalysts for the Suzuki reaction (Scheme V.1) with 4-carboxyphenylboronic acid, several aryl iodides and K_2CO_3 in aqueous medium at 65 °C.[10a] For Heck reaction, styrene iodobenzene, $NaHCO_3$ and cetyl trimethylammonium bromide (CTAB) were used in water at 80 °C. They observed good yields to the corresponding coupled product for Suzuki and Heck reactions with both Core-shell Au–Pd and alloy Au–Pd nanoparticle catalyst with lowest loading of the catalyst of 0.25 mol%.

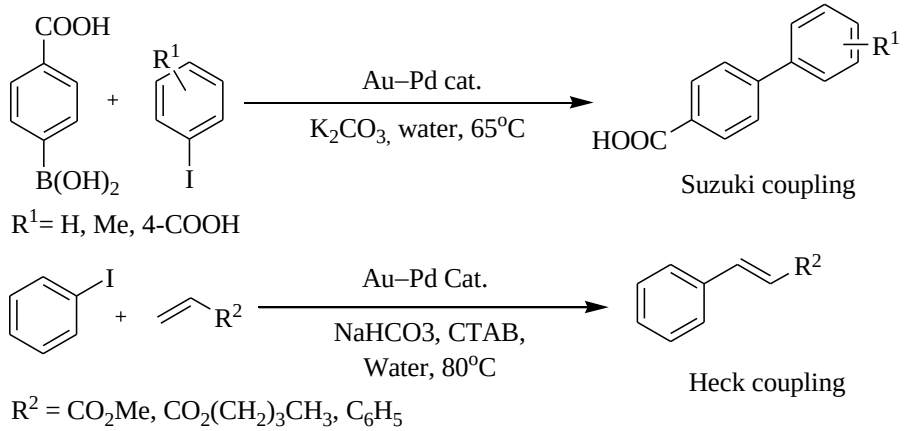

Scheme V.1. Suzuki–Miyaura and Heck reactions catalyzed by Au–Pd bimetallic nanoparticles.

Tang *et al.*[10b] have also synthesised Au–Pd alloy and Core-shell nanoparticle catalyst and stabilised it on SiO_2 to enhance the catalytic activity of catalyst for Suzuki reaction (Scheme V.2). They have synthesised Au/Pd alloy using the various molar ratio of alloy and Core-shell nanoparticles and investigated their catalytic activities for Suzuki reaction. For Suzuki reaction, the order of reactivity of bimetallic alloys is found to be

Au_3Pd_1>Au_1Pd_1>Au_1Pd_3> Core-shell Au–Pd>Pd >Au. Interestingly, the alloy Au–Pd/SiO_2 with lower Pd content shows the highest catalytic activity and selectivity to the coupled products for both the iodobenzene and bromobenzene, indicating that isolated Pd atoms or small ensembles of Pd on Au are favourable for the Suzuki cross-coupling reaction. The stability of the bimetallic nanocrystals is enhanced and the leaching of Pd is inhibited by the protection of the mesoporous shell. The alloy Au–Pd@SiO_2 also shows a higher selectivity and stability than a commercial Pd–C catalyst.

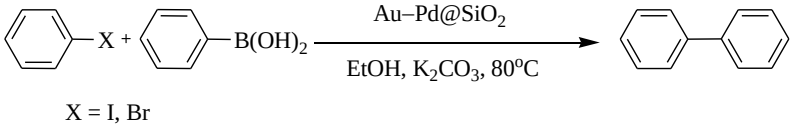

Catalyst	Yield(%)[a]	Yield (%)[b]
Alloy Au_3Pd_1@SiO_2	99.8	84.9
Alloy Au_1Pd_1@SiO_2	98.7	76.3
Alloy Au_1Pd_3@SiO_2	95.3	69.5
Core-shell Au-Pd	92.1	57.1
Pd@SiO_2	88.6	48.6
Au@SiO_2	N.A.	N.A.
Pd-C	99.6	99.1

[a]Yield of products with iodobenzene.
[b]Yield of products with bromobenzene.

Scheme V.2. Suzuki cross-coupling reaction using Au–Pd/SiO_2 as a catalyst.

Gao *et al*. have prepared ultrafine Ag–Pd nanoparticles homogeneously distributed on reduced graphene oxide (rGO) by redox reaction between Pd^{2+}, Ag^{+} and GO and explored their catalytic effect for Suzuki and Sonogashira reactions (Scheme V.3).[16b] The use of rGO as solid support facilitated separation and also the recyclability of the Ag–Pd@rGO catalyst.

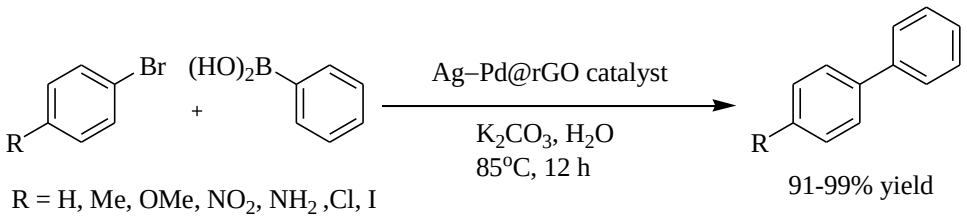

Scheme V.3. Ag–Pd@rGO bimetallic nanoparticles catalyzed Suzuki reaction.

Graphene supported Pd–Co bimetallic nanoparticles prepared by chemical reduction method of GO have employed as efficient catalysts for Suzuki coupling reaction (Scheme V.4).[17] The high stability, dispersibility in liquid-phase solution and also ease of recycling by a magnet make these nanospheres highly efficient catalysts in liquid-phase reaction.

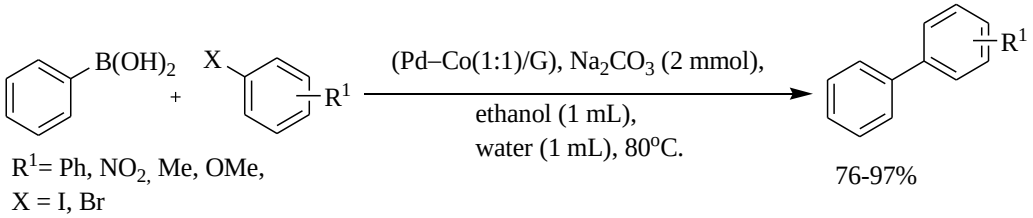

Scheme V.4. Graphene supported Pd–Co bimetallic nanoparticles catalyzed Suzuki-Miyaura coupling.

Reetz *et al.* have synthesised Pd-Ni nanoclusters stabilized by tetra alkyl ammonium salts or poly (vinylpyrrolidone) and observed their catalytic activities towards Suzuki and Heck reactions involving iodo-, bromo- and activated chloroaromatics (Scheme V.5).[15a]

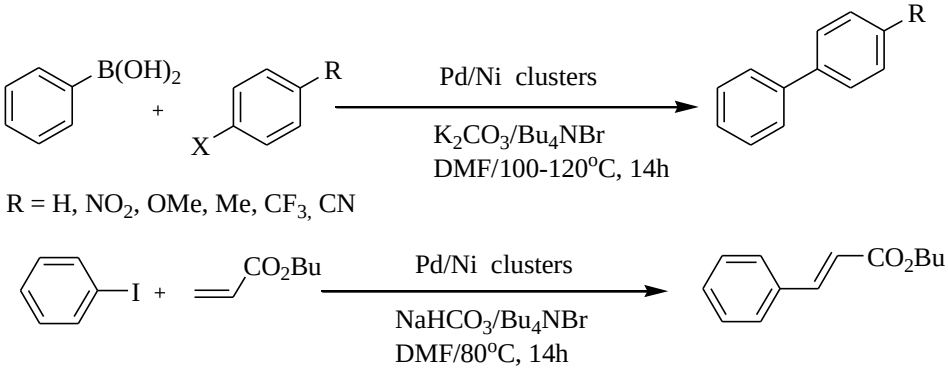

Scheme V.5. Suzuki and Heck coupling reactions catalyzed by bimetallic Pd–Ni nanoclusters.

A simple and efficient solution-based method for the synthesis of Pd–Ni bimetallic nanoparticles (NPs) has been developed by Li *et al.* (Scheme V.6).[15b] They have synthesised a series of Pd–Ni bimetallic NPs by reduction of $PdCl_2$ and $Ni(acac)_2$ in the presence of oleylamine (OAm), oleic acid (OA) and benzyl alcohol. The as-prepared Pd–Ni bimetallic NPs have core–shell structures with a Pd-rich core and a Ni-rich shell. In addition, as-obtained Pd–Ni bimetallic NPs with varying compositions show excellent catalytic activities in the Suzuki-Miyaura reaction.

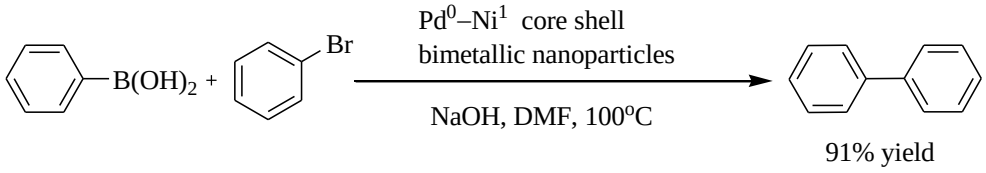

Scheme V.6. Pd–Ni core-shell nanoparticles catalyzed Suzuki coupling reaction.

The bimetallic nanoparticles of Pd/Cu have also been synthesized and explored extensively for Sonogashira reaction.[19] In such bimetallic system copper plays dual role; both as a support for the palladium nanoparticles as well as a co-catalyst. Although, a myriad of Sonogashira reactions have been reported to be catalyzed by Pd/Cu nanoparticles, but a limited number of Suzuki and Heck reactions have been explored which are catalyzed by Pd/Cu bimetallic NPs.

Heshmatpour *et al.*[13e] have synthesized various bimetallic nanoparticles (Pd, Ag, Pd/Ag, Pd/Ni and Pd/Cu) using a water-in-oil micro emulsion system of water/dioctyl sulfosuccinate sodium salt (aerosol-OT, AOT)/isooctane at 25 ^{o}C and investigated their catalytic effect in Heck reaction (Scheme V.7). They have observed that Pd/Cu(4:1) NPs act as superior catalysts among other NPs with high activity and selectivity for Heck reaction with aryl halides having both electron donating and withdrawing groups and methyl acrylate in DMF at 100 °C to achieve high yields of coupled products. In Heck reaction, the order of the catalytic acitivity of as-prepared bimetallic NPs is Pd/Cu (4:1)>Pd>>Pd/Ni (1:1)>Pd/Ag (1:1)>Ag.

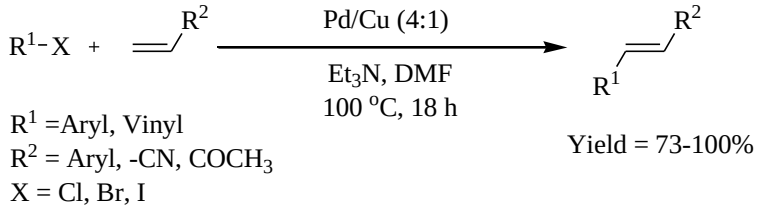

Scheme V.7. Pd/Cu (4:1)-catalyzed Heck–Mizoroki coupling reaction.

Choi *et al.* have synthesized the carbon supported bimetallic Pd–M (M=Ag, Ni, Cu)/C nanoparticles by *γ*-irradiation technique at room temperature without using any reducing agent.[13g] They investigated catalytic activities of these bimetallic nanoparticles for Suzuki and Heck reactions in ethanol and acetonitrile at 78 °C and 82 °C respectively in inert atmosphere to achieve the high yields of the coupled products (Scheme V.8). The Pd- Cu/C showed high catalytic efficiency in the Suzuki- and Heck-type reaction and for Suzuki reaction the catalytic efficiency e has been found to decrease in the order of Pd–Cu/C> Pd/C>Pd–Ag/C> Pd–Ni/C.

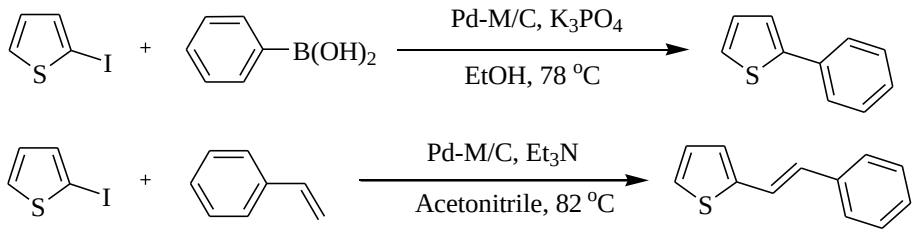

Scheme V.8. Suzuki and Heck reactions catalyzed by Pd-M/C.

Our previous laboratory report depicts about the excellent catalytic effect of monometallic Pd NPs for Suzuki, Heck and Songashira reactions (Please see the Scheme I.22 of Chapter I).[20] Recently, we become interested towards developing bimetallic NPs and also their catalytic application for C–C bond forming reactions.

V.2. Present Work: Background and Objectives

Polystyrene-trimethylammonium anion-exchange resins have been exploited both as a scavenger as well as a solid support to carry out various organic transformations in our laboratory.[20] Amberlite resin formate (ARF) anions obtained by exchanging chloride anion of commercially available Amberlite IRA-420 (chloride form) with formate ($HCOO^-$) ion, have been utilized as scavengers for immobilizing noble (Pd),[20a] and non-noble (Cu),[21] metals (Scheme V.8) and applied in C–C and C–S bond forming reactions in our laboratory (Chapter I, Scheme I.22 & I.23).[20a,21]

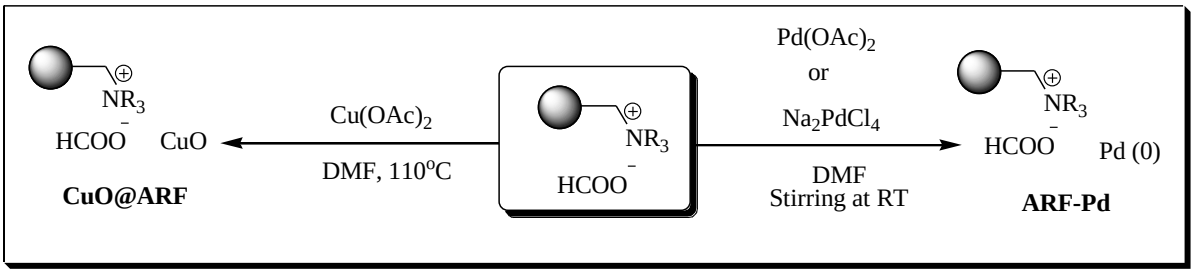

Scheme V.9. Preparation of monometallic Pd NPs and CuO NP embedded on Amberlite Resin Formate (ARF).

Recently, a new heterogeneous Pd/Cu bimetallic nanocomposite embedded on amberlite resin formate (ARF) has been prepared in our laboratory and characterized properly with the help of FT–IR spectroscopy, X-ray powder diffraction (XRD), transmission electron microscopy (TEM) and atomic absorption spectroscopy (AAS).[22] The existence of metallic Pd, PdO and CuO NPs in this nanocomposite has been found by XRD analysis and crystalline nature of the composite has been also observed by TEM analysis. This Pd/Cu–ARF(II) bimetallic nanocomposite exhibited high catalytic activity in the Sonogashira cross-coupling reaction between aryl iodide and terminal alkynes without use of phosphine-ligand (Scheme V.9).[22]

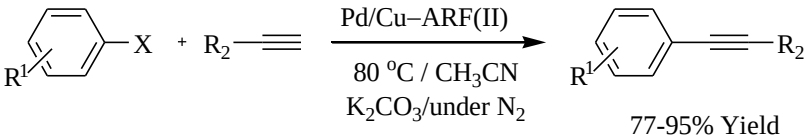

R^1 = -CH_3, -OCH_3, -NO_2, -Br, -$COCH_3$, -C_9H_6
R^2 = Ph, CH_2OCOCH_3, $CH_2OCOCH_2CH_3$, -$CH_2CH_2C_6H_5$, $C_6H_4(4\text{-}CH_3)$
X = Cl, Br, I

Scheme V.10. Sonogashira cross-coupling reaction catalyzed by Pd/Cu–ARF(II).

In continuation with our previous work, herein we have prepared Pd/Cu bimetallic nanocomposite Pd/Cu–ARF following our previous method and applied in Suzuki–Miyaura and Mizoroki–Heck reactions under completely ligand-free conditions. We have also

compared the catalytic activity of these bimetallic NPs with the monometallic Pd NPs embedded on ARF.

V.3. Present Work: Results and Discussion

To investigate our observation we have prepared bimetallic NPs, Pd/Cu−ARF by following our previous lab method and taking the same molar ratio of both metal salts Pd $(OAc)_2$ and Cu $(OAc)_2$.[22]

V.3.1. Preparation of heterogeneous Pd/Cu–ARF nanocomposite

Amberlite resin formate (ARF) was prepared from commercially available inexpensive amberlite resin chloride by ion-exchange process as reported from our laboratory.[20,21] The resin beads were then washed with water followed by acetone, dried under vacuum and used for the preparation of heterogeneous bimetallic nanocomposites. Impregnation of bimetallic Pd/Cu on the ARF was performed by heating an equimolar mixture of solutions of palladium acetate and cupric acetate in dimethylformamide (DMF) using 0.25 mmol of each salts to prepare bimetallic NPs of Pd/Cu−ARF as presented in Scheme V.10.

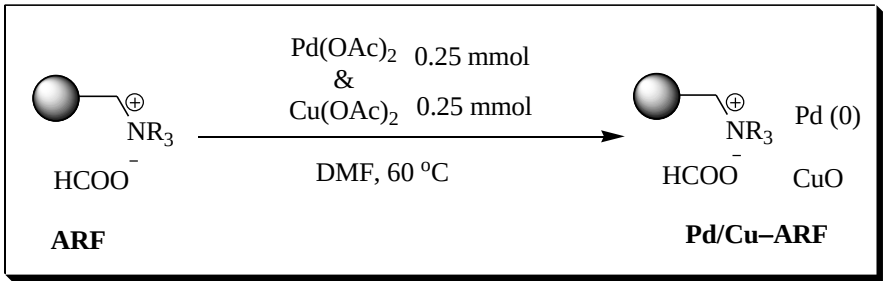

Scheme.V.11. Preparation of bimetallic Pd/Cu–ARF NPs.

❖ **Characterizations of Pd/Cu−ARF**

Characterization of this bimetallic nanocomposite has been already reported in our previous work (reference 23) which was designated as Pd/Cu–ARF (II).

V.3.2. Suzuki–Miyaura reaction catalyzed by Pd/Cu−ARF

For Suzuki–Miyaura cross-coupling reaction, we have taken 4–iodoanisole and phenylboronic acid as model substrates and 100 mg of catalyst to carry out the reaction. At first we have started the reaction at room temperature and found only 48% yield of corresponding cross-coupling product 4–methoxy biphenyl (Table V.1, entry 1). The yield of product increases with the increase of temperature (Table V.1, entries 2–3). In order to optimize the effect of solvent, different solvents including water, water-ethanol mixture,

toluene and DMF were employed for the reaction and found no such increase of yield of the product (Table V.1, entries 7–10). Finally, we found DMF is the best solvent for Suzuki coupling reaction in our condition (table V.1, entry 3). We have also optimised the influence of base using KF, NaOH and NaOAc and found no such increase in the yield of product as compared to K_2CO_3 (Table V.1, entries 4–6) respectively.

Table V.1. Optimization of Suzuki–Miyaura reaction using Pd/Cu–ARF.[a]

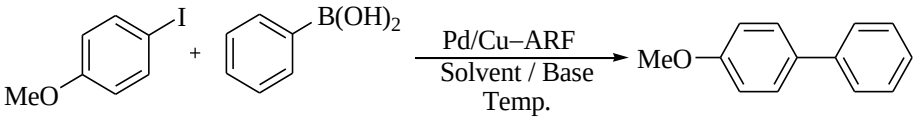

Entry	Base	Solvent	Temperature (^oC)	Time (h)	Yield[b] (%)
1	K_2CO_3	DMF	RT	12	48
2	K_2CO_3	DMF	50	12	88
3	**K_2CO_3**	**DMF**	**65**	**4**	**93**
4	KF	DMF	65	12	68
5	NaOH	DMF	65	12	73
6	NaOAc	DMF	65	12	63
7	K_2CO_3	H_2O	65	12	54
8	K_2CO_3	H_2O:EtOH	65	12	65
9	K_2CO_3	Toluene	65	12	81
10	K_2CO_3	MeOH	65	12	58

[a] 4-Iodoanisole (1 mmol), phenylboronic acid (1.2 mmol), base (1.1 mmol) Pd/Cu−ARF, (100 mg) and solvent (3 mL). [b]Isolated yield. [All optimisation entries were performed and reproduced by the present author as well as one of my co-author D. Sengupta]

By taking our optimized condition, we have go through for the further application of Pd/Cu−ARF nanocomposite to the Suzuki–Miyaura cross-coupling between other aryl halides and different phenyl boronic acids and results are shown in Table V.2. Substituted aryl iodides undergo the reaction without any difficulties forming excellent yield (Table V.2, entries 1−4). The presence of electron donating or withdrawing groups have not found to any retarding effect on the yield of the product in such cases. When aryl bromides smoothly react with boronic acid forming corresponding cross-coupling product in excellent yield (Table V.2, entries 5–6, 9 & 10), aryl chloride remains unaltered under the same condition. Moreover, we have also performed the cross-coupling reaction between a heterocyclic aryl bromide (3-bromoquinoline) with phenyl boronic acid and found 89% of the cross–coupled product 3-phenylquinoline (entry 6). We have further performed the cross-coupling reactions of different aryl di iodo, bromo iodo and di bromo compounds with phenyl boronic acids and obtained corresponding terphenyl compounds with excellent yield (entries 8−10).

Table V.2. Suzuki–Miyaura cross-coupling using Pd/Cu−ARF.[a]

Entry	Aryl halide	Boronic acid	Time (h)	Product	Yield (%)b
1	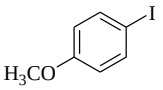	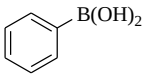	4	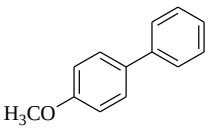	93
2	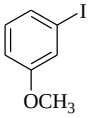	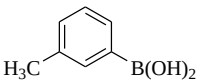	3.5	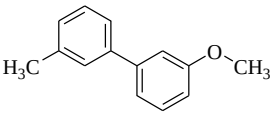	92
3	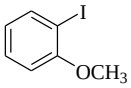	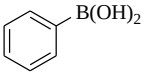	5	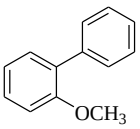	90
4	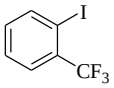	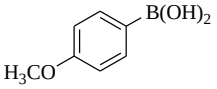	2	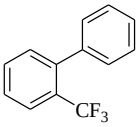	92
5	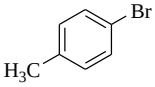	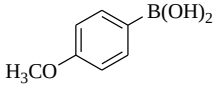	2	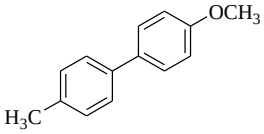	93
6	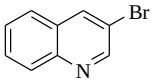	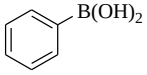	3	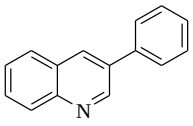	89
7	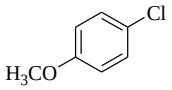	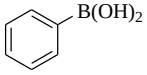	24	No reaction	-
8[c]		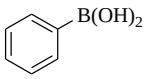	4	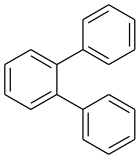	90
9[c]	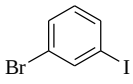	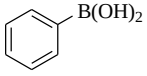	4	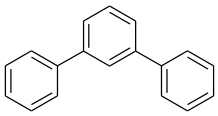	91
10[c]	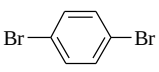	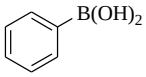	4	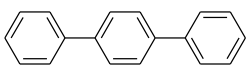	89

[a]Reaction condition: ArX (1 mmol), boronic acid (1.2 mmol), K_2CO_3 (1.1 mmol), Pd/Cu−ARF(II) (100 mg), DMF (3 mL), heating the reaction mixture at 65 ^oC. [b]Isolated yield. [c]ArX_2 (1.0 mmol), boronic acid (2.4 mmol), K_2CO_3 (2.2 mmol), Pd/Cu−ARF (100 mg), DMF (3 mL), heating the reaction mixture at 65 ^oC. [Entries 1, 3, 5, 7, 10 were isolated by the present author and remaining entries were performed by my co-author]

V.3.3. Mizoroki–Heck reaction catalyzed by Pd/Cu−ARF

After the successful application of our bimetallic catalyst to Suzuki–Miyaura cross–coupling, we have further explored the catalytic efficiency of bimetallic Pd/Cu−ARF catalyst in Mizoroki–Heck reaction. We have started our investigation by performing a reaction between 4-iodoanisole and *n*-butyl acrylate using triethylamine as a base and DMF as solvent at room temperature but only 12% of cross-coupled product (Table V.3, entry 1) was isolated after 12 hours. By increasing the temperature the product yield was also increased significantly (entries 2–3) and the best result was achieved at 70 ^{o}C only within 2h, (Table V.3). To know the effect of base on Mizoroki–Heck reation, we have used different bases like NaOAc, K_2CO_3 and KF but found only triethylamine to be most effective over other inorganic bases in our condition.

Table V.3. Optimization of Mizoroki–Heck reaction using Pd/Cu−ARF(II).[a]

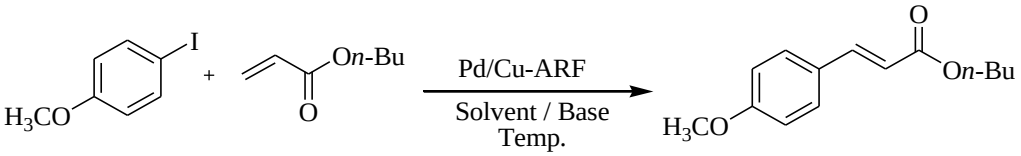

Entry	Base	Solvent	Temperature (^{o}C)	Time (h)	Yield[b] (%)
1	Et_3N	DMF	RT	12	12
2	Et_3N	DMF	55	12	69
3	Et_3N	DMF	60	12	70
4	**Et_3N**	**DMF**	**70**	**2**	**95**
5	NaOAc	DMF	70	6	88
6	K_2CO_3	DMF	70	6	76
7	KF	DMF	70	12	81

[a] 4-Iodoanisole (1 mmol), *n*-butyl acrylate (1.2 mmol), base (1.1 mmol), Pd/Cu−ARF (100 mg) and solvent (3 mL).[b] Isolated yield. [All optimisation entries were performed and reproduced by the present author as well as by my co-author]

With the optimized condition at our hand, we examined its practical with a variety of aryl halides and acrylates. It was observed that aryl iodides undergo Heck reaction with *n*-butyl and ethyl acrylates with the excellent yield of the corresponding cross-coupling products (Table V.4, entries 1−4). Unfortunately, aryl bromides and chlorides are not efficient towards the reaction under the same condition. Di-iodo compound is also give rise to the formation of bis coupled product in good yield (entry 7). We also became successful to synthesize different substituted *trans*-stilbenes of different aryl iodides using styrene as olefin

substrate (entries 8−10). For all of the cases, it is noticed that *trans* selectivity in the coupled product was observed.

Table V.4. Mizoroki–Heck cross-coupling using Pd/Cu−ARF.[a]

Entry	Aryl halide	Olefin	Time (h)	Product	Yield (%)b
1	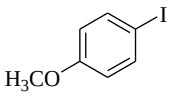		1.5	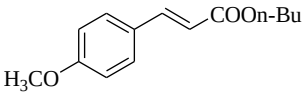	95
2	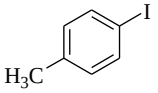	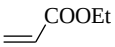	2	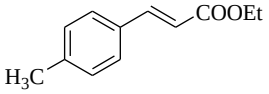	91
3	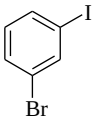	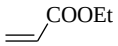	4	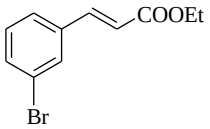	78
4	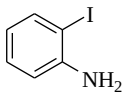	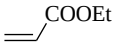	4	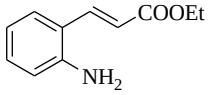	89
5	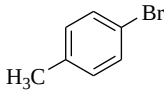	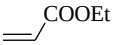	12	No reaction	-
6	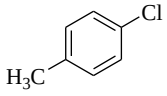	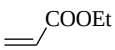	12	No reaction	-
7[c]	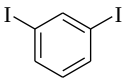	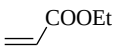	3.5	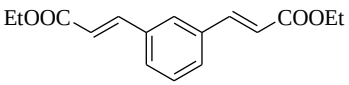	79
8	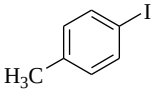		3	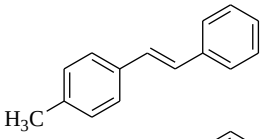	86
9	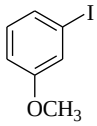		3	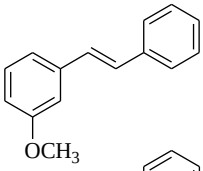	82
10	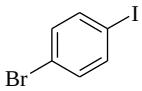		2.5	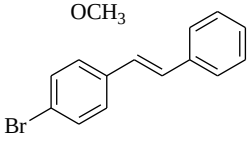	83

[a]Reaction condition: ArX (1 mmol), olefin (1.2 mmol), Et_3N (1.1 mmol), Pd/Cu−ARF (100 mg), DMF (3 mL), heating the reaction mixture at 70 ^oC. [b]Isolated yield. [c] ArI_2 (1.0 mmol), ethylacrylate (2.4 mmol), Et_3N (2.2 mmol), Pd/Cu−ARF (100 mg), DMF (3 mL), heating the reaction mixture at 70 ^oC. [Entries 2, 3, 6, 8, 10 were isolated by the present author and remaining entries were performed by my co-author]

V.3.4. Application of Pd/Cu–ARF bimetallic NPs for the preparation of 3-Methyl-1*H*-indole

To continue our optimization of the catalytic activity of Pd/Cu bimetallic nanocomposite we have extended this Mizoroki–Heck cross-coupling methodology for the preparation of substituted heterocyclic compound like indole. Primarily, we prepared a mono *N*-allylated product of 2-iodoaniline, by the reaction with allyl bromide over silica gel surface following our previous laboratory method.[23] By taking this *N*-allylated product as starting substrate we performed Heck reaction following our optimized condition and finally we get 3-methylindole (Scheme V.11) as the sole product.

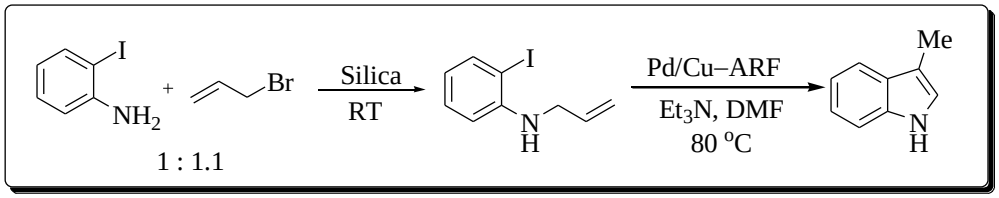

Scheme V.12. Synthesis of 3-methylindole *via* Mizoroki–Heack coupling with Pd/Cu−ARF catalyst. [This one was performed by the present author]

V.3.5. Comparative study

In an attempt to compare the catalytic efficiency of the bimetallic Pd/Cu−ARF nanocomposite with our previously reported monometallic ARF–Pd catalyst,[20a] we performed both Suzuki–Miyaura and Mizroki–Heck coupling reaction using both of the catalysts and monitored the conversion by HPLC. Before the reaction we have also prepared monometallic ARF–Pd following our laboratory method but maintain the molar proportion of palladium same as that of bimetallic catalyst Pd/Cu−ARF.[11] Considering Suzuki–Miyaura coupling, both ARF–Pd and Pd/Cu–ARF shows almost similar activity for entry 1, listed in Table V.2 (Figure V.1a) but when we concerned about Mizoroki–Heck reaction (entry 1, Table V.2), bimetallic catalyst Pd/Cu−ARF shows much higher activity compared to mono metallic catalyst (Figure V.1b). For Mizoroki–Heck coupling Pd/Cu−ARFserve 97% conversion within 2h while using ARF–Pd only 83% conversion was achieved within this period and reaches maximum up to 94% after 3.5 h.

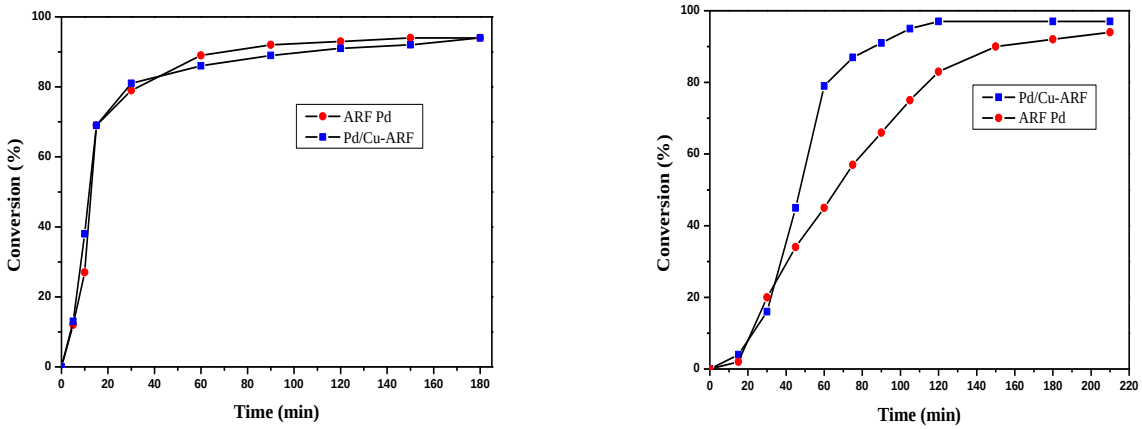

(a) **(b)**

Figure V.1. Time conversion plot for (a) Suzuki–Miyaura and (b) Mizoroki–Heck coupling reaction using Pd/Cu−ARF and ARF–Pd.

V.3.6. Hot filtration Test

To determine leaching of any metallic species from the amberlite resin formate surface we have performed hot filtration test for both of Suzuki and Heck coupling following the literature procedure.[24] We first performed the Suzuki–Miyaura reaction between 4-iodoanisole and phenylboronic acid in DMF. After 10 min the reaction was stopped and the catalyst was recovered by filtration. Then the filtrate was analysed by HPLC (~38% conversion) and heated at 65 ^{o}C for another 3 hr without catalyst resulting in no further conversion (monitored by HPLC). Following the same procedure we have also performed hot filtration test for Mizoroki-Heck reaction between 4-iodoansole and ethyl acrylate at 70 ^{o}C and the result was shown in Figure V.2.

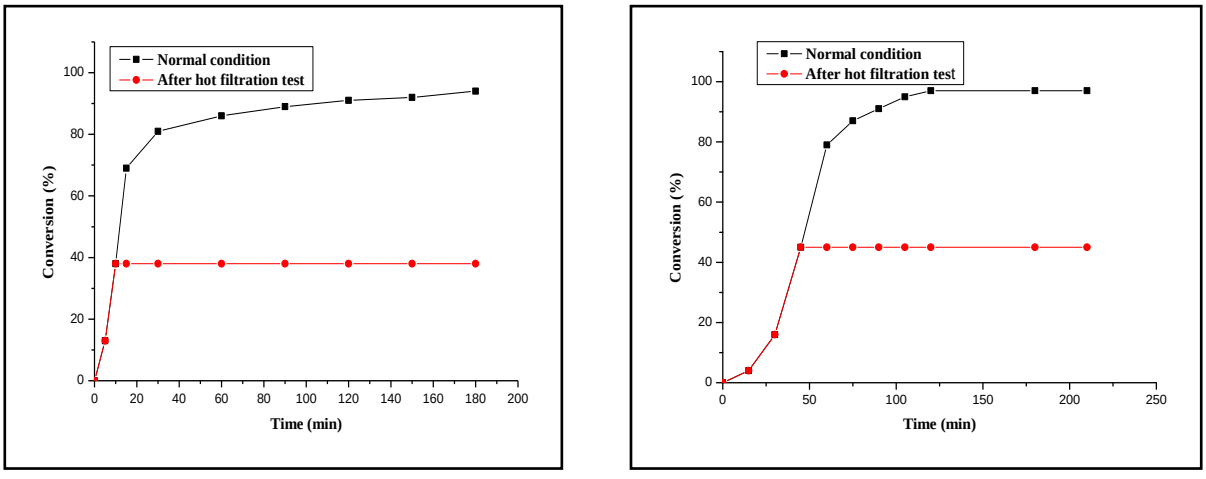

(a) **(b)**

Figure V.2. Comparison of the reaction under normal condition and the reaction after hot filtration test for (a) Suzuki–Miyaura and (b) Mizoroki–Heck coupling reaction catalyzed by Pd/Cu−ARF.

V.3.7. Recyclability of the catalyst

We have also tested the recyclability of the catalyst Pd/Cu−ARF for both Suzuki–Miyaura and Mizoroki-Heck reactions. After the first run, catalysts were collected through simple filtration, and properly washed with water followed by acetone, dried under vacuumed for 30 min and used for next cycle. The results are summarised in Figure V.3. The catalyst can be reused at least seven times for both Suzuki-Miyaura and Mizoroki-Heck reactions separately without decrease in catalytic activity.

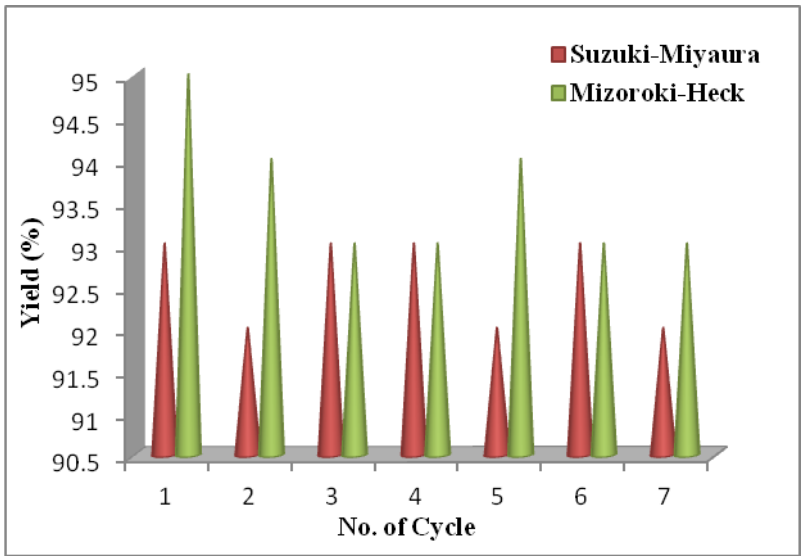

Figure V.3. Recycling experiments using Pd/Cu−ARF for Suzuki–Miyaura cross-coupling between 4-iodoanisole and phenylboronic acid and Mizoroki–Heck cross-coupling between 4-iodoanisoleand *n*-butyl acrylate. [Recycling for Suzuki reaction was performed by the present author and same for Heck was performed by one of my co-author]

V.3.8. Characterization of the recovered catalyst

We have characterized the recovered Pd/Cu−ARF composite material after 7th consecutive run for Mizoroki-Heck reaction by XRD which is shown in the following Figure V.4.

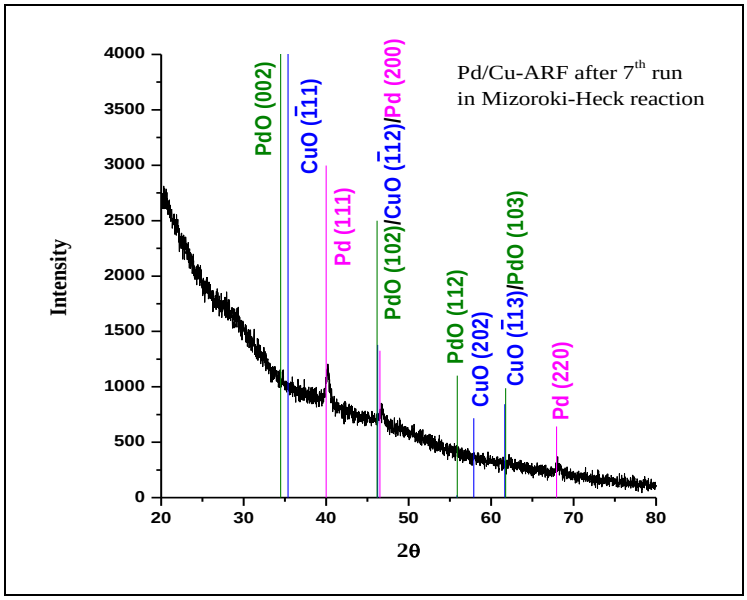

Figure V.4. XRD analysis of Pd/Cu−ARF catalyst recovered after 7th consecutive runs in Mizoroki–Heck reaction**.**

V.4. Conclusion

In summary, we have utilized amberilte resin formate (ARF) as an efficient polymeric support for the preparation of highly active Pd/Cu bimetallic nanocomposite. Furthermore, we have demonstrated Pd/Cu−ARF bi-metallic composite nanoparticles as an efficient heterogeneous catalyst for Suzuki–Miyaura and Mizoroki–Heck coupling reactions under ligand-free and mild conditions. The bimetallic nanocomposite material Pd/Cu−ARF has been found to be more effective as compared to monometallic Pd–ARF catalyst in Mizoroki–Heck coupling. Further studies included a sequential *N*-allylation and Mizoroki–Heck cross–coupling of 2-iodoaniline provides a heterocyclic moiety, 3-methylindole. Recycling of the catalyst up to seven runs without significant loss of catalytic activity can influence its use in a broaden way in industry.

V.5. Experimental Section

V.5.1. General Information

Amberlite IRA 900 (chloride form) was purchased from Acros Organics, Belgium and used after washing with water and acetone followed by drying under vacuum. Other chemicals were purchased and used directly. The X-ray diffraction (XRD) studies of the powder samples were done using the Rigaku SmartLab (9 kW) diffractometer using CuKα radiation. NMR spectra were taken in CDCl3 using Bruker Avance AV-300 spectrometer

operating for 1H at 300 MHz and for 13C at 75 MHz. The spectral data were measured using TMS as the internal standard.

V.5.2. Preparation of Pd/Cu−ARF bimetallic nanocomposite

To a solution of $Pd(OAc)_2$ (56 mg, 0.25 mmol) and $Cu(OAc)_2$ (50 mg, 0.25 mmol) in DMF (10 mL) ARF (1 g) was added in a screw-capped sealed tube and then heated at 60 ^oC for 1h with occasional shaking. The change of colour of supernatant liquid from bluish orange to completely colourless signifies the impregnation of metal NPs on ARF and the greyish beads of ARF turned shiny black. Then the mixture was cooled to room temperature and the resin beads were filtered off and washed with water (3 x 5 mL) and acetone (2 x 5 mL). Resulting black resin beads were dried under vacuum and used for analyses and reactions.

V.5.3. Preparation of monometallic ARF–Pd

In a mixture of $Pd(OAc)_2$ (56 mg, 0.25 mmol) in DMF (10 mL), ARF (1 g) was added and in a screw-capped sealed tube and heated at 60 ^oC for 1h with occasional shaking. The supernatant liquid appeared completely colourless by this time and the greyish beads of ARF turned black. The mixture was cooled to room temperature and the resin beads were filtered off and washed with water (3 x 5 mL) and acetone (2 x 5 mL). Resulting black resin beads were dried under vacuum and used for analyses and reactions.

V.5.4. General procedure for Suzuki–Miyaura cross-coupling using Pd/Cu−ARF

In a mixture of aryl halide (1 mmol), arylboronic acid (1.2 mmol) and potassium carbonate (1.1 mmol) in DMF (3 mL) 100 mg of Pd/Cu−ARF was added and charged in a 15 mL sealed tube and heated the reaction mixture at 65 ^oC under gentle magnetic starring. The reaction progress was monitored by TLC. After completion of reaction the mixture was allowed to cool to room temperature and diluted with water (5 mL). Then, the mixture was passed through a cotton bed and the filtrate part was extracted with diethyl ether. The organic part was dried over sodium sulphate and concentrated under vacuumed. The residue was purified by passing through a short silica gel column and elution with light petroleum. All products were characterized by ^1H, ^{13}C NMR spectral data, and also compared with reported melting point (for known solid compounds).

VI.5.5. General procedure for Mizoroki–Heck coupling using Pd/Cu−ARF

In a mixture of aryl halide (1 mmol), activated alkene (1.2 mmol) and triethylamine (1.1 mmol) in DMF (3 mL), 100 mg of Pd/Cu−ARF was added and charged in a 15 mL sealed tube and heated the reaction mixture at 70 ^{o}C under gentle magnetic starring. The reaction progress was monitored by TLC. After completion of reaction the mixture was allowed to cool to room temperature and diluted with water (5 mL). The mixture was passed through a cotton bed and the filtrate part was extracted with diethyl ether. The organic part was dried over sodium sulphate and concentrated under vacuumed. The residue was purified by passing through a short silica gel column and elution with light petroleum or 2% ethyl acetate-light petroleum. All products were characterized by ^{1}H, ^{13}C NMR spectral data, and also compared with reported melting point (for known solid compounds).

V.5.6. Preparation of 3-Methylindole

We have prepared 3-methylindole in two steps: first step was the formation of *N*-allylated product of 2-iodoaniline followed by the second step of intramolecular Mizoroki–Heck cross-coupling reaction resulting in the formation of final product.

Step I: An equimolar mixture of 2-iodoaniline and allyl bromide was mixed with pre-calcined silica (Grade: TLC; HF_{254}) in a mortar pestle and the solid mixture was transferred into a round bottle flask. Gentle agitation was then provided by a magnetic spin bar at room temperature for 2h. After completion, the reaction mixture was washed repeatedly with diethyl ether and combined ethereal layer was dried over anhydrous Na_2SO_4 and concentrated. The crude product was then purified by column chromatography over silica gel and isolating the desired product *N*-allyl-2-iodobenzenamine (216 mg, 82%).

Step II: A mixture of *N*-allyl-2-iodobenzenamine (1 mmol, 164 mg), triethyl amine (1.1 mmol) and 100 mg of Pd/Cu–ARF in DMF was taken in a sealed tube and heated at 80 ^{o}C for 3 h. After completion of reaction the mixture was cool at room temperature and diluted with water (5 mL). The mixture was extracted with diethyl ether, dried over Na_2SO_4 and concentrated under vacuumed. The crude product was then purified by silica gel column chromatography with light 5% ethyl acetate-light petroleum. Finally, the product was characterized by ^{1}H and ^{13}C NMR.

V.5.7. Physical properties and spectral data of compounds

Table V.2; Entry 1

4-Methoxybiphenyl [25]

The product was obtained as a white solid, mp 91–92 ^{o}C (Lit. mp 90–91 ^{o}C).

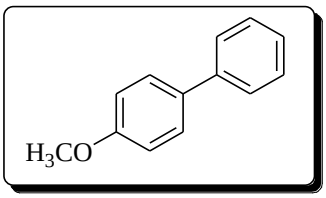

^{1}H NMR ($CDCl_3$, 300 MHz): δ/ppm 3.84 (s, 3H,), 6.97 (dd, *J* = 2.1 and 6.9 Hz, 2H), 7.29-7.32 (m, 1H), 7.38-7.43 (m, 2H), 7.51-7.56 (m, 4H).

^{13}C NMR ($CDCl_3$, 75 MHz): δ/ppm 55.3, 114.2, 126.6, 126.7, 128.1, 128.7, 133.8, 140.8, 159.2.

Table V.2; Entry 2

3-Methoxy-3'-methylbiphenyl[25]

The product was obtained as a colourless liquid.

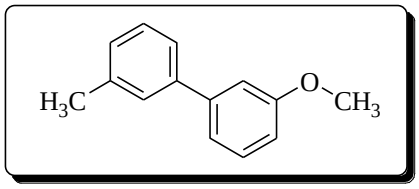

^{1}H NMR ($CDCl_3$, 300 MHz): δ/ppm 2.41 (s, 3H), 3.84 (s, 3H), 6.87-6.89 (m, 1H), 7.11-8.18 (m, 3H), 7.28-7.39 (m, 4H).

^{13}C NMR ($CDCl_3$, 75 MHz): δ/ppm 21.5, 55.2, 112.6, 112.8, 119.6, 124.3, 127.9, 128.1, 128.6, 129.6, 138.3, 141.0, 142.8, 159.8.

Table V.2: entry 3; 2-Methoxybiphenyl.[25]

The product was obtained as a colourless liquid.

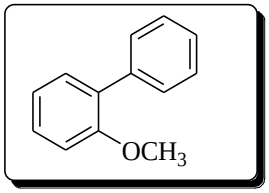

^{1}H NMR ($CDCl_3$, 300 MHz): δ/ppm 3.81 (s, 3H), 6.97-7.06 (m, 2H), 7.29-7.43 (m, 5H), 7.51-7.54 (m, 2H).

^{13}C NMR ($CDCl_3$, 75 MHz): δ/ppm 55.5, 111.2, 120.8, 126.9, 127.9, 128.6, 129.5, 130.7, 130.9, 138.5, 156.4.

Table V.2; Entry 4

4-Methoxy-2'-trifluoromethylbiphenyl [26]

The product was obtained as a colourless liquid.

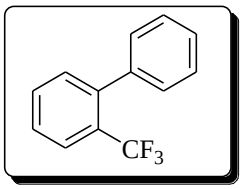

^{1}H NMR ($CDCl_3$, 300 MHz): δ/ppm 3.81 (s, 3H), 6.90-6.94 (m, 2H), 7.22-7.31 (m, 3H), 7.37-7.42 (m, 1H), 7.48-7.53 (m, 1H), 7.71 (d, *J* = 7.8 Hz, 1H).

^{13}C NMR ($CDCl_3$, 75 MHz): δ/ppm 55.1, 113.2, 122.4, 126.0 (q, *J* = 5.4 Hz), 127.0, 128.5 (q, *J* = 29.4 Hz), 130.1 (d, *J* = 1.3 Hz), 131.2, 132.2, 132.3, 141.2 (d, *J* = 1.9 Hz), 159.1.

Table V.2: entry 5; 4-Methoxy-4'-methylbiphenyl.[25]

The product was obtained as a white solid, mp 111–112 ^{o}C (Lit. mp 112–113 ^{o}C).

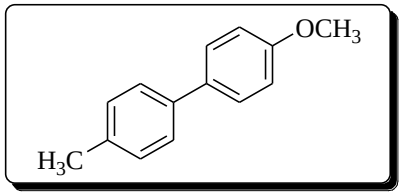

^{1}H NMR ($CDCl_3$, 300 MHz): δ/ppm 2.38 (s, 3H), 3.84 (s, 3H), 6.96 (d, *J* = 8.7 Hz, 2H), 7.22 (d, *J* = 8.4 Hz, 2H), 7.45 (d, *J* = 8.1 Hz, 2H), 7.51 (d, *J* = 8.7 Hz, 2H).

^{13}C NMR ($CDCl_3$, 75 MHz): δ/ppm 21.0, 55.3, 114.1, 126.5, 127.9, 129.4, 133.7, 136.3, 137.9, 158.9.

Table V.2; Entry 6

3-Phenylquinoline[27]

The product was obtained as a colourless liquid.

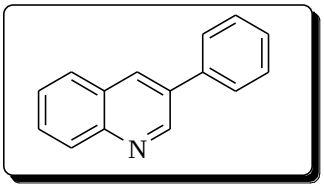

^{1}H NMR ($CDCl_3$, 300 MHz): δ/ppm 7.38-7.56 (m, 4H), 7.65-7.72 (m, 3H), 7.83 (dd, *J* = 1.2 and 7.8 Hz, 1H), 8.14 (d, *J* = 8.4 Hz, 1H), 8.25 (d, *J* = 2.4 Hz, 1H), 9.17 (d, *J* = 2.4 Hz, 1H).

^{13}C NMR ($CDCl_3$, 75 MHz): δ/ppm 126.9, 127.3, 127.9, 128.0, 129.0, 129.3, 133.1, 133.7, 137.7, 147.1, 149.7.

Table V.2; entry 8

***o*-Terphenyl**[25]

The product was obtained as a solid, mp 54–55 ^{o}C (Lit. mp 54–55 ^{o}C).

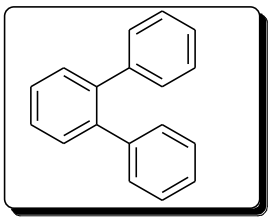

^{1}H NMR ($CDCl_3$, 300 MHz): δ/ppm 7.13-7.26 (m, 10H), 7.40-7.44 (m, 4H).
^{13}C NMR ($CDCl_3$, 75 MHz):δ/ppm 126.4, 127.4, 127.8, 129.9, 130.6, 140.6, 141.5.

Table V.2; Entry 9

***m*-Terphenyl**[25]

The product was obtained as a white solid, m.p. 84–85 ^{o}C (Lit. mp 83–85 ^{o}C).

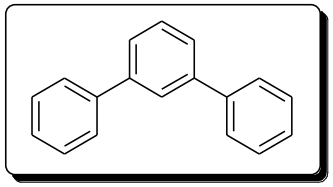

^{1}H NMR ($CDCl_3$, 300 MHz): δ/ppm 7.33-7.38 (m, 2H), 7.43-7.59 (m, 7H), 7.63-7.66 (m, 4H), 7.79-7.80 (m, 1H).
^{13}C NMR ($CDCl_3$, 75 MHz): δ/ppm 126.1, 126.2, 127.3, 127.4, 128.8, 129.2, 141.2, 141.8.

Table V.2; Entry 10

***p*-Terphenyl** [20a]

The product was obtained as a white solid, mp 211–212 ^{o}C (Lit. mp 212–214 ^{o}C).

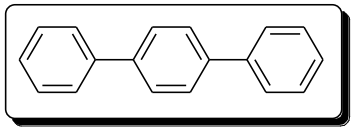

^{1}H NMR ($CDCl_3$, 300 MHz): δ/ppm 7.35-7.38 (m, 2H), 7.43-7.48 (m, 4H), 7.63-7.67 (m, 8H).
^{13}C NMR ($CDCl_3$, 75 MHz): δ/ppm 127.0, 127.3, 127.5, 128.8, 140.1, 140.7.

Table V.4; Entry 1

(*E*)-Butyl 3-(4-methoxyphenyl)acrylate[28]

The product was obtained as a colourless liquid.

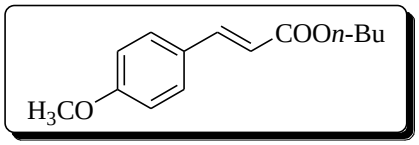

^{1}H NMR ($CDCl_3$, 300 MHz): δ/ppm 0.96 (t, *J* = 7.5 Hz, 3H), 1.42-1.71 (m, 4H,), 3.83 (s, 3H), 4.20 (t, *J* = 6.6 Hz, 2H), 6.31 (d, *J* = 15.9 Hz, 1H), 6.90 (dd, *J* = 2.1 and 6.9 Hz, 2H), 7.48 (dd, *J* = 2.1 and 6.9 Hz, 2H), 7.64 (d, *J* = 15.9 Hz, 1H).
^{13}C NMR ($CDCl_3$, 75 MHz): δ/ppm 13.7, 19.2, 30.7, 55.3, 64.2, 114.2, 115.7, 127.1, 129.6, 144.2, 161.2, 167.4.

Table V.4; Entry 2
(*E*)-Ethyl 3-*p*-tolylacrylate[29]
The product was obtained as a colourless liquid.

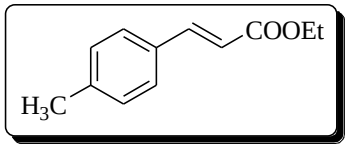

^{1}H NMR ($CDCl_3$, 300 MHz): δ/ppm 1.32 (t, *J* = 7.2 Hz, 3H), 2.35 (s, 3H), 4.25 (q, *J* = 7.2 Hz, 2H), 6.38 (d, *J* = 15.9 Hz, 1H), 7.17 (d, *J* = 7.8 Hz, 2H), 7.41 (d, *J* = 6.6 Hz, 2H), 7.66 (d, *J* = 15.9 Hz, 1H).
^{13}C NMR ($CDCl_3$,75 MHz): δ/ppm 14.2, 21.3, 60.3, 117.0, 127.9, 129.5, 131.6, 140.5, 144.5, 167.1.

Table V.4; Entry 3
(*E*)-Ethyl 3-(3-bromophenyl)acrylate[20a]
The product was obtained as a colourless liquid.

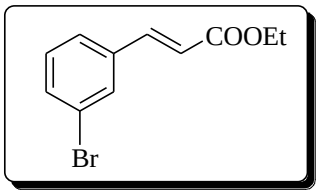

^{1}H NMR ($CDCl_3$, 300 MHz): δ/ppm 1.33 (t, *J* = 7.2 Hz, 3H), 4.26 (q, *J* = 7.2 Hz, 2H), 6.42 (d, *J* = 15.9 Hz, 1H), 7.21-7.26 (m, 1H), 7.41-7.50 (m, 2H), 7.58 (d, *J* = 15.9 Hz, 1H), 7.64-7.66 (m, 2H).
^{13}C NMR ($CDCl_3$, 75 MHz): δ/ppm 14.2, 60.6, 119.6, 122.9, 126.5, 130.2, 130.6, 132.8, 136.4, 142.7, 166.4.

Table V.4; Entry 4

(*E*)-Ethyl 3-(2-aminophenyl)acrylate [20a]

The product was obtained as a yellow solid, mp 75–76 ^{o}C (Lit. mp 76–78 ^{o}C).

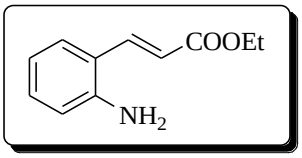

^{1}H NMR ($CDCl_3$, 300 MHz): δ/ppm 1.33 (t, *J* = 7.2 Hz, 3H), 3.89 (br s, 2H), 4.25 (q, *J* = 7.2 Hz, 2H), 6.35 (d, *J* = 15.9 Hz, 1H), 6.68-6.78 (m, 2H), 7.13-7.19 (m, 1H), 7,37 (dd, *J* = 1.5 and 7.5 Hz, 1H), 7.83 (d, *J* = 15.9 Hz, 1H).

^{13}C NMR ($CDCl_3$, 75 MHz): δ/ppm 14.2, 60.4, 116.7, 118.0, 118.9, 119.8, 127.9, 131.2, 140.0, 145.4, 167.3.

Table V.4; Entry 7

Ethyl (*E*)-3-{3-[(*E*)-2-(Ethoxycarbonyl)vinyl]phenyl}acrylate[20a]

The product was obtained as a white solid, mp 50-51 ^{o}C (Lit. mp 50-52 ^{o}C).

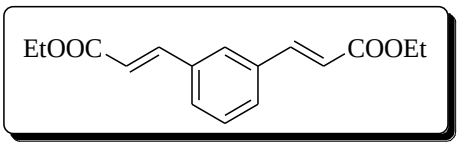

^{1}H NMR ($CDCl_3$, 300 MHz): δ/ppm 1.34 (t, *J* = 7.2 Hz, 3H), 4.23 (q, *J* = 7.2 Hz, 2H), 6.47 (d, *J* = 15.9 Hz, 1H), 7.40-7.54 (m, 4H), 7.67 (d, *J* = 16.2 Hz, 1H).

^{13}C NMR ($CDCl_3$, 75 MHz): δ/ppm 14.2, 60.5, 119.1, 127.5, 129.3, 135.0, 143.5, 166.6.

Table V.4; Entry 8

(*E*)-4-Methylstilbene[30a-c]

The product was obtained as a white solid, 120–121 ^{o}C (Lit mp 121.7–122.3 ^{o}C).

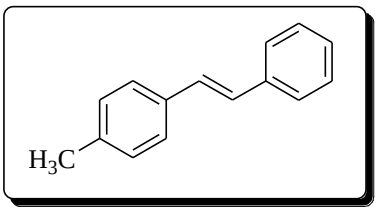

^{1}H NMR ($CDCl_3$, 300 MHz): δ/ppm 2.35 (s, 3H), 7.06 (d, *J* = 1.5 Hz, 2H), 7.16 (d, *J* = 8.4 Hz, 2H), 7.23-7.26 (m, 1H), 7.31-7.42 (m, 4H), 7.48-7.51 (m, 1H).

^{13}C NMR ($CDCl_3$, 75MHz): δ/ppm 21.2, 126.4, 126.41, 127.4, 127.7, 128.6, 129.4, 134.5, 137.5.

Table V.4; Entry 9

(*E*)-3-Methoxylstilbene[31]

The product was obtained as a white solid.

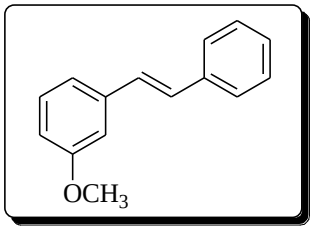

^{1}H NMR ($CDCl_3$, 300 MHz): δ/ppm 3.86 (s, 3H), 6.82 (ddd, *J* = 0.9, 2.7 and 8.1 Hz, 1H), 7.05-7.13 (m, 4H), 7.24-7.38 (m, 4H), 7.50-7.53 (m, 2H).

^{13}C NMR ($CDCl_3$, 75 MHz): δ/ppm 55.2, 111.7, 113.3, 119.2, 126.5, 127.7, 128.6, 128.7, 129.0, 129.6, 137.2, 138.8, 159.9.

Table V.4; Entry 10

(*E*)-4-Bromostilbene[30c,d]

The product was obtained as a white solid, mp 139–140 ^{o}C (Lit mp 136.5–139 ^{o}C).

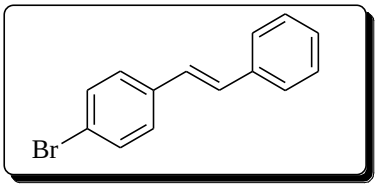

^{1}H NMR ($CDCl_3$, 300 MHz): 7.06 (d, *J* = 7.5 Hz, 2H), 7.26-7.52 (m, 9H).

^{13}C NMR ($CDCl_3$, 75 MHz): δ/ppm 121.3, 126.5, 127.4, 127.9, 128.0, 128.7, 129.4, 131.8, 136.3, 137.0.

Scheme V.11, step II: 3-Methyl-1*H*-indole[32]

The product was obtained as an off white solid, mp 92–93 ^{o}C (Lit. mp 91–92 ^{o}C).

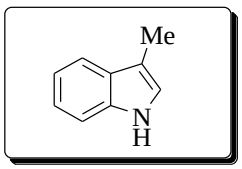

^{1}H NMR ($CDCl_3$, 300 MHz): 2.34 (d, *J* = 0.9 Hz, 3H), 6.96 (d, *J* = 0.9 Hz, 1H), 7.09-7.21 (m, 2H), 7.32-7.36 (m, 1H), 7.86 (br s, 1H).

^{13}C NMR ($CDCl_3$, 75 MHz): δ/ppm 9.6, 110.9, 111.7, 118.8, 119.1, 121.5, 121.8, 128.3, 136.3.

^{1}H NMR spectra of 3-Methyl-1*H*-indole in $CDCl_3$

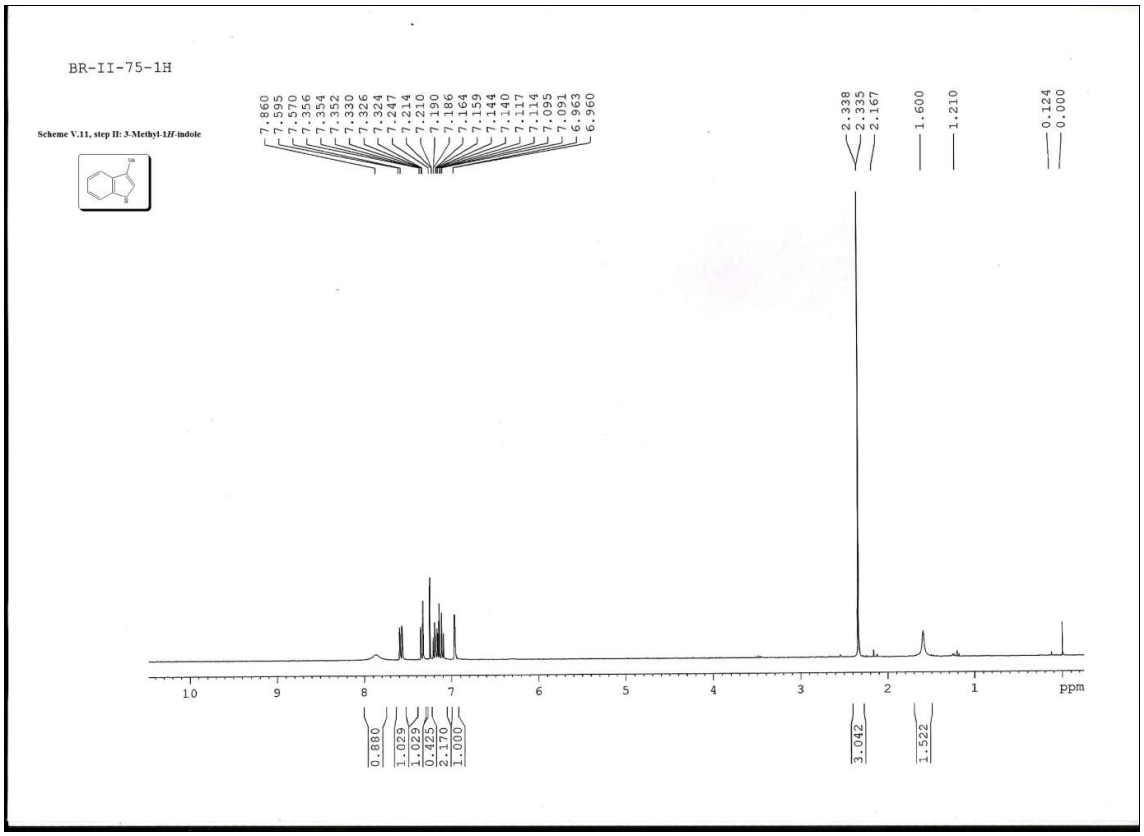

^{13}C NMR spectra of 3-Methyl-1*H*-indole in $CDCl_3$

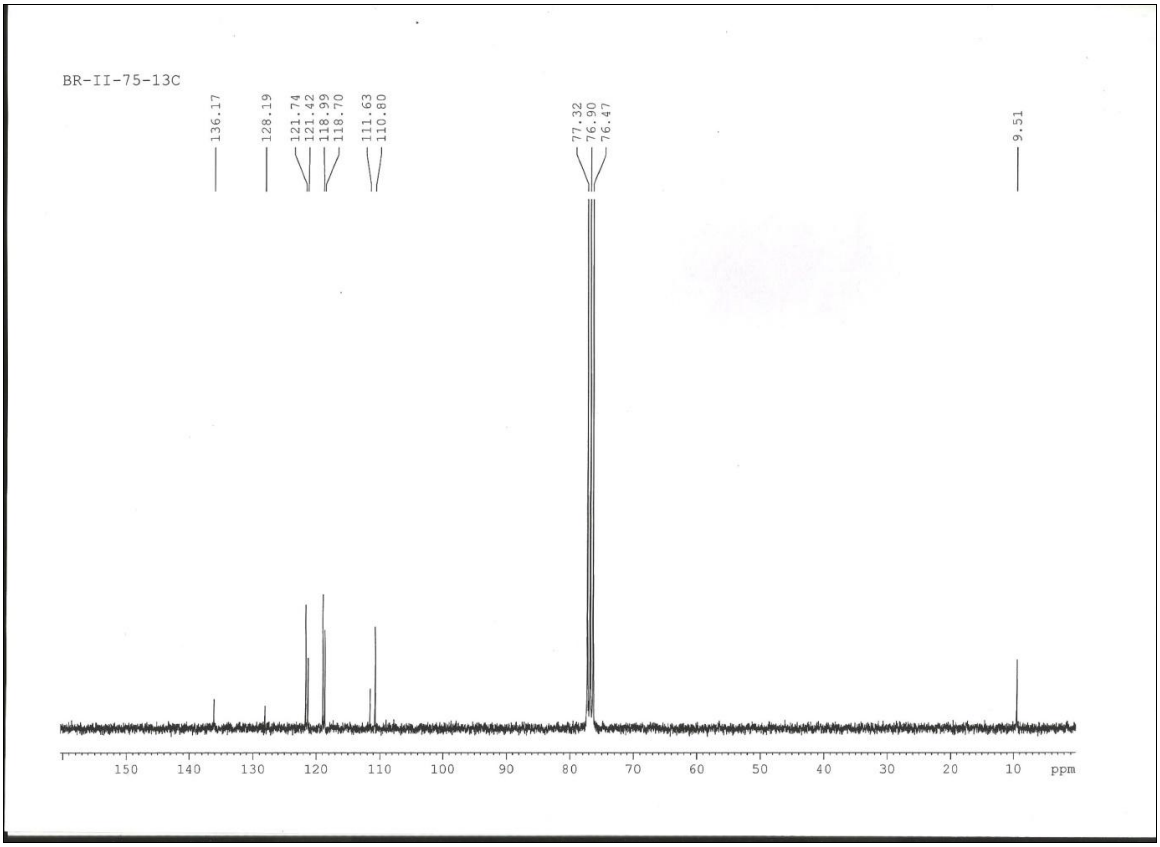

V.6. References

References are given in **BIBLIOGRAPHY** under **CHAPTER V** (pp. 186−190***)***

BIBLIOGRAPHY

CHAPTER I

1. (a) M. Lancaster, *Green Chemistry: An Introductory Text*, 2nd edition, RSC, Cambridge CB40WF, UK; (b) P. T. Anastas and J. C. Warner, *Green Chemistry: Theory and Practice*, Oxford Science Publications, New York, NY, USA, 1998; (c) P. T. Anastas and T. Williamson, *Green Chemistry: Frontiers in Benign Chemical Synthesis and Procedures*, Oxford Science Publications, New York, NY, USA, 1998.
2. (a) M. Lebl, *Biopolymers*, 1998, **47**, 397; (b) N. J. Maeji, R. M. Valerio, A. M. Bray, R. A. Campbell and H. M. Geysen, *React. Polym*., 1994, *22*, 203; (c) N. Hird, I. Hughes, D. Hunter, M. G. J. T. Morrison, D. C. Sherrington and L. Stevenson, *Tetrahedron*, 1999, **55**, 9575–9584.
3. (a) R. C. D. Brown, *J. Chem. Soc., Perkin Trans.* 1, 1998, 3293–3320; (b) E. K. Smith, *Solid Supports and Catalyst in Organic Synthesis*, Ellis Horwood, Chichester, UK, 1992; (c) *Solid-Phase Organic Synthesis*; Burgess, K., Ed.; Wiley-Interscience: New York**,** 2000; (d) *Solid-Phase Synthesis: a Practical Guide*; Kates, S. A. and Albericio, F.; Marcel Dekker, Inc.: New York, 2000.; (e) J. H. Clark, A. P. Kybett, and D. J. Macquarrie, *Supported Reagents: Preparation, Analysis and Applications*, VCH, New York, NY, USA, 1992.
4. R. B. Merrifield, *J. Am. Chem. Soc*., 1963, **85**, 2149–2154.
5. (a) K. S. Novoselov, A. K. Geim, S. V. Morozov, D. Jiang, Y. Zhang, S. V. Dubonos, I. V. Grigorieva and A. A. Firsov, *Science*, 2004, **306**, 666–669; (b) K. S. Novoselov, A. K. Geim, S. V. Morozov, D. Jiang, M. I. Katsnelson, , I. V. Grigorieva, S. V. Dubonos, A. A. Firsov, *Nature*, 2005, **438**, 197−200.
6. (a) S. Navalon, A. Dhakshinamoorthy, M. Alvaro, H. Garcia, *Chem.Rev.*, 2014, **114**, 6179–6212; (b) C. Su and K. P. Loh, Carbocatalysts: Graphene Oxide and Its Derivatives. *Acc.Chem. Res.*, 2012, **46**, 2275–2285; (c) R. Jana, T. P. Pathak, M. S. Sigman, *Chem. Rev*., 2011, **111**, 1417−1492; (d) J. P. Rourke, P. A. Pandey, , J. J. Moore, M. Bates, I. A. Kinloch, R. J. Young, N. R. Wilson, *Angew. Chem. Int. Ed.* 2011, **50**, 3173−3177.

7. (a) P. T. Anastas and R. H. Crabtree, *Handbook of Green Chemistry, Green Catalysis, Homogeneous Catalysis*, John Wiley & Sons, Weinheim, Germany, 2014, Vol-1, 431 pages; (b) B. M. Trost, *Angew. Chem. In. Ed. Engl.*, 1995, **34**, 259–281.
8. (a) J. R. H. Ross, *Heterogeneous Catalysis*, 2012, Elsevier, Oxford OX5 1GB, UK, 232 pages; (b) *Handbook of Green Chemistry, Volume 2: Heterogeneous Catalysi;* R. H. Crabtree, 2009, WILEY-VCH Verlag GmbH & Co. KGaA, Weinheim.
9. (a) P. Serp and J. L. Figueiredo, *Carbon Materials for Catlysis*, 2009 by John Wiley & Sons, Inc., Hoboken, New Jersey, pp-579; (b) E. Lam and J.H.T. Luong, *ACS Catal.*, 2014, **4**, 3393–3410.
10. R. S. Kalhapure , M. K. Kathiravan1 , K. G. Akamanchi , and T. Govender, *Pharm Dev Technol*, 2013, 1–19.
11. D. Zhao, Y. Wan, and W. Zhou, *Ordered Mesoporous Materials***, 2013**, Wiley-VCH Verlag & Co. KGaA Boschstr. 12, 69469 Weinheim, Germany.
12. A.B.D. Nandiyanto, S-G Kim, F. Iskandar and K. Okuyama, "*Microporous Mesoporous Mater.*, 2009, **120**, 447–453.
13. Y. Xia and R. Mokaya, *J. Mater. Chem.*, 2003, **13**, 3112–3121
14. Xu, B., J. Long, H. Tian, Y. Zhu and X. Sun, *Catal. Today*, 2009, **147S**, S46–S50.
15. J. Chen, N. Xia, T. Zhou, S. Tan, F. Jiang and D. Yuan, *Int. J. Electrochem. Sci*., 2009, **4**, 1063–1073.
16. Y. Rao and D. M. Antonelli, *J. Mater. Chem.*, 2009, **19**, 1937–1944.
17. Y. Chen, Y. Huang, J. Xiu, X. Han and X. Bao, *Applied Catalysis A: General*, 2004, **273**, 185–191.
18. T. Tatsumi, K.A. Koyano, Y. Tanaka and S. Nakata, *J Porous Mat.*, 1999, **6**, 13–17.
19. R.K. Iler, "*The Chemistry of Silica: Solubility, Polymerization, Colloid and Surface Properties, and Biochemistry",* Wiley-Interscience, New York, 1979.
20. L.T. Zhuravlev, *Colloids Surf. A Physicochem. Eng. Asp.*, 2000, **173**, 1–38.
21. P.K. Jal, S. Patel and B.K. Mishra, *Talanta*, 2004, **62**, 1005–1028.
22. (a) X.-D. Yang, X.-H. Zeng, Y.-H. Zhao, X.-Q. Wang, Z.-Q. Pan, L. Li, and H.-B. Zhang, *J. Comb. Chem.*, 2010, **12**, 307–310; (b) G.-X. Wan, L. Xu, X.-S. Ma and N. Ma, *Tetrahedron Lett.*, 2011, **52**, 6250–6254; (c) A. Ojeda-Porras, A. Hernandez-Santana and D. Gamba-Sanchez, *Green Chem.*, 2015, **17**, 3157-3163; (d) H. Firouzabadi, N. Iranpoor, M. Jafarpour and A. Ghaderi, *J. Mol. Catal. A: Chem.*, 2006, **249**, 98–102.

23. H. Shinohara, M. Sonoda, N. Hayagane, S. Kita, S. Tanimori, and A. Ogawa, *Tetrahedron Lett*., 2014, **55**, 5302–5305.
24. J. Chen, N. Xia, T. Zhou, S. Tan, F. Jiang and D. Yuan, *Int. J. Electrochem. Sci*., 2009, **4**, 1063–1073.
25. C. Vartuli, W. J. Roth and T. F. Degnan, Jr., in *Dekker Encyclopedia of Nanoscience and Nanotechnology*, Marcel Dekker, 2004, 1797–1811.
26. B. Zhang, , X. Tang, Y. Li, Y. Xu and W. Shen, *Int. J. Hydrogen Energ.*, 2007, **32**, 2367–2373.
27. A. Corma, A. Martínez, V. Martínez-Soria and J. B. Montón, *J. Catal*., 1995, **153**, 25–31.
28. J. Rathousky, A. Zukai, O. Franke and G. Schulz-Ekloff, *J. Chem. Soc., Faraday Trans*., 1995, **91**, 937–940.
29. J. M. Kim, J. H. Kwak, J. Shinae and J. R. Ryoo, *J. Phys. Chem*.,1995, **99**, 16742–16747.
30. X. Feng, G. E. Fryxell, L.-Q. Wang, A. Y. Kilm, J. Liu and K. M. Kemner, *Science*, 1997, **276**, 923–926.
31. Q.S. Huo, D.I. Margolese, U. Ciesla P.Y. Feng, T.E. Gier, P. Sieger, R. Leon, P.M. Petroff, F. Schuth and G. D. Stucky, *Nature*, 1994, **368**, 317–321.
32. (a) C. T. Kresge, M. E. Leonowicz, W. J. Roth, J. C. Vartuli and J. S. Beck, *Nature*, 1992, **359**, 710–712; (b) J. S. Beck, J. C. Vartuli, W. J. Roth, M. E. Leonowicz, C. T. Kresge, K. D. Schmitt, C. T. W. Chu, D. H. Olson, E. W. Sheppard, S. B. McCullen, J. B. Higging and J. L. Schlenker, *J. Am. Chem. Soc*., 1992, **114**, 10834–10843.
33. (a) D. Zhao, Q. Huo, J. Feng, B.F. Chmelka and G.D. Stucky, *J. Am. Chem. Soc*., 1998, **120**, 6024–6036; (b) M. Mesa, L. Sierra and J. L. Guth, *Microporous. Mesoporous. Mater*., 2008, **112**, 338–350.
34. N. Rahmat, A. A. Zuhairi and A. Rahman Mohamed, *Am. J. Appl. Sci*, 2010, **7**, 1579–1586.
35. D. Zhao, J. Feng, Q. Huo, N. Melosh, G. H. Fredrickson, B. F. Chmelka and G. D. Stucky, *Science*, 1998, **279**, 548–552.
36. D. Zhao, J. Sun, Q. Li and G. D. Stucky, *Chem. Mater*., 2000, **12**, 275–279.
37. T. Klimova, A. Esquivel, J. Reyes, M. Rubio, X. Bokhimi and J. Aracil, *Microporous Mesoporous Mater*., 2006, **93**, 331–343.

38. W. Zhao, J. Gu, L. Zhang, H. Chen and J. Shi, *J. Am. Chem. Soc.*, 2005, **127**, 8916–8917.
39. X. Wang, K. S. K. Lin, J. C. C. Chan and S. Cheng, *J. Phys. Chem. B*, 2005, **109**, 1763–1769.
40. S. A. Quintella, R. M. A. Saboya, D. C. Salmin, D. S. Novaes, A. S. Araujo, M. C. G. Albuquerque and C. L. Cavalcante, *Jr. Renew. Energy*, 2012, **38**, 136–140.
41. M. Guan, W. Liu, Y. Shao, H. Huang and H. Zhang, *Microporous Mesoporous Mater.*, 2009, **123**, 193–201.
42. A. Katiyar, S. Yadav, P. G. Smirniotis, N. G. Pinto, *J. Chromatogr. A.*, 2006, **1122**, 13–20.
43. A. Salis, M. S. Bhattacharyya and M. Monduzzi, *J. Phys. Chem. B*, 2010, **114**, 7996-8001.
44. V.S. Lin, C.Y. Lai, J. Huang, S.A. Song and S. Xu, *J. Am. Chem. Soc*., 2001, **123**, 11510–11511.
45. Y. Li, G. Zhou, C. Li, D. Qin, W. Qiao and B. Chu, *Colloids Surf. A*, 2009, **341**, 79–85.
46. L. B. Fagundes, T. G. F. Sousa, A. Sousa, V. V. Silva and E. M. B. Sousa, *J. Non-Cryst. Solids*, 2006, **352**, 3496–3501.
47. A. Sousa, D. Maria, R. Sousa and E. Sousa, *J. Mater. Sci.*, 2010, **45**, 1478–1486.
48. J. Zhao, F. Gao, Y. Fu, W. Jin, P. Yang and D. Zhao, *Chem. Commun.*, 2002, 752–753.
49. T. Yasmin and K. Muller, *J. Chromatogr. A*, 2011, **1218**, 6464–6475.
50. X. Liu, L. Li, Y. Du, Z. Guo, T.T. Ong, Y. Chen, S.C. Ng and Y. Yang, *J. Chromatogr. A*, 2009, **1216**, 7767–7773.
51. D.R. Dreyer, H. P. Jia and C.W. Bielawski, *Angew. Chem. Int. Ed. Engl*., 2010, **49**, 6813–6816.
52. H.P. Boehm, R. Setton and E. Stumpp, *Pure Appl. Chem.*, 1994, **66**, 1893–1901.
53. (a) K. S. Novoselov, A. K. Geim, S. V. Morozov, D. Jiang, Y. Zhang, S. V. Dubonos, I. V. Grigorieva and A. A. Firsov, *Science*, 2004, **306**, 666–669; (b) A. K. Geim and K. S. Novoselov, *Nat. Mater.*, 2007, **6**, 183–191
54. (a) P. Avouris, C. Dimitrakopoulos, *Mater. Today*, 2012, **15**, 86–97; (b) C. Chung, Y.-K. Kim, D. Shin, S.-R. Ryoo, B. H. Hong, D.-H. Min, *Acc. Chem. Res.*, 2013, **46**,

2211–2224; (c) Y. Zhu, S. Murali, W. Cai, X. Li, J.W. Suk , J.R. Potts, R. S. Ruoff, *Adv. Mater.*, 2010, **22**, 3906–3924.

55. A. A. Balandin, S. Ghosh, W. Bao, I. Calizo, D. Teweldebrhan, F. Miao and C. N. Lau, *Nano Lett*., 2008, **8**, 902–907.
56. C. Lee, X. D. Wei, J. W. Kysar and J. Hone, *Science*, 2008, **321**, 385–388.
57. M. D. Stoller, S. Park, Y. Zhu, J. and R. S. Ruoff, *Nano Lett.*, 2008, **8**, 3498–3502.
58. B. Jayasena and S. Subbiah, *Nanoscale Res. Lett.*, 2011, **6**, 95–101.
59. Z.G. Cambaz, G. Yushin, S. Osswald, V. Mochalin, Y. Gogotsi, *Carbon*, 2008, **46**, 841–849.
60. K. Subrahmanyam, L. Panchakarla, A. Govindaraj and C. Rao, *J. Phys.Chem.C*, 2009, **113**, 4257–4259.
61. C. K. Chua and M. Pumera, *Chem. Soc. Rev.*, 2014, **43**, 291–312
62. A. Krishnan, E. Dujardin, M. Treacy, J. Hugdahl, S. Lynum, T. Ebbesen, *Nature*, 1997, **388**, 451–454.
63. (a) S. Stankovich, D. Dikin, G. Dommett, K. Kohlhaas, E. Zimney and E. Stach, *Nature*, 2006, **442**, 282–286; (b) G. Wang, J. Yang, J. Park, X. Gou, B. Wang, H. Liu and J. Yao, *J. Phys. Chem. C*, 2008, **112**, 8192–8195; (c) Z. Fan, K. Wang, T. Wei, J. Yan, L. Song and B. Shao, *Carbon*, 2010, **48**, 1686–1689; (d) Y. Si and E.T. Samulski, *Nano Lett.*, 2008, **8**, 1679–1682; (d) T. Zhou, F. Chen, K. Liu, H. Deng, Q. Zhang, J. Feng, Q. Fu, *Nanotechnology*, 2011, **22**, 045704; (e) X. P. Shen, L. Jiang, Z. Y. Ji, J. L. Wu, H. Zhou and G. X. Zhu, *J. Colloid. Interf. Sci.*, 2011, **354**, 493–497; (f) S. Zhang, Y. Shao, H. Liao, M.H. Engelhard, G. Yin, Y. Lin, *ACS Nano*., 2011, **5**, 1785–1791; (g) J. Che, L. Shen and Y. Xiao, *J. Mater. Chem.* 2010, **20**, 1722–1727; (h) W. B. Wan, Z. B. Zhao, H. Hu, Q. Zhou, Y. R. Fan, J. S. Qiu, *New Carbon Mater.*, 2011, **26**, 16–20; (i) K. Ai, Y. Liu, L. Lu, X. Cheng, L. Huo, *J. Mater. Chem.*, 2011, **21**, 3365–3370.
64. (a) M. Agharkar, S. Kochrekar, S. Hidouri and M. A. Azeez, *Mater. Res. Bull*., 2014, **59**, 323–328; (b) M. T. H. Aunkora, I. M. Mahbubulb, R. Saidurb and H. S. C. Metselaara, *RSC Adv*., 2016, **6**, 27807–27828.
65. Y. Cao, X. Luo, H. Yu, F. Peng, H. Wanga and G. Ning, *Catal. Sci. Technol*, 2013, **3**, 2654–2660.
66. J. Long, X. Xie, J. Xu, Q. Gu, L. Chen, and X. Wang, *ACS Catal.*, 2012, **2**, 622−631.

67. J.-H. Yang, G. Sun, Y. Gao, H. Zhao, P. Tang, J. Tan, A.- H. Lu and D. Ma, *Energy Environ. Sci.*, 2013, **6**, 793–798.
68. X. Zhang, X. Ji, R. Su, B. L. Weeks, Z. Zhang, and S. Deng, *ChemPlusChem*, 2013, **78**, 703–711.
69. L.-S. Bai, X.-M. Gao, X. Zhang, F.-F. Sun and N. Ma, *Tetrahedron Lett.*, 2014, **55**, 4545–4548.
70. E. Lam, J. H. Chong, E. Majid, Y. Liu, S. Hrapovic, A. C. W. Leung and J. H. T. Luong, *Carbon*, 2012, **50**, 1033–1043.
71. M. Wang, X. Song and N. Ma, *Catal Lett*., 2014, **144**, 1233–1239.
72. X. Sun, W. Wang, T. Wu, H. Qiu, X. Wang and J. Gao, *Mater. Chem. Phys*., 2013, **138**, 434–439.
73. L. Tan, B. Wang and H. Feng, *RSC Adv.*, 2013, **3**, 2561–2565.
74. Y. Gao, D. Ma, C. Wang, J. Guan and X. Bao, *Chem. Commun*., 2011, **47**, 2432–2434.
75. B. C. Brodie, *Philos. Trans. R. Soc. London*, 1859, **149**, 249–259.
76. L. Staudenmaier, *Ber. Dtsch. Chem. Ges*., 1898, **31**, 1481–1487.
77. U. Hofmann and E. Konig, *Z. Anorg. Allg. Chem*., 1937, **234**, 311–336.
78. W. S. Hummers Jr. and R. E. Offeman, *J. Am. Chem. Soc*., 1958, **80**, 1339.
79. D. C. Marcano, D. V. Kosynkin, J. M. Berlin, A. Sinitskii, Z. Sun, A. Slesarev, L. B. Alemany, W. Lu and J. M. Tour, *ACS Nano*, 2010, **4**, 4806–4814.
80. C. K. Chua, Z. Sofer and M. Pumera, *Chem. Eur. J.*, 2012, **18**, 13453–13459.
81. T. Szabo, E. Tombacz, E. Illes and I. Dekany, *Carbon*, 2006, **44**, 537.
82. V. Georgakilas, *Functionalization of Graphene*, 2014, Wiley-VCH Verlag GmbH & Co., Weinheim; Germany.
83. T. Szabo, O. Berkesi, P. Forgo, K. Josepovits, Y. Sanakis, D. Petridis and I. Dekany, *Chem. Mater.*, 2006, **18**, 2740–2749.
84. W. Scholz and H. P. Boehm, Z. *Anorg. Allg. Chem*., 1969, **369**, 327–340.
85. U. Hofmann and R. Holst, *Ber. Dtsch. Chem. Ges. B*, 1939, **72**, 754–771.
86. T. Nakajima and Y. Matsuo, *Carbon*, 1994, **32**, 469–475.
87. G. Ruess, Monatsh. Chem., 1946, **76**, 381–417.
88. A. Lerf, H. He, M. Forster and J. Klinowski, J. Phys. Chem. B, 1998, **102**, 4477–4482.

89. (a) D. R. Dreyer and C. W. Bielawski, *Chem. Sci*., 2011, **2**, 1233–1240; (b) D. R. Dreyer, R. S. Ruoff and C. W. Bielawski, *Angew. Chem., Int. Ed.*, 2010, **49**, 9336–9344.
90. A. V. Kumar and K. R. Rao, *Tetrahedron Lett*., 2011, **52**, 5188–5191.
91. H. Wang, T. Deng, Y. Wang, X. Cui, Y. Qi, X. Mu, X. Hou and Y. Zhu, *Green Chem.*, 2013, **15**, 2379–2383.
92. (a) D. R. Dreyer and C. W. Bielawski, *Adv. Funct. Mater*., 2012, **22**, 3247–3253; (b) D. R. Dreyer, K. A. Jarvis, P. J. Ferreira and C. W. Bielawski, *Polym. Chem*., 2012, 3, 757–766; (c) D. R. Dreyer, K. A. Jarvis, P. J. Ferreira and C. W. Bielawski, *Macromolecules*, 2011, **44**, 7659–7667.
93. R. Arshady, *Colloid Polym. Sci*., 1992, **270**, 717–732.
94. E. Bayer, B. Hemmasi, K. Albert, W. Rapp, and M. Dengler, *Peptides, in Proceedings of the Eighth American Peptide Symposium,* 1983, (eds V.J. Hruby and D.H. Rich), Pierce , Rockford, Illinois , pp. 87–90.
95. E. Atherton and R. C. Sheppard, "*Solid Phase Peptide Synthesis: A Practical Approach",* 1989, IRL Press, Oxford.
96. M. Meldal, *Tetrahedron Lett.*, 1992, **33**, 3077–3080.
97. M. Kempe and G. Barany, *J. Am. Chem. Soc.*, 1996, **118**, 7083–7093.
98. S. Cote, *New Polyether Based Monomers, Crosslinkers, and Highly ´ Crosslinked Amphiphile Polyether Resins*. PCT Int. Appl. 2005, WO 2005012277 A1 20050210 CAN 142: 198979 AN 2005: 120909.
99. F. García-Martín , M. Quintanar-Audelo , Y. García-Ramos , L. J. Cruz , C. Gravel , R. Furic , S. Côté , J. Tulla-Puche , and F. Albericio, *J. Comb. Chem.*, 2006, **8**, 213–220.
100. F. García-Martín, P. White, R. Steinauer, S. Côté, J. Tulla-Puche and F. Albericio, *Biopolymers*, 2006, **84**, 566–575.
101. S. Frutos, J. Tulla–Puche, F. Albericio and E. Giralt, *Int. J. Pept. Res. Ther.*, 2007, **13**, 221–227.
102. D. C. Sherrington, *Chem. Commun.*, 1998, 2275–2286. (b) F. Z. Dörwald, in *Organic Synthesis on Solid Phase*, Wiley-VCH Verlag GmbH, Weinheim, Germany, 2000, pp. 19.
103. L. Sinigoi, P. Bravin, C. Ebert, N. D'Amelio, L. Vaccari, L. Ciccarelli, S. Cantone, A. Basso and L. Gardossi, *J. Comb. Chem.*, 2009, **11**, 835–845.

104. R. Kunin, E. Meitzner and N. Bortnick, *J. Am. Chem. Soc.*, 1962, **84**, 305–306.
105. J. R. Millar, D. G. Smith, W. E. Marr and T. R. E. Kressman, *J. Chem. Soc*., 1963, 218–225.
106. M. T. Gokmen and F. E. Du Prez, *Prog. Polym. Sci.*, 2012, **37**, 365–405.
107. B. A. Adams and E. L. Holmes, *J. Soc. Chem. Ind*., 1935, **54**, 1–6.
108. D. Astruc, *Nanoparticles and Catalysis*, Wiley-VCH, Weinheim, Germany, 2008.
109. S. Kobayashi and R. Akiyama, *Chem. Commun.*, 2003, no. 4, 449–460.
110. D. Sengupta and B. Basu, *Tetrahedron Lett.*, 2013, **54**, 2277–2281.
111. (a) M. Bandini, M. Fagioli and A. Umani-Ronchi, *Adv. Synth. Catal*., 2004, **346**, 545–548; (b) B. Das and N. Chowdhury, *J. Mol. Catal. A*: *Chem*., 2007, **263**, 212–215; (c) L. Wu, C. Yang, C. Zhang and L. Yang, *Bull. Korean Chem. Soc*., **2009**, **30**, 1665–1666; (d) M. Vijender, P. Kishore, P. Narender and B. Satyanarayana, *J. Mol. Catal. A*: *Chem*., 2007, **266**, 290–293; (e) T. K. Mandal, R. Pal, R. Mondal and A. K. Mallik, *E-J. Chem*., 2011, **8**, 863–869; (f) B. Das and J. Banerjee, *Chem. Lett*., 2004, **33**, 960–961; (g) S. Ko, C.-F. Yao, *Tetrahedron Lett.*, 2006, **47**, 8827–8829; (h) J.-J. Young, L.-J.; Jung, K.-M. Cheng, *Tetrahedron Lett*., 2000, **41**, 3415–3418.
112. (a) B. Basu, M. M. H. Bhuiyan, P. Das, and I. Hossain, *Tetrahedron Lett.*, 2003, **44**, 8931–8934; (b) B. Basu, P. Das, and S. Das, *Mol. Divers.*, 2005, **9**, 259–262.
113. (a) B. Basu, S. Das, P. Das, B.Mandal, D. Banerjee, and F. Almqvist, *Synthesis*, 2009, 1137–146; (b) D. Sengupta, J. Saha, G. De and B. Basu, *J. Mater. Chem. A*, 2014, **2**, 3986–3992.
114. D. Sengupta and B. Basu, *Org Med Chem Lett.*, 2014, 4:17.
115. B. Basu, S. Das, S.Kundu and B. Mandal, *Synlett*, 2008, 255–259.

CHAPTER II

1. (a) R. Ballini, Ed. *Eco-friendly Synthesis of Fine Chemicals;* RSC Publishing: Cambridge, 2009; pp. 275–292; (b) N. Winterton, *Chemistry for Sustainable Technologies;* RSC Publishing: Cambridge, 2010; (c) P. J. Dunn, A. Well, M. T. Williams, Eds. *Green Chemistry in the Pharmaceutical Industry*;Wiley-VCH: Weinheim, 2010; (d) W. Zhang and B. W Cue, Eds. *Green Techniques for Organic Synthesisand Medicinal Chemistry;* Wiley: Chichester, 2012; pp 69–97; (e) M. Lancaster, *Green Chemistry: An Introductory Text;* RSC Publication: Cambridge, 2002, p-84.

2. J. Lu and P. H. Toy, *Chem. Rev.*, 2009, **109**, 815–838.
3. (a) J. O. Metzger, *Angew. Chem. Int. Edi.*, 1998, **37**, 2975–2978; (b) K. Tanaka, *Solvent-Free Organic Synthesis*, Wiley-VCH GmbH & Co. KGaA, Weinheim, Germany, 2003; (c) R. S. Varma, *Green Chem.*, 1999, **1**, 43–55.(d) K. Wilson and J. H. Clark, *Pure and Applied Chemistry*, 2000, **72**, 1313–1319.
4. (a) B. C. Ranu, S. Bhar, R. Chakroborty, S. R. Das, M. Saha, A. K. Sarkar, R. Chakroborty and D. C. Sarkar, *J. Indian, Inst. Sci.*, 1994, **74**, 15-33; (b) A. K. Banerjee, M. S. Laya Mimo' and W. J. Vera Vegas, *Russ.Chem. Rev.*, 2001, **70**, 971-990.
5. V. A. Basiuk, Russ. *Chem. Rev.*, 1995, **64**, 1003–1019.
6. R. J. Cremlyn, *An Introduction to Organosulfur Chemistry*, Wiley & Sons, New York, 1996.
7. (a) M. E. Peach, *Thiols As Nucleophiles*, In *The Chemistry of the Thiol Group*, ed. S. Patai, John Wiley & Sons, London, 1979, pp. 721; (b) J. Granifo, M.T. Garl, and R. Baggigo, *Inorg. Chim. Acta*, 2003, **348**, 263–270; (c) A. Montaño, M. V. Beato, F. Mansilla and F. Orgaz, *J. Agric. Food Chem.*, 2011, **59**, 1301–1307; (d) C.-R. Jan, H.-R. Lo, C.-Y. Chen and S.-Y. Kuo, *J. Nat.Prod.*, 2012, **75**, 2101–2107; (e) J. Srogl, W. Liu, D. Marshall and L. S. Liebeskind, *J. Am. Chem. Soc.*, 1999, **121**, 9449–9450; (f) C.-N. Huang, J.-S. Horng and M.-C. Yin, *J. Agric. Food Chem.*, 2004, **52**, 3674; (g) A. Daemmrich and E. M. Bowden, *Chem. Eng. News*, 2005, **83**, 28–42.
8. (a) Y. Oudart, V. Artero, J. Pécaut and M. Fontecave, *Inorg. Chem.*, 2006, **45**, 4334–4336; (b) R. Kannan, N. Pillarsetty, H. Gali, J. T. Hoffman and L. C. Barnes, *Inorg. Chem.*, 2011, **50**, 6210–6219; (c) M. Knorr, F. Guyon, A. Khatyr, C. Strohmann, M. Allain, M. S. Aly, A. Lapprand, D. Fortin and D. P. Harvey, *Inorg. Chem.*, 2012, **51**, 9917–9934; (d) J.-R. Li, X.-H. Bu, J. Jiao, W.-P. Du, X.-H. Xu and R.-H. Zhang, *Dalton Trans.*, 2005**,** 464–474; (e) W.Levason, G. Reid, and W. Zhang, *Dalton Trans.*, 2011, **40**, 8491–8506; (f) M. O. Awaleh, A. Badia, F. Brisse and X.-H. Bu, *Inorg. Chem.*, 2006, **45**, 1560–1574.
9. (a) J. Shearer, P. Soh and S. Lentz, *J. Inorg. Biochem.*, 2008, **102**, 2103–2113; (b) E. I. Solomon, R. K. Szilagyi, S. D. George and L. Basumallick, *Chem. Rev.*, 2004, **104**, 419–458; (c) S. T. Prigge, B. A. Eipper, R. E. Mains and L. M. Amzel, *Science*, 2004, **304**, 864–867; (d) T. Osako, Y. Ueno, Y. Tachi and S. Itoh, *Inorg. Chem.*, 2004, **43**, 6516–6518; (e) G. Y. Park, Y. Lee, D.-H. Lee, J. S. Woertink, A. A. N. Sarjeant, E. I.

Solomon and K. D. Karlin, *Chem. Commun.*, 2010, **46**, 91–93; (f) N. W. Aboelella, B. F. Gherman, L. M. R. Hill, J. T. York, N. Holm, V. G.Young Jr., C. J. Cramer and W. B. Tolman, *J. Am. Chem. Soc.*, 2006, **128**, 3445–3458.

10. a) R. H. Holm, P. Kennepohl and E. I. Solomon, *Chem. Rev.*, 1996, **96**, 2239–2314; (b) K. Paraskevopoulos, M. Sundararajan, R. Surendran, M. A. Hough, R. R. Eady, I. H. Hillier and S. S. Hasnain, *Dalton Trans.*, 2006, 3067–3076.
11. (a) L. A. Finney and T. V. O'Halloran, *Science*, 2003, **300**, 931–936; (b) A. V. Davis and T. V. O'Halloran, *Nat. Chem. Biol.*, 2008, **4**, 148–151.
12. A. Cohen, A. Yeori, I. Goldberg and M. Kol, *Inorg. Chem.*, 2007, **46**, 8114–8116.
13. S. Poulain, S. Julien and E. Dunach, *Tetrahedron Lett.*, 2005, **46**, 7075–7077.
14. B. Lian, K. Beckerle, P. T. Spaniol and J. Okuda, *Angew. Chem. Int. Ed*., 2007, **46**, 8507–8510.
15. M. Dieguez, A. Ruiz, C. Claver, M. M. Pereira and M. R. A. Gonsalves, *J. Chem. Soc., Dalton Trans*., 1998, 3517–3522.
16. M. Knorr, F. Guyon, A. Khatyr, C. Daschlein, C. Strohmann, M. S. Aly, S. A. Abd-El-Aziz, D. Fortin and D. P. Harvey, *Dalton Trans.*, 2009, 948–955.
17. (a) A. Ishii, T. Toda, N. Nakata and T. Matsuo, *J. Am. Chem. Soc*., 2009, **131**, 13566–13567; (b) M. G. Meppelder, K. Beckerle, R. Manivannan, B. Lian, G. Raabe, P. T. Spaniol and J. Okuda, *Chem. Asian J.*, 2008, **3**, 1312–1323; (c) T. Kondo and T. Mitsudo, *Chem. Rev.*, 2000, **100**, 3205–3220.
18. Z. Jin, B. Xu and B. G. Hammond, *Eur. J. Org. Chem*., 2010, 168–173.
19. D. P. Curran, In *Comprehensive Organic Synthesis*, Vol. 4; B. M. Trost, I. Fleming, Eds.; Pergamon: New York, 1991, p. 715.
20. (a) T. Posner, Chem. *Ber*., 1905, **38**, 646–657; (b) C. G. Screttas and M. Micha-Screttas, *J. Org. Chem*., 1979, **44**, 713–719; (c) F. Wolf and H. *Z.* Finke, *Chem*., 1972, **12**, 180–181.
21. (a) T. Mukaiyama, T. Izawa, K. Saigo and H. Takai, *Chem. Lett*., 1973, 355–356; (b) M. Belley, R. Zamboni, *J. Org.Chem*., **1**989, **54**, 1230–1232.
22. H. J. Cristau, B. Chabaud, R. Labaudiniere and H. Christol, *J. Org. Chem*., 1986, **51**, 875–878.
23. T. Kondo, S. Uenoyama, K. Fujita and T. Mitsudo, *J. Am. Chem. Soc*., 1999, **121**, 482–483.

24. S.-i. Usugi, H. Yorimitsu, H. Shinokubo, and K. Oshima, *Org. Lett.*, 2004, **6**, 601–603.
25. H. Kuniyasu, A. Ogawa, S. Miyazaki, I. Ryu, N. Kambe and N. Sonoda, *J. Am. Chem. Soc*., 1991, **113**, 9796–9803.
26. Y. Gareau and A. Orellana, *Synlett*, 1997, 803–804.
27. N. Abidi and J. R. Schmink, *J. Org. Chem.*, 2015, **80**, 4123−4131.
28. N. Yamagiwa, Y. Suto and Y. Torisawa, *Bioorg. Med. Chem. Lett.*, 2007, **17**, 6195–6197.
29. Z. Jin, B. Xu and G. B. Hammond, *Eur. J. Org. Chem.*, **2**010, **2010**, 168–173.
30. S. Banerjee, J. Das, R. P. Alvarez and S. Santra, *New J. Chem.*, 2010, **34**, 302–306.
31. B. Basu, P. Das, and I. Hossain, *Synlett*, 2004, 2630–2632,
32. B. Basu, S. Paul and A. K. Nanda, *Green Chem.*, 2010, **12**, 767–771.
33. B. Basu, S. Paul and A. K. Nanda, *Green Chem.*, 2009, **11**, 1115–1120.
34. B. Basu and S. Paul, *Appl. Organometal. Chem*., 2013, **27**, 588–594.
35. (a) C. E. Hoyle, C. N. Bowman, *Angew. Chem., Int. Ed.*, 2010, **49**, 1540–1573; (b) A. Dondoni, *Angew. Chem., Int. Ed.*, 2008, **47**, 8995–8997.
36. (a) S. Patai, Z. Rappoport and C. Stirling, *The Chemistry of Sulphones and Sulfoxide;* John Wiley & Sons: Chichester, 1988; pp. 17–31. (b) J.-E. Bäckvall, *Modern Oxidation Methods;* Wiley-VCH: Hoboken, NJ, 2011.
37. L. T. Zhuravlev, *Colloids Surf. A*, 2000, **173**, 1–38.
38. J. Liu, D. Feng, G. E. Fryxell, L.-Q. Wang, A. Y. Kim and M. Gong, *Chem. Eng. Technol.*, 1998, **21**, 97–100.
39. J. Park, H. Kim and J. Park, *Int. J. Environ. Sci. Dev.*, 2012**, 3**, 81–85.
40. B. C Ranu, and T. Mandal, *Synlett*, 2007, 925–928.

CHAPTER III

Section A

1. K. S. Novoselov, A. K. Geim, S. V. Morozov, D. Jiang, Y. Zhang, S. V. Dubonos, I. V. Grigorieva and A. A. Firsov, *Science,* 2004, **306**, 666–669.
2. (a) S. Navalon, A. Dhakshinamoorthy, M. Alvaro and H. Garcia, *Chem. Rev*., 2014, **114**, 6179–6212; (b) S. Eigler and A. Hirsch, *Angew. Chem., Int. Ed*., 2014, **53**, 7720–7738; (c) C. Su and K. P. Loh, *Acc. Chem. Res*., 2013, **46**, 2275–2285.

3. (a) Z. H. Tang, S. L. Shen, J. Zhuang and X. Wang, *Angew. Chem., Int. Ed.*, 2010, **49**, 4603−4607; (c) J. R. Potts, D. R. Dreyer, C. W. Bielawski and R. S. Ruoff, *Polymer*, 2011, **52**, 5–25; (d) C. Su, R. Tandiana, J. Balapanuru, W. Tang, K. Pareek, C. T. Nai, T. Hayashi and K. P. Loh,. *J. Am. Chem. Soc.*, 2015, **137**, 685−690; (e) S. Bai and X. Shen, *RSC Advances*, 2012, **2**, 64–98.
4. D. R. Dreyer, H.-P. Jia and C.W. Bielawski, *Angew. Chem., Int. Ed*., 2010, **49**, 6813–6816.
5. T. Szabo, E. Tombacz, E. Illes and I. Dekany, *Carbon*, 2006, **44**, 537–545
6. (a) D. R. Dreyer, H.-P. Jia, A. D. Todd, J. Geng and C. W. Bielawski, *Org. Biomol. Chem*., 2011, **9**, 7292–7295; (b) H.-P. Jia, D. R. Dreyer and C. W. Bielawski, *Tetrahedron*, 2011, **67**, 4431–4434; (c) H.-P. Jia, D. R. Dreyer and C. W. Bielawski, *Adv. Synth. Catal*., 2011, **353**, 528–532.
7. (a) A. V. Kumar and K. R. Rao, *Tetrahedron Lett.*, 2011, **52**, 5188–5191; (b) H. Wang, T. Deng, Y. Wang, X. Cui, Y. Qi, X. Mu, X. Hou and Y. Zhu, *Green Chem.*, 2013, **15**, 2379–2383; (c) A. D. Todd and C. W. Bielawski, *Catal. Sci. Technol*., 2013, **3**, 135–139.
8. (a) C.K. Chua and M. Pumera, *Chem. Eur. J.*, 2015, **21**, 1–14; (b) H. Hu, J. H. Xin, H. Hu, X. Wang and Y. Kong, *App. Catal. A*: *General*, 2015, **492**, 1–9; (c) D. R. Dreyer, C.W. Bielawski, *Chem. Sci*., 2011, **2**, 1233–1240; (d) D. R. Dreyer, H.-P. Jia and C. W. Bielawski, *Angew. Chem. Int. Ed.*, 2010, **49**, 6813–6816; (e) S. Kundu and B. Basu, *RSC Adv.*, 2015, **5**, 50178–50185; (f) B. Roy, D. Sengupta and B. Basu, *Tetrahedron Lett*., 2014, **55**, 6596–6600; (g) D. Sengupta, J. Saha, B. Basu and G. De. *RSC Adv*., 2014, **4**, 35442–35448; (h) A. Dhakshinamoorthy, M. Alvaro, M. Puche, V. Fornes and H. Garcia, *ChemCatChem*., 2012, **4**, 2026–2030.
9. Y. Kim, S. Somez and H. Lee, *Chem. Commun.*, 2013, **49**, 5702–5704.
10. S. Verma, H. P. Mungse, N. Kumar, S. Choudhary, S. L. Jain, B. Sain and O. P. Khatri, *Chem. Commun.*, 2011, **47**, 12673–12675.
11. S. M. S. Chauhan and S. Mishra *Molecules*, 2011, **16**, 7256–7266.
12. B. Basu, S. Kundu and D. Sengupta, *RSC Adv*., 2013, **3**, 22130–22134.
13. S. Kundu and B. Basu, *RSC Adv*., 2015, **5**, 50178–50185.
14. G. Lv, H.Wang, Y.Yang,T. Deng, C. Chen, Y.Zhu, and X. Hou, *ACS Catal.*, 2015, **5**, 5636−5646.

15. (a) D. R. Dreyer and C. W. Bielawski, *Adv. Funct. Mater*., 2012, **22**, 3247–3253; (b) D. R. Dreyer, K. A. Jarvis, P. J. Ferreira and C. W. Bielawski, *Polym. Chem*., 2012, **3**, 757–766; (c) D. R. Dreyer, K. A. Jarvis, P. J. Ferreira and C. W. Bielawski, *Macromolecules*, 2011, **44**, 7659–7667.
16. (a) D. R. Dreyer, A. D. Todd and C.W. Bielawski, *Chem. Soc. Rev.*, 2014, **43**, 5288—5301; (b) S. Eigler, C. Dotzer, F. Hof, W. Bauer, and A. Hirsch, *Chem. Eur. J.* 2013, **19**, 9490–9496.
17. A. Dhakshinamoorthy, M. Alvaro, P.Concepcio´n, V.Forne´s and H. Garcia, *Chem. Commun.*, 2012, **48**, 5443–5445.
18. A. Dhakshinamoorthy, M. Alvaro, M. Puche, V. Fornes, and H. Garcia, *ChemCatChem*, 2012, **4**, 2026–2030.
19. (a) T.W. Greene, P.G.M. Wuts, *Protective Groups in Organic Synthesis, third ed*., Wiley, New York, 1999; (b) H. Kunz, H.Waldmann, in: B.M. Trost, I. Fleming (Eds.), *Comprehensive Organic Synthesis*, vol. 6, Pergamon, New York, 1991, pp. 677–681.
20. (a) E. J. Corey and D. Seebach, *J. Org. Chem.*, 1966, **31**, 4097–4099; (b) D. Seebach, *Synthesis*, 1969, 17–36; (c) B.-T. Grobel and D. Seebach, *Synthesis*, 1977, 357–402; (d) D. Seebach, *Angew. Chem. Int. Ed. Engl.*, 1979, **18**, 239–258; (e) P. C. B. Page, M. B. van Niel, J. Prodger, *Tetrahedron*, 1989, **45**, 7643–7677; (f) P. J. Kocienski, *Protecting Groups*, 3rd ed.; Thieme: Stuttgart, 2004.
21. (a) B. J. Grobel and D. Seebach, *Synthesis*, 1977, 357–402; (b) P. K. Mohanta, S. Perunchralathan, H. Ila and H. Junjappa, *J. Org. Chem.*, 2001, **66**, 1503–1508.
22. (a) Y.-C.Wu, and J. Zhu, *J. Org. Chem.*, 2008, **73**, 9522–9524; (b) R. Varala, S. Nuvula and S. R. Adapa, *Bull. Korean Chem. Soc*., 2006, **27**, 1079–1082; (c) S. K. De, *Adv. Synth. Catal*., 2005, **347**, 673–676; (d) S. K. De, *Tetrahedron Lett*., 2004, **45**, 1035–1036; (e) S. K. De, *Tetrahedron Lett*., 2004, **45**, 2339–2341; (f) N. S. Srivastava, K. Dasgupta and B. K. Banik, *Tetrahedron Lett*., 2003, **44**, 1191–1193; (g) A. Kamal and G. Chouhan, *Tetrahedron Lett*., 2002, **43**, 1341–1350; (h) S. Muthusamy, S. A. Babu and C. Gunanathan, *Tetrahedron*, 2002, **58**, 7897–7901; (i) E. Mondal, P. R. Sahu, G. Bose and A. T. Khan, *Tetrahedron Lett*., 2002, 43, 2843–2846; (j) S. Muthusamy, S. A. Babu and C. Gunanathan, *Tetrahedron Lett*., 2001, **42**, 359–362; (k) H. Firouzabadi, N. Iranpoor and H. Hazarkhani, *J. Org. Chem*., 2001, **66**, 7527–7529; (l) J. S. Yadav, B.V. S. Reddy and S. K. Pandey, *Synlett*

2001, 238–239; (m) B. Karimi and H. Seradj, *Synlett*, 2000, 805–806; (n) H. Firouzabadi, N. Iranpoor and B. Karimi, *Synthesis*, 1999, 58–60; (o) T. Ravindranathan, S. P. Chavan and S. W. Dantale, *Tetrahedron Lett*., 1995, **36**, 2285–2288; (p) P. K. Mandal and S. C. Roy, *Tetrahedron*, 1995, **51**, 7823–7828; (q) V. G. Saraswathy and S. J. Sankararaman, *J. Org. Chem.*, 1994, **59**, 4665–4670; (r) V. Kumar and S. Dev, *Tetrahedron Lett*., 1983, **24**, 1289–1292; (s) B. Burczyk and Z. Kortylewicz, *Synthesis*, 1982, 831–833; (t) B. S. Ong, *Tetrahedron Lett*., 1980, 21, 4225–4228; (u) L. F. Fieser, *J. Am. Chem. Soc*., 1954, **76**, 1945-1947; (v) C. Djerassi and M. Gorman, *J. Am. Chem. Soc*., 1953, **75**, 3704–3708; (x) J. W. Ralls, R. M. Dobson and B. Reigel, *J. Am. Chem. Soc*., 1949, 71, 3320–3325.

23. (a) M. H. Ali and M. G. Gomes, *Synthesis*, 2005, 1326–1332; (b) H. Firouzabadi, N. Iranpoor, A. A. Jafari and M. R. Jafari, *J. Mol. Catal. A: Chem.*, 2006, **247**, 14–18; (c) S. Gogoi, J. C. Borah and N.C. Barua, *Synlett*, 2004, 1592–1594; (d) R. Ballini, G. Bosica, R. Maggi, A. Mazzacani, P. Righi and G. Sartori, *Synthesis*, 2001, 1826–1829; (e) T. Aoyama, T. Takido and M. Kodomar, *Synlett*, 2004, 2307–2310; (f) F. Shirini and J. Albadi, *Bull. Korean Chem. Soc*., 2010, **31**, 1119–1120; (g) D. M. Pore, U. V. Desai, R. B. Mane and P. P. Wadgaonkar, *Indian J. Chem.*, 2006, **45B**, 1291–1295; (h) N. Jung, S. D. Grässle, S. Lütjohann and S. Bräse, *Org. Lett*., 2014, **16**, 1036–1039; (i) B. Shaohu, C. Lu, J. Yongjun, Y. Jianguo, *Chin. J. Chem*., **2010**, **28**, 2119–2121; (j) E. J. Lenardao, E. L. Borges, S. R. Mendes, G. Perin and R. G. Jacob, *Tetrahedron Lett.*, 2008, **49**, 1919–1921.
24. M. Rahimizadeh, T. Bazazan, A. Shiri, M. Bakavoli, H. Hassani, *Chin. Chem. Lett.*, 2011, **22**, 435–438.
25. M. H. Ali and M. G. Gomes, *Synthesis*, 2005, 1326–1332;
26. S. Gogoi, J. C. Borah and N.C. Barua, *Synlett*, 2004, 1592–1594.
27. D. M. Pore, U. V. Desai, R. B. Mane and P. P. Wadgaonkar, *Indian J. Chem.*, 2006, **45B**, 1291–1295.
28. N. Jung, S. Grässle, D. S. Lütjohann, and S. Bräse,*Org. Lett.*, 2014, **16**, 1036−1039.
29. (a) W. S. Hummers, R. E. Offeman, *J. Am. Chem. Soc.*, 1958, **80**, 1339; (b) R. K. Layek, S. Samanta, D. P. Chatterjee and A. K. Nandi, *Polymer*, 2010, **51**, 5846–5856.

30. (a) Q. Zhuo, Y. Ma, J. Gao, P. Zhang, Y. Xia, Y. Tian, X. Sun, J. Zhong and X. Sun, *Inorg. Chem*., 2013, **52**, 3141−3147; (b) A. Dhakshinamoorthy, M. Alvaro, P. Concepcion, V. Fornes and H. Garcia, *Chem. Commun*., 2012, **48**, 5443–5445.
31. (a) L. K. Papernaya, E. P. Levanova, L. V. Klyba and A.I. Albanov, *Russ. J. Org. Chem*., 2009, **45**, 1036–1039; (b) L. K. Papernaya, E. P. Levanova, E. N. Sukhomazova, A. I. Albanov, and E. N. Deryagina, *Russ. J. Org. Chem*, 2005, **41**, 952–955.
32. (a) D. R. Dreyer, A. D. Todd and C.W. Bielawski, *Chem. Soc. Rev.*, 2014, **43**, 5288—5301; (b) S. Eigler, C. Dotzer, F. Hof, W. Bauer, and A. Hirsch, *Chem. Eur. J.* 2013, **19**, 9490–9496.
33. M. Vafaeezadeh, Z. B. Dizicheh and M. M. Hashemi, *Catal. Commun*., 2013, **41**, 96–100.
34. (a) H. Firouzabadi, N. Iranpoor and H. Hazarkhani, *J. Org. Chem*., 2001, **66**, 7527–7529; (b) M. Prato, U. Quintily, G. Scorrano and A. Sturaro, *Synthesis*, 1982, 679–680.
35. P. O'Neill and A. F. Hegarty, *J. Org. Chem.*, 1987, **52**, 2114–2116.
36. (a) S. K. De, *Tetrahedron Lett*., 2004, **45**, 2339–2341; (b) S. Muthusamy, S. A. Babu and C. Gunanathan, *Tetrahedron*, 2002, **58**, 7897–7901.

CHAPTER III

Section B

1. (a) G. Brahmachari, *Green Synthetic Approaches for Bilologically Relevant Heterocycles*; Elsevier: Oxford, 2014; pp 632. (b) J. Alvarez-Builla, J. J. Vaquero and J. Barluenga, *Modern Heterocyclic Chemistry*; John Wiley & Sons: Germany, 2011; Vol. 1, pp 2530.
2. (a) J. A. Pereira, A. M. Pessoa, M. N. D. S. Cordeiro, R. Fernandes, C. Prudencio, J. P. Noronha and M. Vieir, *Eur. J. Med. Chem*., 2014, 1–9; (b) F. A. R. Rodrigues, I. S. Bomfim, B. C. Cavalcanti, C. Ó. Pessoa, J. L. Wardell, S. M. S. V. Wardell, A. C. Pinheiro, C. R. Kaiser, T. C. M. Nogueira, J. N. Low, L. R. Gomes and M. V. N. de Souza, *Bioorg. Med. Chem. Lett.,* 2014, **24**, 934–939; (c) N. S. Hari Narayana Moorthy, E. Manivannan, C. Karthikeyan and P. Trivedi, *Mini-Rev. Med. Chem.*, 2013, **13**, 1415–1420 ; (d) A. K. Parhi, Y. Zhang, K. W. Saionz, P. Pradhan, M. Kaul, K. Trivedi, D. S. Pilch and E. LaVoie, *J. Bioorg. Med. Chem. Lett.*, 2013, **23**,

4968–4974; (e) R. A. Smits, H. D. Lim, A. Hanzer, O. P. Zuiderveld, E. Guaita, M. Adami, G. Coruzzi, R. Leurs and I. J. P. de Esch, *J. Med. Chem.*, 2008, **5**, 2457–2467; (f) F. Rong, S. Chow, S. Yan, G. Larson, Z. Hong and J. Wu, *Bioorg. Med. Chem. Lett*., 2007, **17**, 1663–1666; (g) X. Hui, J. Desrivot, C. Bories, P. M. Loiseau, X. Franck, R. Hocquemiller and B. Figadere, *Bioorg. Med. Chem. Lett.*, 2006, **16**, 815–820; (h) Y. B. Kim, Y. H. Kim, J. Y. Park and S. K Kim, *Bioorg. Med. Chem. Lett.*, 2004, **14**, 541–544; (i) S. T. Hazeldine, L. Polin, J. Kushner, J. Paluch, K. White, M. Edelstein, E. Palomino, T. H. Corbett and J. P. Horwitz, *J. Med. Chem.*, 2001, **44**, 1758–1776.

3. (a) E. D. Brock, D. M. Lewis, T. I. Yousaf and H. H. Harper, *The Procter and Gamble Company*, USA, WO9951688, 1999; (b) A. Katoh, T. Yoshida and J. Ohkanda, *Heterocycles*, 2000, **52**, 911–920.
4. J. Granifo, M. T. Garland and R. Baggio, *Inorg. Chim. Acta*, 2003, **348**, 263–270.
5. S. Dailey, W. J. Feast, R. J. Peace, I. C. Sage, S. Till and E. L. Wood, *J. Mater. Chem.*, 2001, **11**, 2238–2243.
6. J. L. Sessler, H. Maeda, T. Mizuno, V. M. Lynch and H. Furuta, *J. Am. Chem. Soc.*, 2002, **124**, 13474–13479.
7. (a) B. D. Lindner, Y. Zhang, S. Hoefle, N. Berger, C. Teusch, M. Jesper, K. I. Hardcastle, X. Qian, U. Lemmer, A. Colsmann, U. H. F. Bunz and M. Hamburger, *J. Mater. Chem. C*, 2013, **1**, 5718–5724; (b) K. R. J. Thomas, M. Velusamy, J. T. Lin, C.-H. Chuen and Y.-T. Tao, *Chem. Mater*., 2005, **17**, 1860–1866.
8. M. J. Crossley and L. A. Johnston, *Chem. Commun.*, 2002, 1122–1123.
9. B.E. Evans, K.E. Rittle, M.G. Bock, R.M. DiPardo, R.M. Freidinger, W.L. Whitter, G.F. Lundell, D.F. Veber, P.S. Anderson, R.S.L. Chang, V.J. Lotti, D.J. Cerino, T.B. Chen, P.J. Kling, K.A. Kunkel, J.P. Springer and J. Hirshfield, *J. Med. Chem.*, 1988, **31**, 2235–2246.
10. (a) J.A. Ellman and L.A. Thompson, *Chem. Rev.*, 1996, **96**, 555–600; (b) M.A. Gallop, R.W. Barrett, W.J. Dower, S.P.A. Fodor and E.M. Gordon, *J. Med. Chem.*, 1994, **37**, 1233–1251.
11. P. Wipf, A. Cunningham, R.L. Rich and J.S. Lazo, *Bioorg. Med. Chem. Lett.*, 1997, **5**, 165–177.
12. D. R. Dreyer, S. Park, C. W. Bielawski and R. S. Ruoff, *Chem. Soc. Rev.*, 2010, **39**, 228–240.

13. S. Navalon, A. Dhakshinamoorthy, M. Alvaro and H. Garcia, *Chem. Rev.*, 2014, **114**, 6179–6212; (b) C. Su and K. P. Loh, *Acc. Chem. Res.*, 2013, **46**, 2275–2285.
14. (a) S. Kundu and B. Basu, *RSC Adv.*, 2015, **5**, 50178–50185; (b) B. Roy, D. Sengupta and B. Basu, *Tetrahedron Lett*., 2014, **55**, 6596–6600; (c) D. Sengupta, J. Saha, B. Basu and G. De., *RSC Adv*., 2014, **4**, 35442–35448; (d) B. Basu, S. Kundu and D. Sengupta, *RSC Adv.*, 2013, **3**, 22130–22134.
15. (a) Y. V. D. Nageswar, K. H. V. Reddy, K. Ramesh andS. N. Murthy, *Org. Prep. Proc. Int*., 2013, **45**, 1–27; (b) B. Basu and B. Mandal, *Sustainable Synthesis of Benzimidazole, Quinoxaline & Congeners*; Elsevier: Oxford, 2014, Chapter 9; pp 209–252.
16. (a) M. Ayaz, Z. Xu and C. Hulme, *Tetrahedron Lett.*, 2014, **55**, 3406–3409; (b) S. Paul and B. Basu, *Tetrahedron Lett.*, 2011, **52**, 6597–6602; (c) T. K. Huang, R. Wang, L. Shi and X. X Lu, *Catal. Commun.*, 2008, **9**, 1143–1147; (d) C. Srinivas, C. N. S. S. P. Kumar, V. J. Rao and S. Palaniappan, *J. Mol. Catal. A: Chem.*, 2007, **265**, 227–230; (e) H. R. Darabi, S. Mohandessi, K. Aghapoor and F. Mohsenzadeh, *Catal. Commun.*, 2007, **8**, 389–392; (f) S. V. More, M. N. V. Sastry, C. C. Wang and C. F. Yao, *Tetrahedron Lett.*, 2005, **46**, 6345–6348; (g) R. S. Bhosale, S. R. Sarda, S. S. Ardhapure, W. N. Jadhav, S. R. Bhusare and R. P. Pawar, *Tetrahedron Lett.*, 2005, **46**, 7183–7186; (h) Z. Zhao, D. D. Wisnoski, S. E. Wolkenberg, W. H. Leister, Y. Wang and C. W. Lindsley, *Tetrahedron Lett.*, 2004, **45**, 4873–4876.
17. S. K. Singh, P. Gupta, S. Duggineni and B. Kundu, *Synlett*, 2003, 2147–2150.
18. Z.Wu and N. J. Ede, *Tetrahedron Lett.*, 2001, **42**, 8115–8118.
19. V. K. Akkilagunta, V. K. Reddy and R. R. Kakulapati, *Synlett*, 2010, 2571–2574.
20. S. Paul and B. Basu, *Tetrahedron Lett.*, 2011, **52**, 6597–6602.
21. H. K. Kadam, S. Khan, R. A. Kunkalkar and S.G. Tilve, *Tetrahedron Lett.*, 2013, **54**, 1003–1007.
22. F. Xie, M. Zhang, H. Jiang, M. Chen, W. Lv, A. Zhenga and X. Jiana, *Green Chem*., 2015, **17**, 279–284.
23. (a) A. Go, G. Lee, J. Kim, S. Bae, B. M. Lee and B. H. Kim, *Tetrahedron*, 2015, **71**, 1215–1226; (b) T. B. Nguyen, P. Retailleau and A. Al-Mourabit, *Org. Lett.*, 2013, **15**, 5238–5241; (c) M. J. Climent, A. Corma, J. C. Hernández, A. B. Hungría, S. Iborra and S. Martínez-Silvestre, *J. Catal.*, 2012, **292**, 118–129; (d) D.-Q. Shi, G.-L. Dou, S.-N. Ni, J.-W. Shi and X.-Y. Li, *J. Heterocycl. Chem.*, 2008, **45**, 1797–1801.

24. (a) C. Allais, J.-M. Grassot, J. Rodriguez and T. Constantieux, *Chem. Rev.*, 2014, **114**, 10829–10868; (b) J. Thomas, J. John, N. Parekh and W. Dehaen, *Angew. Chem., Int. Ed.*, 2014, **53**, 10155–10159.
25. For review: see (a) S. Navalon, A. Dhakshinamoorthy, M. Alvaro and H. Garcia, *Chem. Rev.*, 2014, **114**, 6179–6212; (b) C. Su, and K. P. Loh, *Acc. Chem. Res.*, 2013, **46**, 2275–2285.
26. (a) C. K. Chua and M. Pumera, *Chem. Eur. J.*, 2015, **21**, 1–14; (b) H. Hu, J. H. Xin, H. Hu, X. Wang, and Y. Kong, *Appl. Catal. A: General*, 2015, **492**, 1–9; (c) D. R. Dreyer, A. D. Todd and C. W. Bielawski, *Chem. Soc. Rev.*, 2014, **43**, 5288–5301; (d) D. R. Dreyer and C. W. Bielawski, *Chem. Sci.*, 2011, **2**, 1233–1240; (e) D. R. Dreyer, H.-P. Jia and C. W. Bielawski, *Angew. Chem. Int. Ed.*, 2010, **49**, 6813–6816.
27. Y. Gao, D. Ma, C. Wang, J. Guan and X. Bao, *Chem. Commun*., 2011, 47, 2432–2434.
28. (a) S. Kundu and B. Basu, *RSC Adv*., 2015, **5**, 50178–50185; (b) B. Roy, D. Sengupta and B. Basu, *Tetrahedron Lett*., 2014, **55**, 6596–6600; (c) D. Sengupta, J. Saha, B. Basu and G. De, *RSC Adv*., 2014, **4**, 35442–35448; (d) B. Basu, S. Kundu, and D. Sengupta, *RSC Adv*., 2013, **3**, 22130–22134.
29. (a) W. S. Hummers and R. E. Offeman, *J. Am. Chem. Soc.*, 1958, **80**, 1339.(b) R. K. Layek, S. Samanta, D. P. Chatterjee and A. K. Nandi, *Polymer*, 2010, **51**, 5846–5856.
30. S. Stankovich, D. A. Dikin, R. D. Piner, K. A. Kohlhaas, A. Kleinhammes, Y. Jia, Y. Wu, S. T. Nguyen and R. S. Ruoff, *Carbon*, 2007, **45**, 1558–1565.
31. (a) J. G. S. Moo, B. Khezri, R. D. Webster and M. Pumera, *ChemPhysChem*, 2014, **15**, 2922–2929; (b) Q. Zhuo, Y. Ma, J. Gao, P. Zhang, Y. Xia, Y. Tian, X. Sun, J. Zhong, and X. Sun, *Inorg. Chem*., 2013, **52**, 3141–3147; (c) D. C. Marcano, D. V. Kosynkin, J. M. Berlin, A. Sinitskii, Z. Sun, A. Slesarev, L. B. Alemany, W. Lu, and J. M. Tour, *ACS Nano*, 2010, **4**, 4806–4814.
32. C. D. Zangmeister, X. Ma and M. R. Zachariah, *Chem. Mater*., 2012, **24**, 2554–2557.
33. B. Lakshmi, P. G. Avaji, K. N. Shivananda, P. Nagella, S. H. Manohar and K. N. Mahendra, *Polyhedron*, 2011, **30**, 1507–1515.
34. (a) R. C. Cioc, E. Ruijter and R. V. A. Orru, *Green Chem*., 2014, **16**, 2958–2975; (b) B. H. Rotstein, S. Zaretsky, V. Rai and A. K. Yudin, *Chem. Rev.*, 2014, **114**, 8323–8359.

35. (a) J. W. Larsen, M. Freund, K. Y. Kim, M. Sidovar and J. L. Stuart, *Carbon*, 2000, **38**, 655–661; (b) B. H. Han, D. H. Shin and S. Y. Cho, *Tetrahedron Lett.*, 1985, **26**, 6233–6234.
36. M. R. Karim, K. Hatakeyama, T. Matsui, H. Takehira, T. Taniguchi, M. Koinuma, Y. Matsumoto, T. Akutagawa, T. Nakamura, S.-ichiro. Noro, T. Yamada, H. Kitagawa, S. Hayami, *J. Am. Chem. Soc.*, 2013, **135**, 8097–8100.
37. S. V. More, M. N. V. Sastry, C. C. Wang and C. Yao, *Tetrahedron Lett.*, 2005, **46**, 6345–6348.
38. C. Xie, Z. Zhang, B. Yang, G. Song, H. Gao, L. Wen and C. Ma, *Tetrahedron*, 2015, **71**, 1831–1837.
39. A. Hasaninejad, A. Zare, M. R. Mohammadizadeh and M. Shekouhy, *Arkivoc*, 2006, **13**, 28–35.
40. S. V. More, M. N. V. Sastry and C.-F. Yao, *Green Chem*., 2006, **8**, 91–95.
41. M. M. Heravi, K. Bakhtiari, M. H. Tehrani, N. M. Javadi and H. A. Oskooie, *Arkivoc*, 2006, **16**, 16–22.
42. D.-Q. Shi and G. L. Dou, *Synth. Commun*., 2008, **38**, 3329–3337.
43. H. R. Darabi, K. Aghapoor, F. Mohsenzadeh, F. Taala, N. Asadollahnejad and A. Badiei, *Catal. Lett*., 2009, **133**, 84–89.
44. J.-J. Cai, J.-P. Zou, X.-Q. Pan and W. Zhang, *Tetrahedron Lett.*, 2008, **49**, 7386–7390.
45. S. Sithambaram, Y. Ding, W. Li., X. Shen, F. Gaenzler and S. L. Suib, *Green Chem*., 2008, **10**, 1029–1032**.**
46. A. Shaabani and A. Maleki, *Chin. J. Chem.*, 2007, **25**, 818–821.

CHAPTER IV

1. K. S. Novoselov, A. K. Geim, S. V. Morozov, D. Jiang, Y. Zhang, S. V. Dubonos, I. V. Grigorieva and A. A. Firsov, *Science*, 2004, **306**, 666–669.
2. Z. Zhao, L. Liu, and F. Li, *Graphene oxide: Physics and Applications*, Heidelberg: *Springer*, 2014, 1–154.
3. M. Aliofkhazraei, *Advances In Graphene Science*, Croatia: *InTech*, 2013, 1–271.
4. C. K. Chua and M. Pumera, *J. Mater. Chem. A*, 2013, **1**, 1892–1898.

5. H.-J. Shin, K. K. Kim, A. Benayad, S.-M. Yoon, H. K. Park, I.- S. Jung, M. H. Jin, H.- K. Jeong, J. M. Kim, J.-Y. Choi and Y. H. Lee, *Adv. Funct. Mater*., 2009, **19**, 1987–1992.
6. S. Pei and H.-M. Cheng, *Carbon*, 2011, **50**, 3210–3228.
7. B. F. Machado, P. Serp, *Catal. Sci. Technol*., 2012, **2**, 54–75.
8. V. Singh, D. Joung L. Zhai, S. Das, S.I. Khondaker, S. Seal, *Prog. Mater. Sci*., 2011, **56**, 1178–1271.
9. S. Stankovich, D. A. Dikin, G. H. B. Dommett, K. M. Kohlhaas, E. J. Zimney, E. A. Stach, R. D. Piner, S-B.T. Nguyen and R. S. Ruoff, *Nature*, 2006, **44**, 282–286.
10. D. R. Dreyer, A. D. Todd and C. W. Bielawski, *Chem. Soc. Rev.*, 2014, **43**, 5288–530.
11. D. R. Dreyer, S. Park, C. W. Bielawski and R. S. Ruoff, *Chem. Soc. Rev.*, 2010, **39**, 228–240.
12. D. R. Dreyer and C. W. Bielawski, *Chem. Sci*., 2011, **2**, 1233–1240.
13. D. R. Dreyer, H.-P. Jia and C. W. Bielawski, *Angew. Chem*., *Int. Ed.*, 2010, **122**, 6965 –6968.
14. C. K. Chua, and M. Pumera, *Chem. Eur. J.***,** 2015, **21**, 1–14.
15. S. Navalon, A. Dhakshinamoorthy, M. Alvaro and H. Garcia, *Chem. Rev*., 2014, **114**, 6179–6212.
16. Kundu, S. and Basu, B. *RSC Adv.*, 2015, **5**, 50178–50185.
17. B. Roy, D. Sengupta, and B. Basu, *Tetrahedron Lett*., 2014, **55**, 6596–6600.
18. K. Bhowmik, D. Sengupta, Basu, B. and G. De, *RSC Adv*., 2014, **4**, 35442–35448.
19. B. Roy, S. Ghosh, P. Ghosh and B. Basu, *Tetrahedron Lett.*, 2015, **56**, 6762–6767.
20. C. Su and K. P. Loh, *Acc. Chem. Res*., 2013, **46**, 2275–2285.
21. W. L. Zhang and H. J. Choi, *Soft Matter*, 2014, **10**, 6601–6608.
22. K. S. Novoselov, V. I. Fal′ ko, L. Colombo, P. R. Gellert, M. G. Schwab and K. Kim, *Nature*, 2012, **490**, 192–200.
23. R. K. Layek, A. Kundu and A. K. Nandi, *Macromol. Mater. Eng.*, 2013, **298**, 1166–1175.
24. R. K. Layek, S. Samanta, D. P. Chatterjee and A. K. Nandi, *Polymer*, 2010, **51**, 5846–5856.
25. R. Alam, I. V. Lightcap, C. J. Karwacki and P. V. Kamat, *ACS Nano*, 2014, **8**, 7272–7278.

26. J. Zhu, D. Yang, Z. Yin, Q. Yan, and H. Zhang, *Small*, 2014, **10**, 3480–3498.
27. J. R. Potts, D. R. Dreyer, C. W. Bielawski and R. S. Ruoff, *Polymer*, 2011, **52**, 5–25.
28. X. Huang, X. Qi, F. Boey and H. Zhang, *Chem. Soc.Rev.*, 2012, **41**, 666–668.
29. C. K. Chua and M. Pumera**,** *Chem. Soc. Rev.*, 2014, **43**, 291–312.
30. Kuila, A. K. Mishra, P. Khanra, N. H. Kim and J. H. Lee, *Nanoscale*, 2013, **5**, 52–71.
31. M. Agharkar, S. Kochrekar, S. Hidouri and M. A. Azeez, *Mater. Res. Bull.*, 2014, **59**, 323–328.
32. M. T. H. Aunkora, I. M. Mahbububulb, R. Saidurb and H. S. C. Metselaara, *RSC Adv.***,** 2016, **6**, 27807–27828.
33. S. Gurunathan, J. W. Han, V. Eppakayala and J. H. Kim, *Colloids Surf*., B, 2013, **102**, 772–777.
34. B. Jayasena and S. Subbiah, *Nanoscale Res. Lett*., 2011, **6**, 95-101.
35. Z.G. Cambaz, G. Yushin, S. Osswald, V. Mochalin and Y. Gogotsi, *Carbon*, 2008, **46**, 841–849.
36. Y. Hernandez, V. Nicolosi, M. Lotya, F.M. Blighe, Z. Sun, *Nat. Nanotechnol.,* 2008, **3**, 563–568.
37. B. C. Brodie, *Philos. Trans. R. Soc. London*, 1859, **149**, 249–259.
38. L. Staudenmaier, *Ber. Dtsch. Chem. Ges*., 1898, **31**, 1481–1487.
39. U. Hofmann and E. Konig, *Z. Anorg. Allg. Chem*., 1937, **234**, 311–336.
40. W. S. Hummers Jr. and R. E. Offeman, *J. Am. Chem. Soc*., 1958, **80**, 1339.
41. D. C. Marcano, D. V. Kosynkin, J. M. Berlin, A. Sinitskii, Z. Sun, A. Slesarev, L. B. Alemany, W. Lu and J. M. Tour, *ACS Nano*, 2010, **4**, 4806–4814.
42. (a) S. Stankovich, D. Dikin, G. Dommett, K. Kohlhaas, E. Zimney, E. Stach, Graphene-based composite materials, *Nature*, 2006, **442**, 282–286; (b) G. Wang, J. Yang, J. Park, X. Gou, B. Wang, H. Liu and J. Yao, *J. Phys. Chem. C*, 2008, **112**, 8192–8195; (c) Z. Fan, K. Wang, T. Wei, J. Yan, L. Song and B. Shao, *Carbon*, 2010, **48**, 1686–1689; (d) Y. Si and E.T. Samulski, *Nano Lett.*, 2008, **8**, 1679–1682; (e) T. Zhou, F. Chen, K. Liu, H. Deng, Q. Zhang, J. Feng, Q. Fu, *Nanotechnology*, 2011, **22**, 045704; (f) X. P. Shen, L. Jiang, Z.Y. Ji, J. L. Wu, H. Zhou, G. X. Zhu, *J. Colloid. Interf. Sci.*, 2011, **354**, 493–497; (g) S. Zhang, Y. Shao, H. Liao, M.H. Engelhard, G. Yin and Y. Lin, *ACS Nano*, 2011, **5**, 1785–1791; (h) J. Che, L. Shen, Y. Xiao, *J. Mater. Chem.*, 2010, **20**, 1722–1727; (i) W. B. Wan, Z. B. Zhao, H. Hu, Q. Zhou, Y.

R. Fan and J. S. Qiu, *New Carbon Mater*., 2011, **26**, 16–20; (j) K. Ai, Y. Liu, L. Lu, X. Cheng and L. Huo, *J. Mater. Chem.*, 2011, **21**, 3365–3370.

43. (a) S. Pei, J. Zhao, J. Du, W. Ren and H.M. Cheng, *Carbon*, 2010, **48**, 4466–4474; (b) S. Dubin, S. Gilje, K. Wang, V.C. Tung, K. Cha, A.S. Hall, J. Farrar, R. Varshneya, Y. Yang and R. Kaner, *ACS Nano*, 2010, **4**, 3845–3852; (c) D.A. Sokolov, K.R. Shepperd and T.M. Orlando, *J. Phys. Chem. Lett*., 2010, **1**, 2633– 2636;(d) W. Chen, L. Yan and P.R. Bangal, *Carbon*, 2010, **48**, 1146–1152; (e) K. Vinodgopal, B. Neppolian, I.V. Lightcap, F. Grieser, M. Ashokkumar and P.V. Kamat, *J. Phys. Chem. Lett.*, 2010, **1**, 1987–1993; (f) Z. Wang, X. Zhou, J. Zhang, F. Boey and H. Zhang, *J. Phys. Chem. C*, 2010, **113**, 14071–14075; (g) W. Gao, L.B. Alemany, L. Ci and P.M. Ajayan, *Nat. Chem.*, 2009, **1**, 403–408.
44. (a) C. Zhu, S. Guo, Y. Fang and S. Dong, *ACS Nano*, 2010, **4**, 2429–2437; (b) Y.-K. Kim, M.-H. Kim and D.-H. Min, *Chem. Commun*., 2011, **47**, 3195–3197; (c) J. Li, G. Xiao, C. Chen, R. Li and D. Yan, *J. Mater. Chem.* A, 2013, **1**, 1481–1487; (d) D. Chen, L. Li and L. Guo, *Nanotechnology*, 2011, **22**, 325601; (e) S. Bose, T. Kuila, A. K. Mishra, N. H. Kim and J. H. Lee, *J. Mater. Chem.*, 2012, **22**, 9696–9703; (f) J. K. Ma, X. R. Wang, Y. Liu, T. Wu, Y. Liu, Y. Q. Guo, R. Q. Li, X. Y. Sun, F. Wu, C. B. Li and J. P. Gao, *J. Mater. Chem. A*, 2013, **1**, 2192–2201; (g) T. A. Pham, J. S. Kim, J. S. Kim and Y. T. Jeong, *Colloids Surf., A*, 2011, **384**, 543–548; (h) E. C. Salas, Z. Sun, A. Lu¨ttge and J. M. Tour, *ACS Nano*, 2010, **4**, 4852–4856; (i) G. Wang, F. Qian, C. Saltikov, Y. Jiao and Y. Li, *Nano Res.*, 2011, **4**, 563–570; (j) J. Liu, S. Fu, B. Yuan, Y. Li and Z. Deng, *J. Am. Chem. Soc*., 2010, **132**, 7279–7281; (k) A. Esfandiar, O. Akhavan and A. Irajizad, *J. Mater. Chem.*, 2011, **21**, 10907–10914; (l) M. Agharkar, S. Kochrekar, S. Hidouri and M. A. Azeez, *Mater. Res. Bull*., 2014, **59**, 323–328.
45. S. Thakur and N. Karak, Carbon, 2012, **50**, 5331–5339.
46. J. M. Firdhouse, P. Lalitha, *Carbon Sci. Technol.*, 2013, **5**, 253–259.
47. A. M. Fonseca, F. J. Q. Monte, M. C. F. Oliveira, M. C. Mattos, G. A. Cordell, R. B. Filho, and T. L. G. Lemos, *J. Mol. Catal. B: Enzym.*, 2009, **57**, 78–82.
48. B. Kartick, S.K. Srivastava and I. Srivastava, *J. Nanosci. Nanotechnol.*, 2013, **13**, 4320–4324
49. B. Haghighi and M.A. Tabrizi, *RSC Adv.*, 2013, **3**, 13365–13371.

50. S. Gurunathan, J. W. Han, V. Eppakayala and J. H. Kim, *Colloids Surf. B*, 2013, **102**, 772–777
51. G. Lee and B.S. Kim, *Biotechnol. Prog.*, 2014, 30463–30469.
52. D. Mhamane, W. Ramadan, M. Fawzy, A. Rana, M. Dubey, C. Rode, B. Lefez, B. Hannoyerand and S. Ogale, *Green Chem.*, 2011, **13**, 1990–1996.
53. M. Khan, A. H Al-Marri, M. Khan, M. R. Shaik, N. Mohri, S. F.Adil1, M. Kuniyil, H.Z Alkhathlan, A. Al-Warthan, W. Tremel, M. N.Tahir and M. R. H Siddiqui, *Nano. Res. Lett.*, 2015, 10:281.
54. J. Akhtar, K. M. Siddique, S. Bi and M. Mujeeb *J. Pharm. Bioallied Sci.*, 2011, **3**, 113–117.
55. (a) S. Arulkumar and M. Sabesan, *Int. J. Res. Pharm. Sci.*, **2010,** 1, 417; (b) D. Srinivasrao, A. J. Indira, R. Jayraaj, and M. Lakshmi Prabha, *Indian J. Allergy Asthama Immunol.*, 2006, **20**, 1.
56. R. Suvidya, L. Pravin, B. Shubhangi and J.Satyawati, *Adv. Sci. Eng. Med.*, 2012, **5**, 1-6.
57. L. Berkovich, G. Earon, I. Ron, A. Rimmon, A. Vexler and S. Lev-Ari, *BMC Complementary and Alternative Medicine*, 2013, 13:212.
58. R. Sathyavathi, M. Bala Murali Krishna, and D. Narayana Rao, J. *Nanosci. Nanotechnol*., 2010, **10**, 1–5.
59. P. Banerjee, M. Satapathy, A. Mukhopahayay and P. Das, *Bioresources and Bioprocessing*, 2014, 1:3; (b) M. Pattanayak and P.L. Nayak, *World J. Nano Sci. Technol.*, 2013, **2**, 6–9.
60. M. C. Moulton, L. K. Braydich-Stolle, M. N. Nadagouda, S. Kunzelman, S. M. Hussain and R. S. Varma, *Nanoscale*, 2010, **2**, 763–770; (b) M. N. Nadagouda and R. S. Varma, *Green Chem.*, 2008, **10**, 859–862; (c) S. K. Nune, N. Chanda, R. Shukla, K. Katti, R. R. Kulkarni, S. Thilakavathy, S. Mekapothula, R. Kannan and K. V. Katti, *J. Mater. Chem*., 2009, **19**, 2912–2920.
61. M. F. Abdullah,ab R. Zakariaa and S. H. S. Zein, *RSC Adv.*, 2014, **4**, 34510–34518.
62. T.A. Ajith, K.K. Janardhanan, *J. Clin. Biochem. Nutr.*, 2007, **40**, 157–162; (b) A. Turkoglu, M.E. Duru, N. Mercan, *Eur. J. Anal. Chem*., 2007, **2**, 54–61.
63. D.Philip, *Spectrochim. Acta, Part* A, 2009, **73**, 374–381.
64. S. Stankovich, D. A. Dikin, R. D. Piner, K. A. Kohlhaas, A. Kleinhammes, Y. Jia, Y. Wu, S. T. Nguyen and R. S. Ruoff, *Carbon*, 2007, **45**, 1558–1565.

65. Z.-J. Fan,W. Kai, J. Yan, T. Wei, L. -J. Zhi, J. Feng, Y-M. Ren, L.-P. Song, and F. Wei, *ACS Nano*, 2011, **5**, 191–198.
66. D. Luo, G. Zhang, J. Liu, and X. Sun, *J. Phys. Chem. C*, 2011, **115**, 11327–11335.
67. X. Tong, H. Wang, G. Wang, L. Wan, Z. Ren, J. Bai and J. Bai, *J Solid State Chem.*, 2011, **184**, 982–989.
68. C. Hontoria–Lucas, A. J. Lo´pez–Peinado, Jd. D. Lo´pez–Gonza´lez, M. L. Rojas–Cervantes, R. M. Martı´n–Aranda, *Carbon*, 1995, **33**, 1585–1592.
69. T. Szabo´, O. Berkesi and I. De´ka´ny, *Carbon*, 2005, **43**, 3186–3189.
70. P. Guo, H. Song and X. Chen, *Electrochem. Commun.*, 2009, **11**, 1320–1324.
71. F. Pendolino, E. Parisini and S. Russo, *J. Phys. Chem.* C, 2014, **118**, 28162–28169.
72. A. C. Ferrari, *Solid State Commun.*, 2007, **143**, 47–57.
73. L. M. Malard, M. A. Pimenta, G. Dresselhaus and M. S. Dresselhaus, *Phys. Rep*., 2009, **473**, 51–87.
74. H. Wang, J. T. Robinson, X. Li, and H. Dai, *J. Am. Chem. Soc.*, 2009, **131**, 9910–9911.
75. Y. Hong, Z.Wang and X. Jin, *Scientific Reports*, 2013, **3**, 1–6.
76. A. Kumar and M. Khandelwal, *New J. Chem*., 2014, **38**, 3457–3467.
77. B. K. Barman, P. Mahanandiab and K. K. Nanda, *RSC Adv.*, 2013, **3**, 12621–12624.
78. J. Zhang, H. Yang, G. Shen, P. Cheng, J. Zhang and S. Guo, *Chem. Commun*., 2010, **46,** 1112–1114.
79. T. Szabo´, E. Tomba´cz, E. Ille´s and I. De´ka´ny, *Carbon*, 2006, **44**, 537–545.
80. Z. H. Liu, Z. M. Wang, X. Yang and K. Ooi, *Langmuir*, **2002**, 18, 4926–4932.
81. Y. Gao, D. Ma, C. Wang, J. Guan and X. Bao, *Chem. Commun*., 2011, **47**, 2432–2434.
82. H.Tada, T. Ishida, A. Takao, S. Ito, S. Mukhopadhyay, T. Akita, K. Tanaka and H. Kobayashi, *ChemPhysChem*, 2005, **6**, 1537–1543.
83. Y. Mu, H.-Q. Yu, J.-C. Zheng, S.-J. Zhang and G.-P. Sheng, *Chemosphere*, 2004, **54**, 789–794.

CHAPTER V

1. (a) J. H. Fendler (Eds.), *Nanoparticles and Nanostructured Films. Preparation, Characterizations and Applications*, Wiley -VCH, Weinheim, Germany , 1998; (b) G. Schmid, in *Nanoscale Materials in Chemistry* , K. J. Klabunde (Eds.), Wiley

Interscience, New York, 2001 , pp.15 – 59; (c) G. Schmid, *Chem. Rev.*, 1992 , **92,** 1709–1727; (d) L. N. Lewis, *Chem. Rev.* 1993, **93** , 2693–2730; (e) J. S. Bradley in *Clusters and Colloids* , Ed. G. Schmid (Ed.), VCH, Weinheim, 1994 , Ch. 6, pp 459–544.

2. (a) L. Yin and J. Liebscher, *Chem. Rev*. 2007, **107**, 133-173; (b) H.-U. Blaser, A. Indolese, A. Schnyder, H. Steiner, M. Studer, *J. Mol. Catal. A: Chem.*, 2001, **173**, 3–18; (c) S. Brase, J. H. Kirchhoff and J. Kobberling, *Tetrahedron*, 2003, **59**, 885–939.
3. (a) A. Barge, S. Tagliapietra, L. Tei, P. Cintas and G. Cravotto, *Curr. Org. Chem.*, 2008, **12**, 1588–1612; (b) P. D. Leeson and B. Springthorpe, *Nat. Rev. Drug. Discov.*, 2007, **6**, 881–890.
4. J. Peter and H. Scott., *An introduction to solid-phase palladium chemistry*, 2012:John Wiley & Sons: Inc., Hoboken, New Jersey., vol-2, pp-167
5. E.-I. Negishi and A. Meijere, *Handbook of organopalladium chemistry for organic synthesis.* Wiley-VCH: Weinheim, Volume 1 & 2, 2002.
6. R. Ferrando, J. Jellinek and R. L. Johnston, *Chem. Rev.*, 2008, **108**, 845–910.
7. For selected reviews on bimetallic nanoparticle catalyst see: (a) S. Zafeiratos, S. Piccinin and D. Teschner, *Catal. Sci. Technol.*, 2012, **2**, 1787–1801; (b) S. Shan, J. Luo, L. Yang and C.-J. Zhang, *Catal. Sci. Technol.*, 2014, **4**, 3570–3588; (c) H.-L. Jiang and Q. Xu, *J. Mater. Chem.*, 2011, **21**, 13705–13725; (d) A. K. Singh and Q. Xu, *ChemCatChem*, 2013, **5**, 652–676; (e) D. Wang, Q. Peng and Y. Li, *Nano Res.*, 2010, **3**, 574–580; (f) S. K. Singh and Q. Xu, *Catal. Sci. Technol.*, 2013, **3**, 1889–1900; (g) N. Toshima and T. Yonezawa, *New J. Chem.*, 1998, **22**, 1179–1201; (h) J. Shi, *Chem. Rev.*, 2013, **11**3, 2139–2181; (i) I. Notar Francesco, F. Fontaine-Vive and S. Antoniotti, *ChemCatChem*, 2014, **6**, 2784–2791; (j) R. Ferrando, J. Jellinek and R. L. Johnston, *Chem. Rev.*, 2008, **108**, 845–910.
8. (a) H. Kobayashi, M. Yamauchi, H. Kitagawa, Y. Kubota, K. Kato and M. Takata, *J. Am. Chem. Soc.*, 2010, **132**, 5576–5577; (b) S. K. Singh and Q. Xu, *J. Am. Chem. Soc.*, 2009, **131**, 18032–18033; (c) S. K. Singh and Q. Xu, *Inorg. Chem.*, 2010, **49**, 6148–6152; (d) J. Li, Q.-L. Zhu and Q. Xu, *Catal. Sci. Technol.*, 2015, **5**, 525–530; (e) H. Goksu, S. F. Ho, O. Metin, K. Korkmaz, A. M. Garcia, M. S. Gultekin and S. H. Sun, *ACS Catal.*, 2014, **4**, 1777–1782; (f) J. García-Aguilar, I. Miguel-García, Á. Berenguer-Murcia and D. Cazorla-Amorós, *Carbon*, 2014, **66**, 599–611. (g) S.

Nishimura, Y. Yakita, M. Katayama, K. Higashimine and K. Ebitani, *Catal. Sci. Technol.*, 2013, **3**, 351–359; (h) J. Shen, X. Yin, D. Karpuzov and N. Semagina, *Catal. Sci. Technol*., 2013, **3**, 208–221; (i) J. Zhang, L. Zhang, Y. Jia, G. Chen, X. Wang, Q. Kuang, Z. Xie and L. Zheng, *Nano Res.*, 2012, **5**, 618–629; (j) J. Xu, T. White, P. Li, C. He, J. Yu, W. Yuan and Y.-F. Han, *J. Am. Chem. Soc*., 2010, **132**, 10398–10406; (k) D. I. Enache, J. K. Edwards, P. Landon, B. Solsona-Espriu, A. F. Carley, A. A. Herzing, M. Watanabe, C. J. Kiely, D. W. Knight and G. J. Hutchings, *Science*, 2006, **311**, 362–365.

9. (a) F. Diederich and A. de Meijere, *Metal-Catalyzed Cross-Coupling Reaction*, Wiley-VCH, Weinheim, 2004, pp 41–109; (b) J.-P. Corbet and G. Mignani, *Chem. Rev*., 2006, **106**, 2651–2710.
10. (a) H. M. Song, B. A. Moosa and N. M. Khashab, *J. Mater. Chem.*, 2012, **22**, 15953–15959; (b) L. Tan, X. Wu, D. Chen, H. Liu, X. Meng and F. Tang, *J. Mater. Chem. A*, 2013, **1**, 10382–10388; (c) J. Han, Z. Zhou, Y. Yin, X. Luo, J. Li, H. Zhang and B. Yang, *CrystEngComm*, 2012, **14**, 7036–7042; (d) P. P. Fang, A. Jutand, Z. Q. Tian and C. Amatore, *Angew. Chem., Int. Ed.*, 2011, **50**, 12184–12188; (e) Z. Q. Niu, Q. Peng Z. B. Zhuang, W. He and Y. D. Li, *Chem. Eur. J.*, 2012, **18**, 9813–9817.
11. Md. S. Kutubi, K. Sato, K. Wada, T. Yamamoto, S. Matsumura, K. Kusada, H. Kobayashi, H. Kitagawa and K. Nagaoka, *ChemCatChem*, 2015, **7**, 3887–3894.
12. S.-B. Wang, W. Zhu, J. Ke, M. Lin and Y.-W. Zhang, *ACS Catal.*, 2014, **4**, 2298–2306.
13. (a) M. Nasrollahzadeh, B. Jalehb and A. Ehsani, *New J. Chem*., 2015, **39**, 1148–1153; (b) S. Diyarbakir, H. Can and O. Metin, *ACS Appl. Mater. Interfaces*, 2015, **7**, 3199–3206; (c) M. Korzec, P. Bartczak, A. Niemczyk, J. Szade, M. Kapkowski, P. Zenderowska, K. Balin, J. Lelatko and J. Polanski, *J. Catal*., 2014, **313**, 1–8; (d) W. Xu, H. Sun, B. Yu, G. Zhang, W. Zhang and Z. Gao, *ACS Appl. Mater. Interfaces*, 2014, **6**, 20261–20268; (e) F. Heshmatpour, R. Abazari and S. Balalaie, *Tetrahedron*, 2012, **68**, 3001–3011; (f) B. H. Lipshutz, D. M. Nihan, E. Vinogradova, B. R. Taft and Z. V. Boskovic, *Org. Lett.*, 2008, **10**, 4279–4282; (g) S.-J. Kim, S.-D. Oh, S.-H. Lee and S.-H. Choi, *J. Ind. Eng. Chemi.*, 2008, **14**, 449–456; (h) M. B. Thathagar, J. Beckers and G. Rothenberg, *J. Am. Chem. Soc*., 2002, **124**, 11858–11859.

14. (a) M. T. Reetz, R. Breinbauerm and K. Wanniger, *Tetrahedron Lett.*, 1996, **37**, 4499–4502. (b) J. Xiang, P. Li, H. Chong, L. Feng, F. Fu, Z. Wang, S. Zhang and M. Zhu, *Nano Res.*, 2014, **7**, 1337–1343; (c) O. Metin, S. F. Ho, C. Alp, H. Can, M. N. Mankin, M. S. Gultekin, M. Chi and S. Sun, *Nano Res*., 2013, **6**, 10–18; (d) S. U. Son, Y. J. Jang, J. Park, H. B. Na, H. M. Park, H. J. Yun, J. Lee and T. Hyeon, *J. Am. Chem. Soc*., 2004, **126**, 5026–5027; (e) L. Feng, H. Chong, P. Li, J. Xiang, F. Fu, S. Yang, H. Yu, H. Sheng and M. Zhu, *J. Phys. Chem. C*, 2015, **119**, 11511–11515; (f) J. Saha, K. Bhowmik, I. Das and G. De, *Dalton Trans*., 2014, **43**, 13325–13332.
15. (a) V. K. Rao and T. P. Radhakrishnan, *J. Mater. Chem. A*, 2013, **1**, 13612–13618; (b) M. Chen, Z. Zhang, L. Li, Y. Liu, W. Wang and J. Gao, *RSC Adv.*, 2014, **4**, 30914–30922.
16. Y.-S. Feng, X.-Y. Lin, J. Haob and H.-J. Xu, *Tetrahedron*, 2014, **70**, 5249–5253.
17. W. Tang, J. Li, X. Jin, J. Sun, J. Huang and R. Li, *Catal. Commun.*, 2014, **43**, 75–78.
18. R. Chinchilla and C. Najera, *Chem. Rev.*, 2007, **107**, 874–922.
19. D. Astruc**,** *Nanoparticles and Catalysis,* Wiley-VCH Verlag GmbH & Co. KGaA, Weinheim, 2008.
20. (a) B. Basu, S. Das, P. Das, B. Mandal, D. Banerjee and F. Almqvist, *Synthesis*, 2009, 1137–1146; (b) B. Basu, S. Das, S. Kundu and B. Mandal, *Synlett*, 2008, 0255–0259; (c) B. Basu, S. Das, P. Das and A. K. Nanda, *Tetrahedron Lett*., 2005, **46**, 8591–8593; (d) B. Basu, P. Das and S. Das, *Mol. Diversity*, 2005, **9**, 259–262; (e) B. Basu, Md. M. H. Bhuiyan, P. Das and I. Hossain, *Tetrahedron Lett*., 2003, **44**, 8931–8934.
21. D. Sengupta and B. Basu, *Org Med Chem Lett*., 2014, 4:17.
22. D. Sengupta, J. Saha, G. De and B. Basu, *J. Mater. Chem. A*, 2014, **2**, 3986–3992.
23. B. Basu, S. Paul and A. K. Nanda, *Green Chem.*, 2009, **11**, 1115–1120.
24. B. Basu and S. Paul, *Appl. Organomet. Chem.*, 2013, **27**, 588–594.
25. K. Bhowmik, D. Sengupta, B. Basu and G. De, *RSC Adv*., 2014, **4**, 35442–35448.
26. H. Bonin, D. Delbrayelle, P. Demonchaux and E. Gras, *Chem. Commun*., 2010, **46**, 2677–2679.
27. Y. Zhang, M. Wang, P. Li and L. Wang, *Org. Lett*., 2012, **14**, 2206–2209.
28. T. Fukuyama, M. Arai, H. Matsubara and I. Ryu, *J. Org. Chem*., 2004, **69**, 8105–8105.
29. J. Salabert, R. M. Sebastian, A. Vallribera , J. F. Cívicos and C. Najera, *Tetrahedron*, 2013, **69**, 2655–2659.

30. (a) T. Shimasaki, Y. Konno, M. Tobisu and N. Chatani, *Org. Lett*., 2009, **11**, 4890–4892; (b) H. -J. Xu, Y. -Q. Zhao, and X. –F. Zhou, *J. Org. Chem*., 2011, **76**, 8036–8041; (c) Z. -Y. Peng, F-F. Ma, L-F. Zhu, X-M. Xie and Z. Zhang, *J. Org. Chem*., 2009, **74**, 6855–6858; (d) K. Kikukawa, M. Naritomi, G.-X. He, F. Wada, and T. Matsuda, *J. Org. Chem*., 1985, **50**, 299–301.
31. J. C. Roberts and J. A. Pincock, *J. Org. Chem.*, 2004, **69**, 4279–4282.
32. T. Jensen, H. Pedersen, B. Bang-Andersen, R. Madsen and M. Jorgensen, *Angew. Chem. Int. Ed*., 2008, **47**, 888–890.

INDEX

A

Absorption 72, 96, 102, 104, 125–126, 133, 143
Acetalization 61
Active sites 3–4, 13, 55
Adathoda Vasika 118, 121, 123, 131
Adsorption 2, 4, 5, 7–10
Alloy 122, 139, 140
Allyl bromide 35–18, 41, 43–46, 149, 154
Amberlyst-15 24, 59
Amberlite IRA-420 (Cl^-) 24, 143
Amberlyst® A-26 (OH) 23, 24
Amberlite resin formate (ARF) 25, 143–144, 150–153
Amorphous silica 5, 7– 8, 41
Anti-Markonikov 31, 35–39, 41–42
ArgoGel 20
Atomic absorption spectroscopy (AAS) 96, 104, 143
Azadirachta Indica 118, 121–123, 131
Aza-Michael addition 35, 59

B

Bimetallic 137–144, 147, 149, 152–153
Biocompatibility 10, 119, 120
Bronsted acid 3, 8
Brodie's method 15, 16
Biologically reduced GO (brGO) 116–117, 123–136
Bio-sources 12, 117,121, 122
Bis-thioethers 30, 31
Bridging ligands 29, 30

C

Calcination 41, 45
Camellia Sinensis 118, 121, 123, 131
Cation-exchange capacity 122, 125, 131
Carbon materials 2, 3, 5, 10, 93, 103, 128, 132
Carbon nanotubes (CNT) 2, 5, 11
Catalyst 2-19, 23-26, 29, 31-32, 34, 43-44, 57-66, 71–72, 88–96, 98, 101–104, 117, 133, 138–140, 142, 144, 147–152
Carbocatalysis 10, 57, 58
Carbocatalyst 10, 14, 15, 56–60, 72, 89, 90, 94, 117
Catalysis 1–5, 7, 10, 29, 30, 61, 119

Centrifugation 71, 95, 96, 101
Charcoal 2, 5, 10, 90
Chemisorption 2,7
Chemoselectivity 67, 72
Chemical vapour deposition (CVD) 11, 13, 118
Chemical reduction 12, 117–119, 140
Chemically reduced graphene oxide (CrGO) 117, 124–133, 135, 136
ChemMatrix resin 20, 21
CLEAR 20, 21
Click addition 36
Chromatography 7, 8, 10, 29, 38, 45, 46, 73, 96, 97, 101, 102, 104, 113, 154
Cross-coupling 139, 140, 143−149, 151, 153, 154
Complexes 3, 5, 29, 30, 89
D
Desorption 2, 4
De-ionised (DI) water 95, 123
Diorganyl sulfide 29
Disulfide 23, 24, 30−33, 37, 38, 41, 64−69, 72
Dithioacetalization 62, 63, 68, 72
Dithioether 28–34, 36, 39, 41–42, 44–45
1,3-dithioether 31, 35–39, 42–46
1,2-dithioether 31, 36–39, 42–43
Dithioacetals 62, 63, 64, 68–69, 72–75
DLS 92, 96, 104
E
Environmental Protection Agency (EPA) 2
Embedded 137, 143
F
Friedel-Craft addition 3, 18
Fullerene 2, 5, 11
FT–IR spectroscopy 6, 64, 65, 70, 72, 95, 104, 124, 126, 127, 143
G
Graphene 1, 2, 3, 10-16, 57, 60, 89, 117, 118, 120, 126, 127, 128, 130, 131, 140, 141
Graphene oxide 2, 3, 5, 10, 12, 15, 16, 17, 18, 56, 57, 60, 63, 64, 73, 88, 89, 94, 95, 96, 98, 104, 117−120, 122, 123, 136
Graphite 5, 10, 11, 12, 16, 60, 64, 91, 95, 103, 117, 118, 123, 124, 128, 129
Green chemistry 2, 12, 29, 44, 57, 89, 90, 138

H
Heterogeneous 1, 3, 5, 19, 24, 26, 35, 58, 91, 143, 144
Heterogeneous catalysis 3, 4, 5, 19, 22, 24, 25, 26, 35, 57, 58, 61, 62, 63, 71, 117, 152
HPLC 10, 70, 72−74, 94, 96, 97, 103−106, 113, 149, 150
Hoffman 19
Homogeneous catalysis 3, 4, 8, 62
Hot filtration test 150
Hummers' method 16, 60, 61, 95, 104, 117, 118, 123, 131
Hydrothiolation 31, 36, 37, 41, 42, 57, 58, 59, 60, 62, 68
Hydrazine hydrate 12, 13, 91, 94, 98,102, 114−116, 118, 133
Hydrogel 6
Hydroxylation 13
I
Immobilization 7, 10, 23, 117
Ion-exchange resins 5, 22, 23, 143
Inorganic solid support 2, 3, 5, 28
IUPAC 5
L
Lassaigne's test 71
Leaching 140, 150
Lerf−Klinowski model 16, 17
Lewis acid 3, 8, 31, 34, 62
M
Markovnikov addition 38, 39, 42
Macroporous 5, 18, 19, 21
MCM-41, MCM-48, MCM-50 5, 9
Metal-organic framework (MOF) 29
Mechanism 4, 41, 43, 70, 102, 103
Merrifield resin 2, 18,19, 20
Mesoporous 5, 9, 10, 13, 29, 34, 41, 140
Metal-organic coordination complexes 29, 30
Metal-free catalysts 57, 72, 89, 90
Metalloenzymes 30
Micromechanical cleavage 11, 1118
Microporous 5, 18, 20
Mizoroki-Heck/Heck Reaction 25, 137, 139, 142, 143, 147−152, 154
Moistened silica 37, 39, 41, 42, 44, 45
Monometallic 25, 138, 142−144, 149, 152, 153
Moringa Oleifera 118, 121, 123
N
Nakajima-Matsuo model 16, 17

Nanocomposite 25, 143−145, 149, 152. 153
Nanoparticles (NPs) 26, 34−36, 93, 117, 122, 131−142, 144, 149, 153
NovaGel 20
O
Organometallic 3, 8
Organosulfates 60, 61
Orthosilicate 6, 9, 10
Ordered mesoporous silica 9
Organosulfur compounds 29
Oxidant 13, 17, 18, 58
P
PEGA 20, 21
Physisorption 2
Poly-ionic resin 1, 3, 24, 26, 137
Pd/Cu−ARF 144−151, 153,154
Phase transfer catalysts (PTC) 58
Phenylboronic acid 15, 139, 144, 145
pH 16, 18, 46, 57, 64, 70, 71, 95, 122, 124, 125, 131, 132, 136, 138
Plant extracts 12, 117, 119, 122, 124, 128
Polymer 2, 5, 10, 18−23, 29, 30, 117, 138, 152
Polystyrene 5, 15, 18−20, 23, 141
Poly-ionic resin 1, 3, 25, 135
Pore volume 4
Pore size 5, 9
Pore size distribution 4, 5
Pore structure 4, 10, 21
Porosity 6, 8, 22, 29, 34
Polymerization 6,1 5, 18−22, 30
Pre-calcined silica 37−39, 42−44, 154
Q
Quinoxaline 89−94, 96−99, 101, 103−113
R
Raman spectroscopy 16, 119, 120, 122, 124, 127, 128
Recyclability 2, 25 ,43, 44, 71, 72, 90, 138, 140, 151
Reduced graphene oxide (rGO) 3, 10, 13−15, 88, 89, 104, 117, 118, 121, 122, 124, 136, 140
Regio-selectivity 8, 29, 34, 36, 38, 41, 42
Ruess model 16, 17
S
SBA-15 5, 9, 10
SBA-16 10

Scaffold 26, 68, 104, 122
Scanning electron microscopy (SEM) 16, 120, 122, 124, 125, 130, 140
Scholz-Bohem model 16, 17
Silica gel 5–9, 29, 31, 35–46, 62, 73, 96, 105, 149, 153, 154
Silanol 6, 7, 36, 41
Silicic acid 6
Siloxane bridge 6, 7, 41
Sodium silicate 6, 41, 42, 46
Solid-phase organic synthesis (SPOS) 8, 20–23, 44
Solid-phase peptide synthesis (SPPS) 2, 18, 20
Solid-phase organic reactions 1, 2, 29
Solid supports 1–3, 5, 10, 18, 19, 25, 28, 29, 35, 63, 90, 140, 143
Solid supported reagents 2, 90
Sonogashira reaction 25, 26, 138, 140, 141, 143
Sonication 64, 95, 131
Stereoselectivity 8, 29
Staudenmaier Method 15, 16
Surface area 3–6, 8–13, 29, 34, 57, 58, 103
Sustainability 2,3,10,72,119
Suzuki-Miyaura/Suzuki reaction 26, 35, 139, 141, 144, 146, 147, 149, 151–153

T

Thermo gravimetric analysis (TGA) 16
Transmission electron microscopy (TEM) 16, 124, 125, 130, 131, 143
TentaGel 20
Thioether 29, 30, 31,34, 38, 59, 70
Thioacetalization 58, 61, 65, 67, 69, 71
Thioacetals 31, 62, 63, 67, 70
Titration 122, 125, 131, 132, 136
Tour’s method 15, 16
Tri-block copolymer 9, 10
Trifluoro acetic acid (TFA) 20, 90
Turnover number (TON) 4
Turnover frequency (TOF) 4

U

Uniform particle size (UPS) 22
Unsymmetrical 26, 59, 63, 69, 70, 72, 73, 75
UV-Vis Spectroscopy 16, 119, 120, 122, 124, 125, 126, 133

V

Vander Waals force 10, 119
Vicinal 6, 30, 31, 32, 34, 36, 41, 44, 92, 93

Volvereilla Volvacea 118, 121, 123
X
Xerogel 6
X-ray diffraction (XRD) 16, 119, 120, 122, 124, 129, 143, 151, 152
Z
Zeolite 5, 29, 59
Zuravlev's physico-chemical model 7, 40

REPRINTS

OF

PUBLISHED PAPERS

Beilstein Journal of Organic Chemistry

Silica: An efficient catalyst for one-pot regioselective synthesis of dithioethers

Samir Kundu, Babli Roy and Basudeb Basu*

Full Research Paper

Open Access

Address:
Department of Chemistry, North Bengal University, Darjeeling 734013, India, Fax: +91 353 2699001

Email:
Basudeb Basu* - basu_nbu@hotmail.com

* Corresponding author

Keywords:
allyl halide; dithioether; silica gel; tandem reactions; thiol

Beilstein J. Org. Chem. **2014,** *10,* 26–33.
doi:10.3762/bjoc.10.5

Received: 15 September 2013
Accepted: 11 November 2013
Published: 07 January 2014

Associate Editor: B. Stoltz

Abstract

The development of a silica-promoted highly selective synthesis of 1,2 or 1,3-dithioethers via solvent-free one-pot tandem reactions of an allyl bromide with excess thiol at room temperature is described. The choice of silica gel, either pre-calcined or moistened with water, exhibited notable regioselectivity in the formation of dithioethers. Plausible mechanistic routes were explored and postulated.

Introduction

Organosulfur compounds are important building blocks for the synthesis of various biologically active molecules [1-3]. Versatile applications of organosulfur compounds are known in fields such as the pharmaceutical, the polymer, the pesticide and the food-processing industry [4-8]. For example, organosulfur compounds in garlic are often used in food-processing industries as flavouring and preservative agents and are also used as herbal medicine [4]. Dithioethers are commonly employed as ligands in preparing metal-coordination complexes and also as spacers in metal-organic frameworks [9-14]. For example, vicinal dithioether-based zirconium and titanium complexes have been used for alkene polymerization and hydroamination [15-18]. Chiral dithioethers have been prepared and their iridium complexes have been employed in asymmetric hydrogenation [18]. Vicinal dithioethers are generally synthesised either by the metal-catalyzed addition of disulfides to alkenes [19,20] or by the traditional nucleophilic substitution of 1,2-dihalides with suitable thiols/thiolates [21,22]. They are also prepared by consecutive hydrothiolation of alkynes, both under nucleophilic and radical-induced conditions [22,23]. On the other hand, 1,3-dithioethers can be prepared by the nucleophilic substitution of compounds bearing suitable leaving groups at 1,3-positions of alkyl chains [21]. Because of their versatile applications, a great number of procedures have been developed to synthesize bis(thioethers) with varying degrees of success and a variety of limitations [19-31].

Over the last decade, organic synthesis has taken a major turn towards developing reaction conditions that are environmentally friendly and sustainable [32-36]. Mesoporous inorganic

oxides, which often facilitate various organic reactions, are considered suitable to promote eco-friendly chemical processes [36]. Organic reactions with a high selectivity under eco-friendly and sustainable conditions are attractive features in terms of the concepts of Green chemistry. Previously, we have developed silica-promoted facile and highly selective methods for N and S-alkylations/acylation from amines or thiols, respectively [37,38]. An equimolar mixture of a benzenethiol and allyl bromide on treatment with silica afforded allyl(phenyl)sulfane in excellent yield. Since alkenes are also known to undergo 'click' addition with thiols [39,40], excess use of thiols could effectively produce dithioethers, and based on a regioselective addition one could achieve either vicinal or 1,3-dithioethers in one-pot consecutive substitution–hydrothiolation processes (Scheme 1). Although both reactions are well-known, a search in the literature surprisingly revealed no general one-pot protocols for the preparation of dithioethers from allylic substrates. Recently, Banerjee and co-workers reported on the simple synthesis of thioethers by silica NPs, where a single example of a reaction of an allyl bromide and excess benzenethiol was studied [41,42]. The reaction was carried out in the presence of silica NPs and water, and they isolated 1,3-dithioether by an anti-Markovnikov addition. However, there is no report on the metal-free hydrothiolation of allylic substrates in a Markovnikov fashion to afford 1,2-dithioethers in one-pot reactions. In this paper, we wish to report our investigations on the reaction of allyl halides with excess thiols promoted by silica gel, which finally constitutes distinct protocols for one-pot, solvent-free substitution and regioselective additions to produce either 1,2 or 1,3-dithioethers.

Results and Discussion

Following our previous experience [37,38], we first attempted the magnetic stirring of a mixture of allyl bromide and benzenethiol in a 1:2.5 ratio by using pre-calcined silica gel at room temperature that indeed led to the formation of 1,2-dithioether in 91% yield. On the other hand, if silica gel moistened with a few drops of water was used for the same reaction, the regioselective anti-Markovnikov addition product, i.e., 1,3-dithioether, (1-(3-(phenylthio)propylthio)benzene) was obtained in 83% yield. In both cases, a minimal amount of diphenyldisulfide (5–10%) was formed [43,44], which was easily separable from the reaction mixture by column chromatography. Since the choice of silica led to the production of highly regioselective products, we wanted to optimize both conditions to establish them as general protocols. Table 1 shows the optimization of the reactions of different allylic substrates with benzenethiol. Silica gel (directly from the container, commercially available) was used either pre-activated by heating at 100 °C under vacuum for 1 h and then cooled under vacuum for use under conditions A or moist with water (0.1 mL water for 0.5 g of silica) for use under conditions B. It was observed that allyl bromide or allyl iodide underwent sequential substitution–addition reactions entirely regioselectively with comparable yields (Table 1, entries 1–5), whereas allyl chloride showed varying results under conditions A or B, and allyl acetate did not undergo any desired reaction, but merely produced the disulfide from oxidative dimerization of the thiol (Table 1, entries 6–8). Allyl tosylate, however, produced the desired thioethers in a regioselective manner, but with relatively low yields (Table 1, entries 9 and 10). Interestingly, allylphenylsulfane or allyl phenyl ether entirely followed an anti-Markovnikov addition, under both conditions, A and B (Table 1, entries 11–14).

With the two distinct conditions, we examined the scope of these one-pot tandem reactions of allyl bromide with a variety of thiols under both conditions. The results are presented in Table 2. Arylthiols bearing different functional groups like CH_3, OCH_3, Cl or F were reacted with allyl bromide in the presence of pre-calcined and dry silica affording good to excellent yields of the corresponding 1,2-dithioethers (Table 2, entries 1, 3, 5, 7, 9, 11 and 17). 2-Naphthylthiol also underwent a similar regioselective Markovnikov addition, resulting in the corresponding 1,2-dithioether in 82% yield (Table 2, entry 18). Extending the protocol to aliphatic thiols, such as *n*-pentylthiol and cyclohexylthiol also afforded regioselective dithioether in good yields (Table 2, entries 13 and 15). In all the cases, we observed 100% Markovnikov addition products and no anti-Markovnikov products were detected. We now turned our attention to the other conditions B – the use of moist silica gel. Again, a variety of aromatic thiols, including those that were used for the conditions A, were employed to react with allyl bromide in the presence of silica moist with a few drops of

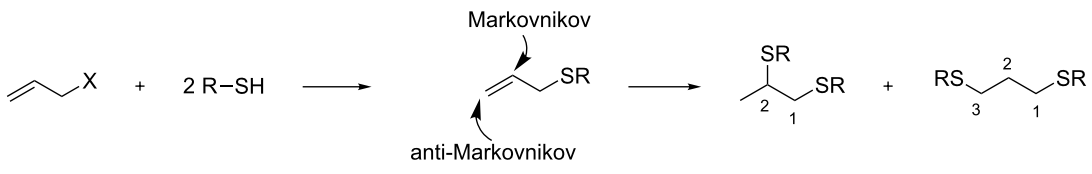

Scheme 1: Sequential substitution-addition reactions of thiols with allyl halides leading to the formation of 1,2 or 1,3-dithioethers.

Table 1: Optimization of one-pot sequential substitution–hydrothiolation of allylic substrate with excess benzenethiol over silica at room temperature.

Entry	CH_2=CH-CH_2-X	Conditions[a]	Time (h)	Product[b]/Yield[c] (%)
1	X = Br	A	6	1,2-dithioether/77
2	X = Br	A	11	1,2-dithioether/91
3	X = Br	B	20	1,3-dithioether/83
4	X = I	A	12	1,2-dithioether/89
5	X = I	B	20	1,3-dithioether/85
6	X = Cl	A	15	1,2-dithioether/57
7	X = Cl	B	30	diphenyldisulfide/83
8	X = OAc	A	24	diphenyldisulfide/90
9	X = OTs	A	8	1,2-dithioether/75
10	X = OTs	B	22	1,3-dithioether/68
11[d]	X = SPh	A	5	1,3-dithioether/83
12[d]	X = SPh	B	12	1,3-dithioether/80
13[d]	X = OPh	A	6	3-phenoxythioether/89
14[d]	X = OPh	B	14	3-phenoxythioether/82
15	X = Br	Neat mixture	20	no dithioether is formed

[a]Conditions A: allylic compound and PhSH (1:2.5 mmol) over pre-calcined dry silica gel (0.5 g); conditions B: allylic compound and PhSH (1:2.5 mmol) over moistened silica gel (0.5 g). [b]In each case 5–10% diphenyldisulfide was formed except in entries 6–8. [c]Yield refers to isolated pure product and no other constitutional isomer was detected. [d]Thiol (1.2 mmol) was used for entries 11–13.

Table 2: Regioselective one-pot synthesis of 1,2 and 1,3-dithioethers using dry (pre-calcined) or moistened silica gel at room temperature.

Entry	Thiol	Conditions[a]	Time (h)	Product	Yield[b] (%)
1	C_6H_5-SH	A	10	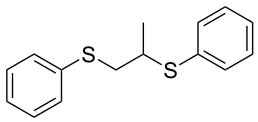	91
2	C_6H_5-SH	B	22	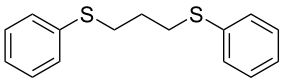	81
3	4-(H_3C)C_6H_4-SH	A	6	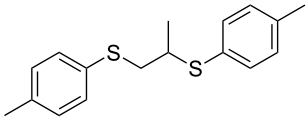	87
4	4-(H_3C)C_6H_4-SH	B	20	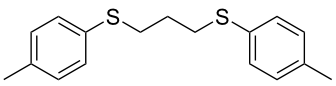	78
5	4-(H_3CO)C_6H_4-SH	A	6.5	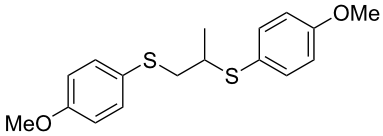	78
6	4-(H_3CO)C_6H_4-SH	B	18	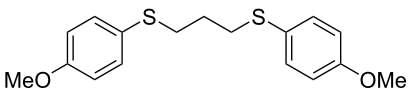	76
7	4-(Cl)C_6H_4-SH	A	6	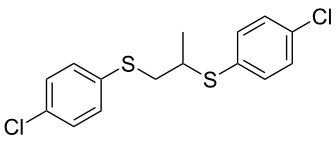	83

Table 2: Regioselective one-pot synthesis of 1,2 and 1,3-dithioethers using dry (pre-calcined) or moistened silica gel at room temperature. (continued)

8	4-(Cl)C_6H_4-SH	B	15	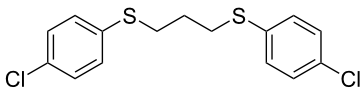	87
9	4-(F)C_6H_4-SH	A	8	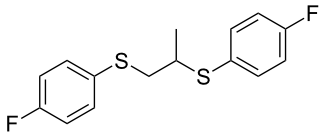	80
10	4-(F)C_6H_4-SH	B	16	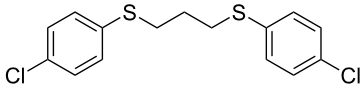	84
11	2,6-$(CH_3)_2$)C_6H_3-SH	A	8	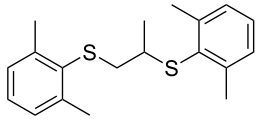	74
12	2,6-$(CH_3)_2$)C_6H_3-SH	B	20	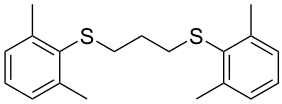	77
13	*n*-C_5H_{11}-SH	A	9	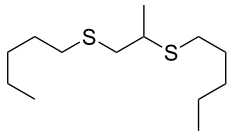	67
14	*n*-C_5H_{11}-SH	B	16	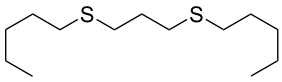	71
15	Cy-SH	A	10	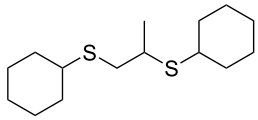	65
16	Cy-SH	B	18	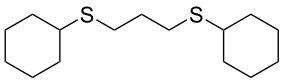	67
17	2-(H_3C)C_6H_4-SH	A	7	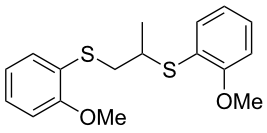	71
18	2-$C_{10}H_7$-SH	A	9	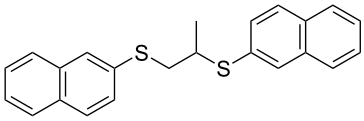	82
19[c]	C_6H_5-SH	B	22	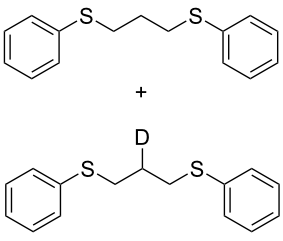	

Table 2: Regioselective one-pot synthesis of 1,2 and 1,3-dithioethers using dry (pre-calcined) or moistened silica gel at room temperature. (continued)

20	C_6H_5-SH	A[d]	15	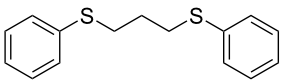	82

[a]Conditions A: allylic compound and PhSH (1:2.5 mmol) over pre-calcined dry silica gel (0.5 g); conditions B: allylic compound and PhSH (1:2.5 mmol) over moist silica gel (0.5 g). [b]Yield refers to isolated pure product; in each case 5–10% diphenyldisulfide was formed and isolated. [c]D_2O (0.5 mL for 0.5 g silica gel) was used instead of H_2O. [d]Mixture of silica and sodium silicate (1:1 w/w; 0.5 g for 1 mmol of allyl bromide) was used after drying under vacuum.

water, and we isolated entirely regioselective 1,3-dithioethers (Table 2, entries 2, 4. 6, 8, 10 and 12). The same selectivity was observed in the reaction of aliphatic thiols (acyclic or alicyclic), viz. *n*-pentane-1-thiol and cyclohexanethiol, with allyl bromide to afford the corresponding 1,3-dithioethers in 71% and 67% yield, respectively (Table 2, entries 14 and 16). In these cases, we did not detect any Markovnikov addition products. Thus, moistened silica gel turns out to be effective for sequential substitution reactions, and entirely anti-Markovnikov addition, while pre-calcined dry silica gel could efficiently give rise to only Markovnikov addition products. The reactions over dry silica gel appear to be faster than the procedure using moist silica. Moreover, the 1,2-dithioethers are formed in slightly better yields than the corresponding 1,3-analogues. We also experienced that aromatic thiols, under both conditions A and B, give better yields than aliphatic thiols.

We assume that the nature of the silica surface and its possible interactions with thiols is responsible for the notable regioselectivity in the hydrothiolation of allylsulfane. It is known that amorphous or mesoporous silica consists of silanol groups and siloxane bridges that determine its surface properties, and the concentration of these OH groups depends mostly on the actual process of calcinations [45-47]. Based on Zhuravlev's physicochemical model of silica surface [45], it may be presumed that the moistened silica surface is covered with a single layer or multilayer of adsorbed water, which might disappear during the calcination process. Since allylphenylsulfane on hydrothiolation affords the anti-Markovnikov product under both conditions A and B (Table 1, entries 11 and 12), we presume that there might be an influence of the generated acid in the first step under dry conditions A. In the absence of water, the generated HBr in the first step might activate the double bond and subsequent assistance by the neighbouring sulfur atom coupled with the stability of the secondary carbocation lead to the Markovnikov addition resulting in the exclusive formation of 1,2-dithioether (Scheme 2, conditions A). On the other hand, the moist silica consisting of a single layer or multilayered adsorbed water promotes thiols to bind with allylsulfane, and the subsequent addition takes place in an anti-Markovnikov approach (Scheme 2, conditions B).

In order to find evidence for the role of silica adsorbed water, we conducted the following experiments: (i) the reaction was carried out under conditions A in the presence of an exogenous base (sodium silicate; see Experimental), which leads to the formation of anti-Markovnikov product only (1,3-dithioether) (Table 2, entry 20); (ii) reactions under conditions B with varying quantities of H_2O (0.5 mL and 1.0 mL) did not exhibit any significant changes producing only 1,3-dithioethers in quantities; (iii) dry HCl gas was passed through pre-calcined silica and was used for the hydrothiolation of allylphenylsulfane, exclusively yielding an Markovnikov addition product (1,2-dithioether); (iv) an experiment was carried out with silica moistened with D_2O (Table 2, entry 19), which afforded a mixture of 1,3-bis(phenylthio)propane and [2-D]1,3-dithioether as seen from the ^{1}H NMR spectrum of the mixture and calculated to be in the ratio of 1:3.9. In the ^{13}C NMR spectrum, the deuterated carbon appeared as a triplet at δ 27.96, J = 20 Hz (see Supporting Information File 1). This observation supports that conditions B might occur through an initial thiol proton exchange with D_2O (PhS–H → PhS–D).

Conclusion

We have demonstrated that the choice of silica gel, either dry or moistened, could lead to highly selective pathways for the preparation of different dithioethers. The sequential reactions in one-pot protocols are robust, neutral, metal-free and notably selective with a broad range of substrates. The diverse reactivity of silica gel in the formation of vicinal or 1,3-dithioethers might not only spur the adaptation of existing procedures for selective dithioether preparation but also attract novel applications. Further utilizations of this diverse reactivity are currently being explored in our laboratory.

Experimental

All chemicals were purchased from commercial suppliers and used without further purification. IR spectra were recorded on

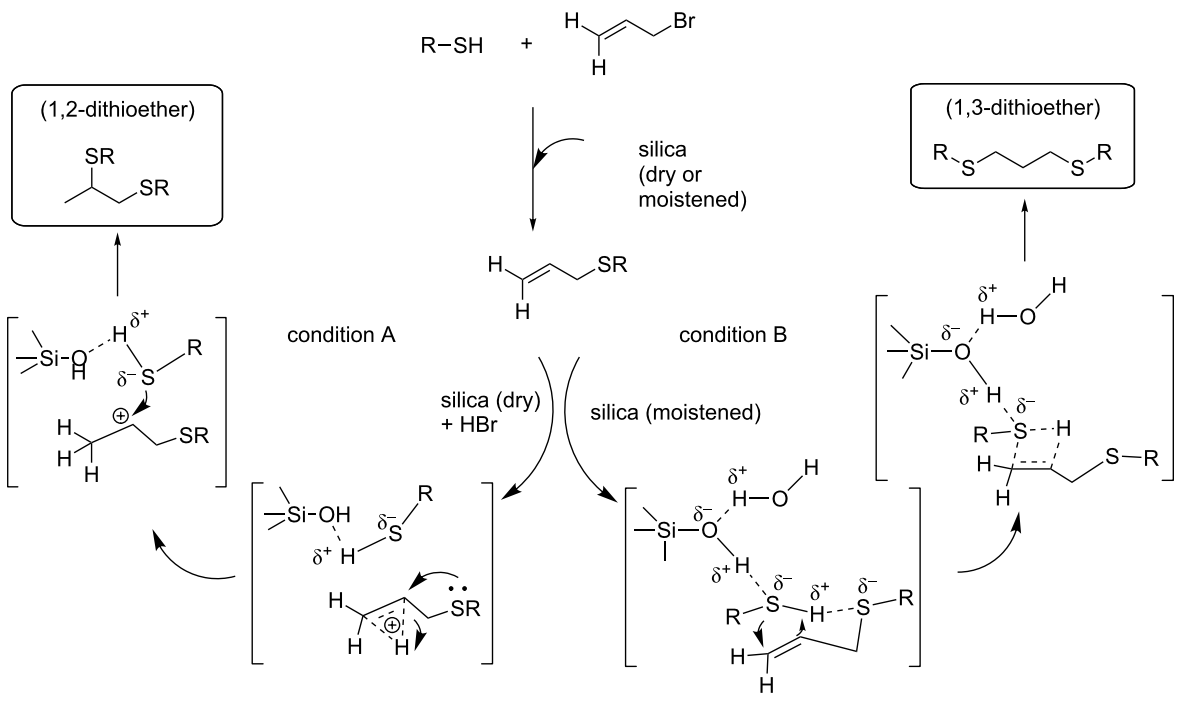

Scheme 2: Plausible mechanisms for the regioselective formation of vicinal and 1,3-dithioethers by using dry or moistened silica gel.

an FTIR spectrophotometer (8300 Shimadzu) using Nujol mulling for liquid compounds and KBr pellets for solid compounds. NMR spectra were recorded on a Varian AV-300 spectrometer with $CDCl_3$ as a solvent. Chemical shifts (δ) are reported in ppm and referenced to TMS for ^{1}H NMR spectra and residual solvent signals for ^{13}C NMR spectra as internal standards. Coupling constants (*J*) are reported in Hertz (Hz). Standard abbreviations indicating multiplicity were used as follows: s = singlet, d = doublet, t = triplet, q = quartet, qnt = quintet, m = multiplet. Melting points were determined by heating in an open capillary tube. High resolution mass spectra (HRMS) were performed in a Micromass Q-TOF Spectrometer under ESI (positive mode) by the services at the Indian Association for the Cultivation of Science, Kolkata.

Calcination: Commercially available silica gel (Merck, India; Grade: TLC; HF_{254}) was heated under vacuum at 100 °C for 1 h, cooled, and then be used for the reaction or stored in a glass-stoppered flask for at least two weeks.

Moistened silica: Commercially available silica gel (Merck, India; Grade: TLC; HF_{254}) was mixed with water and used for the reactions. For column chromatography: silica (60–120 μm) (Thomas Baker, India), and for TLC, Merck plates coated with silica gel 60, F_{254} were used.

General procedure for Table 2 (route A or B)

Route A: A mixture of allyl bromide (1 mmol) and thiol (2.5 mmol) was mixed with pre-calcined dry silica gel (Table 2, for entries 1, 3, 5, 7, 9, 11, 13, 15, 17 and 18)

Route B: A mixture of allyl bromide (1 mmol) and thiol (2.5 mmol) was mixed with silica gel (0.5 g), moistened with two drops of water, (Table 2, for entries 2, 4, 6, 8, 10, 12, 14 and 16), and stirred magnetically by using a spin bar for the respective times listed in Table 2. The reaction was monitored by TLC. After completion the product was purified by column chromatography over silica gel. Elution with light petroleum or mixtures of ethyl acetate/light petroleum (see Supporting Information File 1) furnished the desired dithioether. All products were characterized by IR, ^{1}H NMR, ^{13}C NMR and HRMS data.

Procedure for the reaction using a mixture of silica and sodium silicate under conditions A (Table 2, entry 20)

Equal quantities of silica gel and sodium silicate (1 g each) were mixed, dried under vacuum at 100 °C for 1 h, cooled, and used for the reaction. The mixture (500 mg) was stirred in water (10 mL) and its pH was measured to be 12.7. A mixture of allyl bromide (1 mmol) and benzene thiol (2.5 mmol) was thoroughly mixed with the mixture of dry silica gel and sodium sili-

cate (500 mg), and the solid reaction mixture stirred for 15 h at room temperature. After the reaction, the product was purified by column chromatography (82% yield) and characterized as 1-(3-(phenylthio)propylthio)benzene (1,3-dithioether).

Supporting Information

Supporting information features FTIR, ^{1}H NMR, ^{13}C NMR and HRMS data for 1,2 and 1,3-dithioethers (Table 2, entries 1–19) and ^{1}H NMR and ^{13}C NMR spectra for compounds listed in Table 2, entries 1–19.

Supporting Information File 1

Characterization data for compounds listed in Table 2, entries 1–19.
[http://www.beilstein-journals.org/bjoc/content/supplementary/1860-5397-10-5-S1.pdf]

Supporting Information File 2

^{1}H NMR and ^{13}C NMR spectra for compounds listed in Table 2, entries 1–19.
[http://www.beilstein-journals.org/bjoc/content/supplementary/1860-5397-10-5-S2.pdf]

Acknowledgements

Financial support from the Department of Science and Technology, New Delhi, India (Grant No SR/S1/OC-86/2010) is gratefully acknowledged. SK thanks the University Grants Commission, New Delhi for the award of a fellowship. We wish to thank the reviewers for making useful comments for the improvement of the manuscript.

References

1. Cremlyn, J. R. *An Introduction to Organosulfur Chemistry;* John Wiley and Sons: Chichester, 1996.
2. Whittman, W. W. *Organosulfur Chemistry;* Oxford University Press: New York, 1995.
3. Page, C. B. P. *Organosulfur Chemistry I & II;* Springer: Berlin, 1999.
4. Montaño, A.; Beato, M. V.; Mansilla, F.; Orgaz, F. *J. Agric. Food Chem.* **2011,** *59,* 1301–1307. doi:10.1021/jf104494j
5. Jan, C.-R.; Lo, H.-R.; Chen, C.-Y.; Kuo, S.-Y. *J. Nat. Prod.* **2012,** *75,* 2101–2107. doi:10.1021/np3005248
6. Srogl, J.; Liu, W.; Marshall, D.; Liebeskind, L. S. *J. Am. Chem. Soc.* **1999,** *121,* 9449–9450. doi:10.1021/ja991654e
7. Huang, C.-N.; Horng, J.-S.; Yin, M.-C. *J. Agric. Food Chem.* **2004,** *52,* 3674–3678. doi:10.1021/jf0307292
8. Daemmrich, A.; Bowden, E. M. *Chem. Eng. News* **2005,** *83,* 28–42.
9. Oudart, Y.; Artero, V.; Pécaut, J.; Fontecave, M. *Inorg. Chem.* **2006,** *45,* 4334–4336. doi:10.1021/ic060510f
   See for selected examples.
10. Kannan, R.; Pillarsetty, N.; Gali, H.; Hoffman, J. T.; Barnes, L. C.; Jurisson, S. S.; Smith, J. C.; Volkert, W. A. *Inorg. Chem.* **2011,** *50,* 6210–6219. doi:10.1021/ic200491z
11. Knorr, M.; Guyon, F.; Khatyr, A.; Strohmann, C.; Allain, M.; Aly, M. S.; Lapprand, A.; Fortin, D.; Harvey, D. P. *Inorg. Chem.* **2012,** *51,* 9917–9934. doi:10.1021/ic301385u
12. Li, J.-R.; Bu, X.-H.; Jiao, J.; Du, W.-P.; Xu, X.-H.; Zhang, R.-H. *Dalton Trans.* **2005,** 464–474. doi:10.1039/b416576b
13. Levason, W.; Reid, G.; Zhang, W. *Dalton Trans.* **2011,** *40,* 8491–8506. doi:10.1039/C1DT10317B
14. Awaleh, M. O.; Badia, A.; Brisse, F.; Bu, X.-H. *Inorg. Chem.* **2006,** *45,* 1560–1574. doi:10.1021/ic051357c
15. Cohen, A.; Yeori, A.; Goldberg, I.; Kol, M. *Inorg. Chem.* **2007,** *46,* 8114–8116. doi:10.1021/ic701370t
16. Poulain, S.; Julien, S.; Duñach, E. *Tetrahedron Lett.* **2005,** *46,* 7077–7079. doi:10.1016/j.tetlet.2005.07.161
17. Lian, B.; Beckerle, K.; Spaniol, T. P.; Okuda, J. *Angew. Chem., Int. Ed.* **2007,** *46,* 8507–8510. doi:10.1002/anie.200703218
18. Diéguez, M.; Ruiz, A.; Claver, C.; Pereira, M. M.; d'a Rocha Gonsalves, A. M. *J. Chem. Soc., Dalton Trans.* **1998,** 3517–3522. doi:10.1039/a803626h
19. Kondo, T.; Mitsudo, T. *Chem. Rev.* **2000,** *100,* 3205–3220. doi:10.1021/cr9902749
    See for reviews.
20. Wang, L.; He, W.; Yu, Z. *Chem. Soc. Rev.* **2013,** *42,* 599–621. doi:10.1039/c2cs35323g
21. Jin, Z.; Xu, B.; Hammond, B. G. *Eur. J. Org. Chem.* **2010,** 168–173. doi:10.1002/ejoc.200901101
22. Peach, E. M.; Patai, S., Eds. *The Chemistry of the Thiol Group;* John Wiley & Sons: London, 1979; p 721.
23. Curran, P. D.; Trost, M. B.; Fleming, I., Eds. *Comprehensive Organic Synthesis;* Pergamon: New York, 1991; Vol. 4, pp 715–831. doi:10.1016/B978-0-08-052349-1.00108-6
24. Hartley, F. R.; Murray, S. G.; Levason, W.; Soutter, H. E.; McAuliffe, C. A. *Inorg. Chim. Acta* **1979,** *35,* 265–277. doi:10.1016/S0020-1693(00)93450-9
    See for selected examples.
25. Kitamura, T.; Matsuyuki, J.; Taniguchi, H. *J. Chem. Soc., Perkin Trans. 1* **1991,** 1607–1608. doi:10.1039/p19910001607
26. Usugi, S.; Yorimitsu, H.; Shinokubo, H.; Oshima, K. *Org. Lett.* **2004,** *6,* 601–603. doi:10.1021/ol036391e
27. Troyansky, E. I.; Ismagilov, R. F.; Korneeva, E. N.; Pogosyan, M. S.; Nikishin, G. I. *Mendeleev Commun.* **1995,** *5,* 18–20. doi:10.1070/MC1995v005n01ABEH000441
28. Yorimitsu, H.; Wakabayashi, K.; Shinokubo, H.; Oshima, K. *Bull. Chem. Soc. Jpn.* **2001,** *74,* 1963–1970. doi:10.1246/bcsj.74.1963
29. Ishii, A.; Toda, T.; Nakata, N.; Matsuo, T. *J. Am. Chem. Soc.* **2009,** *131,* 13566–13567. doi:10.1021/ja903369q
30. Meppelder, G.-J. M.; Beckerle, K.; Manivannan, R.; Lian, B.; Raabe, G.; Spaniol, T. P.; Okuda, J. *Chem.–Asian J.* **2008,** *3,* 1312–1323. doi:10.1002/asia.200800064
31. Yamagiwa, N.; Suto, Y.; Torisawa, Y. *Bioorg. Med. Chem. Lett.* **2007,** *17,* 6197–6201. doi:10.1016/j.bmcl.2007.09.021
32. Ballini, R., Ed. *Eco-friendly Synthesis of Fine Chemicals;* RSC Publishing: Cambridge, 2009; pp 275–292. doi:10.1039/9781847559760
33. Winterton, N. *Chemistry for Sustainable Technologies;* RSC Publishing: Cambridge, 2010.
34. Dunn, P. J.; Well, A.; Williams, M. T., Eds. *Green Chemistry in the Pharmaceutical Industry;* Wiley-VCH: Weinheim, 2010.

35. Zhang, W.; Cue, B. W., Eds. *Green Techniques for Organic Synthesis and Medicinal Chemistry;* Wiley: Chichester, 2012; pp 69–97. doi:10.1002/9780470711828
36. Lancaster, M. *Green Chemistry: An Introductory Text;* RSC Publication: Cambridge, 2002; p 84.
37. Basu, B.; Paul, S.; Nanda, A. K. *Green Chem.* **2010,** *12,* 767–771. doi:10.1039/b925620b
38. Basu, B.; Paul, S.; Nanda, A. K. *Green Chem.* **2009,** *11,* 1115–1120. doi:10.1039/B905878H
39. Hoyle, C. E.; Bowman, C. N. *Angew. Chem., Int. Ed.* **2010,** *49,* 1540–1573. doi:10.1002/anie.200903924
40. Dondoni, A. *Angew. Chem., Int. Ed.* **2008,** *47,* 8995–8997. doi:10.1002/anie.200802516
41. Banerjee, S.; Das, J.; Alvarez, R. P.; Santra, S. *New J. Chem.* **2010,** *34,* 302–306. doi:10.1039/b9nj00399a
42. Banerjee, S.; Das, J.; Santra, S. *Tetrahedron Lett.* **2009,** *50,* 124–127. doi:10.1016/j.tetlet.2008.10.110
43. Patai, S.; Rappoport, Z.; Stirling, C. *The Chemistry of Sulphones and Sulfoxide;* John Wiley & Sons: Chichester, 1988; pp 17–31. doi:10.1002/0470034386
44. Bäckvall, J.-E. *Modern Oxidation Methods;* Wiley-VCH: Hoboken, NJ, 2011.
45. Zhuravlev, L. T. *Colloids Surf., A* **2000,** *173,* 1–38. doi:10.1016/S0927-7757(00)00556-2
46. Liu, J.; Feng, D.; Fryxell, G. E.; Wang, L.-Q.; Kim, A. Y.; Gong, M. *Chem. Eng. Technol.* **1998,** *21,* 97–100. doi:10.1002/(SICI)1521-4125(199801)21:1<97::AID-CEAT97>3.0.CO;2-W
47. Park, J.; Kim, H.; Park, J. *Int. J. Environ. Sci. Dev.* **2012,** *3,* 81–85. doi:10.7763/IJESD.2012.V3.192

License and Terms

Tetrahedron Letters 55 (2014) 6596–6600

Contents lists available at ScienceDirect

Tetrahedron Letters

journal homepage: www.elsevier.com/locate/tetlet

Graphene oxide (GO)-catalyzed chemoselective thioacetalization of aldehydes under solvent-free conditions

Babli Roy, Debasish Sengupta, Basudeb Basu *

Department of Chemistry, North Bengal University, Darjeeling 734013, India

ARTICLE INFO

Article history:
Received 7 August 2014
Revised 6 October 2014
Accepted 8 October 2014
Available online 14 October 2014

Keywords:
Aldehydes
Chemoselectivity
Dithioacetal
Graphene oxide
Thiols

ABSTRACT

An efficient method for the synthesis of open chain, cyclic, and unsymmetrical dithioacetals from aryl/hetero-aryl/aliphatic aldehydes is described. The reaction is performed using graphene oxide (GO) as the catalyst under solvent-free and aerobic conditions. High chemoselectivity is observed in the reaction as aryl/alkyl ketones do not give thioketals under the condition.

The efficiency of graphene oxide (GO) and other chemically modified graphenes (CMGs) as the carbocatalysts has raised enormous interest since the seminal papers from Bielawski and coworkers.[1] Catalytic applications of carbonaceous sustainable and easily accessible GO in diverse organic reactions are one of the recent cherished goals.[2] GO possesses rich chemical functionality, is slightly acidic (pH 4.5 at 0.1 mg mL^{-1}),[3] and has long been recognized as having strong oxidizing properties.[4] Accordingly, GO has been mostly employed in oxidation of different functional groups.[5] For example, oxidation of benzyl alcohol to benzaldehyde,[5a,b] oxidation of thiol to disulfide,[5c] or amine to imine etc.[5d] Because of high efficiency and metal-free catalytic activity of GO or partially reduced GO (rGO), efforts are on to develop variety of organic transformations catalyzed by these carbonaceous materials.[2] Although GO has been utilized as an oxidation catalyst in various organic reactions, its use as an acid catalyst has remained relatively unexplored.[5]

Generally, thioacetals are formed as the result of Brønsted and Lewis acid catalyzed condensation reaction of aldehydes and ketones with thiols or dithiols and a vast number of methods are available in the literature.[6] Over the past decade, several heterogeneous acid catalysts such as *p*-TsOH/silicagel,[7a] $H_3PW_{12}O_{40}/SiO_2$,[7b] Montmorillonite K-10 Clay,[7c] Amberlyst-15,[7d] PPA/SiO_2,[7e] Melamine trisulfonic acid (MTSA),[7f] silica-sulfuric acid (SSA),[7g] solid-supported dithiolanylium or dithianylium tetrafluoroborate salts,[7h] and also ionic liquids,[7i,j] have been employed for the preparation of thioacetals. However, moisture sensitivity and reactivity of thioacetals toward acidic sources for reversible reactions pose a great limitation for their preparation in high yield and most of the methods are often unsuitable for use in large-scale applications. Moreover, while in most cases the catalyst is not recoverable, heterogeneous acid catalysts often do not find wide applicability to various substrates. We were interested to explore the feasibility and catalytic efficiency of GO in thioacetalization of aldehydes and ketones. GO has been used in the dimethylacetal formation from aldehydes using methanol.[8] But, use of thiols in place of methanol poses the possibility of intermolecular disulfide formation.[5c] We recently showed that GO can be used as a catalyst under controlled conditions so as to avoid the oxidation of secondary benzyl alcohols as well as minimize that of thiols.[9]

We herein report an efficient and practical method for the preparation of dithioacetal from aryl/alkyl aldehydes with the aid of catalytic amount of graphene oxide (GO). The reaction is highly selective to aldehyde carbonyl groups, can be carried out under solvent-free and mild conditions, and applicable to variety of aryl and alkyl aldehydes including hetero-aryl aldehydes as well as with diverse aromatic/aliphatic thiols. As a further extension of this reaction, unsymmetrical dithioacetals have been prepared in excellent yields by using two different aliphatic thiols (Scheme 1).

Although GO is commonly used as an oxidation catalyst,[4] and thiols can produce disulfides via oxidative coupling in the presence of GO,[5c] we demonstrate here that the catalytic role of GO can be diverse and tuned by changing its loading and reaction conditions.

* Corresponding author.
E-mail address: basu_nbu@hotmail.com (B. Basu).

http://dx.doi.org/10.1016/j.tetlet.2014.10.043
0040-4039/

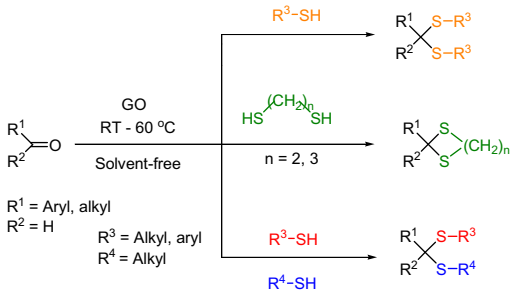

Scheme 1. General scheme illustrating GO-catalyzed diverse dithioacetal formation.

To begin our study, we prepared GO from graphite powder according to the modified Hummers method,[10] followed by exfoliation under sonication and isolation after centrifugation. The FT-IR spectrum of the resulting GO was compared with that of the reported absorption bands,[8,11] and found fairly similar absorption bands for the functional groups (See ESI S3.1). Optimization of the GO-catalyzed thioacetalization was examined with *p*-anisaldehyde and *n*-pentanethiol (1:2.2 ratios) as the model case and the results are shown in Table 1.

Initially, a mixture of the aldehyde and mercaptan (in 1:2.2 ratios) was gently stirred in neat at room temperature in the presence of GO (10 mg $mmol^{-1}$ of the aldehyde) under aerobic condition. Monitoring the reaction by tlc at intervals showed the presence of the starting aldehyde along with the desired dithioacetal even after 24 h. The reaction was stopped and after the separation of the catalyst, the residue was subjected to column chromatography to isolate the desired dithioacetal in 51% yield (entry 1). Increasing the quantity of GO (50 mg $mmol^{-1}$ of the aldehyde) revealed that nearly complete conversion of the aldehyde to dithioacetal could be achieved at room temperature within 3 h under aerobic condition (entry 3). Significantly, there was no detectable amount of disulfide formed in the reaction from the oxidative dimerization of pentanethiol even under the aerobic condition. A control experiment was performed in the absence of the GO under similar reaction condition, which did not produce any dithioacetal even after 24 h (entry 4). In order to see any faster conversion, the reaction was also carried out at 60 °C. This however resulted in partial conversion of the mercaptan into the corresponding disulfide along with the desired dithioacetal in a relatively lower yield (entry 5). Moreover, the same reaction at 60 °C and under a blanket of N_2 did not stop the formation of disulfide (entry 6). Conducting the experiments in a solvent (THF, toluene or water) showed rather a negative effect affording the desired dithioacetal in relatively lower yields (entries 7–9). To scale up the reaction, one set of reaction was performed (in 5 mmol) using the same quantity of catalyst (GO = 50 mg). Excellent yield of the dithioacetal was realized in this case as well signifying that the minimum quantity of the catalyst can promote the reaction in a longer time (entry 10).

With this mild and solvent-free optimized condition at our hand (as in entry 3), we became interested to explore the general applicability of the reaction. Accordingly, a variety of aryl aldehydes were subjected to the reaction in the presence of thiols. The results are presented in Table 2. It can be seen that aryl aldehydes bearing different functional groups react easily with aliphatic thiols in the presence of catalytic amount of GO under solvent-free aerobic condition. The reactions were completed in 3–8 h and the products were realized in excellent yields (Table 2, entries 1–5). Higher temperature was required for α-naphthaldehyde and *p*-chlorobenzaldehyde, which caused partial formation of disulfide (~5–8%) (entries 6 and 7). However, the reaction with *p*-nitrobenzaldehyde needed much longer time and higher temperature, and gave the dithioacetal in a relatively lower yield along with disulfide (Table 2, entry 8). Trying the reaction with aromatic thiols afforded the desired dithioacetal in 80–85% yields but achieved only at higher temperature (60 °C) and was associated with the formation of diaryl disulfides in 8–12% isolated yields (entries 9–11). The disulfides however could be separated easily from dithioacetal by column chromatography over silica gel. In the case of using 1,2- and 1,3-dithiol, corresponding cyclic thioacetals were obtained in excellent yields (95–98%) and the reaction was also successful with aliphatic cyclohexyl aldehyde (entries 12–15). However, there was no such formation of dithioketals from a ketone under the GO-catalyzed reaction condition (entry 16). So, excellent chemoselectivity is observed between the aldehyde and keto- carbonyl groups.

Heteroaryl compounds often exhibit promising pharmacological activities and open chain dithioacetals of heteroaryl aldehydes such as thiophene-based dithioacetals are important scaffolds for design and discovery of new medicines.[12] Since the reaction conditions are mild and solvent-free, we were interested to extend the GO-catalyzed dithioacetalization to thiophene aldehydes and also of other heteroaryl aldehydes. Indeed, 5-bromothiophene-2-carbaldehyde and furfural result in the formation of corresponding dithioacetals with variety of aliphatic and benzenethiol without any difficulty (Table 3, entries 1–5). Other heteroaryl aldehyde indole-3-carbaldehyde also produces corresponding dithioacetals with long chain aliphatic thiols without any difficulty and in excellent yields (Table 3, entry 6). Cyclic dithioacetals of furfural and indole-3-carbaldehyde were obtained in excellent yields under

Table 1
Optimization of dithioacetal formation from *p*-anisaldehyde and *n*-pentane thiol[a]

Entry	GO (in mg $mmol^{-1}$)	Reaction medium	Time (h)/Temp (°C)	Disulfide[b] (%)	Dithioacetal[b] (%)
1	10	Neat	24/rt	Not observed	51
2	25	Neat	24/rt	Not observed	65
3	**50**	Neat	**3/rt**	**Not observed**	**95**
4	Nil	Neat	24/rt	Not observed	Not observed
5	50	Neat	3/60	10	61
6[c]	50	Neat	3/60	8	57
7	50	THF	20/rt	Trace[d]	35
8	50	PhMe	12/rt	Not observed	68
9	50	H_2O	12/rt	Trace[d]	55
10[e]	50	Neat	16/rt	Trace[d]	91

[a] *p*-Anisaldehyde (1 mmol), *n*-pentanethiol (2.2 mmol).
[b] Isolated yield.
[c] Reaction carried out under N_2.
[d] Detected only on tlc, not isolated.
[e] *p*-Anisaldehyde (5 mmol), pentanethiol (11 mmol).

Table 2
GO-catalyzed thioacetalization of aldehydes with different thiols[a]

Entry	Aldehyde	Thiol	Time (h)	Temp.	Product	Yield[b] (%)
1	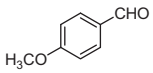	*n*-C_5H_{11}–SH	3	rt	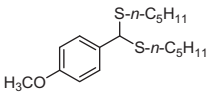	95
2	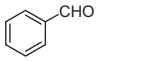	*n*-C_5H_{11}–SH	5	rt	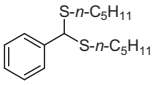	91
3	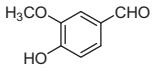	*n*-C_7H_{15}–SH	5	rt	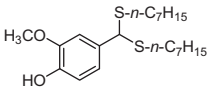	95
4	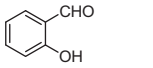	*n*-C_5H_{11}–SH	8	rt	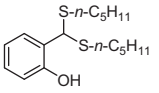	89
5	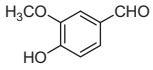	Bu^t–SH	5	rt	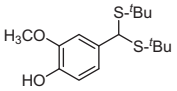	93
6[c]		*n*-C_7H_{15}–SH	3	60 °C	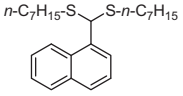	87
7[c]	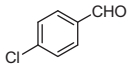	CySH	5	60 °C	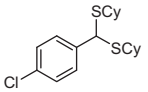	90
8[c]	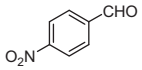	*n*-C_5H_{11}–SH	14	60 °C	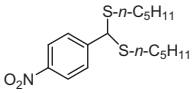	68
9[c]	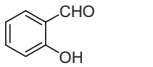	C_6H_5–SH	10	60 °C	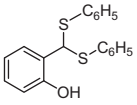	80
10[c]	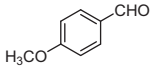	C_6H_5–SH	10	60 °C	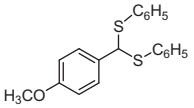	85
11[c]	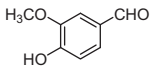	(4-H_3C)C_6H_4–SH	10	60 °C	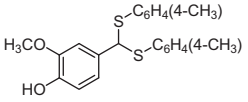	82
12[d]	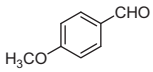		5	rt	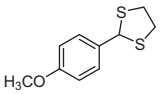	98
13[d]	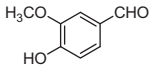		5	rt	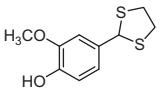	98
14[d]	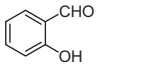		5	rt	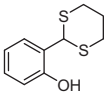	98
15[d]			5	rt	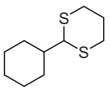	95
16	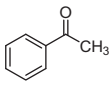	*n*-C_5H_{11}–SH	24	rt/60 °C	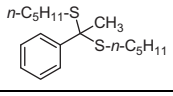	Not observed

[a] Aldehyde/thiol/GO (1 mmol:2.2 mmol:50 mg) and reactions were performed at room temperature.
[b] Isolated yield.
[c] Corresponding disulfides (5–12%) were formed.
[d] Aldehyde/thiol/GO (1 mmol:1.1 mmol:50 mg).

mild conditions (entries 7 and 8). In order to further broaden the scope of the reaction, we attempted synthesis of unsymmetrical dithioacetal using two different thiols. Gratifyingly, the reactions of *p*-anisaldehyde or vanillin with two different aliphatic thiols (*n*-pentyl- and *n*-heptyl thiols) resulted in the formation of unsymmetrical dithioacetals as the only product in 85–88% isolated yields

Table 3
GO-catalyzed thioacetalization of heteroaryl aldehydes[a]

Entry	Aldehyde	Thiol	Time (h)	Product	Yield[b] (%)
1	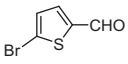	Bu^t–SH	8	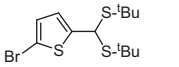	89
2[c]	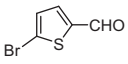	C_6H_5–SH	10	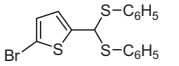	81
3	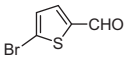	n-C_7H_{15}–SH	8	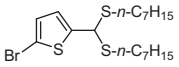	89
4		n-C_5H_{11}–SH	3	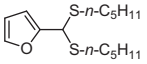	92
5		CySH	3	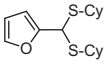	88
6	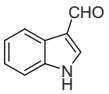	n-C_7H_{15}–SH	8	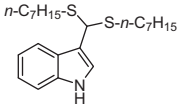	85
7[d]			3	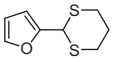	90
8[d]	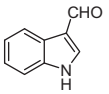		5	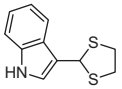	93

[a] Aldehyde/thiol/GO (1 mmol:2.2 mmol:50 mg) and reactions were performed at room temperature.
[b] Isolated yield.
[c] Isolated yield of disulfide was ~5%.
[d] Aldehyde/thiol/GO (1 mmol:1.1 mmol:50 mg).

Table 4
Unsymmetrical thioacetals from aryl aldehydes using two different thiols[a]

Entry	Aldehyde	Thiol (A)	Thiol (B)	Time (h)	Product	Yield[b] (%)
1	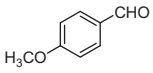	n-C_5H_{11}–SH	n-C_7H_{15}–SH	5	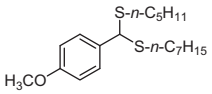	88[b]
2	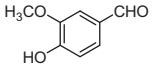	n-C_5H_{11}–SH	n-C_7H_{15}–SH	5	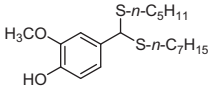	85[b]
3[c]	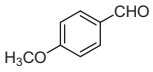	n-C_5H_{11}–SH	C_6H_5–SH	10	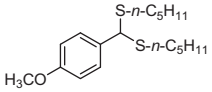	13[d]
					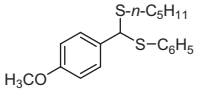	39[d]
					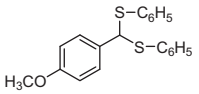	48[d]

[a] Thiol (A)/thiol (B)/GO (1.1 mmol:1.1 mmol:50 mg) for 1 mmol of aldehyde and the reaction was done at RT for entries 1 and 2.
[b] Isolated yield.
[c] Reaction performed at 60 °C.
[d] Product ratios are from HPLC analysis of the crude reaction mixture (See ESI S2.3).

(Table 4, entries 1 and 2). HPLC analysis of the crude product (before column chromatographic purification) showed the unsymmetrical thioether as the sole product. On the other hand, use of one aliphatic and one aromatic thiol gave rise to a mixture of all three possible products in varying proportions, as seen from the analysis of the crude product mixture by HPLC (Table 4, entry 3). Although the exact reason for this selectivity is not known, it might be attributable to the difference in reactivity between the two thiols. Using a mixture of aliphatic or aromatic thiols, formation of the thioacetal from benzenethiol in highest quantity amongst the three possible dithioacetals also supports this rationale. Since in entry 3, all three products were obtained as a non-isolable mixture, we

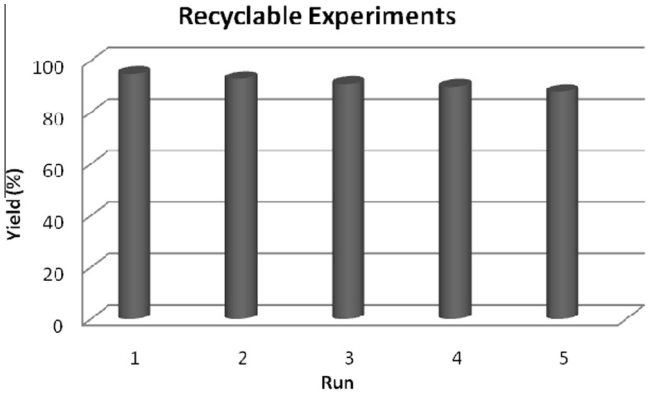

Figure 1. Recyclability of GO in the thioacetalization of *p*-anisaldehyde and *n*-pentanethiol.

tried to analyze the mixture by HPLC and compared the peaks with known products, leaving the third peak likely to be for the unsymmetrical dithioacetal.

As regards the plausible mechanism for the reaction, we wanted to probe the nature of active sites present in GO. In the recent years, the acidic nature of GO has been attributed mostly to the organosulfate group being originated during the oxidation of graphite using Hummers method in the presence of sulfuric acid,[2b,8] though previous measurements of acidic pH were attributable to the presence of surface attached carboxylic functions.[3] The FT-IR spectrum of GO showed the presence of carboxyl (1719 cm^{-1}; COOH stretching) and sulfate functional groups (1052 cm^{-1}; SO_3–H stretching), which are comparable with those reported in the literature (See ESI S3.1, Fig. 3).[8,11] We measured the pH of the GO in aqueous suspension (pH = 3.9; 50 mg in 50 ml 0.5 M aqueous NaCl solution), and found it in fair agreement with previous observations.[3] The pH of GO remains fairly similar when measured after the reaction and also of a mixture of *n*-pentane thiol and GO in water. On the other hand, thioacetal formation is greatly retarded when the reaction is carried out in water or in other organic solvents (Table 1, entries 7, 8 and 9). GO also gave positive Carius test and Lassaigne's test signifying qualitatively the presence of S-containing functional groups. The above results suggest that GO is an acid catalyst and we tend to believe that the acidity of GO might be originating from a combination of both carboxyl and organosulfate groups, which is more pronounced in neat. Mechanistically, surface active acidic functional groups of GO facilitate activation of the aldehyde carbonyl group, more effectively in neat condition, and subsequent nucleophilic attack by the thiol results in the eventual formation of thioacetal.

The reusability of the GO as heterogeneous acid catalyst was examined with the combination of reactants: *p*-anisaldehyde and *n*-pentanethiol in 1:2.2 ratios at room temperature. The GO was recovered from the first batch of reaction by centrifugation and washed with diethyl ether, dried, and reused for subsequent four batches of reactions. In all recycling experiments carried out at room temperature, appreciable conversions were achieved (Fig. 1). A comparison of the FT-IR spectra of the GO before and after use does not indicate any changes of the absorption bands, signifying that the catalyst remains same after the reaction (See ESI S3.1, Fig. 4)

In summary, GO was found to catalyze the formation of thioacetal from a neat mixture of aldehyde and thiol under mild, solvent-free, and aerobic conditions. Notable features of the methodology described herein are: operational simplicity, nil or negligible quantity of disulfide formation, applicability to a large variety of aryl/heteroaryl aldehydes, chemoselectivity, recyclability, and environmental compatibility. Thus it provides a practical approach for the preparation of open chain, cyclic, and unsymmetrical dithioacetals. The present method also demonstrates that controlled loading of GO in combination with reaction conditions could lead to the diversity in reaction types as well as the formation of the products, and is likely to spur more catalytic applications.

Acknowledgments

We thank the Department of Science and Technology, India for financial support (Grant No. SR/S1/OC-86). BR and DS thank UGC, and CSIR, New Delhi respectively, for award of their fellowships.

Supplementary data

Supplementary data associated with this article can be found, in the online version, at http://dx.doi.org/10.1016/j.tetlet.2014.10.043.

References and notes

1. Dreyer, D. R.; Bielawski, C. W. *Chem. Sci.* **2011**, *2*, 1233–1240.
2. (a) Navalon, S.; Dhakshinamoorthy, A.; Alvaro, M.; Garcia, H. *Chem. Rev.* **2014**, *114*, 6179–6212; (b) Eigler, S.; Hirsch, A. *Angew. Chem., Int. Ed.* **2014**, *53*, 7720–7738; (c) Su, C.; Loh, K. P. *Acc. Chem. Res.* **2013**, *46*, 2275–2285.
3. Szabo, T.; Tombacz; Illes, E. E.; Dekany, I. *Carbon* **2006**, *44*, 537–545.
4. Boehm, H. P.; Clauss, A.; Fischer, G.; Hofmann, U. Fifth Conference on Carbon; Pergamon: Oxford, 1962; pp 73–80.
5. (a) Dreyer, D. R.; Jia, H.-P.; Bielawski, C. W. *Angew. Chem., Int. Ed.* **2010**, *49*, 6813–6816; (b) Mirza-Aghayan, M.; Kashef-Azar, E.; Boukherroub, R. *Tetrahedron Lett.* **2012**, *53*, 4962–4965; (c) Dreyer, D. R.; Jia, H.-P.; Todd, A. D.; Geng, J.; Bielawski, C. W. *Org. Biomol. Chem.* **2011**, *9*, 7292–7295; (d) Huang, H.; Huang, J.; Liu, Y.-M.; He, H.-Y.; Cao, Y.; Fan, K.-N. *Green Chem.* **2012**, *14*, 930–934; (e) Jia, H.-P.; Dreyer, D. R.; Bielawski, C. W. *Adv. Synth. Catal.* **2011**, *353*, 528–532.
6. (a) Wu, Y.-C.; Zhu, J. *J. Org. Chem.* **2008**, *73*, 9522–9524; (b) Varala, R.; Nuvula, S.; Adapa, S. R. *Bull. Korean Chem. Soc.* **2006**, *27*, 1079–1082; (c) De, S. K. *Adv. Synth. Catal.* **2005**, *347*, 673–676; (d) De, S. K. *Tetrahedron Lett.* **2004**, *45*, 1035–1036; (e) De, S. K. *Tetrahedron Lett.* **2004**, *45*, 2339–2341; (f) Srivastava, N. S.; Dasgupta, K.; Banik, B. K. *Tetrahedron Lett.* **2003**, *44*, 1191–1193; (g) Kamal, A.; Chouhan, G. *Tetrahedron Lett.* **2002**, *43*, 1341–1350; (h) Muthusamy, S.; Babu, S. A.; Gunanathan, C. *Tetrahedron* **2002**, *58*, 7897–7901; (i) Mondal, E.; Sahu, P. R.; Bose, G.; Khan, A. T. *Tetrahedron Lett.* **2002**, *43*, 2843–2846; (j) Muthusamy, S.; Babu, S. A.; Gunanathan, C. *Tetrahedron Lett.* **2001**, *42*, 359–362; (k) Firouzabadi, H.; Iranpoor, N.; Hazarkhani, H. *J. Org. Chem.* **2001**, *66*, 7527–7529; (l) Yadav, J. S.; Reddy, B. V. S.; Pandey, S. K. *Synlett* **2001**, 238–239; (m) Karimi, B.; Seradj, H. *Synlett* **2000**, 805–806; (n) Firouzabadi, H.; Iranpoor, N.; Karimi, B. *Synthesis* **1999**, 58–60; (o) Ravindranathan, T.; Chavan, S. P.; Dantale, S. W. *Tetrahedron Lett.* **1995**, *36*, 2285–2288; (p) Mandal, P. K.; Roy, S. C. *Tetrahedron* **1995**, *51*, 7823–7828; (q) Saraswathy, V. G.; Sankararaman, S. J. *J. Org. Chem.* **1994**, *59*, 4665–4670; (r) Kumar, V.; Dev, S. *Tetrahedron Lett.* **1983**, *24*, 1289–1292; (s) Burczyk, B.; Kortylewicz, Z. *Synthesis* **1982**, 831–833; (t) Ong, B. S. *Tetrahedron Lett.* **1980**, *21*, 4225–4228; (u) Fieser, L. F. *J. Am. Chem. Soc.* **1954**, *76*, 1945–1947; (v) Djerassi, C.; Gorman, M. *J. Am. Chem. Soc.* **1953**, *75*, 3704–3708; (x) Ralls, J. W.; Dobson, R. M.; Reigel, B. *J. Am. Chem. Soc.* **1949**, *71*, 3320–3325.
7. (a) Ali, M. H.; Gomes, M. G. *Synthesis* **2005**, 1326–1332; (b) Firouzabadi, H.; Iranpoor, N.; Jafari, A. A.; Jafari, M. R. *J. Mol. Catal. A: Chem.* **2006**, *247*, 14–18; (c) Gogoi, S.; Borah, J. C.; Barua, N. C. *Synlett* **2004**, 1592–1594; (d) Ballini, R.; Bosica, G.; Maggi, R.; Mazzacani, A.; Righi, P.; Sartori, G. *Synthesis* **2001**, 1826–1829; (e) Aoyama, T.; Takido, T.; Kodomar, M. *Synlett* **2004**, 2307–2310; (f) Shirini, F.; Albadi, J. *Bull. Korean Chem. Soc.* **2010**, *31*, 1119–1120; (g) Pore, D. M.; Desai, U. V.; Mane, R. B.; Wadgaonkar, P. P. *Indian J. Chem.* **2006**, *45B*, 1291–1295; (h) Jung, N.; Grässle, S. D.; Lütjohann, S.; Bräse, S. *Org. Lett.* **2014**, *16*, 1036–1039; (i) Shaohu, B.; Lu, C.; Yongjun, J.; Jianguo, Y. *Chin. J. Chem.* **2010**, *28*, 2119–2121; (j) Lenardao, E. J.; Borges, E. L.; Mendes, S. R.; Perin, G.; Jacob, R. G. *Tetrahedron Lett.* **2008**, *49*, 1919–1921.
8. Dhakshinamoorthy, A.; Alvaro, M.; Puche, M.; Fornes, V.; Garcia, H. *ChemCatChem* **2012**, *4*, 2026–2030.
9. Basu, B.; Kundu, S.; Sengupta, D. *RSC Adv.* **2013**, *3*, 22130–22134.
10. (a) Hummers, W. S.; Offeman, R. E. *J. Am. Chem. Soc.* **1958**, *80*, 1339; (b) Layek, R. K.; Samanta, S.; Chatterjee, D. P.; Nandi, A. K. *Polymer* **2010**, *51*, 5846–5856.
11. (a) Zhuo, Q.; Ma, Y.; Gao, J.; Zhang, P.; Xia, Y.; Tian, Y.; Sun, X.; Zhong, J.; Sun, X. *Inorg. Chem.* **2013**, *52*, 3141–3147; (b) Dhakshinamoorthy, A.; Alvaro, M.; Concepcion, P.; Fornes, V.; Garcia, H. *Chem. Commun.* **2012**, 5443–5445.
12. (a) Papernaya, L. K.; Levanova, E. P.; Klyba, L. V.; Albanov, A. I. *Russ. J. Org. Chem.* **2009**, *45*, 1036–1039; (b) Papernaya, L. K.; Levanova, E. P.; Sukhomazova, E. N.; Albanov, A. I.; Deryagina, E. N. *Russ. J. Org. Chem.* **2005**, *41*, 952–955.

Tetrahedron Letters 56 (2015) 6762–6767

Contents lists available at ScienceDirect

Tetrahedron Letters

journal homepage: www.elsevier.com/locate/tetlet

Graphene oxide (GO) or reduced graphene oxide (rGO): efficient catalysts for one-pot metal-free synthesis of quinoxalines from 2-nitroaniline

Babli Roy, Sujit Ghosh, Pranab Ghosh, Basudeb Basu *

Department of Chemistry, North Bengal University, Darjeeling 734013, India

ARTICLE INFO

Article history:
Received 29 August 2015
Revised 18 October 2015
Accepted 19 October 2015
Available online 19 October 2015

Keywords:
Graphene oxide (GO)
Hydrazine hydrate
2-Nitroaniline
Quinoxaline
Reduced graphene oxide (rGO)

ABSTRACT

A straightforward one-pot preparation of library of quinoxalines from 2-nitroanilines under entirely metal-free conditions is described. Initial reduction of nitroaniline with hydrazine hydrate is efficiently catalyzed by graphene oxide (GO) or reduced graphene oxide (rGO), and further one-pot tandem reactions with 1,2-dicarbonyl compounds or with α-hydroxy ketones afford quinoxalines in excellent yields. The catalyst is recovered, characterized, and found to be recyclable for consecutive four runs examined with appreciable conversions.

Heterocyclic compounds are ubiquitous in nature.[1] Among different *N*-heterocyclic compounds, quinoxaline, and its congeners have broad spectrum of biological activities such as antiviral, anti-inflammatory, antitumour, antibacterial, anthelmintic, kinase inhibitory, anti-HIV, and anticancer activities.[2] In addition, these heterocycles are widely applied to other technical fields. For example, in the preparation of dyes,[3] metal complexes,[4] organic semiconductors,[5] cavitands,[6] luminescent materials,[7] chemically controllable switches,[8] etc. owing to vast and outstanding applications, several synthetic strategies have been developed for their synthesis over the years.[9] The most common method involves the condensation of an aryl 1,2-diamine with 1,2-dicarbonyl compound.[10] Since aryl 1,2-diamines are carcinogenic and relatively unstable than its precursor nitro compounds,[11] a few methods are also reported in the recent years via reduction of nitro compounds to anilines and subsequent condensation reaction, preferably in one-pot procedure, resulting in the formation of quinoxaline (Scheme 1).[11,12] The reduction of nitro to amine has however been carried out in the presence of different metal catalysts. For example, ruthenium-catalyzed hydrogen transfer strategy,[11] indium-acetic acid or indium(III) chloride,[12a] in situ generated iron sulfide from elemental sulfur and ferric chloride,[12b] gold NPs supported with cerium oxide,[12c] stannous chloride in ethanol,[12d] etc have been employed for the reduction of nitro group and subsequently, synthesis of quinoxaline was achieved by the reaction with 1,2-dicarbonyl compounds or analogues.

The primary demands of green synthesis include minimization of steps, that is, one-pot tandem reactions as well as catalytic processes under metal-free conditions.[13] Since there is no method developed for the one-pot and metal-free tandem synthesis of quinoxalines from nitroaniline or dinitrobenzene, we were interested to develop an alternative metal-free greener process for the synthesis of quinoxalines directly from 2-nitroaniline. The biomass derived carbon materials has been considered as potential catalyst for diverse organic reactions.[14] Since the seminal report by Bielawski in 2010, the use of graphene oxide (GO) as the 'carbocatalyst' in organic reactions has evolved enormous interests among the synthetic organic chemists.[14,15] While searching the literature, we find that reduced graphene oxide (rGO) in combination with large excess of hydrazine hydrate can perform the reduction of nitrobenzene to aniline, which is as good as commonly used noble metal catalyst like Pt/SiO_2.[16]

In connection with our interest to harness the utilization of sustainable carbonaceous materials in catalyzing diverse organic reactions,[17] we envisioned that GO or rGO could serve as an eco-friendly alternative catalyst for the synthesis of quinoxaline through the metal-free tandem reduction-condensation in one-pot protocol. Although the reported procedure using rGO for the reduction of nitroaniline is quite useful, further one-pot

* Corresponding author. Tel.: +91 353 2776 381; fax: +91 353 2699 001.
E-mail address: basu_nbu@hotmail.com (B. Basu).

http://dx.doi.org/10.1016/j.tetlet.2015.10.065
0040-4039/

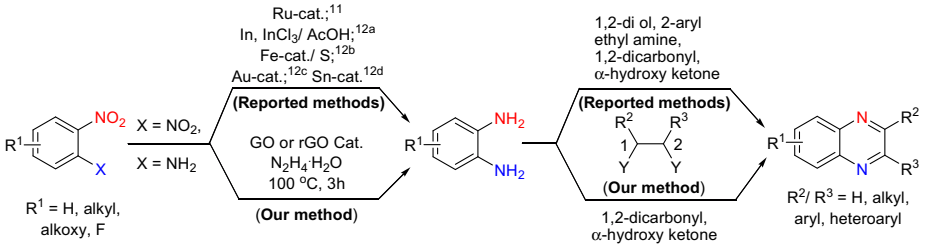

Scheme 1. One-pot reduction of nitro compounds and subsequent condensation resulting quinoxalines.

condensation with 1,2-dicarbonyl compound might lead to multifarious results due to the presence of excess hydrazine in the reaction mixture. In our strategy, it was therefore necessary to find out an optimized condition that could avoid the excess use of the reducing source hydrazine.

We report herein our findings that finally established a practical and clean procedure for the synthesis of quinoxalines directly from 2-nitroaniline via one-pot reduction-condensation reactions under metal-free condition. There was no other by-product detected by analysis of the crude product, the conversion was high (HPLC) and the isolation of the desired quinoxaline was achieved in excellent yield. A large variation of functional groups attached with the aromatic rings of either of the condensing partners was observed with excellent conversions to quinoxalines (Scheme 1).

Our studies began with the reaction of 2-nitroaniline and benzil in the presence of GO and hydrazine hydrate. Since benzil can also react with hydrazine to form hydrazone,[18] we set up the reaction by adding the reacting components in a step-wise manner and not in the multi-component reaction approach.[19] Thus a neat mixture of 2-nitroaniline (1 mmol), graphene oxide (5 mg), and hydrazine (6 mmol) was heated at 100 °C for 3 h (tlc monitoring showed complete disappearance of the nitroaniline), and then benzil (1 mmol) was added to the reaction mixture. After stirring for another 3 h at 100 °C, tlc showed complete disappearance of benzil on tlc plate. Ethyl acetate was added to the reaction mixture and the catalyst GO was separated out by centrifugation. HPLC analysis of the crude mixture showed the ratios of quinoxaline and dihydrazone derivative of benzil (prepared separately for comparison) in 70:30 mixtures. Separation of the crude mixture by column chromatography over silica gel afforded the quinoxaline (68%). The observation is presented in Table 1 (entry 1). Further optimization of the reaction conditions by changing the quantity of GO and/or hydrazine hydrate led us to achieve only quinoxaline as the sole product in 92% isolated yield (entries 2–7). However, as in entry 7, there was un-reacted benzil (6%) observed by HPLC analysis of the crude reaction mixture. Decreasing the temperature of the reaction furnished the hydrazone again (entry 8). Use of solvents like water, methanol or ethyl acetate however resulted in significant quantity of the hydrazone (entries 9–11). Further examination of the second step, that is, the condensation reaction carried out at room temperature was not favorable but the same at 60 °C afforded the quinoxaline in isolated yield (93%) (entries 12 and 13). Since hydrazine can also reduce the GO to reduced GO (rGO), we had separately prepared rGO using hydrazine,[20] and used it for the same one-pot reaction. It was observed that the rGO is also an equally effective catalyst for the reduction of 2-nitroaniline and subsequent condensation with benzil (entry 14). The control experiment without using GO did provide only trace amount of quinoxaline (⩽10%) signifying the catalytic role of the graphene oxide (entry 15). In another experiment, the reaction was scaled up using 2-nitroaniline (5 mmol) and the catalyst GO (50 mg), which afforded finally the quinoxaline in 88% isolated yield (entry 16). Thus the optimized condition was found to be the reaction of 2-nitroaniline (1 mmol) hydrazine hydrate (2.2 mmol),

Table 1
Optimization of reaction conditions for GO-catalyzed one-pot reduction and heterocyclization of 2-nitroaniline (1 mmol) and benzil (1 mmol)

Entry no.	GO (mg)	Temp (°C)	Solvent	Hydrazine hydrate ($N_2H_4·H_2O$) (mmol)	Time (h) (reduction & condensation)	Conversion[a] (%)	
						Quinoxaline (% yield)	Hydrazone[a]
1	5	100	No	6	(3 & 2)	70 (68)	30
2	10	100	No	4	(3 & 2)	78 (76)	22
3	15	100	No	4	(3 & 2)	80 (78)	20
4	15	100	No	3	(3 & 2)	87 (85)	13
5	15	100	No	2.5	(3 & 2)	90 (88)	10
6	15	100	No	2.2	(3 & 2)	91 (89)	09
7[b]	20	100	No	2.2	(3 & 2)	94 (92)	No
8	20	80	No	2.2	(3 & 2)	87 (81)	13
9	20	100	Water	2.2	(4 & 2)	75 (71)	25
10	20	100	MeOH	2.2	(4 & 2)	71 (68)	29
11	20	100	EtOAc	2.2	(4 & 2)	75 (68)	25
12[c]	20	100	No	2.2	(3 & 12)	83 (81)	17
13[d]	**20**	**100**	**No**	**2.2**	**(3 & 3)**	**95 (93)**	**No**
14[e]	20	100	No	2.2	(3 & 3)	93 (91)	07
15[f]	No	100	No	2.2	(6 & 3)	09	65
16[g]	50	100	No	11	(4 & 3)	88	No

[a] Conversion was checked by HPLC and yield of quinoxaline (in the parenthesis) represents the isolated product after column chromatography.
[b] Un-reacted benzil (6%).
[c] Condensation with benzil was performed at room temperature.
[d] Condensation with benzil was performed at 60 °C and un-reacted benzil.
[e] rGO was used instead of GO and condensation with benzil was performed at 60 °C.
[f] Un-reacted benzil (26%).
[g] Reaction carried out with 2-nitroaniline (5 mmol).

Table 2
GO-catalyzed reduction of various 2-nitroanilines and subsequent heterocyclization with 1,2-dicarbonyl compounds or with α-hydroxy ketones[a]

Entry	2-Nitro aryl amine	1,2-Dicarbonyl compound/α-hydroxy ketone	Temp (°C) (reduction & condensation)	Time (h) (reduction & condensation)	Product	Yield[b] (%)
1	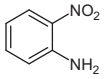	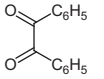	100 & 60	3 & 3	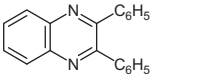	93
2	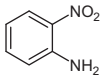	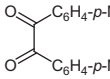	100 & 60	3 & 3	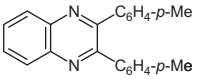	91
3	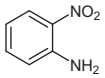	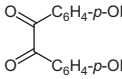	100 & 60	3 & 3	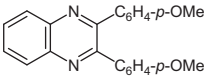	92
4	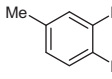	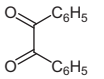	100 & 60	4 & 3	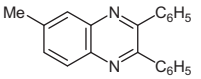	89
5	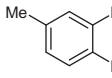	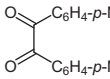	100 & 60	4 & 3	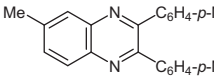	91
6	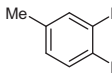	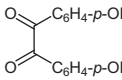	100 & 60	4 & 3	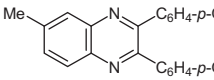	90
7	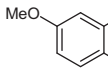	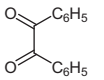	100 & 60	4 & 3	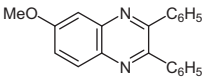	90
8	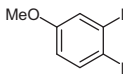	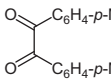	100 & 60	4 & 3	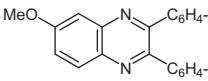	88
9	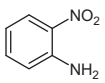	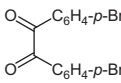	100 & 60	3 & 3.5	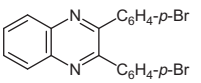	95
10	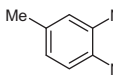	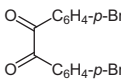	100 & 60	4 & 3.5	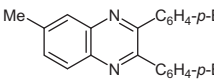	92
11	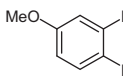	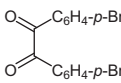	100 & 60	4 & 3	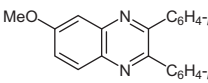	90
12	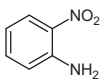	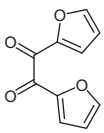	100 & 60	3 & 3	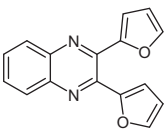	91
13	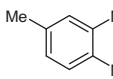	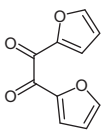	100 & 60	4 & 3	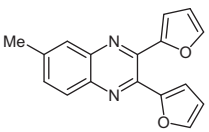	90
14	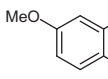		100 & 60	4 & 3		89
15			100 & 60	3 & 2		85
16			100 & 60	3 & 3		84
17			100 & 60	4 & 2		87
18			100 & 60	3 & 2.5		83

Table 2 (*continued*)

Entry	2-Nitro aryl amine	1,2-Dicarbonyl compound/α-hydroxy ketone	Temp (°C) (reduction & condensation)	Time (h) (reduction & condensation)	Product	Yield[b] (%)
19	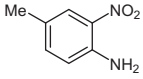		100 & 60	4 & 3	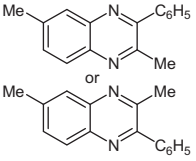	88
20	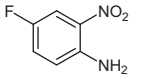		100 & 60	4 & 4	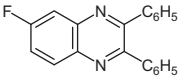	87
21[c]	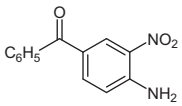		100 & 60	5 & 4	Inseparable mixture of different products	–
22[d]	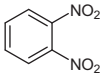		100 & 60	4 & 3	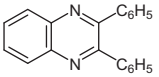	48
23	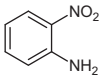	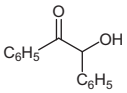	100 & 80	3 & 1.5	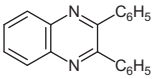	91
24	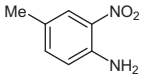	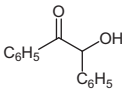	100 & 80	4 & 2	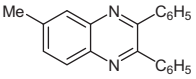	90
25	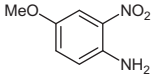	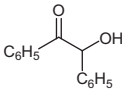	100 & 80	4 & 2	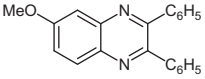	92
26	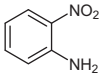	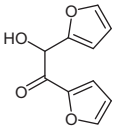	100 & 80	3 & 2	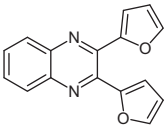	87
27	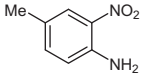	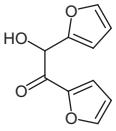	100 & 80	4 & 2	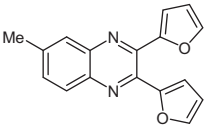	88
28	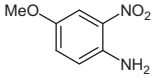	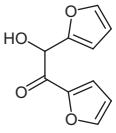	100 & 80	4 & 2	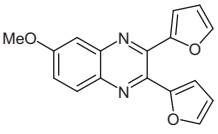	86

[a] Reaction conditions: a mixture of 2-nitro aryl amine (1 mmol), hydrazine monohydrate (2.2 mmol) and GO (20 mg) was heated in a sealed tube with magnetic stirring for hours and then 1,2-dicarbonyl compound or α-hydroxy ketone (1 mmol) was added to the reaction mixture and stirred.
[b] Isolated yield after column chromatography.
[c] The reaction furnished a non-separable mixture of compounds.
[d] The reaction was carried out using 4.4 mmol of hydrazine hydrate.

and GO (20 mg), stirring the mixture in neat at 100 °C for 3 h, then benzil (1 mmol) was added and further stirring at 60 °C for 3 h.

With the optimized condition at our hand (as in Table 1, entry 13), we examined its practical applications with a variety of nitroanilines and benzil derivatives. The results are presented in Table 2. It can be seen that different nitroanilines undergo one-pot reduction and condensation with benzils gave rise to the formation of corresponding quinoxalines in excellent yields (Table 2, entries 1–8). Since the present reducing condition is metal-free, it was interesting to examine whether halogen substituents could survive the overall reaction conditions. We employed 4,4′-dibromobenzil as the condensing partner and indeed the corresponding bromo-substituted quinoxalines were isolated in 90–95% yields (entries 9–11). Heteroaromatic benzils like α-furil also yielded corresponding furyl-containing quinoxaline derivatives in isolated yield (>90%) (entries 12–14). Further studies with glyoxal, aliphatic 1,2-diketones, and phenylpropane-1,2-dione also resulted in the formation of quinoxaline in good to excellent yields (entries 15–19). Thus, functional groups like methyl, methoxyl, furyl, or bromide being present with either nitroaniline or dicarbonyl compounds as well as the ketone or aldehyde functions worked without any difficulty yielding the final quinoxalines in excellent yields. We then examined similar reactions using 2-nitroaniline bearing an electron-withdrawing group such as F or –COPh (entries 20 and 21) as well as with 1,2-dinitrobenzene (entry 22). While 4-fluoro-2-nitroaniline resulted in the formation of the desired quinoxaline in excellent yield, 4-benzoyl-2-nitroaniline gave rise to a mixture of four spots on tlc and one of those was matched with the authentic sample [(phenyl(2,3-diphenylquinoxalin-6-yl) methanone)].[10b] However, the desired quinoxaline could not be separated and its actual yield was not obtained. Possibly, the benzoyl group suffers from reaction with hydrazine causing an

Table 3
Recycling of the catalyst tested with 2-nitroaniline and benzil in one-pot reactions

Entry[a]	Recovered catalyst (mg)	Catalyst used (mg)	Time (h) (reduction & condensation)	Yield[b] (%)
1st run	—	40	3 & 3	93
2nd run	28	20	3 & 3	91
3rd run	16	15	4 & 3	85
4th run	14	10	5 & 3	84

[a] First experiment was performed with 2-nitroaniline (2 mmol), hydrazine hydrate (4.4 mmol), benzil (2 mmol) and GO (40 mg), and subsequently in 1, 0.75 and 0.5 mmol scales.
[b] Isolated product after column chromatography.

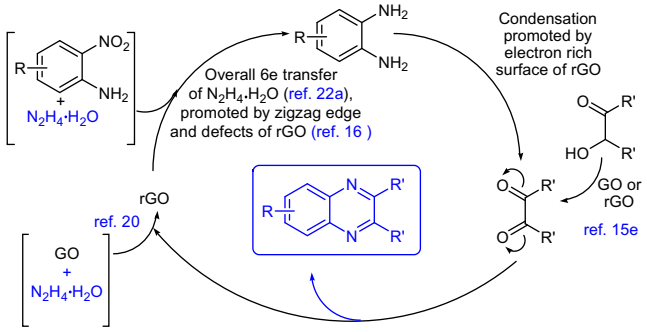

Scheme 2. Plausible mechanism.

inseparable mixture of products. In the case of 1,2-dinitrobenzene, similar reaction was sluggish and the desired quinoxaline was isolated in 48% yield. Since GO is known by its intriguing properties as an oxidizing agent, dual role of GO might be expected if α-hydroxy ketone is used as the condensing partner instead of 1,2-diketone. Acyloins are often considered as the precursor of diketo equivalent compounds. The reaction with benzoin indeed resulted in the formation of quinoxaline in isolated yield (91%) (entry 23). Substituted nitroanilines and other variety of acyloin such as furoin also gave rise to the formation of quinoxaline in 86–92% yields (entries 24–28).

We also tested the reusability of the catalyst GO. The catalyst was recovered from the reaction mixture as follows: The reaction mixture was taken in water (2 mL), subjected to the centrifugation (5000 rpm) and removed the supernatant liquid. The residue was washed with ethyl acetate followed by acetone. Drying under vacuum furnished the free-flowing powder, which is visibly blackish as compared to the first-time used GO. We can assume that the recovered catalyst may be the reduced graphene oxide (rGO), which was confirmed by comparison of the FT-IR spectroscopic characteristic absorption peaks (see SI, S3). The average particle size of GO was measured by DLS studies and found to be 544 ± 37 nm (0.1 mg/mL H_2O), which is comparable with the literature report (see SI, S6).[21]

After the first run, the recovered catalyst by weight was low, which could possibly be attributed to the removal of several oxygenated functional groups. It was then used in the second run with nearly equal catalytic efficiency in the reduction and subsequent condensation producing the quinoxaline product in 91% isolated yield. In the third and fourth runs, the quantity of the recovered catalyst by weight was nearly equal (from the second run) and indeed found to be significantly active with appreciable conversions. The results are presented in the Table 3.

Mechanistically, carbon-catalyzed reduction of nitrobenzene to aniline by hydrazine is believed to involve four-electron process occurring through the formation of phenylhydroxylamine.[22] While hydrazine is a two-electron reducing agent, the role of carbon materials such as graphite, GO or rGO might be to serve as an adsorbent as well as the conductor of electrons.[16,22] In order to find out the possible involvement of GO or rGO in the second step of condensation, we performed few reactions starting from *o*-phenylenediamine. In the case of graphite-promoted quinoxaline formation from *o*-phenylenediamine, it was postulated that the attack of amine *N*-lone pair to the carbonyl group is facilitated by the presence of graphite.[23] At our hand, the condensation of *o*-phenylenediamine with benzil in neat in the absence of GO afforded only 30% conversion to quinoxaline after 3 h at 60 °C, while the same reaction carried out in ethyl acetate resulted in >90% conversion to quinoxaline. Similarly, heating the neat reaction mixture of *o*-phenylenediamine, benzoin, and rGO at 80 °C gave nearly complete conversions after 2 h (analyzed by HPLC). The above observations suggest that the catalyst GO or rGO plays a positive role in promoting the second step of condensation as well as the oxidation of benzoin to benzil. Although the exact function of GO or rGO is not clearly understood, we tend to believe that GO is at first reduced to rGO and its electron-rich large surface area might act favorably as the conductor of electrons thereby facilitating release of hydrogen source from hydrazine that is finally responsible for the reduction of nitro group,[16,24] as well as assisting to promote the condensation between the diamine and diketone to form quinoxaline. Plausible mechanism is presented in Scheme 2 indicating the role of GO or rGO.

In summary, the present work demonstrates synthesis of bio-active scaffold quinoxalines directly from 2-nitroaniline via one-pot reduction-condensation reactions using hydrazine as the reductant and GO/rGO as the catalysts under complete metal-free conditions. The conditions are straightforward, mild and no other side-products are obtained. Green process of preparation of quinoxalines from 2-nitroaniline is developed that could override existing metal-catalyzed reaction conditions.

Acknowledgments

B.R. and S.G. thank the UGC, New Delhi, for award of their fellowships under UGC-FDP program.

Supplementary data

Supplementary data associated with this article can be found, in the online version, at http://dx.doi.org/10.1016/j.tetlet.2015.10.065.

References and notes

1. (a) Brahmachari, G. *Green Synthetic Approaches for Biologically Relevant Heterocycles*; Elsevier: Oxford, 2014. p 632; (b) Alvarez-Builla, J.; Vaquero, J. J.; Barluenga, J. In *Modern Heterocyclic Chemistry*; John Wiley & Sons: Germany, 2011; Vol. 1,
2. (a) Pereira, J. A.; Pessoa, A. M.; Cordeiro, M. N. D. S.; Fernandes, R.; Prudencio, C.; Noronha, J. P.; Vieir, M. *Eur. J. Med. Chem.* **2014**, 1–9; (b) Rodrigues, F. A. R.; Bomfim, I. S.; Cavalcanti, B. C.; Pessoa, C. Ó.; Wardell, J. L.; Wardell, S. M. S. V.; Pinheiro, A. C.; Kaiser, C. R.; Nogueira, T. C. M.; Low, J. N.; Gomes, L. R.; de Souza, M. V. N. *Bioorg. Med. Chem. Lett.* **2014**, *24*, 934–939; (c) Hari Narayana Moorthy, N. S.; Manivannan, E.; Karthikeyan, C.; Trivedi, P. *Mini-Rev. Med. Chem.* **2013**, *13*, 1415–1420; (d) Parhi, A. K.; Zhang, Y.; Saionz, K. W.; Pradhan, P.; Kaul, M.; Trivedi, K.; Pilch, D. S.; LaVoie, E. *J. Bioorg. Med. Chem. Lett.* **2013**, *23*, 4968–4974; (e) Smits, R. A.; Lim, H. D.; Hanzer, A.; Zuiderveld, O. P.; Guaita, E.; Adami, M.; Coruzzi, G.; Leurs, R.; de Esch, I. J. P. *J. Med. Chem.* **2008**, *51*, 2457–2467; (f) Rong, F.; Chow, S.; Yan, S.; Larson, G.; Hong, Z.; Wu, J. *Bioorg. Med. Chem. Lett.* **2007**, *17*, 1663–1666; (g) Hui, X.; Desrivot, J.; Bories, C.; Loiseau, P. M.; Franck, X.; Hocquemiller, R.; Figadere, B. *Bioorg. Med. Chem. Lett.* **2006**, *16*, 815–820; (h) Kim, Y. B.; Kim, Y. H.; Park, J. Y.; Kim, S. K. *Bioorg. Med. Chem. Lett.* **2004**, *14*, 541–544; (i) Hazeldine, S. T.; Polin, L.; Kushner, J.; Paluch, J.; White, K.; Edelstein, M.; Palomino, E.; Corbett, T. H.; Horwitz, J. P. *J. Med. Chem.* **2001**, *44*, 1758–1776.
3. (a) Brock, E. D.; Lewis, D. M.; Yousaf, T. I.; Harper, H. H. The Procter and Gamble Company, USA, WO9951688, 1999.; (b) Katoh, A.; Yoshida, T.; Ohkanda, J. *Heterocycles* **2000**, *52*, 911–920.

4. Granifo, J.; Garland, M. T.; Baggio, R. *Inorg. Chim. Acta* **2003**, *348*, 263–270.
5. Dailey, S.; Feast, W. J.; Peace, R. J.; Sage, I. C.; Till, S.; Wood, E. L. *J. Mater. Chem.* **2001**, *11*, 2238–2243.
6. Sessler, J. L.; Maeda, H.; Mizuno, T.; Lynch, V. M.; Furuta, H. *J. Am. Chem. Soc.* **2002**, *124*, 13474–13479.
7. (a) Lindner, B. D.; Zhang, Y.; Hoefle, S.; Berger, N.; Teusch, C.; Jesper, M.; Hardcastle, K. I.; Qian, X.; Lemmer, U.; Colsmann, A.; Bunz, U. H. F.; Hamburger, M. *J. Mater. Chem. C* **2013**, *1*, 5718–5724; (b) Thomas, K. R. J.; Velusamy, M.; Lin, J. T.; Chuen, C.-H.; Tao, Y.-T. *Chem. Mater.* **2005**, *17*, 1860–1866.
8. Crossley, M. J.; Johnston, L. A. *Chem. Commun.* **2002**, 1122–1123.
9. (a) Nageswar, Y. V. D.; Reddy, K. H. V.; Ramesh, K.; Murthy, S. N. *Org. Prep. Proc. Int.* **2013**, *45*, 1–27; (b) Basu, B.; Mandal, B. *Sustainable Synthesis of Benzimidazole, Quinoxaline & Congeners*; Elsevier: Oxford, 2014. Chapter 9; pp 209–252.
10. (a) Ayaz, M.; Xu, Z.; Hulme, C. *Tetrahedron Lett.* **2014**, *55*, 3406–3409; (b) Paul, S.; Basu, B. *Tetrahedron Lett.* **2011**, *52*, 6597–6602; (c) Huang, T. K.; Wang, R.; Shi, L.; Lu, X. X. *Catal. Commun.* **2008**, *9*, 1143–1147; (d) Srinivas, C.; Kumar, C. N. S. S. P.; Rao, V. J.; Palaniappan, S. *J. Mol. Catal. A: Chem.* **2007**, *265*, 227–230; (e) Darabi, H. R.; Mohandessi, S.; Aghapoor, K.; Mohsenzadeh, F. *Catal. Commun.* **2007**, *8*, 389–392; (f) More, S. V.; Sastry, M. N. V.; Wang, C. C.; Yao, C. F. *Tetrahedron Lett.* **2005**, *46*, 6345–6348; (g) Bhosale, R. S.; Sarda, S. R.; Ardhapure, S. S.; Jadhav, W. N.; Bhusare, S. R.; Pawar, R. P. *Tetrahedron Lett.* **2005**, *46*, 7183–7186; (h) Zhao, Z.; Wisnoski, D. D.; Wolkenberg, S. E.; Leister, W. H.; Wang, Y.; Lindsley, C. W. *Tetrahedron Lett.* **2004**, *45*, 4873–4876.
11. Xie, F.; Zhang, M.; Jiang, H.; Chen, M.; Lv, W.; Zhenga, A.; Jiana, X. *Green Chem.* **2015**, *17*, 279–284.
12. (a) Go, A.; Lee, G.; Kim, J.; Bae, S.; Lee, B. M.; Kim, B. H. *Tetrahedron* **2015**, *71*, 1215–1226; (b) Nguyen, T. B.; Retailleau, P.; Al-Mourabit, A. *Org. Lett.* **2013**, *15*, 5238–5241; (c) Climent, M. J.; Corma, A.; Hernández, J. C.; Hungría, A. B.; Iborra, S.; Martínez-Silvestre, S. *J. Catal.* **2012**, *292*, 118–129; (d) Shi, D.-Q.; Dou, G.-L.; Ni, S.-N.; Shi, J.-W.; Li, X.-Y. *J. Heterocycl. Chem.* **2008**, *45*, 1797–1801.
13. (a) Allais, C.; Grassot, J.-M.; Rodriguez, J.; Constantieux, T. *Chem. Rev.* **2014**, *114*, 10829–10868; (b) Thomas, J.; John, J.; Parekh, N.; Dehaen, W. *Angew. Chem., Int. Ed.* **2014**, *53*, 10155–10159.
14. For review: see (a) Navalon, S.; Dhakshinamoorthy, A.; Alvaro, M.; Garcia, H. *Chem. Rev.* **2014**, *114*, 6179–6212; (b) Su, C.; Loh, K. P. *Acc. Chem. Res.* **2013**, *46*, 2275–2285.
15. (a) Chua, C. K.; Pumera, M. *Chem. Eur. J.* **2015**, *21*, 1–14; (b) Hu, H.; Xin, J. H.; Hu, H.; Wang, X.; Kong, Y. *Appl. Catal. A: General* **2015**, *492*, 1–9; (c) Dreyer, D. R.; Todd, A. D.; Bielawski, C. W. *Chem. Soc. Rev.* **2014**, *43*, 5288–5301; (d) Dreyer, D. R.; Bielawski, C. W. *Chem. Sci.* **2011**, *2*, 1233–1240; (e) Dreyer, D. R.; Jia, H.-P.; Bielawski, C. W. *Angew. Chem., Int. Ed.* **2010**, *49*, 6813–6816.
16. Gao, Y.; Ma, D.; Wang, C.; Guan, J.; Bao, X. *Chem. Commun.* **2011**, 2432–2434.
17. (a) Kundu, S.; Basu, B. *RSC Adv.* **2015**, *5*, 50178–50185; (b) Roy, B.; Sengupta, D.; Basu, B. *Tetrahedron Lett.* **2014**, *55*, 6596–6600; (c) Sengupta, D.; Saha, J.; Basu, B.; De, G. *RSC Adv.* **2014**, *4*, 35442–35448; (d) Basu, B.; Kundu, S.; Sengupta, D. *RSC Adv.* **2013**, *3*, 22130–22134.
18. Lakshmi, B.; Avaji, P. G.; Shivananda, K. N.; Nagella, P.; Manohar, S. H.; Mahendra, K. N. *Polyhedron* **2011**, *30*, 1507–1515.
19. (a) Cioc, R. C.; Ruijter, E.; Orru, R. V. A. *Green Chem.* **2014**, *16*, 2958–2975; (b) Rotstein, B. H.; Zaretsky, S.; Rai, V.; Yudin, A. K. *Chem. Rev.* **2014**, *114*, 8323–8359.
20. Stankovich, S.; Dikin, D. A.; Piner, R. D.; Kohlhaas, K. A.; Kleinhammes, A.; Jia, Y.; Wu, Y.; Nguyen, S. T.; Ruoff, R. S. *Carbon* **2007**, *45*, 1558–1565.
21. Zangmeister, C. D.; Ma, X.; Zachariah, M. R. *Chem. Mater.* **2012**, *24*, 2554–2557.
22. (a) Larsen, J. W.; Freund, M.; Kim, K. Y.; Sidovar, M.; Stuart, J. L. *Carbon* **2000**, *38*, 655–661; (b) Han, B. H.; Shin, D. H.; Cho, S. Y. *Tetrahedron Lett.* **1985**, *26*, 6233–6234.
23. Kadam, H. K.; Khan, S.; Kunkalkar, R. A.; Tilve, S. G. *Tetrahedron Lett.* **2013**, *54*, 1003–1007.
24. Karim, M. R.; Hatakeyama, K.; Matsui, T.; Takehira, H.; Taniguchi, T.; Koinuma, M.; Matsumoto, Y.; Akutagawa, T.; Nakamura, T.; Noro, S.-ichiro; Yamada, T.; Kitagawa, H.; Hayami, S. *J. Am. Chem. Soc.* **2013**, *135*, 8097–8100.